UNIVERSITÀ DEGLI STUDI DI TRIESTE
UNIVERSITÀ DEGLI STUDI DI UDINE

XXXV CICLO DEL DOTTORATO DI RICERCA IN AMBIENTE E VITA

EXPLORATION OF PLANT EARLY RESPONSE MECHANISMS TO SELF-DNA EXPOSURE

Settore scientifico-disciplinare: **BIO/07 ECOLOGIA**

DOTTORANDA/PH.D. STUDENT

ALESSIA RONCHI

COORDINATORE/PH.D. PROGRAM COORDINATOR

PROF. GIORGIO ALBERTI

SUPERVISORE DI TESI/THESIS SUPERVISOR

PROF. GUIDO INCERTI

CO-SUPERVISORE DI TESI/THESIS CO-SUPERVISOR

PROF. EMANUELE DE PAOLI

ANNO ACCADEMICO 2021/2022

Summary

CHAPTER 1: GENERAL INTRODUCTION AND SYNOPSIS 7

1.1. FUNCTIONAL ROLES OF PLANT EXTRACELLULAR DNA 9
1.1.1. EXTRACELLULAR DNA IN ROOT EXTRA-CELLULAR TRAPS (RETS) 10
1.1.2. DNA AS A DAMAGE-ASSOCIATED MOLECULAR PATTERN (DAMP) 12
1.1.3. SELF-DNA AS A DRIVER FOR SPECIES-SPECIFIC PLANT–SOIL NEGATIVE FEEDBACKS 15
1.2. THE PHENOMENON OF SELF-DNA INHIBITION IN PLANTS 17
1.3. MECHANISMS UNDERLYING SELF-DNA INHIBITION 19
1.3.1. CELL SELF-DNA SENSING AND DISCRIMINATION FROM NONSELF-DNA 20
1.3.2. MOLECULAR MECHANISMS OF SELF-DNA INHIBITION 22
1.4. AIMS AND SCOPE 28

CHAPTER 2: SPECIES-SPECIFICITY OF ROOT GROWTH INHIBITION BY SELF-DNA IN CULTIVATED AND WEEDY *SETARIA* SPECIES 35

2.1. ABSTRACT 37
2.2. INTRODUCTION 38
2.3. MATERIALS AND METHODS 41
2.3.1. LEAF BIOMASS PRODUCTION FOR DNA EXTRACTION 41
2.3.2. DNA EXTRACTION AND RNASE TREATMENT 42
2.3.3. DNA TREATMENT SOLUTION PREPARATION 43
2.3.4. CROSS-FACTORIAL EXPERIMENT SETUP 45
2.3.5. STATISTICAL ANALYSIS 48
2.4. RESULTS 48
2.5. DISCUSSION 52
2.6. CONCLUSIONS 53

CHAPTER 3: TARGETED GENE EXPRESSION ANALYSIS IN *SETARIA* SPECIES AFTER SELF-DNA EXPOSURE 55

3.1. ABSTRACT 57
3.2. INTRODUCTION 58
3.3. MATERIALS AND METHODS 62
3.3.1. GENE SELECTION AND PRIMER DESIGN 62
3.3.2. SELF-DNA EXPOSURE 65
3.3.3. RNA EXTRACTION, PURIFICATION AND CDNA SYNTHESIS 65
3.3.4. REAL TIME QPCR 66
3.3.5. STATISTICAL ANALYSIS 67
3.4. RESULTS 68
3.5. DISCUSSION 70
3.5.1. DROUGHT AND DEHYDRATION STRESS 70
3.5.2. OSMOTIC AND OXIDATIVE STRESS 73
3.5.3. THERMIC STRESS 74
3.6. CONCLUSIONS 75

CHAPTER 4: INVESTIGATION OF DNA-RNA HYBRID FORMATION IN *ARABIDOPSIS THALIANA* SEEDLINGS EXPOSED TO SELF-DNA **77**

4.1. ABSTRACT **78**
4.2. INTRODUCTION **79**
4.3. MATERIALS AND METHODS **87**
4.3.1. GENE SELECTION, PROBE AND PRIMER DESIGN 87
4.3.2. *IN VITRO* TESTING OF DNA-RNA IMMUNOPRECIPITATION (DRIP) PROTOCOL 89
4.3.2.1. RNA-DNA hybridization and dsRNA purification 90
4.3.2.2. DNA-RNA immunoprecipitation (DRIP) 91
4.3.2.3. DNase treatment, RNA reverse transcription and PCR amplification 93
4.3.2.4. Non-denaturing Polyacrylamide Gel Electrophoresis 94
4.3.3. *IN VIVO* INVESTIGATION OF DNA-RNA HYBRID FORMATION AFTER SELF-DNA EXPOSURE 95
4.3.3.1. Seed sterilization, vernalization and germination 95
4.3.3.2. Self-DNA exposure 95
4.3.3.3. Total nucleic acid extraction 97
4.3.4. VERIFICATION OF THE ACTUAL MOLECULAR PROCESS CAUSING HYBRID FORMATION *IN VIVO* 98
4.3.4.1. TESTING HYBRID FORMATION DURING THE EXTRACTION PHASE DUE TO PROBE CARRY-OVER 98
4.3.4.2. Preventing hybrid formation during the extraction phase 99
4.4. RESULTS **101**
4.4.1. *IN VITRO* RESULTS 101
4.4.2. *IN VIVO* RESULTS 103
4.5. CONCLUSIVE REMARKS AND PERSPECTIVES **108**

CHAPTER 5: INVESTIGATION OF EPIGENETIC CHANGES IN *ARABIDOPSIS THALIANA* SEEDLINGS EXPOSED TO SELF-DNA **111**

5.1. INTRODUCTION **113**
5.2. MATERIALS AND METHODS **130**
5.2.1. SEED STERILIZATION AND GERMINATION 130
5.2.2. GROWTH MEDIUM SLICES PREPARATION 130
5.2.3. SELF-DNA EXPOSURE AND ROOT COLLECTION 132
5.2.4. RNA EXTRACTION AND MRNA SEQUENCING 134
5.2.5. DNA EXTRACTION AND WHOLE GENOME BISULFITE SEQUENCING ANALYSIS 135
5.2.6. BIOINFORMATIC ANALYSIS 136
5.3. RESULTS **136**
5.3.1. RNA-SEQ AND GENE EXPRESSION IN TREATED VS CONTROL SAMPLES 136
5.3.2. WGBS AND METHYLATION LEVEL IN TREATED VS CONTROL SAMPLES 142
5.4. CONCLUSIVE REMARKS AND PERSPECTIVES **146**

CHAPTER 6: GENERAL CONCLUSIONS **149**

REFERENCES **157**

APPENDICES **181**

ACKNOWLEDGEMENTS 193

Chapter 1: General introduction and synopsis

1.1. Functional roles of plant extracellular DNA

Extracellular DNA (eDNA) is defined as "…located outside the cell and originating from intracellular DNA by active or passive extrusion mechanisms or by cell lysis" (Ceccherini *et al*., 2009). DNA normally exists in the living cell as genetic material, but it can be released either actively or passively from damaged or infected cells to the extracellular space. After release, these extracellular DNA (eDNA) can be degraded into fragments in a variable size range (Kuriyama & Fukuda, 2002; Wu *et al*., 2013; De Lorenzo *et al*., 2018). It is abundant in many habitats, including soil, sediments, oceans, and freshwater, and can be found in both the double and single stranded, as well as more or less fragmented forms (Levy-Booth *et al*., 2007; Ceccherini *et al*., 2009; Thierry *et al*., 2016; Nagler *et al*., 2018). eDNA serves several biological functions: in plants, it can have important roles in defence response and immunity induction (Monticolo *et al*., 2020), horizontal gene transfer (Aubin *et al*., 2021), as source of nutrients (Paungfoo-Lonhienne *et al*., 2010), and as driver of negative plant-soil feedbacks, as recently discovered (Mazzoleni *et al*., 2015a,b).

Bacteria, archaea, fungi, and in general, microbial communities, but also multicellular organisms, like animals and plants, are able to actively release genetic material into the extracellular environment, where it is often present in matrices located outside the cells. In plants, they identify as high molecular weight compounds, mostly carbohydrates, produced by the root border cells and surrounding the plant root cap (Monticolo *et al*., 2020). These extracellular structures, named Root Extracellular Traps (RETs), have been described to play a crucial role in plant defence, appearing as barrier against pathogen invasion or for their recognition (Hawes *et al*., 2011; Hawes *et al*., 2016; Driouich *et al*., 2013).

Moreover, extracellular self-DNA (esDNA) in soil might function as a signaling molecule for self-damage recognition, triggering plant resistance and inducing immunity response against environmental stresses and dangers like pathogen infection, herbivore feeders, and intraspecific competition (Duran-Flores & Heil, 2015; Barbero *et al*., 2021).

The discovery of the additional role of esDNA as a main driver of species-specific plant-soil negative feedbacks (PSNF) (Mazzoleni *et al*., 2015a,b; Bonanomi *et al*., 2022; Rietkerk, 2022) highlighted its importance also in determining biodiversity patterns throughout the world, depending on the environment, soil characteristics and weather conditions, with terrestrial ecosystems, like tropical forests where fragments of DNA produced by litter decomposition accumulate in the soil, generally showing high biodiversity levels, and aquatic tropical communities showing low diversity (Cartenì *et al*., 2016; Givnish, 1999).

1.1.1. Extracellular DNA in root extra-cellular traps (RETs)

The plant root cap, in the external part of the root apex, adjacent to the apical meristem, represents a dynamic and multifunctional tissue extremely resistant to both biotic and abiotic stimuli thanks to the presence of root border cells at the cap periphery (Monticolo *et al*., 2020). These cells are morphologically and physiologically different from the root cap cells (Hawes *et al*., 2016) and constitute a metabolically active population of cells released into the rhizosphere as free cells or in clump (Brigham *et al*., 1998; Gunawardena & Hawes, 2002; Wen *et al*., 2007; Hawes *et al*., 2016). Both root cap cells and border cells are able to secrete the root mucilage, the high molecular weight sticky matrix that surrounds the plant root cap, through an active continuous process, that piles up materials outside the root (Figure 1.1). The root mucilage is mostly composed by both mono and polysaccharides, proteins and amino acids, minerals and lipids (Carminati & Vetterlein, 2013; Koocheki *et al*., 2013; Alizadeh Behbahani *et al*., 2017), where proteins seem to play a major role in the structural integrity of the matrix (Matsuyama *et al*., 1999). Interestingly, the root mucilage was also revealed to be formed by known intracellular markers, such as histone H4 (Wen *et al*., 2007; Weiller *et al*., 2017). Together with the histone H4, the presence of DNA in the root mucilage was also reported (Wen *et al*., 2009).

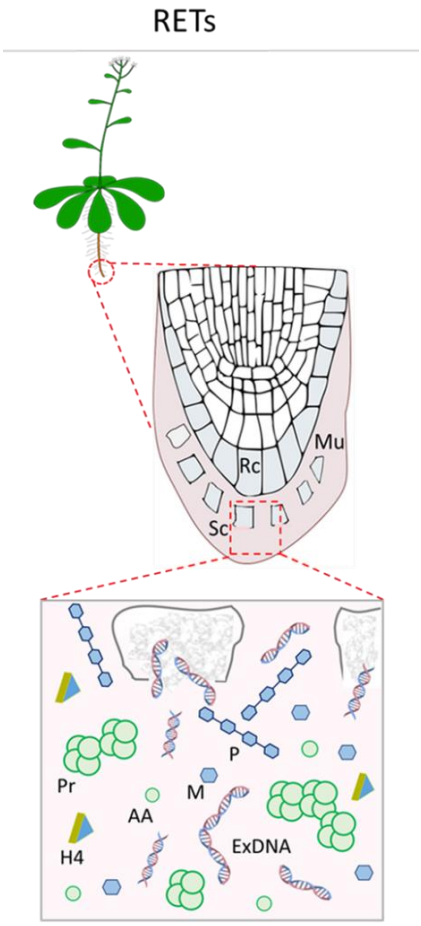

Figure 1.1. Schematic representation of RETs (plants) structures. RC, root cap cells; MU, mucilage; SC, sloughed cells (border cells); Pr, proteins; AA, aminoacids; H4, histones; M, monosaccharides; P, polisaccharides; ExDNA, extracellular DNA (adapted from Monticolo *et al*., 2020).

Recent research has shed light on the fascinating phenomenon of extracellular DNA (eDNA) release in plants. Specifically, studies have shown that plant root border cells and mucilage secretions form intricate networks known as root extracellular traps (RETs) (Driouich *et al*., 2019). It appears that plant eDNA is actively exported into RETs by vital root cap cells, although it is worth noting that the leakage of nuclear content from dead cells cannot be entirely ruled out (Wen *et al*., 2009). Initial analyses have indicated that the eDNA found within RETs primarily consists of nuclear DNA enriched in repetitive sequences (Hawes *et al*., 2012). So far, there is no evidence supporting the presence of mitochondrial DNA sequences within these structures (Driouich *et al*., 2019). Many roles were associated with the root mucilage, such as: lubricant protecting the root tips while growing into the soil (Greenland, 1979); carrier of gravitropic signals from the root cap to the root tip (Moore *et al*., 1990); protection of roots from the toxicity of ions such as copper, cadmium, boron, lead, mercury, iron, arsenic, aluminium (Mench *et al*., 1987; Hawes *et al*., 2016); as carbon source for soil microbes (Knee *et al*., 2001); or as an “extra-root” digestive system (Rogers *et al*., 1942), that functions as an exoenzyme system releasing substances, like phosphatases, into the rhizosphere (Driouich *et al*., 2019). Moreover, the root cap secretion plays a crucial role as a primary site for the colonization of microbial symbionts and pathogens present in the rhizosphere (Monticolo *et al*., 2020).

The rhizosphere, the zone surrounding the fine roots, is a complex ecosystem known to harbour diverse microbial communities that interact with the plant. These communities include bacteria and mycorrhizal organisms engaged in symbiotic and mutualistic relationships with the root (Lambers *et al*., 2009; McNear, 2013). In a similar fashion to the formation of neutrophil extracellular traps (NETs) in animals, border cells in plants are also involved in interactions with various plant pathogens: it has been suggested that the root slime works by “trapping” pathogens, forming aggregates that hinder their growth, to safeguard the root tip meristem, a critical component for root development and overall plant survival, which lacks specific resistance to biotic or abiotic stresses (Whipps, 2001; Raaijmakers *et al*., 2009). Interestingly, the extracellular trapping phenomenon is host-microbe specific, with no aggregation or growth inhibition of non-pathogenic organisms (Jaroszuk-Ściseł *et al*., 2009). All the constituents of the RETs play an important role in the host defence against pathogens (Wen *et al*., 2007a,b; Hawes *et al*., 2011). For example, the degradation of eDNA has been found to compromise the resistance of root tips to infection: when DNase 1, an enzyme that breaks down DNA, is introduced at the time of pathogen inoculation, it leads to necrosis in 100% of the root tips within 48-72 hours (Hawes *et al*.,

2011). Furthermore, studies involving the plant pathogen *Ralstonia solanacearum* have demonstrated that inactivation of extracellular DNases in the pathogen reduces its virulence, suggesting that the ability of the pathogen to dissolve the structural organization of the extracellular trap is related to its infection strategy, as it diminishes the trap's protective function (Tran *et al*., 2016; Wen *et al*., 2017). Indeed, similar to NETs, both histones H4 and eDNA found in RETs have been proposed to possess antimicrobial activity, with the former having the potential to bind and disrupt microbial cell membranes, and the DNA possibly playing a structural role, acting as a scaffold for the adhesion of antimicrobial components and as a trap for pathogens, preventing their spread throughout the organism (Tran *et al*., 2016; Driouich *et al*., 2019). Furthermore, the DNA in RETs is also known to exhibit direct bactericidal properties (Halverson *et al*., 2015). Finally, evidence suggest that eDNA may play a relevant role in the innate immunity response to pathogen invasion, being released into the extracellular environment along with other molecules such as callose, reactive oxygen species (ROS), and cell wall extensins, triggered by pathogen molecules (Plancot *et al*., 2013).

Despite the fact that eDNA function and mechanisms in RETs remain to be further elucidated, its release by viable border cells suggests an active role in plant root defence against pathogens in the rhizosphere and maintaining the protective function of the extracellular trap, which serves as a physical barrier against potential environmental threats. Further investigations will enhance our understanding of the intricate interplay between eDNA, pathogens, and the immune response in plants.

1.1.2. DNA as a Damage-Associated Molecular Pattern (DAMP)

Damage-associated molecular patterns (DAMPs) are endogenous signals generated in wounded or infected tissue under insect or pathogen attacks (Duran-Flores & Heil, 2016; Gust *et al*., 2017; DeFalco & Zipfel, 2021). They are defined as molecules that, if present in the inappropriate compartment, are recognized as a self-damage and can initiate and perpetuate a non-infectious inflammatory response (Seong & Matzinger, 2004; Roh & Sohn, 2018). Indeed, after being released from damaged or dying cells, DAMPs may activate the innate immune system, an induction of immunity in damaged organisms that is independent of exogenous molecules such as microbe- or pathogen-associated molecular patterns (MAMPs or PAMPs) (Heil, 2009; Heil & Land, 2014).

In mammals, well-studied DAMPs include, for example, high-mobility group box proteins (HMGBs), extracellular ATP, or extracellular and cytosolic (i.e. extranuclear) DNA fragments

(Garg *et al*., 2015; Vénéreau *et al*., 2015). Whereas eDNA molecules of nuclear and mitochondrial origin are considered DAMPs (Toussaint *et al*., 2017), bacterial and viral DNA molecules are considered Microbe-Associated Molecular Patterns (MAMPs) or Pathogen-Associated Molecular Patterns (PAMPs) (Altfeld & Gale, 2015; Dempsey & Bowie, 2015; Jounai *et al*., 2013; Kaczmarek *et al*., 2013; Tang *et al*., 2012; Wang *et al*., 2016; Wu & Chen, 2014). In animals, DNA of nuclear or mitochondrial origin is frequently reported to be involved in various types of diseases, e.g. cancers (Hawes *et al*., 2015), hypertension (McCarthy *et al*., 2015), Parkinson and Alzheimer (Lowes *et al*., 2020), autoimmune diseases such as rheumatoid arthritis (Rykova *et al*., 2017) and systemic lupus erythematosus (Barrat *et al*., 2005). Mammalian cells sense DAMPs as well as MAMPs via a range of receptor-dependent and -independent pathways that involve, among others, Toll-like receptor 9 (TLR9), DNA-dependent activator of interferon regulatory factors (DAI), inflammasome-forming receptors absent in melanoma 2 (AIM2), and receptor for advanced glycation end products (RAGE) (Hemmi *et al*., 2000; Takaoka *et al.*, 2007; Fernandes-Alnemri *et al*., 2009; Sirois *et al*., 2013). In fact, mammalian immune cells sense eDNA independently of whether it has been released from dying host cells or produced, e.g., by retroviral reverse transcriptase (Altfeld & Gale, 2015; Gallucci & Maffei, 2017). The activation of these sensors triggers immunity-related responses like mitogen-activated protein kinase (MAPK) signalling, the formation of reactive oxygen species (ROS), the synthesis of interferons (IFNs) and multiple other signalling processes that lead to inflammation, the maturation of dendritic cells to antigen-presenting cells and, ultimately, to active innate and adaptive immune response (Land, 2015).

Plants have evolved sophisticated strategies to perceive exogenous and endogenous danger signals (Ronald & Beutler, 2010; DeFalco & Zipfel, 2021). Examples of molecules that serve as DAMPs include cell wall fragments, cutin monomers, oligogalacturonides, oligosaccharides, adenosine 5′-triphosphate, methanol, ethanol, and systemin (Akira *et al*., 2006; Gust *et al*., 2017). Plants perceive most of these molecules via cell surface proteins called pattern recognition receptors (PPRs) (Roh & Sohn, 2018). The recognition induces early immunity responses, including calcium fluxes across the plasma membrane, the production of reactive oxygen species (ROS), and the activation of mitogen-activated protein kinases, thus leading to rapid defence gene expression (Seybold *et al*., 2014; DeFalco & Zipfel, 2021) (Figure 1.2).

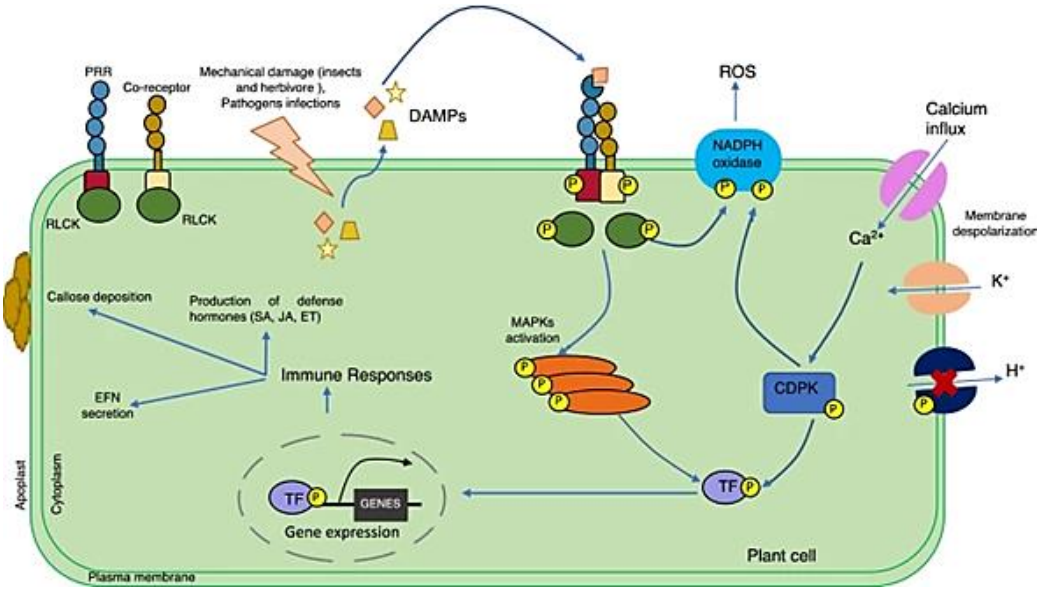

Figure 1.2. Perception and common responses triggered by DAMPs in plants. DAMPs recognition by pattern recognition receptors (PRRs) initiates the downstream signal transduction. These signals are passed via phosphorylation of mitogen-activated protein kinases (MAPKs) and calcium-dependent protein kinases (CDPKs). Some early immune responses triggered by DAMPs are reactive oxygen species production (ROS), calcium signaling, membrane potential depolarization (Ca2+ and K+ influxes), phosphorylation of plasma membrane (PM)-resident H + -ATPases and transcriptional factors (TFs); which leads to the integration of a robust defence response. These defence responses include callose deposition, extrafloral nectar (EFN) secretion, and production of hormones as salicylic acid (SA), ethylene (ET) and jasmonic acid (JA) (source: Ferrusquía-Jiménez *et al*., 2021).

In plants, self-DNA (i.e. endogenous or conspecific DNA) in the extracellular environment has often been discussed for its possible role as DAMP (Barbero *et al*., 2016; Duran-Flores & Heil, 2018; Vega-Muñoz *et al*., 2018). First, delocalized self nucleic acids — such as extranuclear DNA or extracellular RNA — like previously mentioned, are well-known DAMPs in mammals, “because they are reliable indicators of cellular damage” (Desmet & Ishii, 2012). Second, eDNA has been suggested to act in plant immunity (Duran-Flores & Heil, 2015, Gallucci & Maffei, 2017, Gust *et al*., 2017, Hawes *et al*., 2011) because it was reported as an indicator of bacterial infection in *Arabidopsis thaliana* (Yakushiji *et al*., 2009), as an inducer of immunity to fungal infections in pea roots (*Pisum sativum*) (Wen *et al*., 2009) and, most recently, as a trigger of Ca^{2+} signalling and membrane depolarization in lima bean (*Phaseolus lunatus*) and maize (*Zea mays*) (Barbero *et al*., 2016). Moreover, extracellular self-DNA (esDNA) can trigger the generation of ROS, calcium influx, induce defence gene expressions, and enhance resistance in plants against pathogens (Barbero *et al*., 2016; Duran-Flores & Heil, 2018; Vega-Muñoz *et al*., 2018; Ferrusquia-Jimenéz *et al*., 2022). Third, the effects of eDNA can depend on the taxonomic distance between the source and the receiver, again

suggesting its role as DAMP (Duran-Flores & Heil, 2018; Vega-Muñoz *et al*., 2018). Finally, the esDNA mainly functions through the JA signaling pathway, a phytohormone that is critical for damage responses triggered by herbivore and pathogen attack; also, wounding and esDNA induce similar changes in the transcriptome profile (Zhou *et al*., 2023). Regarding the perspective of extracellular self-DNA (esDNA) as a damage-associated molecular pattern (DAMP), it is plausible that esDNA could contribute to the taxonomic specificity observed in the recognition of damaged-self in plants (Duran-Flores & Heil, 2015).

Although esDNA is a promising candidate of plant DAMPs, the underlying mechanisms through which the esDNA functions are largely unknown. For example, it is a challenge to unravel the molecular mechanism through which the esDNA in the environment can be detected and perceived by plant cells.

1.1.3. Self-DNA as a driver for species-specific plant–soil negative feedbacks

Plant–soil negative feedback (PSNF) occurs when plants alter soil properties, negatively affecting the performance of other plants, with relevant effects in shaping natural plant communities (Van der Putten *et al*., 2013) (Figure 1.3). In particular, species-specific or direct NF refers to the diminished vigour of conspecific seedlings (Bennett & Klironomos, 2019; Van der Putten *et al*., 2013). The majority of conspecific plant–soil feedback effects reported are negative, consistently with soil feedbacks contributing to plant species coexistence and maintenance of biodiversity (Bever *et al*., 1997; Bever, 2003; Kulmatiski *et al*., 2008).

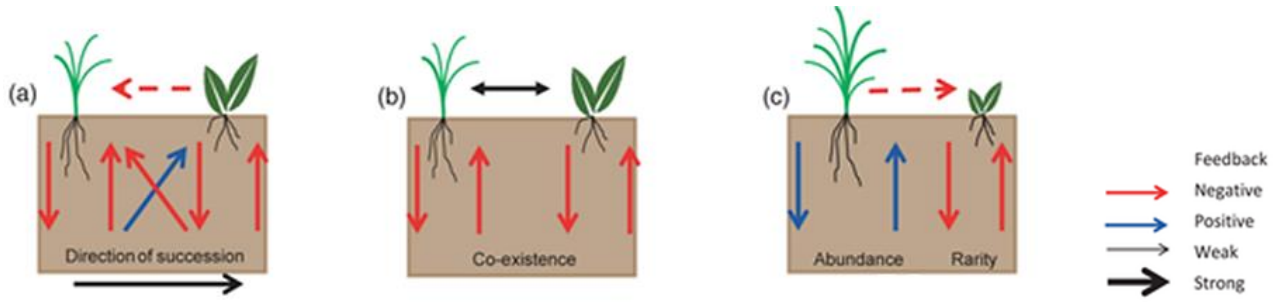

Figure 1.3. Emergent properties of plant communities subject to plant-soil feedback mechanisms with different direction (positive vs. negative) and species-specificity. a) Directionality of ecological succession, b) coexistence of different species c) abundance or rarity of a species (source: Van der Putten *et al*., 2013).

This natural phenomenon has been linked to several non-mutually exclusive hypotheses of the possible underlying mechanisms, among which: soil nutrient and resource depletion (Ehrenfeld *et al*., 2005), accumulation of natural enemies, e.g. soilborne pathogen

populations (Packer & Clay, 2000; Kardol *et al*., 2007) or excretion of autotoxic compounds, such as the release of phytotoxins during litter and organic matter decomposition (An *et al*., 2001; Trifonova *et al*., 2008). However, the hypothesis of litter autotoxicity has been widely criticized since such toxins are known to be rapidly degraded by soil microbial activity (Hodge, 2004; Bonanomi *et al*., 2011) and hundreds of organic compounds, extracted, purified and identified from plant tissues only showed a general toxicity without species-specific effects (e.g. Rice, 1984; Rizvi & Rizvi, 1992; Reigosa *et al*., 2006). Nonetheless, the hypothesis of a chemical origin of NF was not dismissed and while the observation that plant–soil NF occurs mainly in terrestrial systems and rarely in aquatic environments (Mazzoleni *et al*., 2007) suggested that the inhibiting factor causing NF could be a water-soluble compound, in 2015 a research group from Naples confirmed that this inhibiting factor was indeed DNA (Mazzoleni *et al*., 2015a). They studied the litter inhibitory effect in different bioassays carried out both *in vitro* and in greenhouse and noticed that undecomposed litter caused nonspecific inhibition of root growth, while autotoxicity was produced by aged litter. The addition of activated carbon (AC) removed the phytotoxicity related to known labile allelopathic compounds but was ineffective against autotoxicity. Spectroscopy methods highlighted that nucleic acids were the only ones negatively correlated with root growth on conspecific substrates and DNA accumulation was observed in both litter decomposition and soil history experiments. Finally, extracted total DNA showed evident species-specific toxicity. This work demonstrated that fragmented eDNA accumulating in aged litter during the decomposition process has a concentration dependent inhibitory effect on conspecifics, reducing root growth and seed germination, acting as a driver of species-specific PSNF.

In this context, the release, degradation and persistence of DNA in soil holds great importance. The decomposition of plant tissues by microbial enzymes facilitates the release of undegraded eDNA into the rhizosphere, which is accessible to decomposing microorganisms (Ceccherini *et al*., 2003). In general, eDNA release during plant residue decomposition is poorly characterized quantitatively. In temperate climates and agricultural systems, the entry of crop residue DNA into soil is believed to follow seasonal oscillations following patterns of plant growth and senescence, while in tropical systems the entry of DNA in soil may be continuous (Levy-Booth *et al*., 2007). Degradation of DNA in soil follows different phases: once free in the interstitial water the DNA is restricted and digested by extracellular DNases of microbial origin (Demaneche *et al*., 2001), which are ubiquitous in the soil environment, and provide oligonucleotides and nutrients then used in metabolism by microorganisms and plants (Levy-Booth *et al*., 2007). eDNA is able to persist in soil because

of its chemical stability and its protection against enzymatic degradation by absorption and binding onto soil minerals and organic matter components (Levy-Booth *et al*., 2007). Nonetheless, its persistence is influenced by a number of factors such as its composition, methylation or conformation and the prevailing environmental conditions (Nagler *et al*., 2018). Rapid desiccation, low temperatures, high salt concentrations, low pH and a high content of expandable clay minerals have all been found to slow down eDNA accumulation (Crecchio *et al*., 2005; Pietramellara *et al*., 2009), while flushing water can easily remove DNA from soil (Mazzoleni *et al*., 2015a; Cartenì *et al*., 2016). Consistently, in general, monospecific stands occur both in salt and freshwater condition irrespectively of the latitudinal level (e.g. floating plants, perennial species in wetlands and marshes, gallery and mangrove forests, seagrass, seaweed and kelp forests), while monospecific stands in terrestrial ecosystems can only be found when the accumulation of DNA in the soil is reduced either by slow decomposition (e.g., boreal forests) or by its degradation due to acidic soil conditions and/or burning (e.g. conifers and eucalypts forests). Similarly, monospecific crops typically show reduced establishment and yield after several cultivation cycles, which can be recovered only by traditional agricultural practices such as either crop rotation or burning and flooding, likely to remove accumulated DNA (Cartenì *et al*., 2016).

1.2. The phenomenon of self-DNA inhibition in plants

As mentioned in the previous chapters, Mazzoleni *et al*. (2015a) reported evidence that fragmented eDNA accumulating in litter during the decomposition process produces a concentration-dependent, species-specific inhibitory effect reducing root growth and seed germination of conspecifics, providing an explanation for negative plant–soil feedbacks (Mazzoleni *et al.,* 2015a,b; Bonanomi *et al*., 2022). Moreover, there now is experimental evidence supporting esDNA as a DAMP that can cause the species specificity in plant damaged-self recognition*,* triggering immunity induction and enhancing resistance to pathogens (Barbero *et al*., 2016; Duran-Flores & Heil, 2018; Vega-Muñoz *et al*., 2018; Ferrusquia-Jimenéz *et al*., 2022). The phenomenological evidence on self-DNA inhibition has been now repeatedly verified, also in organisms from different kingdoms and environments, including bacteria, fungi, algae, protozoa and insects, suggesting a more general biological process (Mazzoleni *et al*., 2015b; Palomba *et al*., 2022). In plants, it has been consistently observed after an exposure time ranging between 3 days and 4 weeks (Mazzoleni *et al*., 2015a; Duran-Flores & Heil, 2018), correlated to a fragmented (either by natural or artificial

decomposition) esDNA in the growing substrate, mostly present in fragment size between 50 and 2000 bp, and its concentration level (Mazzoleni *et al*., 2015a; Cartenì *et al*., 2016). Minimum self-DNA concentration to observe root growth inhibition depends on the specific sensitivity of the target species: for example, in *Arabiopsis thaliana*, the inhibition effect has been observed for concentration as low as 2 ng/µL after 7 days exposure (Mazzoleni *et al*., 2015a), while in common bean seedlings a significant inhibition of the growth of the primary root was observed at a concentration of 50 ng/µL after 4 days exposure (Duran-Flores & Heil, 2018). On the other hand, toxic effects, like root apex necrosis, were found at high concentrations of self-DNA (e.g. 200 ng/µL), inducing death of both seeds and seedlings (Mazzoleni *et al*., 2015a). Nonself-DNA treatments showed a magnitude of the effect proportionate to the phylogenetic distance between the DNA source and the receiver species (Mazzoleni *et al*., 2015a,b; Duran-Flores & Heil, 2018; Vega-Muñoz *et al.* 2018). Indeed, the inhibitory effect of eDNA on the growth of organisms in different phyla (Mazzoleni *et al*., 2015a,b; Mazzoleni *et al*., 2014) showed taxonomic specificity: eDNA of *Lepidium sativum* inhibited the root growth of *Arabidopsis* in a dosage-dependent manner (sharing the same taxonomic family), but 'self eDNA' prepared from *Arabidopsis* had a much stronger effect (Mazzoleni *et al*., 2015a).

In 2018, Vega-Muñoz et al. (2018) suggested that the response to self- and non-self-DNA could depend on the degree of self damage detected by the plant, confirming that, in line with previous findings (Mazzoleni *et al*., 2015a,b; Barbero *et al*., 2016; Duran-Flores & Heil, 2018), this could depend on the concentration of either self-DNA or non-self-DNA and on the phylogenetically distance of non-self-DNA. It is tempting to speculate that there is a sequence-specific recognition of small-sized eDNA mechanism in plants (Mazzoleni *et al*. 2015a), since the toxic effect was also evident, although to a lower extent, when exposing plants to decomposing litters of phylogenetically similar plants. Despite the previous evidence, the mechanisms behind the sensing and differential response of plants to self- and nonself-DNA remain still unclear. Clearly, the existence and identification of esDNA receptors in plants need to be a priority research subject, since it can help answer another critical question, that is, how the species-specific effect of esDNA is achieved. However, these studies paved the way to further investigations on possible novel roles of eDNA in ecology, plant physiology, and in translational research, introducing, under an applicational point of view, the possibility to use self-DNA inhibitory effect in agriculture for pest and weed control (Ferrusquía-Jiménez *et al*., 2021), as well as for the development of novel pharmaceuticals (Mazzoleni *et al*., 2014). For example, esDNA could be used for biotechnological approaches

in agriculture with two main ways of action (Figure 1.4): the first one by generating a specie-specific inhibitory effect on the organism from which it comes using significant high esDNA doses, and the second one by inducing positive immune responses that lead to stress tolerance by applicating low esDNA doses (Vega-Muñoz *et al*. 2018; Duran-Flores & Heil, 2018; Mazzoleni *et al*., 2014; Quintana-Rodriguez *et al*., 2018).

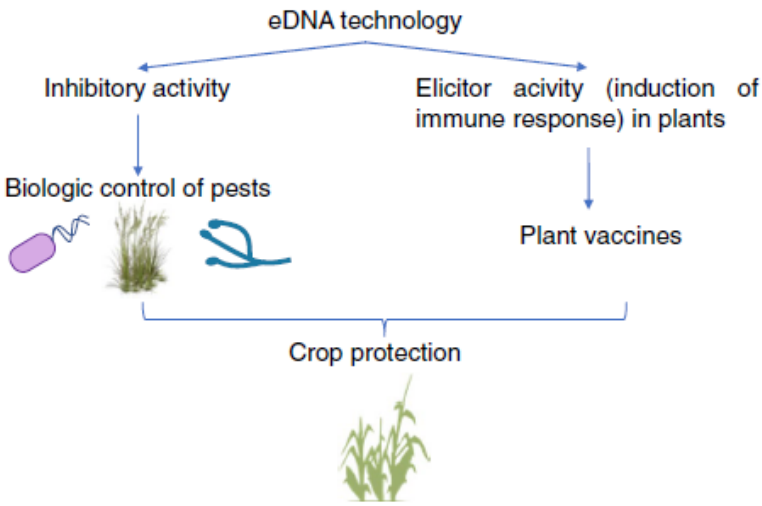

Figure 1.4. Dual eDNA activity and its biotechnological potential. Based on the action of eDNA as DAMP, this technology could be used for the development of biologic control products and as plant vaccines. Using the technology for pest control the application of esDNA in doses ≥ 200 µg/mL is proposed, where the source of eDNA can be any type of soil pathogen or pest organism (bacteria, weeds, fungi). For immunity induction, as "plant vaccine" approach, doses < 200 µg/mL could be used in developed plants (for example, 4-week-old plants); DNA must be obtained from plants of agronomic interest (source: Ferrusquía-Jiménez *et al*., 2021).

1.3. Mechanisms underlying self-DNA inhibition

The reported phenomenological observations raised basic questions on eDNA sensing and esDNA inhibition underlying cellular and molecular mechanisms. Unfortunately, at present, little is known about specific DNA receptors in plants (Monticolo *et al*., 2020), while growth inhibition mechanism by esDNA is still unclear, although explored by some recent papers (Duran-Flores & Heil, 2018; Vega-Muñoz *et al*., 2018; Heil & Vega-Muñoz, 2019; Barbero *et al*., 2016; Lanzotti *et al*., 2022; Chiusano *et al*., 2021; Zhou *et al*., 2023).

Even if the molecular processes of eDNA recognition in plants remain uncertain, several authors have proposed various mechanisms to shed light on this phenomenon. The first of these is the classic process of recognition by means of membrane receptors capable of

recognizing fragments of eDNA and activating a signaling cascade inside the cell. Another mechanism is the use of transport channels that can bind fragments of eDNA and translocate them to the cytoplasm. Internalization by vesicles containing eDNA residues has also been proposed, where such fragments could be recognized by intracellular sensors (Bhat & Ryu, 2016). As an alternative hypothesis, Mazzoleni *et al*., (2015a) and later Cartenì *et al*., (2016) suggested a different explanation based on a more direct effect, i.e., the possible "interference" of extracellular self- or "similar" DNA (e.g.: homologous, i.e., from phylogenetically related species or even similar, i.e., with convergent structure similarity, although not phylogenetically related) causing inhibition of the whole cell functionality, mediated by sequence-specific recognition of small-sized nucleotide molecules (Gruenert *et al*., 2003), which could hamper cell and gene expression functionality (Nisa *et al*., 2019), or affect genome stability (Kim, 2021), inhibiting the growth. A recent study indicates that possibly eDNA signaling is linked to the methylation processes that DNA naturally suffers. In lettuce, DNA acts as DAMP and induces changes in DNA methylation and defence-related responses (Vega-Muñoz *et al*., 2018), when applied at different doses.

To date, this phenomenon is of crucial interest due to its possible applicational prospective and further studies are required to provide additional insights and clarity regarding the mechanisms underlying the self-DNA recognition and processing, including the signaling pathways and genetic adaptations involved in the inhibitory effect.

1.3.1. Cell self-DNA sensing and discrimination from nonself-DNA

In mammals, eDNA has been demonstrated to be sensed by receptors located in various cellular compartments, such as the nucleus (Brázda *et al*., 2012; Wang *et al*., 2019), the cytoplasm (Hornung *et al*., 2009; Herzner *et al*., 2015; Szczesny *et al*., 2018), and the endosomes (Hemmi *et al*., 2000). eDNA can be sensed by specific transmembrane Toll-like receptors (TLRs) or, alternatively, is taken up by phagocytosis and then released and sensed inside the cell, in both cases triggering proinflammatory responses (Heil & Land, 2014). It is known that cells developed several defence mechanisms to protect from heterologous (foreign) eDNA, like degradation or excretion, excision and loss of previously integrated DNA from the host genome, targeted inactivation of foreign molecules by specific modifications like methylation (Doerfler, 1991).The distinction between self and nonself-DNA is a relevant aspect and while there is some evidence of bacterial and viral genome recognition as nonself thanks to, respectively, the detection of poor CpG methylation patterns in the endosomal compartment through the TLR9 receptor (Barton *et al*., 2006), or DNA with unpaired open

ends containing guanosines in the cytoplasm (Herzner *et al*., 2015), there are no reports on the capability of these receptors to distinguish self- from nonself-DNA within the same kingdom (Duran-Flores & Heil, 2015).

It is suggested that the exposure to both self- and nonself-DNA induces an immunological response in plants (Duran-Flores & Heil, 2015; Heil & Vega-Muñoz, 2019) and that the recognition of eDNA could involve a membrane-bound eDNA receptor that, upon recognition, triggers a downstream signaling cascade, or a membrane-bound eDNA transporter or channel, and/or a vesicle-mediated internalization that, after the eDNA internalization, could favour the detection via an intracellular sensor (Bhat & Ryu, 2016). Nonetheless, in plants, TLRs have not been described (Couto & Zipfel, 2016) and there is no indication of specific DNA receptor (Monticolo *et al*., 2020). PAMPs and DAMPs are mainly recognised via pattern-recognition receptors (PRRs), which are single transmembrane proteins belonging to the receptor-like kinase (RLK) and receptor-like protein (RLP) super families and sense microbe- and host-derived molecular patterns to activate immune responses (Zhou & Zhang, 2020). The low degree of specificity makes it unlikely that these receptors allow for a species-specific recognition of eDNA able to explain self-DNA inhibition. Indeed, the suggested mechanisms for eDNA perception by a plant cell involving membrane-bound receptors or intracellular sensors able to recognize specific eDNA moieties (Bhat & Ryu, 2016) seem to be a non-parsimonious explanation for esDNA detection and discrimination, since it would imply a great number of specific receptors for all the possible sequences deriving from its natural or experimental fragmentation (Duran-Flores & Heil, 2015). On the other hand, it is possible to assume that a first sensing of exogenous self-DNA may occur at the level of the DNA based NET-like mantles located at the external membrane surface, since it was shown that treatments with DNases destroy the resistance to pathogen infection (Gunawardena *et al*., 2005; Wen *et al*., 2009).

The sensing of eDNA molecules has also been ascribed to mechanisms similar to the “well-known processes of interference, based on sequence-specific recognition of small-sized nucleotide molecules” (Mazzoleni *et al*., 2015a), that could justify the specific inhibitory roles of extracellular self-DNA. In animals, nuclear-encoded RNAs stably attached to the cell surface and exposed to the extracellular space have been recently discovered, mostly associated with monocytes, suggesting an expanded role for RNA in cell-cell and cell-environment interactions (Huang *et al*., 2020). Rather than specific receptors, nuclear encoded RNAs displayed on the cell surface could represent an interesting way for cells to discriminate between self- and nonself-DNA through complementary sequence recognition.

Alternatively, the perception of fragmented free esDNA might involve its entrance into living cells through membrane-bound channels or vesicular translocation and the potential disruption of mRNA translation with the consequent trigger of plant immune response (Cartenì *et al*., 2016). This could happen through the direct interaction with the genome structure based on mechanisms like the Small Fragment Homologous Replacement (Gruenert, 2003): once within the cell, Small DNA Fragments (SDFs) trigger the exchange between their sequences and the genomic DNA (Leclerc, 2009) likely by a mechanism in which the fragment recognizes and anneals to its homologous target, promoting the formation of a D-loop, a triple-stranded DNA structure where the two strands of a double-stranded DNA molecule are separated for a stretch and held apart by a third strand of DNA. This hybrid structure could activate the endogenous machinery involved in DNA repair and, by homologous recombination, allow the SDF to be integrated into the genomic DNA (Gruenert, 1999). Upon esDNA entrance inside the cell, the disruption of mRNA translation could also occur following a pattern of action similar to RNA interference (Bhat & Ryu, 2016) based on sequence-specific recognition involving RNA/DNA interactions (Moazed, 2009).

These latter mechanisms could also explain more directly the species-specificity of the inhibitory effect, attributed to self-DNA or DNA from phylogenetically related species (Mazzoleni *et al*., 2015a), causing either complete interference or inhibition of the whole cell functionality and protein synthesis. Accordingly, cultured mammalian cells can absorb and integrate eDNA added to the culture medium (Groneberg *et al*., 1975) and confocal microscope analysis suggests that eDNA is taken up into root cells of living plants upon exposure, without artificial aid (Paungfoo-Lonhienne *et al*., 2010). However, in a recent paper esDNA of *Arabidopsis* is shown to remain outside the root cell while nonself-DNA enters the cells at the early stage of exposure (60 min), suggesting that plant cells are able to perceive esDNA at the cell surface (Chiusano *et al*., 2021). Despite this evidence, the molecular mechanisms at the base of esDNA sensing and discrimination from the nonself-DNA in plants are not yet clarified.

1.3.2. Molecular mechanisms of self-DNA inhibition

As previously highlighted, little is known about the cellular and molecular mechanisms underlying growth inhibition by esDNA, despite being explored by some recent papers (Duran-Flores & Heil, 2018; Vega-Muñoz *et al*., 2018; Heil & Vega-Muñoz, 2019; Barbero *et al*., 2016; Lanzotti *et al*., 2022; Chiusano *et al*., 2021; Zhou *et al*., 2023), mostly referring to the time window preceding the inhibition phenomenological observation. Indeed, Vega-

Munoz *et al*. (2018) is the only study carrying out biochemical and epigenetic tests after 5 days of exposure in *Lactuca sativa* plants. It highlighted that fragmented esDNA induces changes in CpG genomic DNA methylation levels, altered gene expression associated with oxidative burst (induced expression of superoxide dismutase, catalase and phenylalanine ammonia lyase in a concentration-dependent manner) and increases the production of secondary metabolites associated with defence responses to stress (phenylpropanoids). Except for Vega-Munoz *et al*. (2018), the studies addressing the inhibition mechanisms refer to an observation time spanning between 30 min and 16 h after exposure. In particular, Duran-Flores and Heil observed the activation of Mitogen-Activated-Protein-Kinases (MAPK) at 30 min and H_2O_2 production at 2 h post exposure to self-DNA at 200 ng/µL, and extra-floral nectar (EFN) production at 24 h post self-DNA treatment at 50 ng/µL in Lima bean (*Phaseolus lunatus*), suggesting that self-DNA acts as a damage-associated molecular pattern (DAMP) inducing early immunity-related signaling responses. Accordingly, a reduced rootlet growth would result as consequence of the energetic cost of the immunity response (Heil & Vega-Muñoz, 2019). Further previous evidence on Lima bean and maize includes an increase of cytosolic flux of Ca^{2+} after 30 min from leaves exposure to 50 µL of self-DNA at 200 ng/µL, associated with a concentration-dependent plasma transmembrane potential (Vm) depolarization at 2 h, already observed at concentrations as low as 2–20 ng/µL (Barbero *et al*., 2016). This was later confirmed by the same authors on tomato (*Solanum lycopersicum*) leaves, also coupled to the opening of K^+ channels at 50 min and followed by ROS production after 180 min (Barbero *et al*., 2021). Moreover, 1 h exposure to self-DNA at 200 ng/µL elicited an alteration of the transcriptomic profile involving several genes related to Ca^{2+} signaling, ROS scavenging and ion homeostasis (Barbero *et al*., 2021). A very recent metabolomic profiling during self-DNA exposure at 200 ng/µL between 1 and 15 h in *Arabidopsis thaliana* plantlets (Lanzotti *et al*., 2022), highlighted a striking, progressive accumulation of nucleobases, ribonucleosides, dinucleotide and trinucleotide oligomers, in particular cyclic AMP and GMP, and N6 methylated adenosine. Such finding was interpreted as an indication of RNA degradation and lack of disposal or recycling with consequent metabolic impairment, based on previous findings of a dramatic reduction of gene expression along the same time frame, observed on the same model plant by Chiusano *et al*. (2021). However, this latter study, a whole-plant transcriptomic profiling, had highlighted a remarkable pattern of differential gene expression and fragment localization across treatments (self-DNA vs. nonself-DNA at high concentration, 200 ng/µL) and timing (1, 8 and 16 h), suggesting that cells are capable of specifically sensing and processing self-DNA and

discriminating it from nonself-DNA. In particular, exposure to extracellular, fragmented self-(conspecific) DNA seems to elicit a significant differential expression of several pools of genes, among which, noteworthy, were those responsive to abiotic stress under self-DNA exposure, while nonself-treatment seems to be related to the upregulation of genes responsive to biotic stress. This was mostly evident after 1 h exposure and then was apparently released after 8 h. Finally, a very recent research (Zhou *et al*., 2023) confirmed that esDNA inhibits root growth (tested after 3-4 days from treatment) and triggers reactive oxygen species (ROS) early production (60 min after treatment) in plant leaves in a concentration- and species-specific manner in Arabidopsis (*Arabidopsis thaliana*) and tomato (*Solanum lycopersicum* L.). Furthermore, by combining RNA sequencing, hormone measurement and genetic analysis, they found that esDNA-mediated growth inhibition and ROS production are achieved through the jasmonic acid (JA) signaling pathway. Specifically, RNA-seq data (60 min after treatment at 200 ng/µL) revealed a total of 3343 genes differentially expressed between the esDNA and nonself-eDNA treatments. Gene Ontology (GO) analysis indicated that esDNA-regulated genes were mainly enriched in pathways related to responses to ROS, chitin, JA (including those involved in JA biosynthesis, signal transduction and response), wounding, and oxidative stress. This analysis is consistent with the observation that esDNA can induce ROS production. Accordingly, esDNA induces JA production at 60 min. post treatment and the RT-qPCR analysis confirmed the expression of JA responsive genes and ROS production within 2 h, inducing plant immunity and providing insight into how esDNA functions as a DAMP. Very interestingly, a new paper (Vega-Muñoz *et al*., 2023) tests and elucidates current knowledge on self- and nonself-DNA recognition and mechanism of action in *Arabidopsis*, giving valuable insights on the highly self/nonself-DNA-specific differential induction of immune response, ROS production and the defence hormones, jasmonic acid (JA, the hormone controlling the wound response to chewing herbivores) and salicylic acid (SA, the hormone controlling systemic acquired resistance, SAR, to biotrophic pathogens). It has been observed that the application of plant or algal extracts, which arguably contain DAMPs, enhanced the resistance, trigger early immune responses, against herbivory in tomato, maize, cabbage and other major crops (Quintana-Rodriguez *et al*., 2018). Strikingly, stronger responses to self- in comparison to nonself-DNA were reported in most of the studies that compared DNA from different sources (Table 1.1). Differential responses to self- versus nonself-DNA are significant even when nonself-DNA from closely related genotypes (species of the same genus or ecotypes of the same species) is used (Duran-Flores & Heil, 2018; Rassizadeh *et al*., 2021; Palomba *et al*., 2022; Zhou *et*

al., 2023; Duran-Flores & Heil, 2023; Germoglio *et al*., 2022). In particular, Vega-Muñoz *et al*., (2023) suggest a hypothetical model with differential sensing of self- versus nonself-DNA fragments, respectively as damage- (abiotic stress) versus pathogen-associated (biotic stress) molecular patterns (DAMPs/PAMPs), with self-DNA triggering stronger responses by early immune signals such as JA-dependent wound response and H_2O_2 formation than nonself-DNA from closely related plant species.

Table 1.1. List of experimental activity on plant response to DNA exposure. For each experiment, the target species, the DNA source species for self- and non-self-DNA, and a synthesis of results and conclusion are showed. A, Original references can be found in the source paper (Vega-Muñoz *et al*., 2023).

Model	Self-DNA	Nonself-DNA	Response	Result	Conclusion
A. thaliana Col-0	No	Plasmid and genomic bacterial DNA	H_2O_2 formation, callose deposition and inhibition of seedling growth	Enzymatically digested plasmid or bacterial genomic DNA was active, but intact DNA was inactive. Enzymatic methylation of 5'-CG-3' or cleavage of 5'-CCGG-3'reduced the immunogenic activity	Bacterial linear DNA containing unmethylated CpG motifs has immunogenic properties in plants.
Several plant species	Yes	Mixture of several plant species	Root and seedling growth inhibition	Self-DNA inhibited root growth in a concentration-dependent manner while the mixture of nonself-DNA did not.	Extracellular DNA has species-specific inhibitory effects on plants.
A. thaliana Col-0	No	*Pst* DC3000	Disease severity	Bacterial DNA did not trigger a significant reduction of disease severity	Bacterial RNA, but not DNA, triggers a plant immune response
Lima bean (*P. lunatus*) and maize (*Z. mays*)	Yes	*Spodoptera littoralis* larvae, maize for *P. lunatus*, lima bean for *Z. mays*	Plasma membrane potential depolarization and CA^{2+} fluxes	Perfusion with fragmented self-DNA triggered depolarization and CA^{2+}-influxes, no detectable response to nonself-DNA or non-sonicated self-DNA	Fragmentation and the self-origin of DNA are crucial to activate early immune signals.
Common bean (*P. vulgaris*)	Yes	*P. lunatus* and *Acacia farnesiana*	Seedling growth, H_2O_2 formation, MAPK activation, extrafloral nectar (EFN) secretion, resistance to *P. syringae* pv. *syringae*	Self-DNA triggered a dosage-dependent inhibition of seedling growth and induced H_2O_2, MAPKs and resistance to *P. syringae* more strongly than nonself-DNA, and only self-DNA induced EFN secretion	The phylogenetic distance affects the immune response to DNA, in particular in case of the JA-dependent EFN-secretion
Lettuce (*Lactuca sativa*)	Yes	*Capsicum chinense* and *Acaciella angustissima*	Seedling growth, expression of SOD, CAT and PAL and global level of CpG DNA methylation	Self-DNA and nonself-DNA from *C. chinense* triggered a dosage-dependent inhibition of seedling growth, induced CAT and SOD expression and reduced CpG DNA methylation, while all three types of DNA induced PAL expression	The phylogenetic distance affects the immune response to DNA, but even nonself-DNA from a distant species induces PAL, a SA-synthetic enzyme
A. thaliana Col-0, including mutants mpk3 and npr1-3	No	ssODNs IMT 504 and 2006	Resistance to *B. cinerea* and *Pst* DC3000, stomatal closure, a H_2O_2 -dependent response	Both ssODNs induced resistance to *B. cinerea* and *Pst* DC3000 with no detectable difference, and they triggered stomatal closure in a mpk3- and npr1-3 dependent way	DNA triggers resistance to pathogens independently of the presence of CpG motifs but depending on MAPK signalling and NPR1, a central activator of PR-gene expression
A. thaliana	Yes	*Clupea harengus* (fish)	Transcriptomic response, microscopy for DNA uptake.	Nonself-DNA enters root cells and triggers differential expression of ca 6000 genes while self-DNA remains in the apoplast and affects the expression of ca 1500 genes	An as-yet unknown self/nonself-specific transport of DNA that generates differential ## that might contribute to the differential immune responses

517

Tomato (*S. lycopersicum*)	Yes	No	Membrane depolarization, CA^{2+} fluxes, H_2O_2 formation, and RNAseq of transcriptomic responses	Self-DNA triggered membrane depolarization, CA^{2+}-influxes, increased H_2O_2 levels and induced enhanced expression of genes related to plant defence and phytohormones, but reduced expression of shock proteins, heat shock factors, pumps and photosynthesis-related genes	The physiological and transcriptomic changes in response to self-DNA treatment are consistent with general patterns of induced plant resistance
A. thaliana Col-0	Yes	Various *A. thaliana* ecotypes and other plant species:	H_2O_2 formation. expression of MPK3, OXI1 and CML37, resistance to *B. cinerea*, *Hyaloperonospora arabidopsidis, Myzus persicae and Pst* DC3000,	Self-DNA induced H_2O_2, resistance to biological enemies and marker gene expression, nonself-DNA from other ecotypes had similar effects, while nonself-DNA from other species had lower or no effects on marker gene expression	The phylogenetic distance affects the immune response to DNA
Capsicum annuum	No	*Phytophthora capsici* *F. oxysporum*	Phenolics and total flavonoids contents, PAL, Mn-SOD and	Pathogen eDNA treatment reduce severity of disease and plant mortality, while also increasing levels of total phenols and flavonoids, and expression of PAL and CHS	Using pathogen eDNA as treatment induced the plant immune system, reducing mortality and disease severity.
		Rhizoctonia solani	CHS expression, disease resistance		
Musa acuminata	No	*F. oxysporum*	Disease resistance, ROS detection, PR1, chitinase 1, SOD, CAT gene expression	High concentrations of pathogen DNA increased plantlets' disease resistance. ROS accumulation (24 h) and defence-related genes were highly induced in plantlets after treatment (9 days)	eDNA exhibits antifungal activity combining an inhibition of fungal growth with a priming of the plant immune system.
Capsicum annuum	No	*Phytophtora capsici*	Resistance to *P. capsici*, increment in phenols and total flavonoids	Low concentrations of pathogen eDNA (2 μg ml^{-1}) induced resistance against the pathogen while higher concentrations (60 and 100 μg ml^{-1}), on the contrary, made the plant more susceptible	The dose versus quantity of inoculum may interfere with the plant-pathogen interaction.
Alnus glutinosa	Yes	*Festuca drymeja*	Root growth inhibition in open and closed systems	Self-DNA application affected the root health only in closed systems.	Self-DNA but not nonself-DNA, caused toxic effects on the roots in closed systems while in open systems the harmful effects of self-DNA were dramatically reduced.
Chlamydomonas reinhardtii *Nannochloropsis gaditana*	Yes	*Sardina pilchardus* (fish)	Culture cell density inhibition, Morphological changes.	Presence of self-DNA affects cell density and generation time in both freshwater and marine microalgae in a concentration-dependent manner as low concentrations (3 μg ml^{-1}) favored growth while higher concentrations (10 μg ml^{-1}) inhibited it.	Inhibitory effects are dosage-dependent.
A. thaliana	Yes	*Z. mays*, *Clupea harengus* (fish)	Metabolite profiling	Self-DNA treatment induced the four ribonucleosides and its corresponding bases along with AMP, GMP and N6-methyl-AMP.	Self-DNA treatment induces the accumulation of RNA building blocks.
S. lycopersicum	Yes	*F. oxysporum*	ROS formation, CAT, SOD and PAL activity and total phenolics and flavonoids content.	Self-DNA induced the phenylpropanoid pathway, nonself-DNA induced an intense response of the antioxidant system and lower ROS formation.	The intensity of the immune responses depends on the plant ontogenetic stage. Adult plants have a higher response threshold, thus the stimulus must be higher to obtain the same results for younger plants.
Peach fruits (*Prunus persica*)	Yes	No	Resistance to *Rhizopus stolonifera*, RNAseq of transcriptomic responses	Self-DNA treatments of peach fruits enhanced resistance to fungal infection *via* a pathway that depends on the co-receptor BAK1 and includes ethylene-dependent genes	Self-DNA can be used for postharvest biocontrol of fungal infections, resistance is linked to ethylene signalling

518

519

A. thaliana Col-0 and *S. lycopersicum*, incl. mutants affected in JA synthesis or signalling	Yes	Different ecotypes/ cultivars, different species from same genus/ family, species from different families	Root growth inhibition, ROS formation, gene expression, resistance to *B. cinerea*	Self-DNA triggered a dosage-dependent inhibition of root growth in seedlings, increased levels of H_2O_2, of a JA precursor, of JA-Ile and of the expression of JA-related genes. Lower/no growth inhibition in response to nonself-DNA from related/ distant species and in JA-signalling mutants treated with self-DNA.	Confirms that the dosage and the taxonomical distance affect the immune response to DNA and indicates that the JA-controlled wound response is involved in this response.
P. vulgaris	Yes	*P. lunatus* and *Acacia farnesiana, as well as self-DNA with enzymatically manipulated CpG methylation*	Induction of ROS, JA and SA, resistance to 1 herbivore, 4 fungi and 4 bacteria, seed production in the open field	Self/nonself-specific induction of JA and herbivore resistance and enhancement of seed yield but non-specific induction of SA and resistance to microbial pathogens by all three types of DNA tested. Self-DNA with enzymatically altered CpG methylation had lower but still significant ROS-inducing effects	The presence of unmethylated CpG motifs contributes to the immunogenic effects of DNA. DNA triggers a self/non-self-specific induction of the WR and a non-specific induction of SAR, leading to net effects that can be adaptive under natural enemy pressure.

In conclusion, present evidence highlights that self-DNA in soil might function as a signaling molecule for self-damage recognition (DAMP), just like ATP, small signalling peptides (AtPeps), or cell wall fragments released by mechanical damage, feeding by chewing herbivores and even infection by necrotrophic pathogens that cause the cell disruption, and activate the plant response (Bacete *et al*., 2017; Li *et al*., 2020; Heil & Land, 2014; Duran-Flores & Heil, 2016; Wang *et al*., 2018). This signalling cascade comprises membrane depolarization, Ca^{2+} fluxes, ROS production and MAPK activation and the subsequent induction of a JA dependent broad-spectrum immunity against chewing herbivores and necrotrophic pathogens (Vos *et al*., 2013). The JA-dependent immune response causes dosage-dependent metabolic costs which, at the phenotypic level, may become apparent as stunted growth or a transient growth arrest (Guo *et al*., 2018; Heil & Baldwin, 2002; Pearce *et al*., 2010). esDNA inhibition is dosage-dependent and depends on the phylogenetic scale, that is the taxonomic distance between the source and the receiver species (Duran-Flores & Heil, 2014; Mazzoleni *et al*., 2015a; Barbero *et al*., 2016). For example, eDNA from *A. thaliana* inhibited the growth of *Lepidium sativum* seedlings and vice versa, but DNA from *A. thaliana* did not inhibit *Acanthus mollis* growth (Mazzoleni *et al*., 2015a). Interestingly, *A. thaliana* and *Lepidium* belong to the same order (*Brassicaceae*), whereas the *Acanthaceae* belongs to a different order, the *Lamiales*. Similarly, DNA from *Capsicum chinense* inhibited *Lactuca sativa* (both *Asterales*), whereas DNA from *Acaciella angustissma* (*Fabales*) did not (Vega-Muñoz *et al*., 2018), and DNA from lima bean inhibited common bean growth whereas DNA from *Acacia farnesiana* did not (Duran-Flores & Heil, 2018).

eDNA from phylogenetically unrelated species was even reported to promote growth, being used as a phosphorous source (Paungfoo-Lonhienne *et al*., 2010). The application of esDNA can elicit the expression of defence genes and induce resistance against environmental stresses, like pathogens, herbivores, and intraspecific competition, in plants, such as *Arabidopsis* (*Arabidopsis thaliana*), chili pepper (*Capsicum annuum* L.), lettuce (*Lactuca sativa* L.), and common bean (*Phaseolus vulgaris* L.) (Duran-Flores & Heil 2018; Vega-Muñoz *et al*., 2018; Rassizadeh *et al*., 2021; Ferrusquia-Jimenéz *et al*., 2022). Even if the sensing mechanisms and way of action of self-DNA are not fully clarified, there are evidence that self-DNA treatment triggers an electric response, starting with a sensing at membrane level, with calcium spikes followed by a reduced permeability of the roots, and a cascade of events involving the chloroplasts and inducing ROS production, whereas nonself-DNA enters the cells where it is metabolized activating a cascade of events inducing a hypersensitive response (Chiusano *et al*., 2021). It has also been suggested that eDNA methylation patterns could explain the mechanism for self-DNA recognition in plants (Vega-Muñoz *et al*., 2018). Consistent with the results from Chiusano *et al*., (2021), reporting the upregulation of the response to biotic stress prevailing in the nonself treatments and , together with the triggering of the hypersensitive response in the later stages of this treatment, and the upregulation of the response to abiotic stress prevailing in the self treatments, nonself-DNA is reported to be sensed as a PAMP with specific immunogenic effect and self-DNA as DAMP (Vega-Muñoz *et al*., 2023).

1.4. Aims and Scope

In the first chapter of this thesis, we discussed the current knowledge on extracellular DNA main roles in the plant-environment interaction, with a particular focus on the newly added function in plant-soil negative feedbacks, where the accumulation of fragmented extracellular DNA causes the reduction of conspecific seed germination and plantlet growth in a concentration-dependent fashion. Despite the numerous evidence on this natural phenomenon, included in different kingdoms, the underlying mechanisms are not fully clarified and many questions remain open, paving the way to further studies that could address the role and the molecular mechanisms involved in esDNA sensing and growth inhibition of conspecifics. The desirable application of self-DNA inhibitory effect as pest and weed control in agriculture (Ferrusquía-Jiménez *et al*., 2021) requires further clarification and trials, especially in open fields, on the degree of species-specificity of the inhibition, in

particular in the case of species phylogenetically close (e.g. congeneric species). The molecular mechanisms involved in this phenomenon should as well be investigated for applicational purposes, including possible epigenetic changes related to transposon activation and mobilization, as previously suggested (Germoglio *et al*., 2022). Finally, it is of paramount importance to understand the process allowing plant cell sensing and discrimination between self- and nonself- DNA, considering that at present we are unaware of DNA receptors able to such degree of specificity in plants (Couto & Zipfel, 2016; Monticolo *et al*., 2020).

Therefore, during my first activity, we investigated the species-specificity of self-DNA inhibition (Figure 1.5) in cultivated vs. weed congeneric species (respectively, *Setaria italica* and *Setaria pumila*), under the hypothesis that the species-specificity of self-DNA inhibition still holds when tested on phylogenetically related species, even on weed plants that are expected to be more resistant to allelopathic effects. As previously mentioned, from an application perspective, evidence of species-specific self-DNA inhibition on the invasive weed *S. pumila* but not on the cultivated species *S. italica* could provide promising data for innovative weedicide treatments in agriculture.

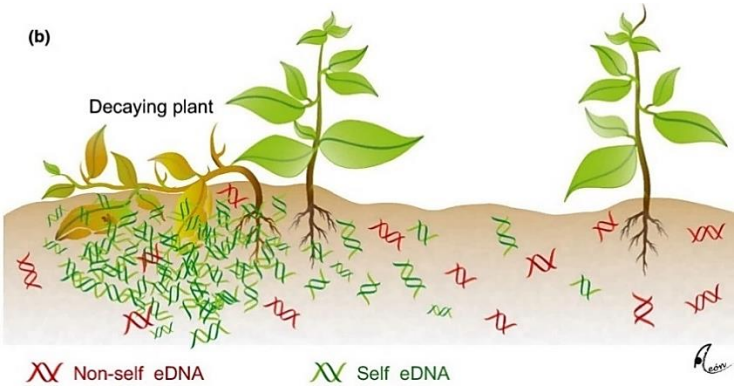

Figure 1.5. Representation of species-specific effect of self eDNA. High concentrations of esDNA can occur in the soil below, and around, a decaying plant, affecting nearby conspecifics. As the concentration of nonself-eDNA can be expected to be homogenous throughout the soil, plants of a certain species will be exposed to different concentrations and ratios of self- to nonself-DNA, depending on their distance from the decaying conspecific plant (adapted from Duran-Flores & Heil, 2015).

Secondly, we explored the early expression of genes responsive to abiotic stress in the two *Setaria* species over the time window spanning between 1 and 3 h since exposure to self-DNA, testing previously reported evidence by a whole transcriptome profiling (Chiusano *et*

al., 2021). Our intent was to contribute to the ongoing investigation on the molecular mechanisms underlying the observed phenomenon of self-DNA inhibition (Figure 1.6), with particular focus on the early response to exposure, at gene expression scale. In this respect, we hypothesized that early exposure to self-DNA elicits molecular pathways known as responsive to abiotic stressors. This study represents the first exploration of early response to self-DNA inhibition at molecular level in C4 model plants.

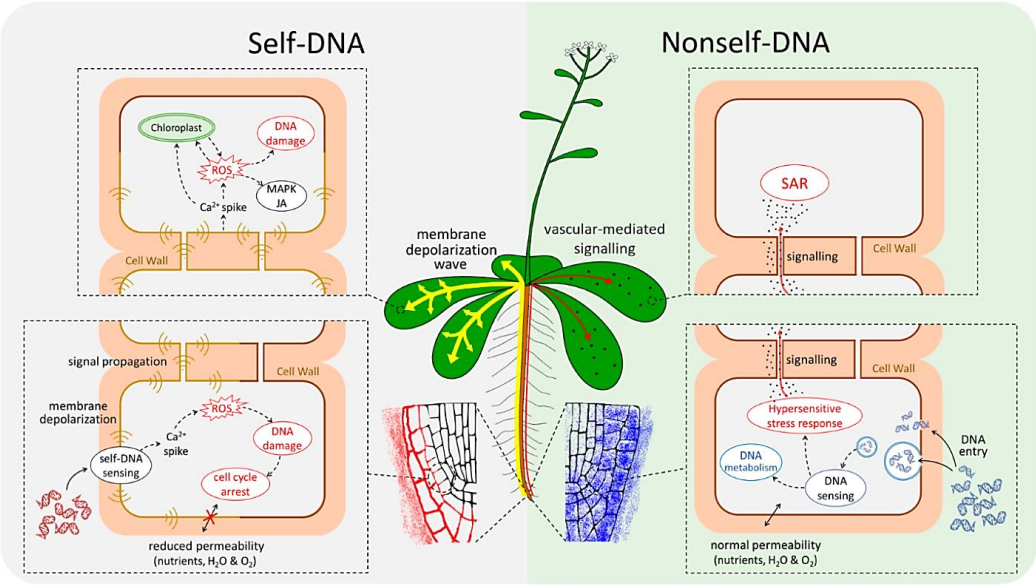

Figure 1.6. Model of the molecular mechanisms responsive to self- and nonself- DNA based on current evidence. The exposure to either self- or nonself-DNA produces differential cellular responses and fragment localization (adapted from Chiusano *et al*., 2021).

In my third activity we set up to study cell sensing and discrimination between self- and nonself-DNA mechanism based on sequence-specific recognition involving RNA/DNA interactions (Mazzoleni *et al*., 2015a; Cartenì *et al*., 2016). Since we consider the presence of membrane-bound receptors or intracellular sensors able to recognize specific eDNA moieties a non-parsimonious explanation, we hypothesized a complementary sequence recognition either at extracellular level (for example through nuclear encoded RNAs possibly present on the cell surface, similar to those displayed on animal cell surface, Huang *et al*., 2020) with a consequent signalling cascade that triggers immunity, or in the cell cytoplasm upon eDNA entrance (through mRNA/esDNA complementary sequence pairing). In the case of intracellular recognition, the binding of esDNA onto the mRNA strands may block the translation machinery causing a blockage in the protein synthesis, with a mechanism similar to RNA interference (Bhat & Ryu, 2016; Moazed, 2009), explaining the resulting plant growth

inhibition. Moreover, this hypothesis explains the specific recognition of esDNA for sequence complementary compared to nonself-DNA. In both scenarios, this hypothesis implies the formation of DNA-RNA hybrids for esDNA recognition and could be easily tested experimentally by the assessment of DNA-RNA hybrid formation *in vivo* for specific targets, which, to the best of our knowledge, has never been performed in plants (Figure 1.7).

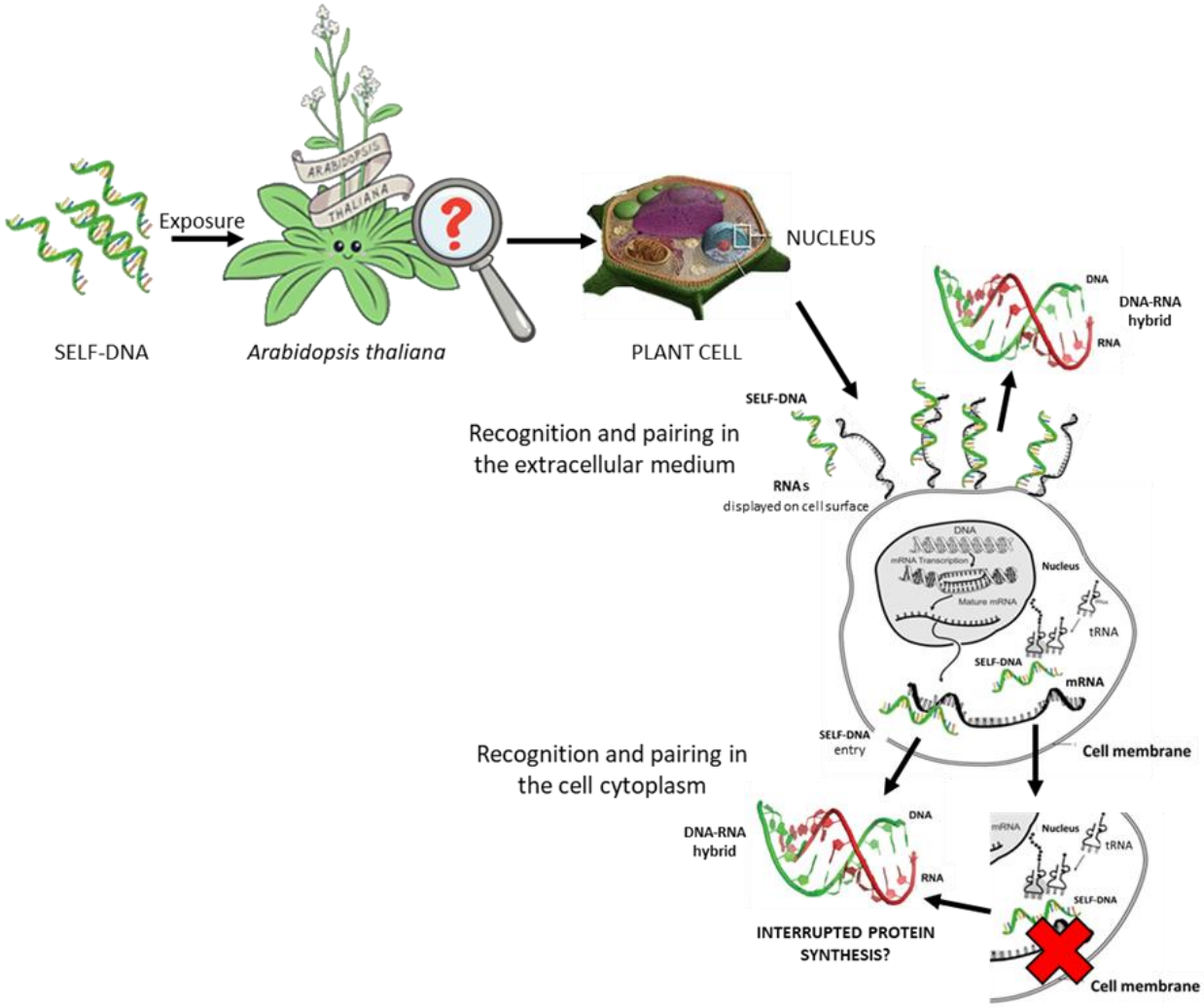

Figure 1.7 – Schematic representation of our hypothesis of cell sensing and discrimination between self- and nonself-DNA based on DNA-RNA hybrid formation either in the extracellular medium or in the cytoplasm for complementary sequence recognition and pairing.

Continuing on the investigation of self-DNA early molecular mechanisms in plants, in my final activity we examined whether self-DNA could cause epigenetic changes, in particular methylation changes, in the genome of the receiver plant (in our case, *Arabidopsis thaliana* seedlings), leading to significant changes in gene expression, as well as gene silencing (Figure 1.8). Interestingly, changes in 5-methylcytosine levels associated with self-DNA exposure in plants have already been previously reported (Vega-Muñoz *et al*., 2018).

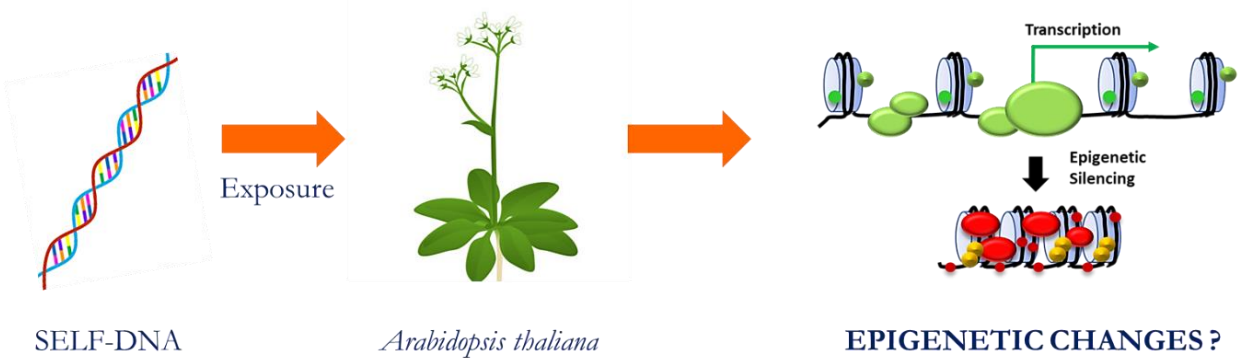

Figure 1.8. Schematic representation of the hypothesis of gene silencing caused by epigenetic changes in the receiver plant *Arabidopsis thaliana* after self-DNA exposure.

The subsequent chapters of this thesis provide detailed descriptions of the key activities conducted as part of this PhD research. Specifically, the second and third chapters encompass the research material recently published in the Plants journal (Ronchi *et al*., 2023). These chapters focus on a cross-factorial experiment investigating the species-specificity of self-DNA in *Setaria* species, as well as a gene expression analysis utilizing real-time quantitative PCR (qPCR). The fourth chapter delves into the investigation of possible methylation changes in the genome following exposure to self-DNA in *Arabidopsis thaliana*. This chapter represents the material for a manuscript currently in preparation. Moving on, the fifth chapter outlines an experiment concerning DNA-RNA hybrid immunoprecipitation. The aim of this experiment is to explore potential mechanisms for discriminating self-DNA from non-self-DNA. This chapter also serves as the basis for another manuscript currently being prepared. Lastly, the final chapter provides a comprehensive summary of the general conclusions drawn from this research work.

Along the following chapters, this thesis delves into various facets of the self-DNA inhibition topic in plants, among which the species-specificity of the effect, the molecular response by gene expression analysis, possible sensing mechanisms for discriminating self- from non-self-DNA, and patterns of DNA methylation changes associated to exposure. All these studies, which differ by observation scale, methodologies and experimental setup, are bound together by the common goal of exploring plant early response mechanisms to self-DNA exposure. Each chapter features exploratory, hypothesis-driven experiments that serve as a platform for testing existing hypotheses, generating new ones, collecting preliminary data, refining research methodologies, and validating innovative approaches. Furthermore, these chapters offer valuable insights into the numerous unresolved questions regarding self-DNA recognition and its implications and applications in plant biology, contributing to a broader

understanding of this significant phenomenon, while paving the way for further focused research and advancements in this captivating field. Ultimately, through their exploratory nature, these experiments aim to provide a solid foundation for investigating self-DNA mechanisms, pushing the boundaries of knowledge in plant biology.

677

Chapter 2: Species-specificity of root growth inhibition by self-DNA in cultivated and weedy *Setaria* species

2.1. Abstract

In this chapter, we present the methods and results of our first activity, which aimed to verify the species-specificity of root growth inhibition by self-DNA in cultivated and weedy Setaria species. The study was recently published in the Plants journal by Ronchi et al., (2023). The phenomenon of self-DNA inhibition, caused by the accumulation of fragmented extracellular DNA, has been previously reported, but its underlying mechanisms remain unclear. In this activity, we focused on investigating the species-specific effects of self-DNA on seed germination and plantlet growth in Setaria italica (cultivated species) and S. pumila (weedy congeneric species). We chose these two species due to the economic importance of S. italica as a globally relevant crop and its interesting comparison with the weedy congeneric species, S. pumila, to assess the species-specificity of self-DNA inhibition. Additionally, the Setaria genus has been recognized as a model plant genus for C4 metabolism, and its genetics and genomics have been extensively studied, including the availability of the fully sequenced genome of S. italica.

The experimental design involved a cross-factorial experiment where four types of DNA solutions (self, congeneric, plant, and animal heterospecific) at three different concentrations (2, 10, and 50 ng/µl) were tested on seedlings of each target species. The seedlings were grown on Petri dishes under controlled conditions. The DNA solutions were extracted, purified, sonicated to achieve the desired fragment size range, and diluted. The Setaria DNA solutions underwent an additional ultra-purification step using the AMPure XP system to ensure high purity. The experimental setup comprised 78 experimental units, including three replicated dishes for each target species and treatment combination, as well as control dishes. The radicle length of each seedling was measured before and after four days of treatment using ImageJ software. Root elongation was calculated for each seed and expressed as the average of the replicates and as a percentage of the corresponding control. Statistical analyses, including three-way ANOVA, Tuckey's test, and one-sample t-tests, were performed to assess the species-specific effects of self-DNA, DNA source, and concentration on root elongation.

The results confirmed the concentration-dependent and species-specific nature of self-DNA inhibition. The inhibitory effect of self-DNA was significantly higher compared to non-self treatments, and the magnitude of the effect correlated with the phylogenetic distance between the DNA source and the target species. This study provides confirmatory evidence on the concentration dependency and species-specificity of self-DNA inhibition, specifically

in cultivated and weedy Setaria species. The findings also suggest potential applications for species-specific weed control in agriculture. However, the study highlights the need for further investigations, including scaled-up field tests, to address critical concerns. These concerns include the purity of treatment solutions and the potential impact of self-DNA on the growth of native or crop plants closely related to the target weed species. Field-scale experiments with highly purified DNA solutions and realistic field conditions, such as mesocosms with topsoil from the field, are necessary to determine the species-specific concentration levels required for effective weed control.

Furthermore, the use of microbial libraries, both artificial (e.g., BAC libraries) and naturally produced through microbial insertion and amplification, should be prioritized and adequately tested as a promising approach. These assessments and field-scale experiments are crucial for evaluating the potential use of self-DNA in controlling invasive weed species like S. pumila. By addressing these issues, we can develop effective and environmentally sustainable strategies for weed management.

2.2. Introduction

In the context of extracellular self-DNA inhibitory effect previously discussed, we present the results of an experiment carried out on two target species belonging to the genus *Setaria*: *S. italica* (L.) P. Beauvois and *S. pumila* (Poir.) Roem. and Schult. We purposely chose these two species for three main reasons. First, the genus *Setaria* can be considered a model plant genus for C4 metabolism (Morrone *et al*., 2014), with an increasing number of published studies addressing its genetics and genomics (Doust & Diao, 2017). Second, the two species provide, for the first time, an interesting case study to test the species-specificity of self-DNA inhibition in cultivated vs. weed congeneric species of global relevance. Third, the availability of the sequenced genome of *S. italica* (Bennetzen *et al*., 2012) also allows for the assessment of the species response to conspecific and congeneric DNA exposure at a genetic level.

S. italica (the foxtail millet) is a monocotyledon belonging to the *Poaceae* family with a short vegetative cycle. It is one of the oldest domesticated millet species, mainly cultivated in Asia and in third world countries, where it is used as feed for livestock, as food for humans and also for healing purposes. In recent years, *Setaria italica* has become a model species for the study of C4 plants as it has a small genome, it is economically important, and some varieties are particularly resistant to abiotic stresses (Lata *et al*., 2013) (Fig. 2.1).

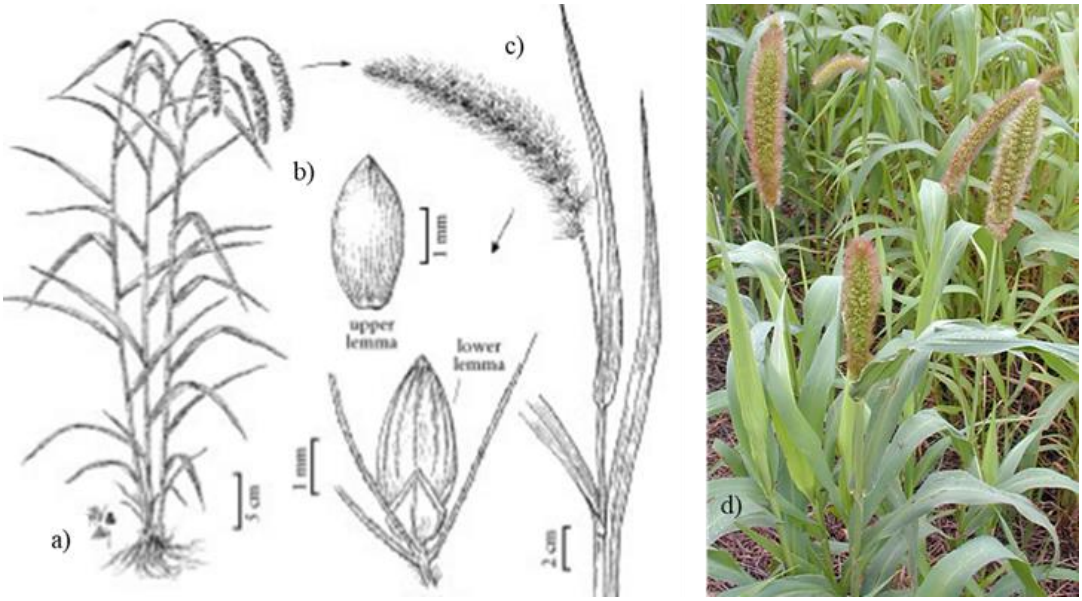

Figure 2.1. *S. italica* morfology. a) Mature plant, b) seeds, c) mature inflorescence (source: Foxtail Millet/Bristlegrass (*Setaria italica*) (soilcropandmore.info)).

S. pumila (the yellow foxtail) (Figure 2.2) is a weed of global concern with a severe impact on dairy pastures, such as in New Zealand (Tozer *et al*., 2015) and in Switzerland (Orlandi *et al*., 2015), and on cereal crops, as in the United States and Canada (Satchivi *et al*., 2017; Steel *et al*., 1983). *S. pumila* presence has also been reported in the Region within some sites of community interest (ZSC Greto del Tagliamento and ZSC Confluence of Torre and Natisone rivers) (Fabian *et al*., 2019a,b), probably due to the abandonment of traditional land management, which have generally favoured the establishment of ruderal plants. Like other invasive plants of genus *Setaria*, produce great environmental damage and negatively affect agriculture, leading to significant economic impacts due to the decline in yields (Dekker *et al*., 2003). In the case of wheat, the extent of yield loss due to infestation can be substantial, potentially reaching up to 44% depending on the severity of the infestation. The density of plants plays a crucial role, with infestation densities surpassing 600 plants per square meter (Satchivi *et al*., 2017).

The genus Setaria is native to Africa from which it has spread throughout the globe through successive waves caused in part also by anthropic activity (Orlandi *et al*., 2015; James, 2008), adapting to first sub-tropical and then temperate climates, thanks to its great genotypic plasticity. Due to the ability to self-pollinate and the phenomenon of dormancy, plants of the genus Setaria can colonize and remain for long periods in different environments; they are also very competitive with other native plants as they manage to exploit the resources of the soil and produce a very large number of seeds, up to 8000 per plant, which contribute to the

persistence of the problem (Steel et al., 1983). Their diffusion within agricultural crops has been contrasted in recent decades with a massive use of herbicides, but this has led to the appearance of various resistance genes that make herbicide treatments useless (Dekker et al., 2003). Within the pastures, the presence of species belonging to the genus Setaria is even more problematic given that few selective herbicides are available and weed control in these environments is generally more difficult to implement (Tozer *et al*., 2009).

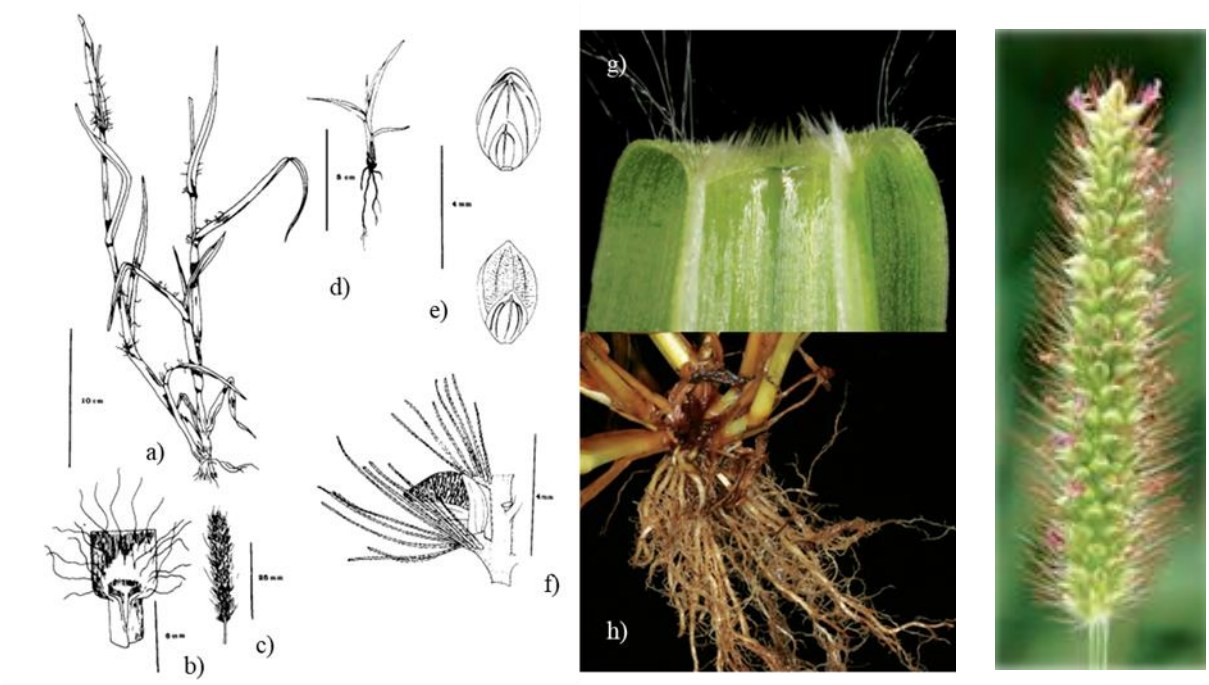

Figura 2.2. *S. pumila* morfology. a) Mature plant, b) base of a leaf lamina with detail of the ligule, c) mature inflorescence, d) seedling at the 4-leaf stage, e) mature seeds, f) mature seed supported by the bristles, g) photo of the ligule equipped with hairs, h) photo of the root system (sources: a-f) Steel *et al*., 1983; g-h) James, 2008).

As pointed out by James & Rahman, (2009), herbicides commonly used in pastures also cause damage to forage species and require a high number of applications to lead to a decrease in the target species. In particular, a study carried out by Orlandi *et al*., (2015) in the Ticino river valley in Switzerland highlighted that the increase in temperatures caused by global warming and the recent change in the rainfall regime has favoured the diffusion of the *Setaria pumila* species, particularly harmful in pastures, where it lowers the quality of forage. In fact, these plants contain a lot of organic matter that is difficult for cattle to digest, resulting in a drop in milk production. Furthermore, the ears of Setaria pumila can lead to the appearance of ulcers in the mouth of ruminants, reducing the amount ingested, and sometimes predisposes them to hypomagnesaemia (Steel *et al*., 1983). The test presented in our study could provide interesting insights on the application perspective of the self-DNA

inhibition principle as species-specific weed control (Mazzoleni, 2014). In order to assess whether the self-inhibition principle still holds for the two target species, we exposed seedlings to treatment with DNA extracts from four different sources (i.e., conspecific, congeneric, plant heterospecific from *Brassica napus* L., and animal from *Salmon salar* L.) at three different concentrations in a cross-factorial experiment. While the effects of self-DNA on species belonging to the same family (Mazzoleni *et al*., 2015a) and on congeneric species (Duran-Flores & Heil, 2018) were previously investigated, this is the first study comparatively and simultaneously testing self-DNA inhibition on a cultivated and an invasive congeneric species. Our hypothesis is that the species-specificity of self-DNA inhibition still holds when tested on phylogenetically related species, even on weed plants that are expected to be more resistant to allelopathic effects. From an application perspective, evidence of species-specific self-DNA inhibition on the invasive weed *S. pumila* but not on the cultivated species *S. italica* could provide promising data for innovative weedicide treatments in agriculture.

2.3. Materials and Methods

2.3.1. Leaf Biomass Production for DNA Extraction

S. pumila seeds were collected in the field in Cadenazzo (Switzerland) in the late summer of 2020; seeds of *S. italica* (Indo American Hybrid Seeds (I) pvt. Ltd. Bangalore, India) and *B. napus* (not tanned Gordon variety, KWS Italy S.p.a.) were purchased from the Friulian Agricultural Club of Udine (Udine, Italy). Seeds of each species were imbibed with Milli-RO water for 24 h into in 50 mL lab grade tubes and then transferred to plastic saucers filled with a standard peat:perlite growing substrate, where they were kept until germination. After germination, seedlings were transplanted in 8 cm pots (2 seedlings per pot) previously filled with the substrate. Plants of all three species were grown under controlled conditions (day T = 22 °C; night T = 20 °C; photoperiod = 12 h; relative humidity = 50%; PPFD = 600 µmol photons m^{-2} s^{-1}) for 60 days (Fig 2.3). Finally, the foliar biomass was harvested.

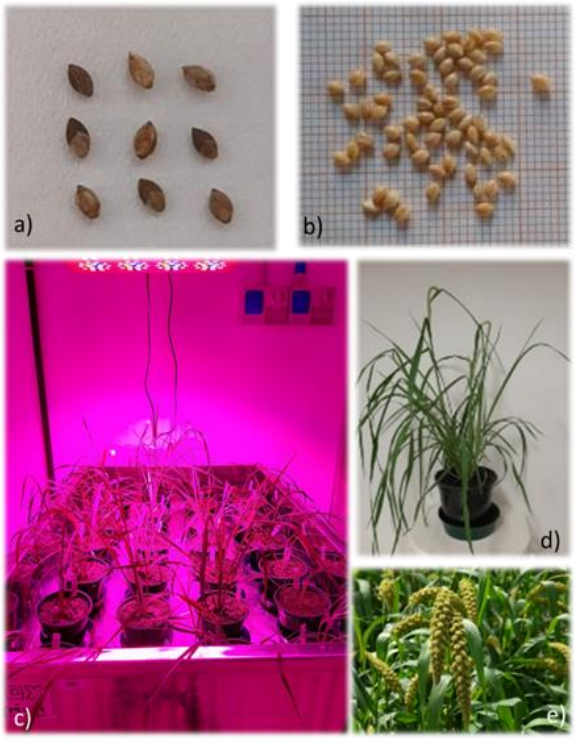

Figure 2.3. Images of *Setaria* plants. a) *S. pumila* seeds, b) *S. italica* seeds, c) *Setaria* plants in the growth chamber with LED lights on, d) 60-day-old *S. pumila* plants, e) 60-day-old *S. italica* plants.

2.3.2. DNA Extraction and RNase Treatment

Nucleic acid extraction from leaf material of *S. italica*, *S. pumila*, and *B. napus* was carried out by a modified Doyle & Doyle, (1987) protocol. For each extraction, 5 g of fresh leaves were grounded in liquid nitrogen and placed in a 50 mL Falcon tube containing the lysis solution composed of 20 mL CTAB (2.5%), 2 µL Proteinase K (20 µg/µL), and 200 µL β-mercaptoethanol (0.1%). The tube was incubated at 65 °C for 30 min and then transferred on ice for 10 min. To separate nucleic acids from cellular components (proteins, lipids, polysaccharides) and other interfering substances (polyphenols), 20 mL of the chloroform–isoamyl alcohol mixture (24:1) were added. The tube was stirred by inversion for 10 min and centrifuged for 30 min at 6800 rpm. Then, the aqueous supernatant fraction was gently pipetted out. Sodium acetate (3 M, 1/10 starting volume) and pure 2-propanol (2/3 of the final volume) were added, followed by incubation at −20 °C for 1 h and centrifugation for 30 min at 6800 rpm. Liquid was discarded, and the residual pellet was washed with 2 mL of 80% ethanol twice. All traces of ethanol were removed by heat volatilization (37 °C for 10–15 min). At the end, the nucleic acid pellet was resuspended in 2 mL of sterile deionized water (Figure 2.4).

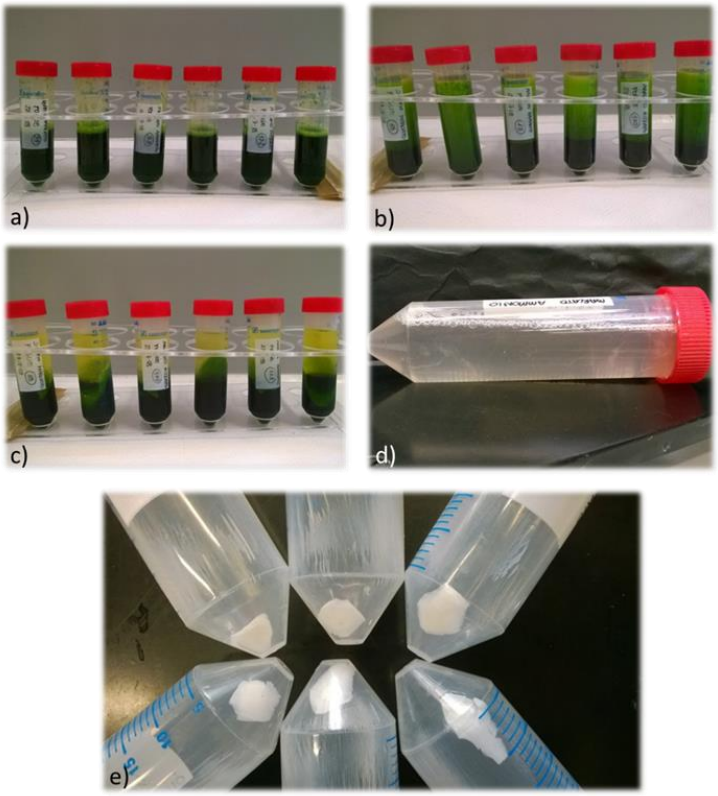

Figure 2.4. Illustrative images of some phases of the nucleic acid extraction process. a) Mixing of the plant material with the lysis solution, b) Purification with organic solvent and isoamyl alcohol, c) Separation of the aqueous supernatant fraction containing the nucleic acids, d) Nucleic acid precipitation, e) Nucleic acid pellets.

To remove RNA, 20 µL of RNase A enzyme (10 mg/mL) was added to the tube and incubated for 1 h at 37 °C. A further precipitation step was performed by adding ammonium acetate (10 M, pH = 7, 1/3 starting volume) and 100% ethanol (2 final volume). The DNA pellet was washed with ethanol as described above. Finally, the DNA pellet was resuspended in 2 mL of sterile deionized water.

2.3.3. DNA Treatment Solution Preparation

In order to replicate the molecular size observed in natural conditions and produced by chemical–physical degradation after plant debris decomposition (Mazzoleni *et al*., 2015a), extracted DNA solutions (about 20 mL for each of the three plant species) were sonicated using the sonicator model UP200S (Hielscher, Teltow, Germany) for 4 min at full power, with alternating high and low-pressure cycles of 1 s. Commercial *Salmon salar* DNA solution (deoxyribonucleic acid from salmon sperm, Merck, Darmstadt, Germany) was already bought at low molecular weight, so it was not exposed to the fragmentation process. The fragment length distribution in all DNA solutions was assessed by 0.8% agarose gel electrophoresis (Figure 2.5).

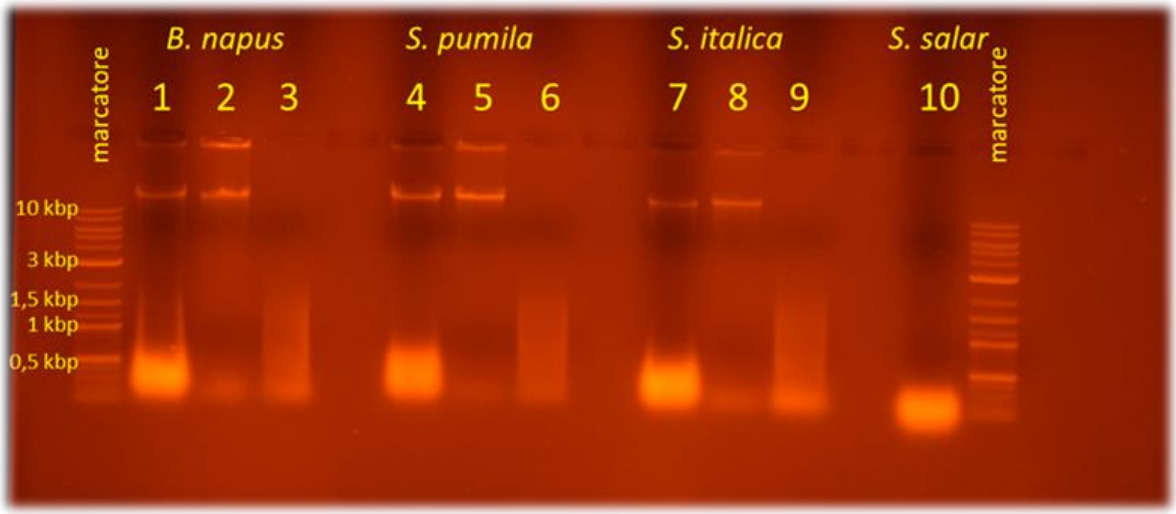

Figure 2.5. Agarose gel electrophoresis of the nucleic acid samples. Pre-RNase-treatment samples (wells labelled with numbers 1, 4 and 7); post-RNase-treatment samples (2, 5 and 8); and post-sonication (3, 6, 9) are shown. The final expected DNA fragment size ranges between 0.1 and 1.5 Kpb for the three plant species considered (*B. napus*, *S. pumila* and *S. italica*) and the commercial solution of *S. salar* (10).

All DNA solutions were diluted at 2, 10, and 50 ng/µL to be used for treatments in the cross-factorial experiment. Limited to *Setaria* DNAs, that showed lower purity values (see Nanodrop ratios before and after beads treatment, Tables 2.1 and Table 2.2), the treatment solutions were also ultra-purified with the AMPure XP system (Beckman Coulter, Brea, CA, USA), a paramagnetic bead SPRI (Solid-Phase Reversible Immobilization) technology generally used for the preparation of highly-pure genetic material (Rudi *et al*., 1997; Beckman Coulter, 2016), following the manufacturer's recommendations (Figure 2.6).

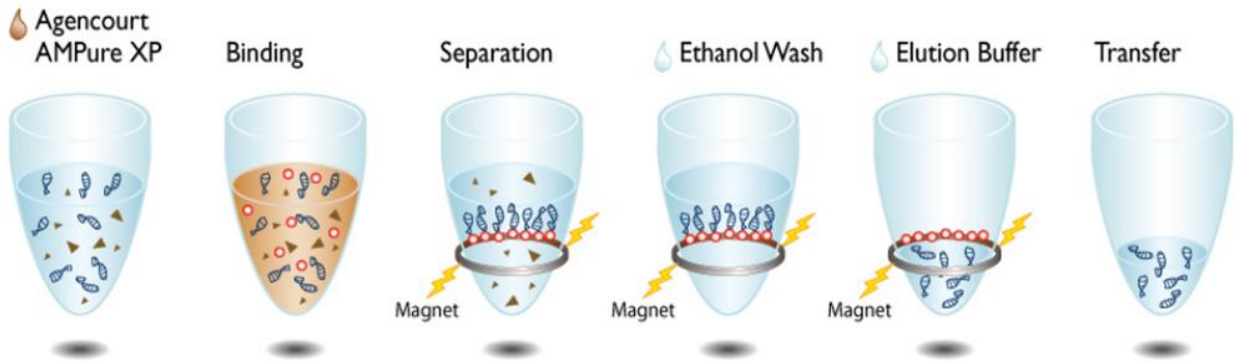

Figure 2.6. Illustrative images of the protocol of DNA solution purification with the magnetic beads AMPure XP system.

Table 2.1. Nanodrop ratios of the treatment solutions before purification with the AMPure XP beads.

DNA source	Absorbance values before beads		
	ng/µl	A260/280	A260/230
	2.2	2.30	0.80
S. pumila	10.1	2.35	0.80
	50.6	2.43	0.75
	2.2	2.23	1.00
S. italica	10.3	2.23	1.00
	51.7	2.28	0.90
	2.2	2.00	2.20
B. napus	10.8	2.00	2.18
	50.1	2.20	2.28
	2.0	1.35	2.33
S. salar	10.0	1.45	2.58
	49.7	1.50	2.58

Table 2.2. Average Nanodrop ratios of the *Setaria* treatment solutions after purification with the AMPure XP beads.

DNA source	Average absorbance values after AMPure beads		
	ng/µl	A260/280	A260/230
S. pumila	51.7	1.82	1.93
S. italica	56.5	1.80	1.72

All DNA solutions were quantified by fluorimeter Qubit 3.0 (Life Technology, Carlsbad, CA, USA), and the quality was assessed by spectrophotometer Nanodrop ND 1000 (Thermo Fisher Scientific, Waltham, MA, USA).

2.3.4. Cross-factorial experiment setup

Seeds of *S. pumila* and *S. italica* were sterilized with a 20% sodium hypochlorite solution, thoroughly washed with sterile deionized water, and placed in Petri dishes (Vetrotecnica, Padova, Italy) over three sheets of filter paper (Grade 1 qualitative filter paper, Whatman, Maidstone, UK) soaked with 4 mL of sterile deionized water. Dishes were placed in a growth chamber under standard controlled conditions (22 ± 2 °C, 50% RH, 16 h day and 8 h night

photoperiod) for 4/5 days. After germination, seedlings with radicle length between 2 and 5 mm were selected for each species and transferred in new Petri dishes (12 seedlings per dish) over three sheets of filter paper soaked with 4 mL of either sterile deionized water (controls) or one of the DNA solutions (treatments) described in Section 2.2.3 and exposed for 4 days under the same previous standard controlled conditions. For the cross-factorial root elongation experiment, 3 replicated dishes were set up, plus 3 control dishes, for each target *Setaria* species and for each treatment combination of DNA source and concentration for a total of 78 experimental units (3 replicates × 2 species × 4 DNA sources × 3 concentration levels + 6 controls) (Figure 2.7).

At the end of the exposure phase, all the seedlings from each Petri dish were moved onto graph paper and photographed (Figure 2.8). The images obtained before and after the exposure were analysed with the software ImageJ version 1.51 (https://imagej.nih.gov/ij, accessed on 7 March 2023, National Institutes of Health, Bethesda, MD, USA), and root elongation was calculated for each seed. Root elongation data, within each target species and treatment, were expressed as averages of the replicates (each calculated over the seeds in the dish) and as percentage of the corresponding control.

a)

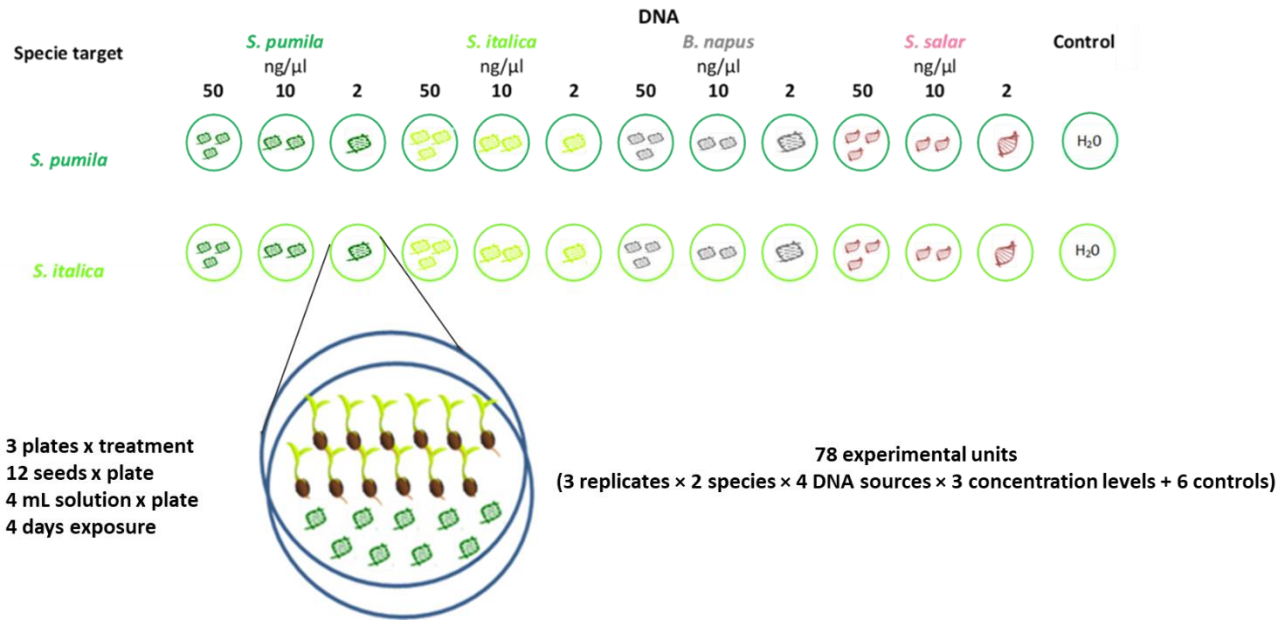

b)

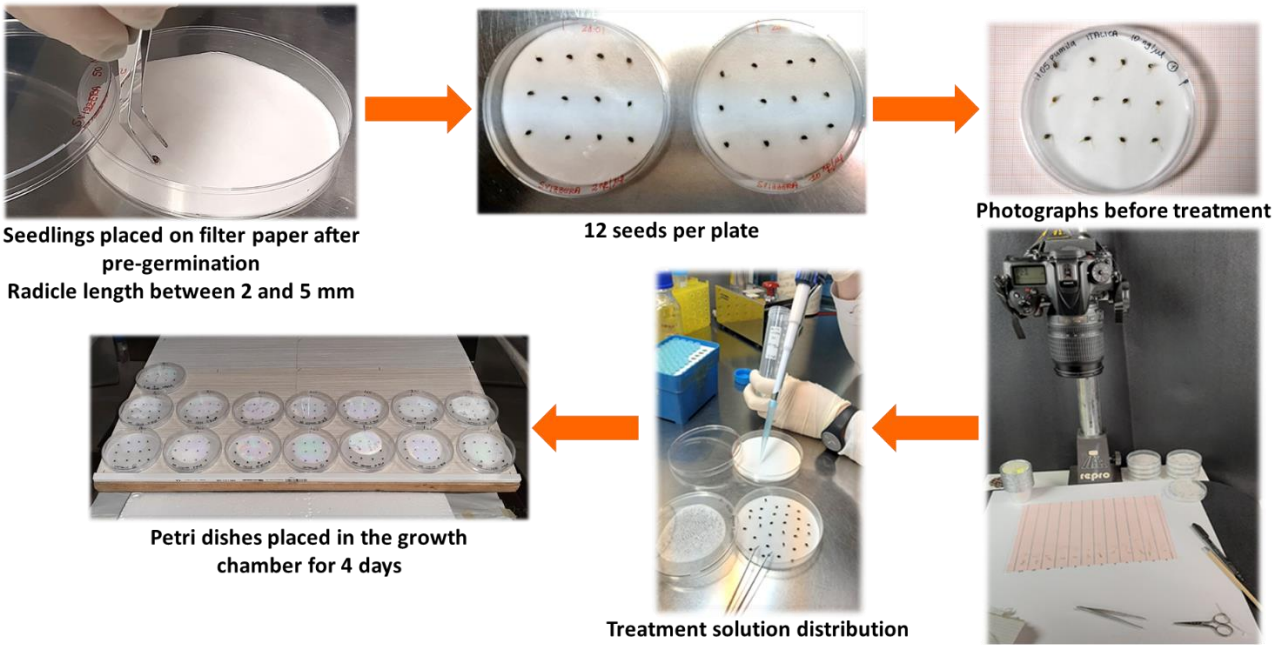

Figure 2.7. a) Cross-factorial experiment setup, representing treatment solution exposure scheme; b) cross-factorial experiment workflow.

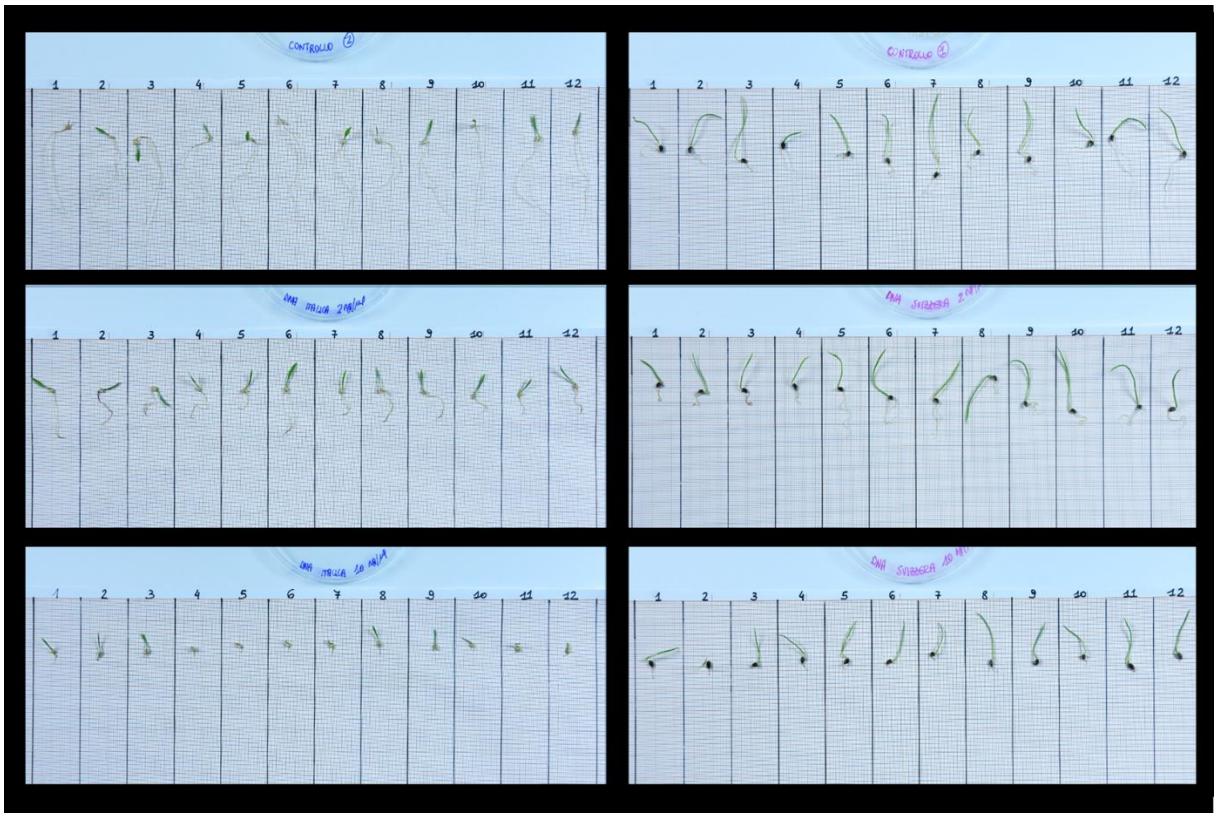

Figure 2.8. Examples of photographs of the seedlings from selected Petri dishes moved onto graph paper. Images refer to seedlings of *S. italica* (left) and *S. pumila* (right), unexposed (top) or exposed to self-DNA solutions, at lower (center) and higher (bottom) concentration.

2.3.5. Statistical Analysis

To evaluate the effect of the DNA solution treatments on the target species root elongation, we fitted a factorial ANOVA model, including main and second order interactions of target species (S, two levels, *S. pumila* and *S. italica*): DNA source (D, four levels, *S. pumila*, *S. italica*, *B. napus*, and *S. salar*) and DNA concentration (C, three levels, 2, 10, and 50 ng/µL). The interaction terms were included in the model, considering that previous evidence (Mazzoleni *et al*., 2015a) showed that self-DNA effects are species-specific, with magnitude depending on the target species' sensitivity, DNA source, and concentration. Then, it was expected to observe significant S × D (due to species-specificity), S × C (due to species sensitivity), and D × C (due to different effects of different DNA sources at different concentration levels) terms. Root elongation data were further investigated with Tuckey's test to assess the significance of pair-wise differences in the average root elongation percentage among all treatment groups ($\alpha = 0.05$). We purposely decided to express response data for both target species as percentages of the respective controls in order to allow a comparison of the treatments' effects between the two target species, while controlling for the different species-specific root elongations. Then, to assess the occurrence of significant differences in the comparisons between treatment groups and the respective controls, the average root elongation percentage of each treatment group was tested against the value 100 (i.e., the control mean) by one-sample t tests with the application of Bonferroni's correction for multiple comparisons ($\alpha = 0.05/24$). Borderline statistical significance was considered for tests producing marginal p-values ($0.05 < p < \alpha$). Statistical analyses and graphs were performed using Excel 2013 (Microsoft Inc., Redmond, WA, USA), STATISTICA v. 10 (Statsoft Inc., Tulsa, OK, USA), and R software version 3.6.2 (R Core Team, 2019) using the following packages: base version 3.6.2, stats version 3.6.2, and ggplot2 version 3.2.1.

2.4. Results

Our cross-factorial experiment showed a significant effect of target species, DNA source, concentration, and their interactions on the root elongation of *S. italica* and *S. pumila* seedlings (Table 2.3). Both target species showed significantly lower root elongation when exposed to self-DNA, as compared to all other treatments, and consistently across all the tested concentration levels (Table 2.4 and Figure 2.10). Moreover, DNA from congeneric species produced higher inhibition as compared to DNA from other heterospecifics, especially when comparing congeneric vs. *S. salar* DNA effects, although this was more

evident at the highest DNA concentration (Table 2.4, Figure 2.10). Such a pattern was consistent with the significant effects of the D and D × C terms in the ANOVA model (Table 2.3, Figure 2.9). Sensitivity to treatments was species-specific, as indicated by the significant S × D term in the ANOVA model (Table 2.3, Figure 2.9), with *S. italica* showing root growth inhibition at all tested self-DNA concentration levels, while *S. pumila* rootlet was not inhibited at the lowest self-DNA concentration (Table 2.4, Figure 2.10).

Table 2.3. Results of the ANOVA carried out on root elongation data from the cross-factorial experiment. Tested effects include main and second order effects of target species (S, two levels, *S. italica* and *S. pumila*), DNA source (D, four levels: *S. italica*, *S. pumila*, *B. napus*, *S. salar*), and concentration (C, three levels, 2, 10, and 50 ng/µL). Df = Degrees of freedom; SS = Sum of Squares; MS = Mean Sum of Squares; F = F statistic ratio; *p* = *p* value.

Effect	Df	SS	MS	F	*p*
Target species (S)	1	178.8	178.8	4.66	0.0353
DNA source (D)	3	24,862.5	8287.5	216.13	<0.0001
Concentration (C)	2	15,268.6	7634.3	199.09	<0.0001
S × D	3	13,069.7	4356.6	113.61	<0.0001
S × C	2	279.5	139.7	3.64	0.0328
D × C	6	3641.8	607.0	15.83	<0.0001
Error	54	2070.7	38.3		

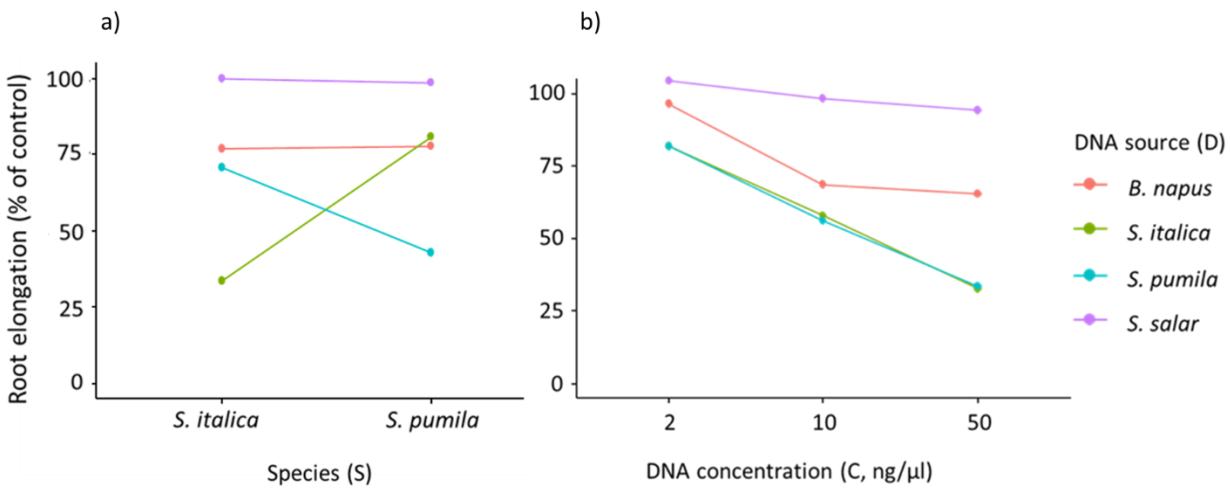

Figure 2.9. Interaction plot for the term S × D (a) and interaction plot for the term D × C (b) of the ANOVA model presented in Table 2.3.

Table 2.4. Results of the cross-factorial experiment. Data refer to the inhibition tests on root elongation of the two *Setaria* species exposed to purified extracellular DNA solutions at different concentrations and from different sources. For each treatment combination (target species, DNA source and DNA concentration) mean and standard deviation of root elongation (expressed as percentage of the control) are shown. Different small letters in brackets indicate significant differences among combinations of target species and DNA source within each concentration level (i.e. table column, see also lettering in Figure 2.10), whereas different capital letters in brackets indicate significant differences among combinations of DNA source and concentration within each target species (table blocks). All pairwise comparisons were tested with Tukey's post hoc test (α = 0.05). Asterisks indicate means significantly different from the control (one-sample t test with Bonferroni's correction for multiple comparisons). The symbol § indicates borderline p-values (0.002 < P < 0.05) in the treatment vs. control tests.

Target Species	**DNA source**	**DNA Concentration (ng/µl)**		
		2	**10**	**50**
S. italica	*S. italica*	58.47 ± 3.20 (a, CD) *	27.44 ± 2.53 (a, AB) *	14.91 ± 3.06 (a, A) *
	S. pumila	93.18 ± 8.93 (b, F)	72.68 ± 6.38 (bc, DE) §	46.06 ± 4.23 (b, BC) *
	B. napus	89.68 ± 7.45 (b, EF)	68.81 ± 2.67 (bc, D) §	67.91 ± 7.69 (c, D) §
	S. salar	104.48 ± 7.88 (b, F)	98.45 ± 2.84 (d, F)	95.81 ± 7.88 (d, F)
S. pumila	*S. italica*	104.98 ± 7.20 (b, F)	87.99 ± 5.00 (cd, EF) §	50.26 ± 4.29 (bc, BC) *
	S. pumila	70.08 ± 6.88 (a, DE) §	39.63 ± 6.89 (a, AB) *	24.64 ± 3.95 (a, A) *
	B. napus	105.68 ± 6.41 (b, F)	68.32 ± 6.17 (bc, CD) §	63.88 ± 9.46 (bc, CD) §
	S. salar	104.42 ± 5.75 (b, F)	97.57 ± 3.12 (d, F)	92.15 ± 6.41 (d, F)

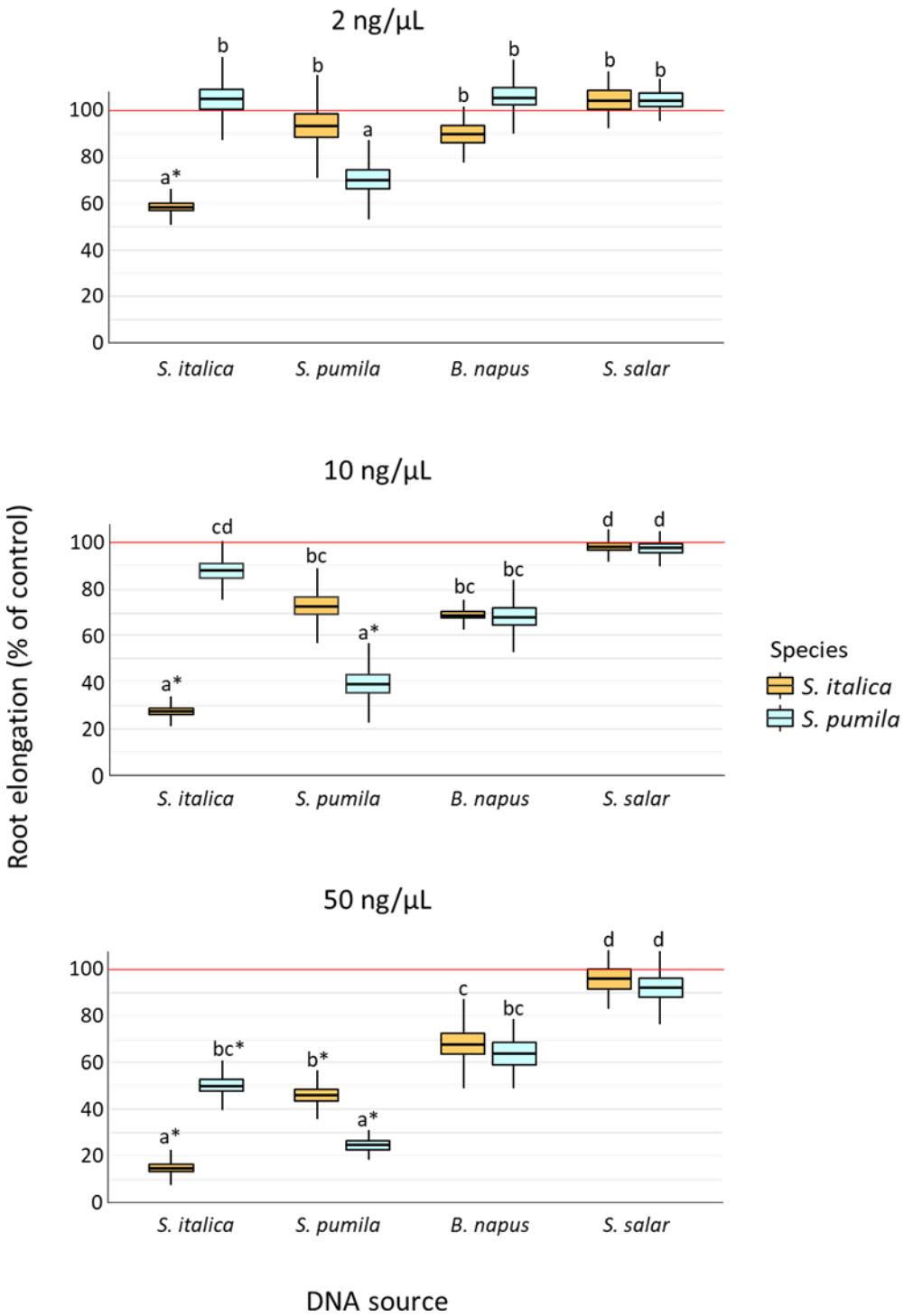

Figure 2.10. Effects of the treatment solutions containing DNA from different sources (*S. italica*, *S. pumila*, *B. napus*, *S. salar*) at three concentrations (2, 10, and 50 ng/µL) on the root elongation (% of control = 100, horizontal red lines) of *S. italica* and *S. pumila* seedlings after 4-day exposure in controlled conditions. Data refer to mean ± 1 standard error (box) and 95% confidence limits (whiskers) of 3 replicates for each treatment combination. Different letters above bars indicate significantly different means within each panel (Tuckey's test, $p < 0.05$. Detailed results in Table 2.4). Asterisks indicate significant root elongation inhibition as compared to the control (one-sample *t* test with Bonferroni's correction for multiple comparisons).

2.5. Discussion

A self-inhibition by fragmented extracellular DNA, mostly for fragment size between 50 and 1500 bp, has been reported in previous studies as dependent on the concentration of DNA in the growing substrate and on the phylogenetic distance between the DNA source and the receiver species (Mazzoleni *et al*., 2015a,b; Barbero *et al*., 2021). Since its discovery, the magnitude of self-DNA inhibition was related to the species-specificity of the molecular agent. In particular, in Mazzoleni *et al*., (2015a), a stronger effect of conspecific DNA is highlighted, as compared to heterospecific DNA, with intermediate magnitude of the inhibition when the target and the DNA source species belong to the same taxonomic family. Duran-Flores & Heil (2018) confirmed the species-specificity of self-DNA, showing that common bean (*Phaseolus vulgaris*) root growth was strongly inhibited by self-DNA, weakly inhibited by congeneric DNA (*Phaseolus lunatus*), but substantially unaffected by heterologous DNA from acacia (*Acacia farnesiana*), indicating that the species-specificity of the self-DNA effect still holds at the infrageneric level. Along this line, we tested the species-specificity of self-DNA inhibition in congeneric species with the novelty of investigating a cultivated (*Setaria italica*) and a weedy, invasive species (*Setaria pumila*), with the latter expected to be more resistant to environmental stressors (Zerebecki & Sorte, 2011; Godoy *et al*., 2011; Podda, *et al*., 2017; Clements & Jones, 2021; Leal *et al*., 2022). In our cross-factorial experiment, the absence of detectable effects of *S. salar* DNA and a marginal effect of heterospecific DNA from *B. napus* on *Setaria* rootlets are fully consistent with the above-mentioned previous findings, confirming the absence of inhibition in the case of species exposed to DNA from phylogenetically distant species, while still showing a weak, marginal concentration-dependent inhibition exerted by heterologous plant DNA at a supra-familiar phylogenetic distance (Mazzoleni *et al*., 2015a,b; Duran-Flores & Heil, 2018). Taken together, our results provided confirmatory evidence on the absence of a substantial effect of extracellular DNA from phylogenetically distant species, on the root elongation of target plants.

Considering in more detail our results on the two congeneric target plants and the effects cross-factorially exerted by exposure to their DNA, the observed pattern of significant inhibition of root elongation was fully consistent with previous findings and our expectations. In particular, the inhibitory effect of conspecific DNA, on both *S. italica* and *S. pumila* root growth, was significantly higher than the one exerted by congeneric DNA at the same concentration levels, highlighting the species-specificity of the self-DNA effect at infrageneric level. The magnitude of self-DNA inhibition observed in our experiment is also consistent with

that previously observed at similar concentration levels for different plant species (Mazzoleni *et al*., 2015a,b; Duran-Flores & Heil, 2018). At the lowest concentration level (2 ng/µL), only the *S. italica* seedlings were significantly inhibited by self-DNA, thus providing support to the general hypothesis of a higher susceptibility of cultivated species, compared to invasive weeds, towards environmental stress factors (Zerebecki & Sorte, 2011; Godoy *et al*., 2011; Podda, *et al*., 2017; Clements & Jones, 2021; Leal *et al*., 2022). Accordingly, *S. pumila* DNA at 10 ng/µL, besides inhibiting conspecific seedlings, also showed a marginal inhibitory effect on congeneric (*S. italica*) seedlings, although in this latter case the treatment vs. control comparison produced a borderline p-value. Therefore, in the context of species-specific biological control, our study highlights the promising role of *S. pumila* DNA as a potential species-specific weedicide in analogy to its previously suggested use as a species-specific pesticide (Ferrusquía-Jiménez *et al*., 2021; Serrano-Jamaica *et al*., 2020; Germoglio *et al*., 2022; Ferrusquía-Jiménez *et al*., 2022). However, upscaling tests in an open field are obviously required in order to clarify the persistence of extracellular DNA and the reliability of its self-inhibitory effects under more realistic conditions, as well as the possible interference with cultivations of phylogenetically related crops.

2.6. Conclusions

Our root inhibition experiment provided confirmatory evidence on the concentration dependency and species-specificity of self-DNA inhibition. More importantly, the hypothesis that the self-DNA inhibitory effect still holds at infrageneric level was also confirmed for congeneric species with different ecological traits, such as the weedy invasive *S. pumila* and the cultivated *S. italica*. However, our research also highlighted some critical concerns deserving verification by appropriate upscaled field tests, such as the extent of possible inhibition of crop species treated with DNA targeting closely related weeds.

In conclusion, considering the results obtained in this work, with regard to the possible use of self-DNA in the field for the control of the invasive *S. pumila* species, some specific issues must be carefully considered and possibly require further assessment.

- Attention must be posed not only towards the level of concentration, but also on the degree of purity of the treatment solutions.
- It is of paramount importance to ensure that self-DNA is harmful to the target weed species and does not compromise the growth of other native or crop plants, especially if phylogenetically close to the target weed.

- The necessary concentration level, which is species-specific and depends on the sensitivity of the species, can only be assessed following biological assays based on highly purified solutions in realistic settlements resembling open field conditions (such as mesocosms with topsoil from the field). Adopting the methods used in our work it is possible to obtain sufficient DNA amount for the purposes of the experimental tests, but the procedure may not be adequate when the scope is obtaining larger DNA quantities, like those needed to carry out field-scale experiments.
- A promising approach based on microbial libraries, both artificial (i.e. BAC libraries) or naturally produced by microbial insertion and amplification, should be prioritized and adequately tested.

In light of these evidence and considerations, further assessments and field-scale experiments are necessary to fully evaluate the potential use of self-DNA for controlling invasive weed species like *S. pumila*. Addressing these issues will contribute to the development of effective and environmentally sustainable strategies for weed management. The results of this work have been published on Plants journal (Ronchi, A., Foscari, A., Zaina, G., De Paoli, E., & Incerti, G., 2023. Self-DNA Early Exposure in Cultivated and Weedy Setaria Triggers ROS Degradation Signaling Pathways and Root Growth Inhibition. Plants (Basel, Switzerland), 12(6), 1288. https://doi.org/10.3390/plants12061288).

Chapter 3: Targeted gene expression analysis in *Setaria* species after self-DNA exposure

3.1. Abstract

In this second activity, we conducted a targeted gene expression analysis to investigate the early response of Setaria species to exposure to self-DNA. This study aimed to test the hypothesis proposed by Chiusano et al., (2021) that self-DNA elicits molecular pathways associated with abiotic stress responses. We selected seven genes known to be responsive to abiotic stress in S. italica within a timeframe of 6 hours and performed a targeted Real-Time qPCR analysis.

To begin, we conducted a literature search to identify a set of genes that are constitutively expressed in S. italica roots and selectively responsive to abiotic stress factors within the first 6 hours of exposure. These stress factors include drought, dehydration, osmotic, oxidative, and thermal stresses. We also selected RNA Polymerase II as a reference gene for the RT-qPCR experiment. Primers for the target and reference genes were designed considering the genomic sequences of S. italica as a reference for both S. italica and S. pumila. We verified the specificity of the primers by checking for sequence similarities with other regions of the S. italica genome and ensuring that there were no high similarities among gene members of the same family. The amplification specificity was confirmed through qualitative PCR and agarose gel electrophoresis using retrotranscribed RNA from both S. italica and S. pumila.

For the experimental setup, seedlings of the two target species were exposed to ultra-purified self-DNA solutions for 1 and 3 hours. Control replicates were also included, where seedlings were treated with deionized sterile water. After the treatment, radicles were collected, and total RNA was extracted using a plant total RNA kit. The quantity and quality of the extracted RNA were assessed using Nanodrop, agarose gel electrophoresis, and capillary electrophoresis. The RNA samples were then reverse-transcribed into cDNA using a reverse transcription kit. Real-time qPCR analysis was performed using the SsoFast EvaGreen Supermix and the CFX96 Real-Time PCR system. The expression levels of the target genes were calculated as fold change using the $\Delta\Delta$Cq method. Statistical analysis was performed to evaluate the significance of differences in gene expression between the control and self-DNA-treated samples at 1 and 3 hours.

The results showed that the selected target genes exhibited similar expression patterns in both S. italica and S. pumila, with S. pumila generally showing a higher response level. Genes responsive to specific abiotic stressors, such as drought, osmotic, oxidative, and cold stresses, were upregulated in both species at both observation times. These results were consistent with their known response to abiotic stressors. However, two genes, WD40-144

and WD40-155, showed a unique expression pattern, being downregulated in response to self-DNA exposure. These genes are known to be responsive to osmotic, oxidative, and cold stresses. Additionally, MPK17, involved in dehydration and hyper-osmotic stress, showed an initial upregulation followed by a decrease in expression levels.

The differential expression of these abiotic stress-responsive genes in both species supports the hypothesis that self-DNA exposure activates molecular pathways associated with abiotic stress responses. The upregulation of genes involved in ROS degradation and management indicates the involvement of reactive oxygen species (ROS) production during the early stages of self-DNA exposure. Moreover, the analysis revealed that invasive species exhibit greater resilience compared to cultivated species, possibly due to a more rapid and efficient initiation of the immune response.

Overall, this study provides valuable insights into the early response of Setaria species to self-DNA inhibition at the molecular level. It contributes to our understanding of the molecular mechanisms underlying self-DNA inhibition, particularly focusing on the early response and gene expression changes associated with abiotic stress pathways. Further investigations using more comprehensive gene sets are warranted to delve deeper into specific cellular processes.

3.2. Introduction

The discovery of the self-DNA inhibitory effect bears important implications for plant ecology, as the accumulation, persistence, or removal of DNA in the soil, depending on the environment, soil characteristics, and weather conditions, could play a fundamental role in determining biodiversity levels and patterns in different ecosystems (Cartenì *et al*., 2016). Self-DNA in soil might also function as a signaling molecule for self-damage recognition, triggering plant resistance against environmental stresses and dangers such as pathogen infection, herbivore feeders, and intraspecific competition (Duran-Flores & Heil, 2015; Duran-Flores & Heil, 2018; Barbero *et al*., 2021; Vega-Muñoz *et al*., 2018; Vega-Muñoz *et al*., 2023). The nature of the molecular mechanisms of the observed inhibitory effect is yet to be clarified, although some exploratory works have highlighted specific early events following exposure of seedlings to self-DNA (e.g. Barbero *et al*., 2016). In particular, Duran-Flores & Heil (2018) highlighted the involvement of response signals linked to immunity pathways such as H_2O_2 and the activation of MAPK, as well as the increase in ROS (Reactive oxygen species) production. Moreover, a recent study on *Arabidopsis thaliana* (Chiusano *et al*., 2021)

confirmed that cells distinguish self- from nonself-DNA, suggesting, through confocal microscope analysis, that nonself-DNA enters root tissues and cells, while self-DNA remains outside. Specifically, exposure to self-DNA is associated with a DAMP-induced innate immunity (or PTI, Pattern Triggered Immunity) that leads to limited cell permeability, chloroplast disfunction and ROS production, eventually causing cell cycle arrest, consistently with macroscopic observations of root apex necrosis, increased root hair density and leaf chlorosis. Such early response is peculiar to exposure to self-DNA and highlights a possible analogy between the response to self-DNA and that to abiotic stress at early term, confirmed by differential expression of gene ontology associated with abiotic stress response (Chiusano *et al*., 2021; Vega-Muñoz *et al*., 2023) (Figure 3.1). In contrast, nonself-DNA seems to enter the cells triggering the activation of a hypersensitive response, a rapid and localized response that includes cell death, qualitatively similar to PTI, that occurs at the point of pathogen penetration, and that evolves into systemic acquired resistance (SAR), a mechanism of induced defence that confers long-lasting protection against a broad spectrum of microorganisms, associated with the signal molecule salicylic acid (SA) and the accumulation of pathogenesis-related proteins. In this sense, nonself-DNA seems to be related to biotic stress response, also confirmed by gene ontology expression analysis (Chiusano *et al*., 2021).

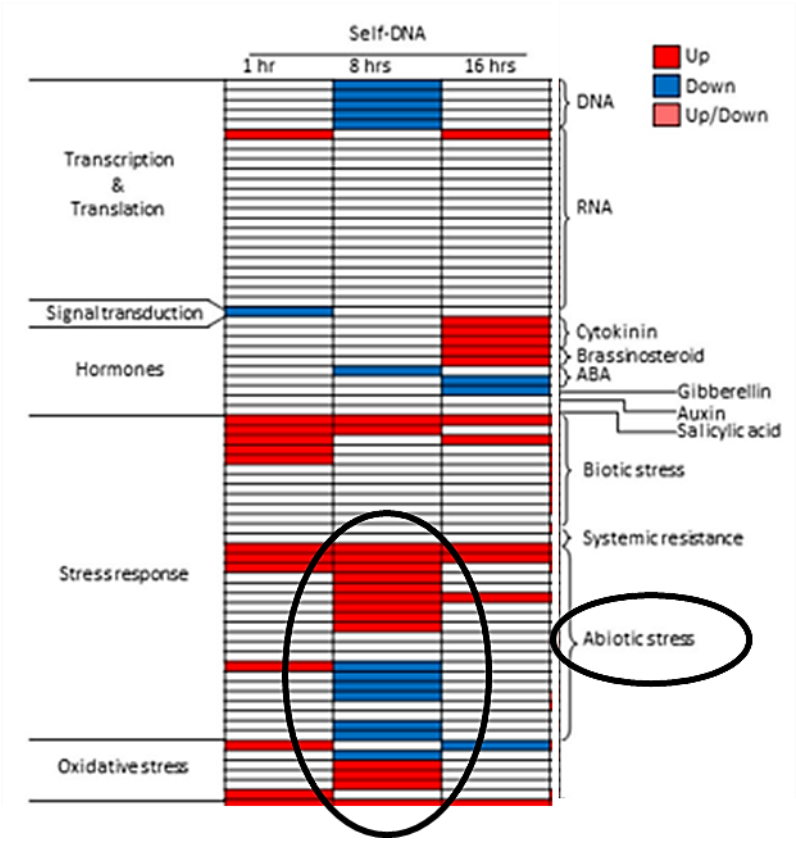

Figure 3.1. Summary of the Gene Ontology (GO) enrichment analysis on filtered differentially expressed genes (DEGs), with most enriched GOs (rows) grouped by functional process or cell compartment. The colour of each cell in the columns (indicating treatment type and stage) shows the pattern of expression of the enriching genes (full red: upregulated DEGs; blue: downregulated; light red: both up- and downregulated, with enrichment in upregulated DEGs showing lower p-value compared to the downregulated ones). In white, absence of enrichment is shown.

In light of this preliminary evidence, it is of great interest to explore the early response to exposure to self-DNA in terms of variation in gene expression that leads to an impairment of cell functionality. Therefore, we present the results of a RT-qPCR (Reverse Transcription - quantitative Polymerase Chain Reaction) analysis carried out on two target species belonging to the genus *Setaria*, *S. italica* (L.) P. Beauvois and *S. pumila* (Poir.) Roem. and Schult, in order to understand which genes linked to particular abiotic stresses may be involved in the early stages of response to self-DNA exposure at root level. For the *S. italica* species, all the needed gene information can be retrieved from the Setaria italica genome, which has been completely sequenced by the JGI (Joint Genome Institute) of the State Department of Energy United States of America (DOE) and by the BGI (Bijing Genome Initiative) in China, and is freely available on the Phytozome database (JGI, USA). A literature research was carried out to identify a set of genes constitutively expressed in *S. italica* root and selectively and differentially responsive to abiotic stress factors within the first 6 h of exposure to the abiotic

stressor, which refer to adverse environmental conditions caused by non-living agents, such as drought and dehydration, osmotic, oxidative and thermic. The list of the seven selected genes is presented in Table 3.1. In order to comparatively assess the expression level among different genes and samples/treatments, a number of reference genes of known expression levels must be also included in the RT-qPCR experiment (Kozera & Rapacz, 2013). Among the reference genes used in literature for *Setaria*, we selected RNA Polymerase II (Kumar *et al*., 2013). Also, the necessary primers of target and reference genes for the real-time amplification were identified.

Table 3.1. List of selected genes responsive to abiotic stress in *S.italica* for RT-qPCR.

Gene	Gene Family	Function	Reference
Gene1_SiFSD2	SUPEROXIDE DISMUTASE (FeSOD)	Defence against ROS and apoptotic stimuli, convert superoxide(O_2^-) into hydrogen peroxide (H_2O_2) and dioxygen (O_2)	Wang *et al*., 2018
Gene2_SiALDH22A1	ALDEHYDE DEHYDROGENASE (ALDH)	Oxidation of aldehydes to carboxylic acids, reducing the effect of lipid peroxidation under various environmental stresses	Chen *et al*., 2014
Gene3_SiALDH7B1	ALDEHYDE DEHYDROGENASE (ALDH)	Oxidation of aldehydes to carboxylic acids, reducing the effect of lipid peroxidation under various environmental stresses	Chen *et al*., 2014
Gene4_SiCSD3	SUPEROXIDE DISMUTASE (CuZnSOD)	Defence against ROS and apoptotic stimuli, convert superoxide(O_2^-) into hydrogen peroxide (H_2O_2) and dioxygen (O_2)	Wang *et al*., 2018
Gene5_SiWD40-144	WD REPEATS include conserved tryptophan (W) and aspartic acid (D) residues and a repeat length of 40 amino acids	Scaffolding molecule, WD repeat-containing protein 26 isoform X2 (WDR26) may act as a negative regulator in MAPK signalling pathway	Mishra *et al*., 2014
Gene6_SiWD40-155	WD REPEATS include conserved tryptophan (W) and aspartic acid (D) residues and a repeat length of 40 amino acids	Scaffolding molecule, WD repeat-containing protein DWA2, known as a negative regulator of ABA signaling	Mishra *et al*., 2014
Gene7_SiMPK17-1	Mitogen-activated protein kinase (MAPK/MPK)	MPK signalling cascades transduce and amplify endogenous and exogenous stimuli. MPK17 can be firstly triggered by ROS production; its downregulation seems to significantly reduce growth	Lata *et al*., 2010

In particular, data from the whole-plant transcriptomic profiling by Chiusano *et al*., (2021), highlighted a remarkable pattern of differential gene expression of several pools of genes

across treatments (self-DNA vs. non-self-DNA) and timings (1, 8, and 16 h), mostly evident after 1 h exposure and then apparently released after 8 h. Therefore, in this study, we test if the evidence reported by Chiusano *et al*. (2021) still holds for the two *Setaria* species over the time window spanning between 1 and 3 h since exposure. From a pure science perspective, our study, being the first exploration of early response to self-DNA inhibition at molecular level on C4 model plants, contributes to the ongoing investigation on the molecular mechanisms underlying the observed phenomenon of self-DNA inhibition, with a particular focus on the early response to exposure, at gene expression scale. In this respect, we hypothesize that early exposure to self-DNA elicits molecular pathways known to be responsive to abiotic stressors.

3.3. Materials and Methods

3.3.1. Gene Selection and Primer Design

Since only the *S. italica* genome has been fully sequenced (Joint Genome Institute, USA, and Bijing Genome Initiative China), in this study, we used *S. italica* as a reference genome also for *S. pumila*. We selected 7 genes (*FSD2*, *ALDH22A1*, *ALDH7B1*, *CSD3*, *WD40-155*, *WD40-144*, *MPK17*) involved in *S. italica* root signaling pathways responsive to abiotic stress and known to be up or downregulated within the first 6 h of exposure (Wang *et al*., 2018; Mishra *et al*., 2014; Lata *et al*., 2010; Zhu *et al*., 2014) and the reference gene coding for RNA Polymerase II (Kumar *et al*., 2013). Real-time qPCR primers (Table 3.2) were selected as follows: for the reference gene and the target genes *ALDH22A1* and *ALDH7B1* we used the same primers proposed by the authors (Kumar *et al*., 2013; Zhu *et al*., 2014), as they met the analysis requirements for amplicon length, melting temperature, and position on the genomic sequence. For all the other target genes, instead, we proceeded to design the primers using the Primer3web v.4.1.0 software (ELIXIR Estonia), setting the following parameters: primer length (Min. 18; Opt. 20; Max. 24 bases), primer melting temperature (Min. 64 °C; Opt. 65 °C; Max. 66 °C), and amplicon length (130–210 bases). Inputs for Primer3 software were *S. italica* CDS (coding DNA sequence) of the target genes, available on the Phytozome database (Phytozome v.13, Joint Genome Institute, JGI, Berkeley, CA, USA).

Table 3.2. Primers used in real-time qPCR analysis. For each source gene, the Phytozome ID, strand and position on the genome are shown, with the forward and reverse primer sequences, and either the reference paper for the primer or the reference tool used to design it.

Source gene	Phytozome ID and position	Primer (5'-3')	Reference/Tool
FSD2	Seita.4G031200 plus strand Scaffold_4:2020702..2023953	Fwd: TGGTTGGGTTTGGCTTGTCTTG Rev: TGTCCCAAGAGATGAGATGGTCCA	(Primer3web v.4.1.0)
ALDH22A1	Seita.2G440100 minus strand Scaffold_2:48874364..48880144	Fwd: CAAGAAGAGGCATTTGGACC Rev: TTGATTGCTGCTACACCACAG	(Zhu *et al*., 2014)
ALDH7B1	Seita.2G218400 minus strand Scaffold_2:32046039..32052337	Fwd: TCTGCGGAAACTGTGTTGTC Rev: TGAACCATTAGACCAGCCCT	(Zhu *et al*., 2014)
CSD3	Seita.9G403600 minus strand Scaffold_9:46291516..46295065	Fwd: CTCAAGCCTGGCCTCCACGG Rev: CAGTGGGATCTGGCTGTCGGT	(Primer3web v.4.1.0)
WD40-144	Seita.6G076200 minus strand Scaffold_6:6733603..6739573	Fwd: TACCATCTCGCACGCTACAGGTTT Rev: TCCATGCAACCATCATCACCGACT	(Primer3web v.4.1.0)
WD40-155	Seita.6G247500 minus strand Scaffold_6:35501203..35506269	Fwd: TCAAGGAGGAGAACGAGGTGCAC Rev: GCAGCGCCATAACCCTCACCA	(Primer3web v.4.1.0)
MPK17	Seita.4G273900 plus strand Scaffold_4:39101196..39106532	Fwd: CGAGAGCCACAGGAAGAACTCAGT Rev: CCTGTGCGGGTATCTACTGCTGC	(Primer3web v.4.1.0)
RNA Polymerase II	Seita.2G142700 plus strand Scaffold_2:17011362..17018255	Fwd: TAGGAAAGGAATTGGCAAGG Rev: TAGGACTGCTTTCGACCCA	(Kumar *et al*., 2013)

Primers were designed to be placed on two contiguous exons to detect genomic residual traces during controls with qualitative PCR or partly on one exon and partly on the following one to be able to amplify only retrotranscribed RNA sequences (Figure 3.3). Primers used in the present study are listed in Table 3.2 and were sourced from Sigma Aldrich (Rome, Italy). Eventually, we verified that the region amplified by the selected primers did not have high similarity with other sequences of the *S. italica* genome (through BLAST tool on Phytozome website) to prevent primers from amplifying unspecific targets. Moreover, we verified that there were no high similarities in the sequences of gene members belonging to the same family: in particular, *ALDH22A1* and *ALDH7B1*, as well as *WD40-155* and *WD40-144*. For this analysis, we utilized the Clustal Omega software (EMBL-EBI, Wellcome Genome Campus, Hinxton, Cambridgeshire, UK), which allows to find the best alignment among a given number of nucleotide sequences. Specific primer amplification was also verified on a retrotranscribed RNA for both *S. italica* and *S. pumila* through qualitative PCR (50 ng per cDNA sample, T annealing = 58 °C, 35 cycles, using OneTaq Hot Start DNA Polymerase

from New England Biolabs, Ipswich, MA, USA) and 2% electrophoresis agarose gel (Figure 3.2).

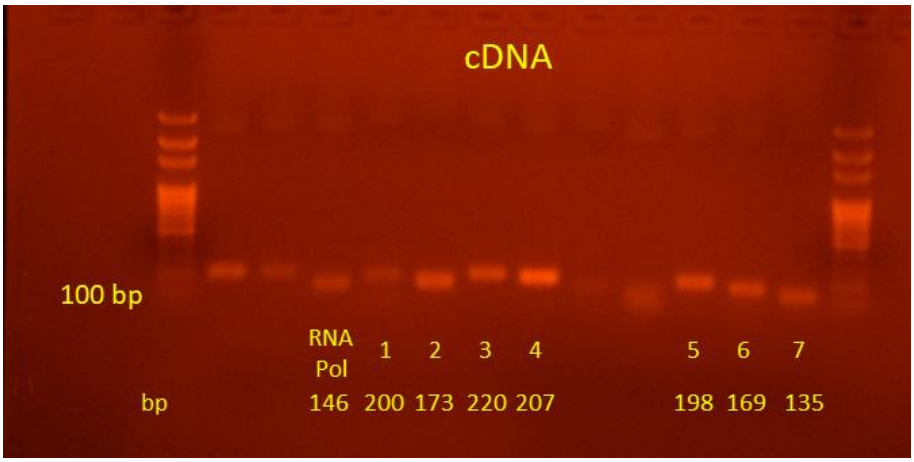

Figure 3.2. Qualitative PCR to test the amplification of target and reference genes on *S.pumila* cDNA using the primers designed on *S.italica* gene CDS sequences. Target genes displayed are named as follows: 1) *FSD2*; 2) *ALDH22A1*; 3) *ALDH7B1*; 4) *CSD3*; 5) *WD40-144*; 6) *WD40-155*; 7) *MPK17*.

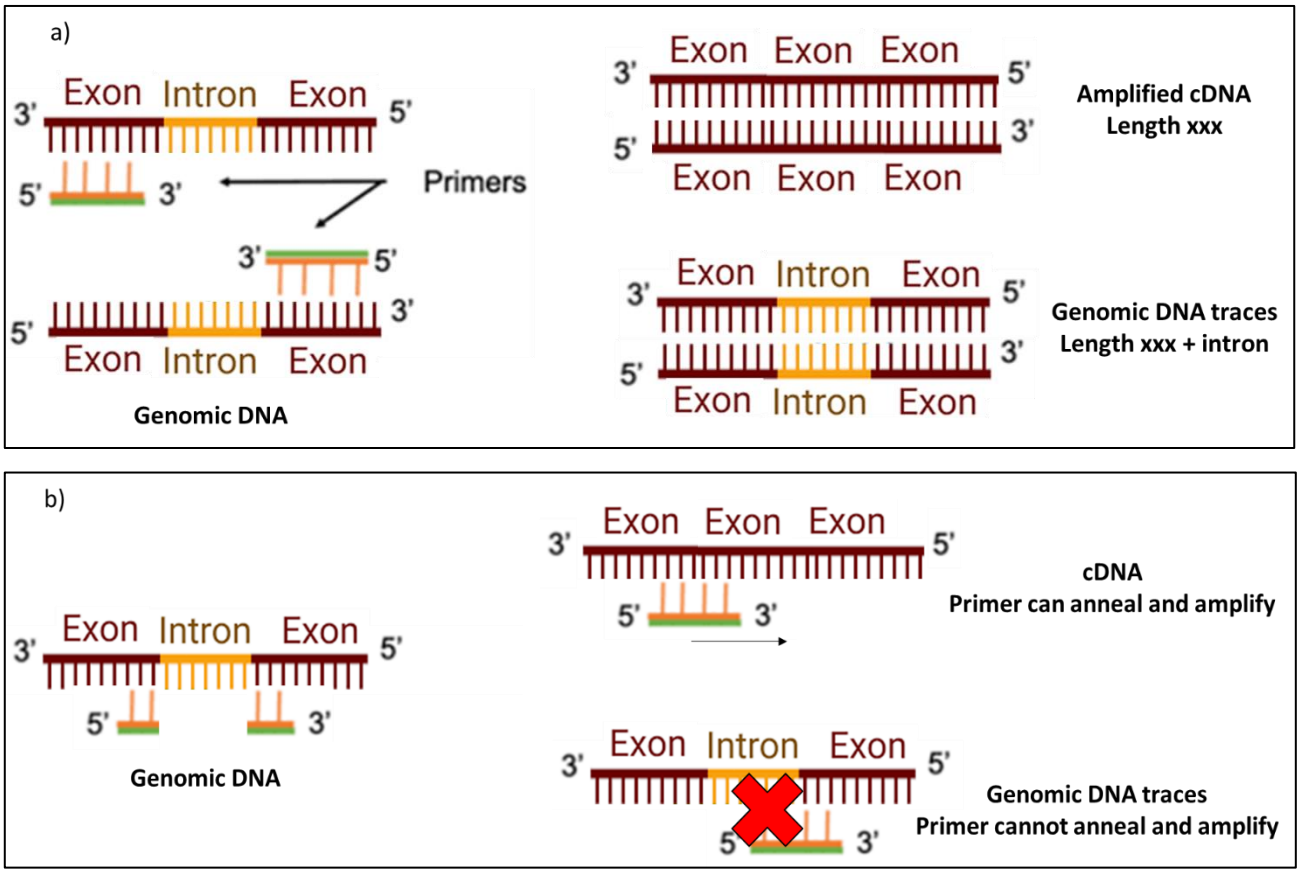

Figure 3.3. Primers were designed with Primer3web software using *S.italica* gene CDS sequences. a) Primers were placed on two contiguous exons, in order to detect genomic residual traces in the cDNAs during controls with qualitative PCR; b) or partly on one exon and partly on the following one to be able to amplify only retrotranscripted RNA sequences.

3.3.2. Self-DNA Exposure

Seeds of the two target species, *S. italica* and *S. pumila*, were prepared as described in Section 2.2.4. After germination, seedlings with radicle length between 5 and 10 mm were selected for exposure. Each seedling was placed on a Petri dish and exposed to 10 µL of 90 ng/µL ultra-purified self-DNA solutions (Section 2.2.3) by micro pipetting on the root apex. Petri dishes were placed at room temperature and closed with lids during exposure, in order to minimize the evaporation of the treatment solution. We tested 3 biological replicates (i.e., Petri dishes with 20 germinated seeds each) for each combination of target species and exposure time (1 and 3 h) plus 3 control replicates (dishes containing seedlings micro pipetted with deionized sterile water), for each species and time, for a total of 24 Petri dishes (3 replicates × 2 species × 2 exposure times + 12 controls) (Figure 3.4). After undergoing the self-DNA treatment, seedling radicles were collected from each Petri dish, fresh-weighed, and stored at −80 °C.

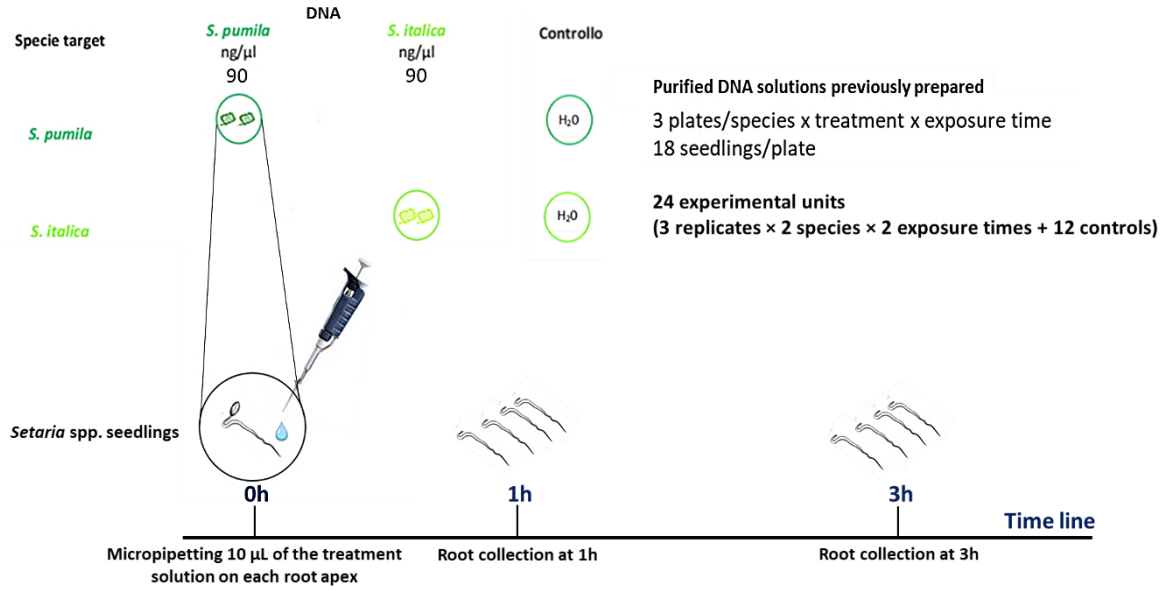

Figure 3.4. Targeted gene expression experiment setup, representing treatment solution exposure scheme. In particular, the two target species, *S. italica* and *S. pumila*, were exposed to 10 µL of 90 ng/µL ultra-purified self-DNA solutions by micro pipetting on the root apex.

3.3.3. RNA Extraction, Purification and cDNA Synthesis

Total RNAs were extracted from the radicles of each replicate with the Spectrum™ Plant Total RNA Kit (Sigma-Aldrich), scaling the reagent volumes recommended by the manufacturer to the low amount of root material per sample (12 mg on average), as follows: 300 µL of the Lysis Solution/2-ME Mixture, 500 µL of the Binding Solution, 300 µL for every

washing step, and 2 subsequent elutions with 35 µL of the Elution Solution. Extracted RNA's quantity was measured by Nanodrop 3.0 (Thermo Scientific), quality was assessed by 1% electrophoresis agarose gel, and integrity was measured by on-chip capillary electrophoresis using Agilent RNA 6000 Nano kit and Bioanalyzer 2100 (Agilent technologies, Santa Clara, CA). Then, 1 µg of each RNA sample was purified from residual genomic DNA and reverse-transcribed to cDNA with Qiagen QuantiTect Reverse Transcription Kit, following the manufacturer's instructions (Figure 3.5). RNA's and cDNA's yield and quality were estimated by Nanodrop, while the absence of residual genome traces was checked through qualitative PCR.

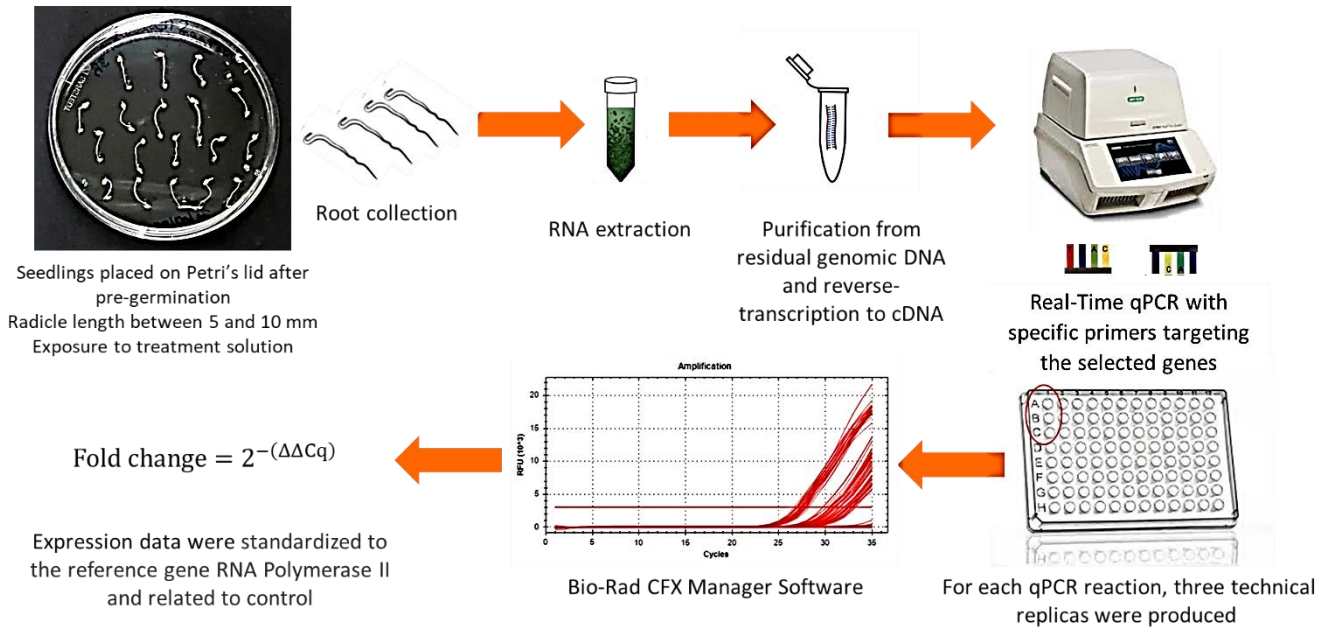

Figure 3.5. Targeted gene expression experiment workflow, indicating the main experiment passages from seedling self-DNA exposure to Real Time performance.

3.3.4. Real Time qPCR

Real-time qPCR analysis was performed using the SsoFast EvaGreen Supermix (Bio- Rad, Hercules, CA, USA) and the CFX96 Real-Time PCR system (Bio-Rad Laboratories, Hercules, CA, USA). Each PCR reaction contained 10 µL of SsoFast EvaGreen Supermix, 10 µM of each primer, and 2 µL of cDNA (25 ng/µL) from each sample (final volume was 20 µL per reaction with sterile water). For each qPCR reaction, three technical replicas were produced. Real-time qPCR conditions were used as follows: 95 °C for 30 s; 35 cycles of 95 °C for 5 s; 58 °C for 5 s; the melting curve was assessed from 65 °C to 95 °C in increments of 0.5 °C. Standard curves for each primer pair and for each species were generated by

plotting the quantification cycle (Cq) values from qPCRs executed with a pool of all cDNA samples as templates, as well as the log10 concentration of the cDNA template (5, 25, 50 and 100 ng/µL). The amplification efficiency (E) of each primer pair in each species was calculated from the slope of the corresponding standard curve as:

$$E = 10^{-1/slope}$$

$$\%E = (E - 1) \times 100$$

and ranged from 98 to 103% in *S. italica* and from 97 to 103% in *S. pumila*, with an average correlation value (R2) of 0.995.

Expression levels of the 7 target genes for the 24 cDNAs samples (12 for each species) were calculated as fold change:

$$\text{Fold change} = 2^{-(\Delta\Delta Cq)}$$

where ΔΔCq value represents the difference between the average 1-h-self-DNA-treatment or the average 3-h-self-DNA-treatment ΔCq and the average control ΔCq. The average ΔCq values were calculated over the three biological replica ΔCq values, except for the control treatment. In this case, each gene average ΔCq was calculated over six biological replicates, given that the three replicates per exposure time were put together, assuming non-variation of gene expression under controlled conditions.

3.3.5. Statistical Analysis

To evaluate the significance of the differences in average ΔCq values between 1 h and 3 h treatment and between 1 h treatment and control and 3 h treatment and control within each target gene, we carried out two independent-sample t tests with the application of Bonferroni's correction for multiple comparisons ($\alpha = 0.05/21$) for both species.

Statistical analyses and graphs were performed using Excel 2013 (Microsoft Inc., Redmond, WA, USA), STATISTICA v. 10 (Statsoft Inc., Tulsa, OK, USA), and R software version 3.6.2 (R Core Team, 2019) using the following packages: base version 3.6.2, stats version 3.6.2, and ggplot2 version 3.2.1.

3.4. Results

Mean extracted RNA yields were 1207 ng per root mg (*S. italica*) and 1125 ng per root mg (*S. pumila*). RNA integrity was satisfactory, with RIN values ranging between 5.00 and 6.60. Mean cDNA yields (DNA-50) from 1 µg of RNA were 32 µg (*S. italica*) and 30 µg (*S. pumila*). The pool of genes selected for the real-time qPCR experiment showed a very similar expression pattern for both target species (Figure 3.6), although *S. pumila* generally presented the highest response level (the range of fold change in gene expression was 0.195–2.305 in *S. italica* and 0.234–2.960 in *S. pumila*, Table 3.3).

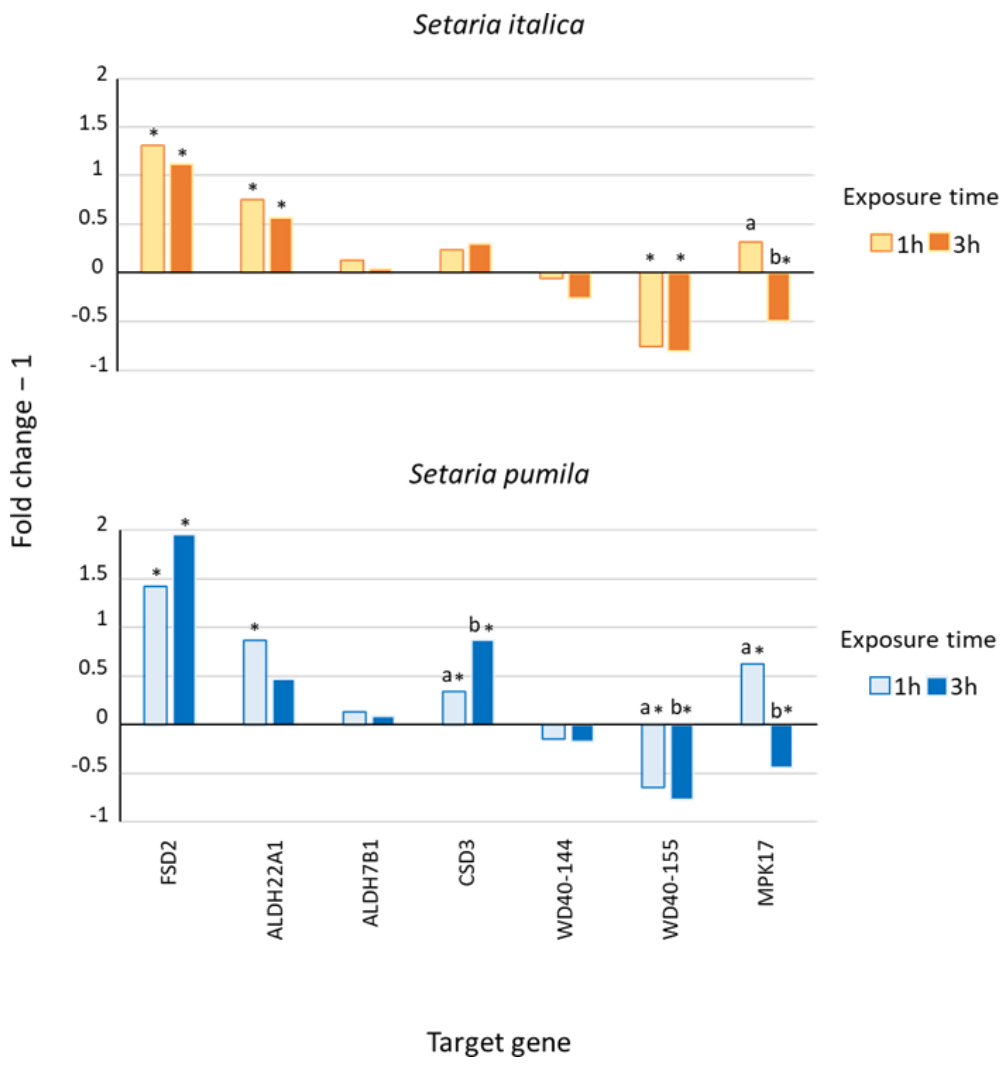

Figure 3.6. Target gene expression profiles in the two *Setaria* species after 1 and 3 h exposure to self-DNA. Data refer to fold change −1 for each target gene after exposure to ultra-purified self-DNA solutions for 1 and 3 h, at the concentration of 90 ng/µL. Different letters above bars indicate statistically significant differences in ΔCq means between exposure times within each gene (t test for independent samples with Bonferroni's correction for multiple comparisons). Asterisks indicate ΔCq means that are significantly different from the controls (t test for independent samples with Bonferroni's correction for multiple comparisons. Detailed results in Table 3.3).

Table 3.3. Results of the real-time qPCR test on *S. italica* and *S. pumila* exposed to self-DNA. Data refer to mean and standard deviation of ΔCq, calculated over 3 biological replicates, for each species, target gene and exposure time. Mean and standard deviation of ΔCq observed in the unexposed controls are also shown. Different letters indicate significant differences between 1 h and 3 h ΔCq for each species and gene, as resulting from two-independent-sample t test with Bonferroni's correction for multiple comparisons. Asterisks indicate means significantly different from control (two-independent-sample t test with Bonferroni's correction). The symbol § indicates borderline P-values (0.00238 < P < 0.05) in the treatment vs. control comparisons.

Species	Target Gene	1h	3h	Control
S. italica	SiFSD2	1.259 ± 0.169 *	1.380 ± 0.133 *	2.464 ± 0.103
	ALDH22A1	-0.938 ± 0.148 *	-0.778 ± 0.104 *	-0.131 ± 0.156
	ALDH7B1	-1.855 ± 0.197	-1.740 ± 0.119	-1.685 ± 0.194
	CSD3	-3.807 ± 0.203	-3.885 ± 0.156	-3.507 ± 0.193
	WD40-144	-0.867 ± 0.073	-0.523 ± 0.073 §	-0.954 ± 0.127
	WD40-155	1.495 ± 0.068 *	1.795 ± 0.102 *	-0.562 ± 0.116
	MPK17-1	-0.374 ± 0.127 (a) §	0.990 ± 0.094 (b) *	0.018 ± 0.156
S. pumila	SiFSD2	1.782 ± 0.191 *	1.495 ± 0.123 *	3.060 ± 0.194
	ALDH22A1	-1.533 ± 0.169 *	-1.189 ± 0.170 §	-0.631 ± 0.088
	ALDH7B1	-1.112 ± 0.182	-1.053 ± 0.156	-0.931 ± 0.165
	CSD3	-4.851 ± 0.027 (a) *	-5.332 ± 0.106 (b) *	-4.427 ± 0.115
	WD40-144	-0.810 ± 0.127	-0.769 ± 0.130 §	-1.040 ± 0.131
	WD40-155	1.575 ± 0.084 (a) *	2.165 ± 0.085 (b) *	0.069 ± 0.173
	MPK17-1	-0.063 ± 0.150 (a) *	1.474 ± 0.184 (b) *	0.639 ± 0.168

In particular, the target genes *FSD2*, *ALDH22A1*, *ALDH7B1,* and *CSD3*, respectively responsive to drought, osmotic, oxidative and cold stress (*FSD2*), osmotic and oxidative stress (*ALDH22A1* and *ALDH7B1*) as well as osmotic, oxidative, and cold stress (*CSD3*), were upregulated in both species at both observation times (Figure 3.6) and substantially consistent with their known response to abiotic stressors. In the cases of *FSD2* and *ALDH22A1*, mean ΔCq values were also significantly different from the respective controls, while in the case of *CSD3* the expression values were significantly different from the control only in *S. pumila*, with an increase, with time, of its expression levels from 1 h to 3 h (Table 3.3). The genes *WD40-144* and *WD40155*, respectively responsive to osmotic, oxidative, and cold stresses (*WD40-144*) and to drought, osmotic, oxidative, and cold stress (*WD40155*), showed a peculiar expression pattern. In fact, they were characterized by a generalized downregulation in response to self-DNA not previously reported for other abiotic stressors (Figure 3.6). Specifically, *WD40-155* mean ΔCq values resulted significantly

different from the control at each exposure time and for both species, while also showing a significant decrease in its expression levels with time (Table 3.3). Finally, *MPK17*, normally involved in dehydration and hyper-osmotic stress, was initially upregulated in both species (mean ∆Cq at 1 h was significantly different from the control, Table 3.3), as previously reported for other abiotic stressors, and then showed a significant decrease in its expression levels in both species (Figure 3.6).

3.5. Discussion

As different genes are known to respond to several stress factors, we separately discuss all abiotic factors considered in this study (i.e., drought, dehydration, osmotic, oxidative, and thermic stress), as previously suggested (Fraire-Velázquez & Balderas-Hernández, 2013; Mareri *et al*., 2022), to better investigate the potential connection between the expression response of the target genes after self-DNA exposure and their expression levels under a specific abiotic stress.

3.5.1. Drought and Dehydration Stress

Drought stress in plants means that transpiration or evaporation exceeds water uptake in plants (Zhang *et al*., 2018), and it is closely intertwined with dehydration, as the first event during drought stress is the loss of water from the cell (Martignago *et al*., 2019) with consequent reduction in water potential and turgor (Shao *et al*., 2008). Drought is considered one of the most important environmental stresses in agriculture (Fahad *et al*., 2017). It leads to physiological and morphological adaptations to reduce evapotranspiration, such as decreased leaf area or leaf folding, ABA-mediated stomatal closure, increased leaf thickness, and enlargement of the root system, together with plant growth and productivity decrease (Abobatta, 2019; Anjum *et al*., 2011). From a molecular point of view, several genes are activated and involved in response and signaling pathways in *S. italica* under drought conditions, among which we selected *FSD2*, *WD40-155*, and *MPK17-1* (Wang *et al*., 2018; Mishra *et al*., 2014; Lata *et al*., 2010).

FSD2 encodes an iron–superoxide dismutase (FeSOD), and its expression level is reported to decrease (relative to control) after 1 h of drought stress and to significantly increase (fold change ~= 5) and peak after 4 h (Wang *et al*., 2018). In our real-time qPCR analysis, *FSD2* was also significantly upregulated (fold change ranging between 2 and 3) at both exposure times (1 h and 3 h) in both species. Comparatively, this result suggests an earlier activation

in response to self-DNA as compared to drought stress, although a direct quantitative comparison is not straightforward as it is possibly biased by the different stress nature and intensity between our experimental conditions and those of the reference study. However, since SODs are known to play a crucial role by the dismutation of O_2^- radicals in the protection against oxidative damage (Scandalios, 1993), our result is consistent with an enhanced early superoxide production under self-DNA exposure. This finding aligns with the results from the transcriptomic study conducted by Chiusano *et al*., (2021), where enhanced expression of genes associated with antioxidant activity was observed in *A. thaliana* after 1 hour of exposure to self-DNA. Notably, this included the upregulation of five peroxidases and the Fe superoxide dismutase 1 (FSD1), which shares functional similarities with our target gene. The parallel findings in both studies provide further support for the involvement of antioxidant-related genes in the plant's response to self-DNA exposure. Interestingly, a very recent work (Tjia *et al*., 2023) showed higher levels of O_2^- and H_2O_2 in rice (*Oryza sativa* L.) roots, after 7 days of exposure to self-DNA, compared to the unexposed control, although the experimental timing prevents us from assessing if this corresponded to a prolonged ROS production or a decreasing trend after an earlier peak. However, it is important to note that the authors of the study also observed a downregulation of genes encoding ROS-scavengers at the same time-point, which was interpreted as a signal of decreasing ROS levels. However, despite the downregulation, the ROS content remained relatively high, suggesting that the plant was still experiencing oxidative stress and that the downregulation of ROS-scavenging genes may be informative of a preceding cytotoxic redox state. Differently, Vega-Muñoz *et al*., (2018), in a qPCR assay after whole plant total RNA extraction, reported that antioxidant genes (superoxide dismutase/SOD, catalase/CAT, and phenylalanine ammonia lyase/PAL) were up-regulated in a concentration-dependent manner after 5 days of self-DNA exposure in lettuce (*Lactuca sativa* L.). The function of ROS production and scavenging, along the response dynamics to self-DNA, cannot be clarified by summing up our and previous findings, due to several experimental differences, including the target species and plant organ, experimental timing, and exposure dose. However, both cited studies suggest a long-term role in self-DNA stress management. At an earlier term, ranging between 1 and 3 h, our observation of ROS activation is consistent with the studies of Barbero *et al*., (2021) and Duran-Flores & Heil (2018). In both cases, peroxidase activity was found, respectively, by fluorescent dye and enzymatic assay in the chloroplasts of tomato leaves and in lima bean leaves 3 and 2 h after exposure to self-DNA. However, it is important to note that mechanical

damage to the leaf material before or after exposure to self-DNA has been employed in these studies, which may potentially have exacerbated the production of H_2O_2, which is a well-known end product of the DAMP cascade (Yeats & Rose, 2013).

WD40-155 encodes the WD repeat-containing protein DWA2 and was found to be upregulated during dehydration stress at 1 and 3 h, reaching its peak expression at 3 h, and then decreasing at a longer term (Mishra *et al*., 2014). We observed the opposite response pattern for this gene, with a significant downregulation in all tested conditions. Its trend in *S. pumila* even suggests an increasing downregulation with time. Since DWA2 protein is known as a negative regulator of ABA signaling in *A. thaliana* (Lee *et al*., 2010), it could be inferred that such a signaling pathway plays an important role during early response to self-DNA exposure, as already pointed out by the work of Chiusano *et al*. (2021), that showed an early upregulation of genes related to ABA and jasmonic acid at 1 h of self-DNA treatment. In fact, ABA is a very important stress hormone in plants, accumulated in response to stress conditions in different organs and able to initiate a cascade of signal transduction pathways that regulate stomatal aperture and expression of genes involved in resistance to environmental stresses (Dar *et al*., 2017). It also interacts with the jasmonic acid (JA) and salicylic acid (SA) signaling pathways, both hormones engaged in the early response to self-DNA (Vega-Muñoz *et al*., 2023), and it is reported to be involved in signaling crosstalks between biotic and abiotic stress responses (Ku *et al*., 2018). However, its most important function is the regulation of plant water balance and osmotic stress tolerance (Dar *et al*., 2017). Accordingly, in *Setaria*, the negative regulator of ABA signaling, DWA2 protein, is downregulated for prolonged drought conditions, while self-DNA exposure seems to trigger an earlier onset of ABA signaling cascade.

Finally, *MPK17* encodes a mitogen-activated protein kinase that exhibited the highest expression level (around 6-fold induction) after 1 h of dehydration stress in a tolerant cultivar of *S. italica* and an earlier, but lower, peak in a non-tolerant cultivar. Then, it was released at 3 h in both cultivars (Lata *et al*., 2010). Consistently, in our analysis, *MPK17* is firstly upregulated after 1 h of self-DNA exposure, then significantly downregulated after 3 h in both species. Interestingly, the upregulation at 1 h is perfectly consistent with the MAPKs activation previously described in common bean after 30 min of exposure to self-DNA (Duran-Flores & Heil, 2018), which, in turn, can be triggered by ROS production (Son *et al*., 2011). Moreover, a recent genetic study (Zhu *et al*., 2022) in rice (*Oryza sativa* L.), a species phylogenetically closely related to *S. italica* (Lu *et al*., 2006), highlighted that the downregulation of *MPK17* enhances Xa21-mediated resistance to the bacterial

Xanthomonas oryzae pv. Oryzae (Xoo). The downregulation of *MPK17* at 3 h, in our analysis, could be related to the plant immunity response to self-DNA, which is already hypothesized to function as DAMP, indicating self-damage and triggering self-specific immunity induction (Barbero *et al*., 2021; Duran-Flores & Heil, 2018; Vega-Muñoz *et al*., 2018; Chiusano *et al*., 2021; Vega-Muñoz *et al*., 2023). Finally, the downregulation of *MPK17* seems to affect plant morphology, significantly reducing growth, development, and reproduction (Zhu *et al*., 2022).

3.5.2. Osmotic and Oxidative Stress

High salt concentration in soil alters plant performance by causing metabolic damage, ion toxicity, secondary oxidative stress, and osmotic stress, and it induces gene expression alterations fitting an efficient salt stress response (Fraire-Velázquez & Balderas-Hernández, 2013). Oxidative stress, which can be triggered by different severe environmental stress factors, is associated with an excessive production and accumulation of ROS, toxic molecules that can cause damage by lipid peroxidation, affecting nucleic acids and protein oxidation, which promote programmed cell death (Qamer *et al*., 2021). Among the genes involved in salinity and osmotic stress response in *S. italica*, we selected *ALDH22A1*, *ALDH7B1*, *CSD3*, and *WD40-144* (Wang *et al*., 2018; Mishra *et al*., 2014; Zhu *et al*., 2014), in addition to the three genes described above and already selected as responsive to drought and dehydration (*FSD2*, *WD40-155*, *MPK17*) (Wang *et al*., 2018; Mishra *et al*., 2014; Lata *et al*., 2010).

ALDH22A1 and *ALDH7B1* encode aldehyde dehydrogenases (ALDHs), enzymes known to reduce oxidative stress, catalysing the oxidation of a wide range of aldehydes into corresponding carboxylic acids, detoxifying cellular ROS, and/or reducing lipid peroxidation (Zhu *et al*., 2014; Singh *et al*., 2013). During salinity stress in *S. italica*, *ALDH22A1* is upregulated after 1 h, reaching its peak after 6 h, while *ALDH7B1* results upregulated only after 6 h, suggesting a later activation (Zhu *et al*., 2014). Our analysis in response to self-DNA substantially highlighted the same pattern, with *ALDH7B1* expression not significantly different from the control at 1 and 3 h, as well as a significant upregulation at 1 and 3 h for *ALDH22A1*.

CSD3 encodes for a Cu–Zn superoxide dismutase, and its expression level is reported to decrease after 1 h and then increase after 4 h (Wang *et al*., 2018). This is in line with the non-significant changes in expression level of *CSD3* after 1 and 3 h exposure to self-DNA in *S. italica*. Interestingly, *CSD3* was significantly upregulated in *S. pumila*, already, at 1 and 3 h, indicating an expression progressively increasing with time, as reported for other invasive

plants, which show superior tolerance to drought and salinity stress in connection to a more efficient upregulation of SODs (Filippou *et al*., 2014). Then, this might be related to a higher stress resistance of the weedy invasive *Setaria* species as compared to the cultivated one (Zerebecki & Sorte, 2011; Godoy *et al*., 2011; Podda, *et al*., 2017; Clements & Jones, 2021; Leal *et al*., 2022). In addition, *S. pumila* showed a wider range of gene expression variation relative to the control, as compared to *S. italica* (Table 3.3), possibly indicating a more rapid and intense response to stress onset.

WD40-144 was found to be strongly upregulated under salt stress after 1, 3, and 6 h (Mishra *et al*., 2014). On the contrary, in our analysis the expression level of this gene did not vary significantly among treatments, indicating that it is not likely involved in the response to self-DNA, at least at an early stage.

Concerning the genes already mentioned in the previous subsection, *WD40-155* presents an oscillating pattern in response to salt and osmotic stress, being slightly upregulated at 1 h, but not at 3 h, and then reaching its peak at 6 h (Mishra *et al*., 2014), while it was significantly downregulated in response to self-DNA at 1 and 3 h. *MPK17*, which we mentioned in the previous subsection as being responsive to water stress in *S. italica*, is also reported as responsive to salt stress in other plant species. In *Arabidopsis thaliana* (Moustafa *et al*., 2008; Frick & Strader, 2018), it is transiently induced after 3 h of hyperosmolarity influencing the proliferation and cellular distribution of peroxisomes; in maize (*Zea mays* L.), both PEG and H_2O_2 treatment caused a decline in the expression of *ZmMPK17* in roots, correlated to increased Ca^{2+}, and the lower peaks appeared at 24 and 3 h, respectively (Pan *et al*., 2012). In our analysis, *MPK17* results significantly downregulated at 3 h; this is intriguingly consistent with the findings by Barbero *et al*. (2016), reporting an increase in cytosolic Ca^{2+} concentration after early exposure to self-DNA in *Z. mays*.

3.5.3. Thermic Stress

We considered the gene expression response to cold stress, a dangerous environmental stressor that can cause cell membrane damage and cell-cycle disruption, affecting plant germination, growth, development, and reproduction (Aslam *et al*., 2022). Among the genes involved in the early response to cold stress in *S. italica*, we had selected two SODs, *FSD2* and *CSD3* (Wang *et al*., 2018), already discussed above as also responsive to other abiotic stressors. Both genes were found upregulated in response to cold stress, which is consistent with the generalized enhancement of the SOD gene family in foxtail millet under stress conditions (Wang *et al*., 2018). Treatments with self-DNA elicited, substantially, the same

pattern, especially for the more tolerant weed *S. pumila*, with the only exception of *CSD3* in *S. italica* showing a non-significant upregulation. Given the prominent function of these two genes in the antioxidant response to several stress factors, including self-DNA exposure, the observed pattern does not provide useful insight about the relationships between the response to self-DNA and that to thermal stress.

3.6. Conclusions

At the molecular level, among the seven tested abiotic stress-responsive genes (*FSD2*, *ALDH22A1*, *ALDH7B1*, *CSD3*, *WD40-155*, *WD40-144*, *MPK17*), we observed differential expression in four genes in *S. italica* (*FSD2*, *ALDH22A1*, *WD40-155*, *MPK17*) and five genes in *S. pumila* (*FSD2*, *ALDH22A1*, *CSD3*, *WD40-155*, *MPK17*) after 1 and/or 3 hours of exposure. This supports previous indications of the involvement of abiotic stress pathways in the early response to self-DNA. Importantly, our qPCR experiment revealed a clear functional link between self-DNA exposure and ROS production during the early stage, as evidenced by the upregulation of genes associated with antioxidant activity. Furthermore, our analysis confirmed that invasive species exhibit greater resilience compared to cultivated species, likely due to a more rapid and efficient initiation of the immune response, with SOD (superoxide dismutase) proteins playing a crucial role. Overall, our exploratory molecular experiment provides valuable insights and should be followed by further tests addressing more specific cellular processes with fully representative gene sets.

The results of this work have been published on Plants journal (Ronchi, A., Foscari, A., Zaina, G., De Paoli, E., & Incerti, G., 2023. Self-DNA Early Exposure in Cultivated and Weedy Setaria Triggers ROS Degradation Signaling Pathways and Root Growth Inhibition. Plants (Basel, Switzerland), 12(6), 1288. https://doi.org/10.3390/plants12061288).

Chapter 4: Investigation of DNA-RNA hybrid formation in *Arabidopsis thaliana* seedlings exposed to self-DNA

4.1. Abstract

During this third activity, we focused on the exploration of esDNA (extracellular DNA) sensing and discrimination, aiming to gain a more comprehensive understanding of the self-DNA inhibition phenomenon. In mammals, eDNA is detected either through specific transmembrane Toll-like receptors (TLRs) or by being phagocytosed, released inside the cell, and sensed internally. Both scenarios trigger proinflammatory responses. However, there is no evidence of these receptors being capable of distinguishing between self-DNA and nonself-DNA within the same kingdom.

In contrast, plants currently lack evidence of specific DNA receptors. One plausible approach for eDNA sensing in plants could involve the presence of nuclear-encoded RNAs displayed on the cell surface, similar to what has been observed in animals. These RNA molecules could enable cells to differentiate between self- and nonself-DNA through complementary sequence recognition. Another possibility is that fragmented free eDNA may enter living cells through membrane-bound channels or vesicular translocation. This process could disrupt mRNA translation and trigger a plant immune response, resembling the pattern of action seen in RNA interference. These mechanisms could explain the species-specific inhibitory effect attributed to self-DNA or DNA from phylogenetically related species.

To investigate these possibilities, we propose a specific sequence recognition through DNA-RNA complementarity either at the level of nuclear-encoded RNAs present on the cell surface or through binding with mRNAs upon the entry of small-size fragmented eDNA into living cells. These scenarios involve the formation of DNA-RNA hybrids. To test the hypothesis of self-recognition by sequence homology, the formation of DNA-RNA hybrids *in vivo* could be experimentally assessed. Among the available techniques for detecting hybrid formation, DNA-RNA immunoprecipitation (DRIP) based on DNA-RNA hybrid immunoprecipitation (DRIP) is a common and well-known method.

In our study, we implemented a modified version of the DRIP protocol to investigate DNA-RNA hybrid formation. We used single-stranded DNA probes (ssDNA probes) designed to bind to RNA fragments of target genes highly expressed in *Arabidopsis thaliana* roots. Primers for the target genes were designed using appropriate software. Initially, we tested the protocol *in vitro* to verify its efficiency in isolating DNA-RNA hybrids. We induced hybrid formation by incubating RNA extracted from roots with ssDNA probes and then subjected the DNA-RNA mixture to RNase III treatment to degrade double-stranded RNA and RNase H treatment to eliminate RNA moieties in negative controls. Antibody S9.6 and magnetic beads

(Dynabeads Protein A), instead of agarose beads, were used for immunoprecipitation, and amplification was performed using qualitative PCR.

Subsequently, we exposed *Arabidopsis thaliana* seedling roots to short self-DNA probes for one hour and applied the DRIP protocol to investigate DNA-RNA hybrid formation *in vivo*. To minimize the potential carry-over of probes on roots during the extraction process, we implemented root washing-up techniques with DNase I. The results showed the expected amplification of target genes and the absence of amplification in control genes, confirming DNA-RNA hybrid formation *in vivo*.

However, some challenges and questions remain unresolved. It is unclear whether the observed hybrid formation occurred during the exposure phase or the extraction process. Carry-over of DNA probes on roots during extraction could lead to the formation of hybrids unrelated to the exposure. We are actively exploring various approaches to address these challenges, including developing new and more efficient washing methods, optimizing DNase treatments based on hypothesized carry-over percentages, and refining experimental setups.

In conclusion, our methodologically innovative approach could contribute to a better understanding of the interactions between eDNA and the cell environment, shedding light on the advantages and limitations of immunoprecipitation techniques. Although there are challenges to overcome, the DRIP protocol holds promise in studying DNA-RNA hybrids and can provide valuable insights into hybrid formation, epigenetic modifications, and related molecular mechanisms. Further refinement and optimization of the protocol will enhance its reliability and applicability in various biological contexts.

4.2. Introduction

As extensively discussed in the previous chapters of this thesis, extracellular self-DNA (esDNA) inhibitory effect is a natural phenomenon caused by the accumulation of fragmented self-DNA in decomposing aged litter. By inhibiting conspecific root growth and seed germination in a concentration-dependent manner, esDNA could represent a main driver of plant–soil negative feedbacks (Mazzoleni *et al*., 2015a). While the phenomenological evidence on esDNA inhibition has been repeatedly reported, much less is known about the underlying mechanisms at cellular and molecular levels. esDNA has been proposed to function as a damage-associated molecular pattern (DAMP), triggering an early innate immune response in plants characterized by reactive oxygen species (ROS) production, mitogen-activated protein kinase (MAPK) activation, and induction of extra-floral nectar

(Duran-Flores & Heil, 2018). Additionally, studies have shown that exposure to esDNA leads to increased intracellular calcium concentration ([Ca^{2+}]) and plasma membrane depolarization (Barbero *et al*., 2016). Recent research conducted by Chiusano *et al*. (2021) using whole-plant transcriptome profiling in *Arabidopsis thaliana* revealed distinct gene expression patterns and fragment localization in response to exposure to extracellular fragmented self-DNA (conspecific) or nonself-DNA (heterologous). This suggests that plant cells possess the ability to specifically sense and process self-DNA, discriminating it from nonself-DNA. However, despite these findings, the molecular mechanisms underlying esDNA sensing and discrimination from nonself-DNA in plants remain largely unresolved. In summary, while the inhibitory effect of esDNA has been well-documented, our understanding of the cellular and molecular mechanisms involved is still incomplete. Further research is needed to unravel the intricate processes of esDNA sensing, discrimination, and the subsequent plant responses, which will contribute to a comprehensive understanding of this intriguing phenomenon.

As previously mentioned, in mammals extracellular DNA (eDNA) is detected through specific transmembrane Toll-like receptors (TLRs) or, alternatively, eDNA is taken up by phagocytosis and then released and sensed inside the cell, in both cases triggering proinflammatory responses (Heil & Land, 2014) (Figure 4.1). While there is some evidence of bacterial and viral genome recognition as nonself thanks to, respectively, the detection of poor CpG methylation patterns (Barton *et al*., 2006) or DNA with unpaired open ends containing guanosines (Herzner *et al*., 2015), there are no reports on the capability of these receptors to distinguish self- from nonself-DNA within the same kingdom (Duran-Flores & Heil, 2015). Recently, nuclear-encoded RNAs stably attached to the cell surface and exposed to the extracellular space have been discovered, mostly associated with monocytes, suggesting an expanded role for RNA in cell-cell and cell-environment interactions (Huang *et al*., 2020). The potential pairing for sequence homology with complementary sequences could help explaining the mechanism of recognition between self- and nonself-DNA.

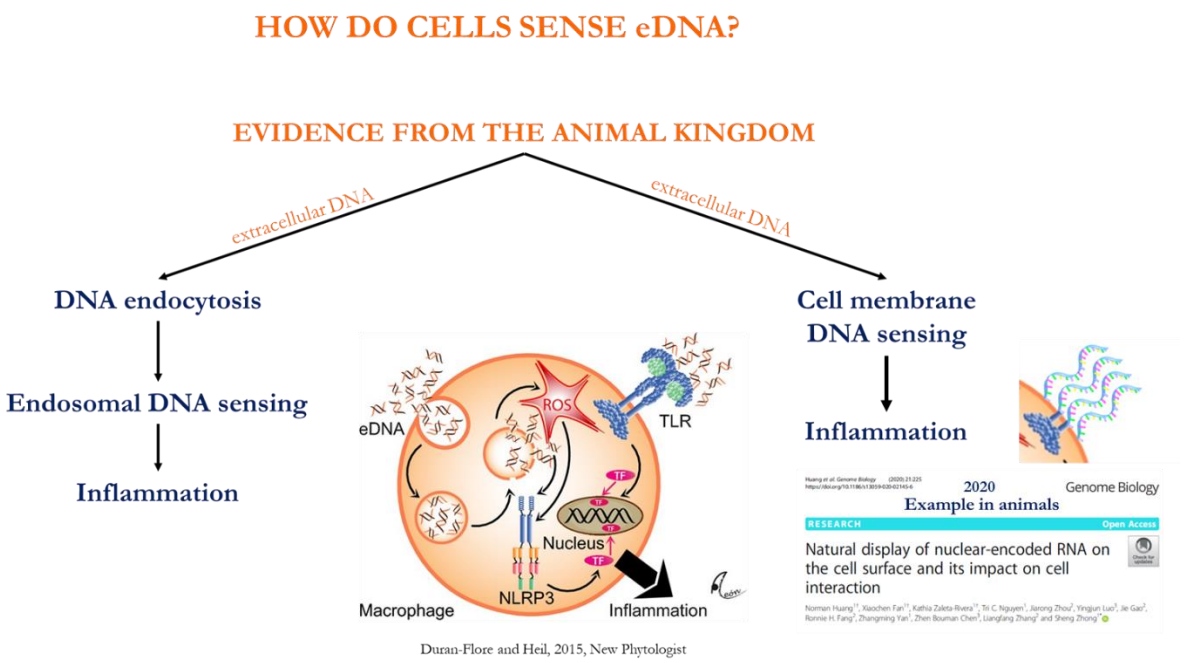

Figure 4.1. Extracellular and intracellular perception of extracellular DNA (eDNA). Mammalian macrophages perceive eDNA both within and outside the cell. Toll-like receptors (TLRs) sense eDNA at their extracellular domains and release transcription factors (TF) that induce gene-expression leading to pro-inflammatory responses. Moreover, there is evidence of recently discovered nuclear-encoded RNAs displayed on the cell surface that could explain the self- vs nonself-DNA recognition for sequence homology. Alternatively, fragmented eDNA can be taken up via phagocytosis, re-released into the cell plasma and then directly or indirectly (via the formation of reactive oxygen species, ROS) activate the NOD-like receptor family protein 3 (NLRP3) inflammasome to trigger proinflammatory responses (adapted from Duran-Flores & Heil, 2015).

Although there is currently no evidence of specific DNA receptors in plants (Monticolo *et al*., 2020), the proposed mechanisms involving membrane-bound receptors or intracellular sensors for eDNA perception and recognition (Bhat & Ryu, 2016) appear to be an unlikely explanation for the detection and discrimination of esDNA. In fact, such mechanism would require a vast array of specific receptors capable of recognizing all the numerous possible sequences resulting from natural or experimental DNA fragmentation (Duran-Flores & Heil, 2015). Instead, a more plausible approach in plants could involve the presence of nuclear-encoded RNAs displayed on the cell surface, similar to what has been observed in the animal kingdom. These RNA molecules could enable cells to differentiate between self- and nonself-DNA through complementary sequence recognition. Alternatively, the perception of fragmented free eDNA may occur through the entry of eDNA into the living cells via membrane-bound channels or vesicular translocation. This process could potentially disrupt mRNA translation and trigger a plant immune response, resembling the pattern of action seen in RNA interference (Bhat & Ryu, 2016). These mechanisms could also provide an

explanation for the species-specificity of the inhibitory effect attributed to self-DNA or DNA from phylogenetically related species (Mazzoleni *et al*., 2015a). In summary, we consider unlikely that the mechanisms of esDNA detection and discrimination in plants involve a large number of specific receptors. Instead, specific sequence recognition through DNA-RNA complementary, either at the level of nuclear-encoded RNAs potentially present on the cell surface, or through binding with mRNAs upon entrance of small-size fragmented eDNA into living cells, could represent a better explanation, able to justify such specific self- nonself-DNA recognition. Noteworthy, both these scenarios would involve the formation of DNA-RNA hybrids. Therefore, the hypothesis of self recognition by sequence homology could be easily tested experimentally by the assessment of DNA-RNA hybrid formation *in vivo* for specific targets, which however has never been performed, to the best of our knowledge, in plants.

Among the various techniques available for the detection of naturally occurring hybrid formation, the most common and well-known is based on DNA-RNA hybrid immunoprecipitation (DRIP). DRIP is a powerful technique used to identify and study DNA-RNA hybrids in biological samples and utilizes specific antibodies that recognize and bind to the hybrids, enabling their isolation from a complex mixture of nucleic acids. Normally this technique is applied *in vitro* to map genomic R-loop formation (Ginno *et al.*, 2012), three-stranded structures ranging from 100 bp to 1–2 kilobases forming during transcription and involved in genome stability and regulation of gene expression, comprising a DNA-RNA hybrid and a displaced single-stranded DNA (Santos-Pereira & Aguilera, 2015). The isolated hybrids can then be further analysed using various approaches, such as sequencing or quantitative PCR, to gain insights into their formation and functions. By utilizing DRIP, researchers can investigate the occurrence of DNA-RNA hybrids under different biological conditions, explore their roles in gene regulation, genome stability, and other cellular processes, and uncover their potential implications in various diseases and biological phenomena.

The DRIPc-seq (DNA–RNA immunoprecipitation followed by cDNA conversion coupled to high-throughput sequencing) protocol from Sanz & Chédin, (2019), in particular, relies on the recovery of the RNA moiety of the DNA-RNA hybrid followed by its conversion in cDNA before amplification, while the DNA moiety is entirely degraded. Specifically, they used the antibody S9.6 for the immunoprecipitation step, a highly specific mouse monoclonal antibody that targets DNA-RNA hybrid but possesses substantial residual affinity also for double-stranded RNA (dsRNA), particularly AU-rich dsRNA (Phillips *et al*., 2013). This binding can be problematic, especially when the DRIP protocol retrieves material for sequencing and

amplification derived originally from RNA, as in DRIPc-seq. To remedy this problem, extracted nucleic acids can be treated with RNase III, which specifically cleaves dsRNA, before DRIP (Hartono *et al*., 2018) (Figure 4.2).

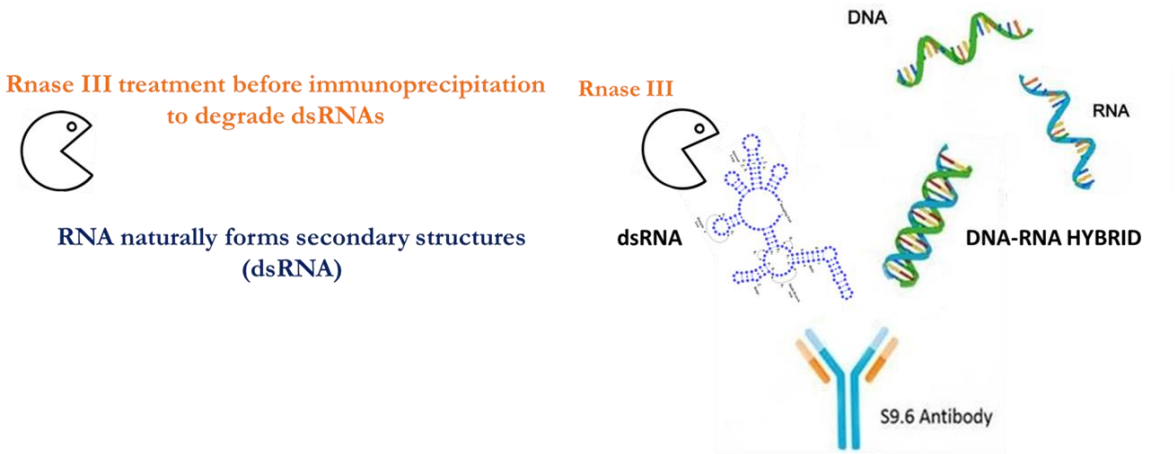

Figure 4.2. S9.6 antibody affinity for DNA-RNA hybrids and ds-RNA. dsRNA binding by S9.6 antibody can be prevented by treating the extracted nucleic acids with RNase III before immunoprecipitation.

In this study, we modified and adapted the Sanz & Chédin, (2019) protocol, used to map genomic R-loops, to investigate the *in vivo* formation of DNA-RNA hybrids after self-DNA exposure. This brought us to face many challenges, in particular contamination and lack of selective target amplification. Moreover, to the best of our knowledge, this is the first implementation of a DNA-RNA immunoprecipitation protocol *in vivo*. Usually, DRIP protocols involve a DNA fragmentation process after extraction and before immunoprecipitation, a step that can threaten the already unstable R-loop structures and makes DRIP-based methods not suitable to query *in vivo* R-loop formation (Sanz & Chédin, 2019). This fragmentation step should not be necessary when the target DNA-RNA hybrids are expected to be short. Moreover, when the focus is solely the detection of the potentially formed target DNA-RNA hybrids, like in our case, not their quantification, a partial loss of signal due to the extraction and immunoprecipitation process would not be a definitive impediment. We started by selecting target genes always highly expressed in *Arabidopsis thaliana* roots (see FPKM - fragments per kilobase of transcript per million fragments mapped- values in Table 4.1 by Liu *et al*., 2012). Single stranded DNA probes (ssDNA probes) of 70-90 nt were designed using the OligoMiner application (Passaro *et al*., 2020) to bind a RNA fragment of the corresponding target gene. Both were selected (probe and target binding sequence) in order to minimize the risk of secondary structure formation, which could compromise the annealing of the

complementary sequences. Primers for the target genes were designed trough the Primer3web v.4.1.0 software (ELIXIR Estonia).

Table 4.1. List of the selected target genes for DNA-RNA immunoprecipitation experiment with FPKM values (Liu *et al*., 2012), coded protein and function.

Number	Gene_ID	Gene_Name	FPKM root (Liu2012)	Coded protein	Function
1	AT1G09780	PGM1	208	2,3-bisphosphoglycerate-independent phosphoglycerate mutase 1	Cellular carbohydrate metabolic process
2	AT3G24503	ALDH2C4	135	Aldehyde dehydrogenase family 2 member C4 (NAD+)	Oxidation of aldehydes to carboxylic acids
3	AT4G37870	PCKA	427	Phosphoenolpyruvate carboxykinase (ATP)	Gluconeogenesis pathway
4	AT5G23020	MAM3	127	Methylthioalkylmalate synthase 3	Glucosinolate biosynthetic process
5	AT5G43780	APS4	232	ATP sulfurylase 4	Sulfur metabolism subpathway
6	AT1G01580	FRO2	117	Ferric reduction oxidase 2	Ferric-chelate reductase for iron uptake
7	AT2G25980	JAL20	139	Jacalin-related lectin 20	Carbohydrate binding
8	AT3G14940	PPC3	192	Phosphoenolpyruvate carboxylase 3	Phosphoenolpyruvate carboxylase
9	AT3G23430	PHO1	227	Phosphate transporter PHO1	Phosphate ion transmembrane transporter
10	AT3G44300	NIT2	124	Nitrilase 2	Detoxification of nitrogen compound
11	AT4G38470	STY46	159	Serine/threonine-protein kinase STY46	Phosphorylation chloroplast precursor proteins
12	AT5G44790	RAN1	157	Copper-transporting ATPase RAN1	Copper import into the cell

Afterwards, we tested our modified version of the DRIP protocol by Sanz & Chedin *in vitro*, to verify that the adapted protocol and selected antibody was suitable and efficient in DNA-RNA hybrid isolation. In our *in vitro* trials, we induced the formation of DNA-RNA hybrids by subjecting RNA extracted from roots to incubation with ssDNA probes, utilizing a hybridization thermal cycle. We then treated the DNA-RNA mixture with RNase III (to degrade dsRNA) and

RNase H, this last one only in the case of negative controls, before the immunoprecipitation step. RNase H is an enzyme that specifically cleaves the RNA of RNA/DNA hybrids that form during replication and repair, like Okazaki fragments and R-loops (Cerritelli & Crouch, 2008; Lee *et al*., 2022). Therefore, by treating our DNA-RNA mixture before immunoprecipitation, we eliminate the RNA moiety impeding hybrid isolation. Through this approach, we can ascertain whether the signals obtained from the positive controls, which were not treated with RNase H, are indeed attributed to the presence of DNA-RNA hybrids or if they stem from other factors (Hartono *et al*., 2018; Sanz & Chédin, 2019). Moreover, instead of using agarose beads like in the Sanz & Chédin, (2019) protocol, we implemented magnetic beads, in particular Dynabeads Protein A. They are superparamagnetic beads with recombinant Protein A (~45 kDa) covalently coupled to the surface and provide a superior alternative to Sepharose resin or agarose resin for immunoprecipitation (IP) by performing a more rapid and gentle magnetic separation, causing minimal physical stress to the target proteins. They allow for isolation of most mammalian immunoglobulins (Ig) with low non-specific binding (Figure 4.3). The amount of Ig captured depends on the concentration of Ig in the starting sample and on the type and source of the Ig (ThermoFisher Scientific, 2023). We also did not perform library construction and sequencing, but rather amplification by qualitative PCR with the probe target gene primers and visualization on agarose electrophoresis gel.

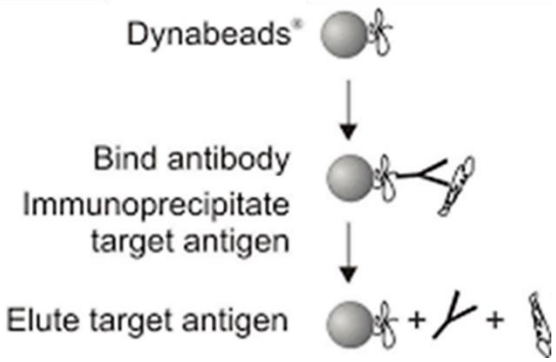

Figure 4.3. Magnetic beads bind the S9.6 antibody, already bound to the target DNA-RNA hybrid, to separate it from the other components in the solution. Then, they release the antibody and target hybrid during the elution phase.

Finally, we exposed *Arabidopsis thaliana* seedling roots to the designed short self-DNA probes during 1 h and applied our tested DRIP protocol to investigate the potential formation of DNA-RNA hybrids and its prospect as a possible mechanism for self-DNA sensing. After DNA-RNA hybrid isolation *in vivo*, we decided to verify if the observed hybrids actually formed during the exposure time or, alternatively, during the extraction process, due to cell lysis,

nucleic acids release into the extraction medium and binding with potential ssDNA probe carried over on roots (Figure 4.4). Moreover, we implemented root washing-up techniques with DNase I to minimize the risk of the above-mentioned carry-over.

Similar applications for the on-purpose creation of hybrids, that testify the feasibility of the method we hereby suggest, involve recent technological advances that have allowed the development of tools and applications based on purposely elicited DNA-RNA hybridization. Among these, Wu *et al*., (2020) developed a novel fluorescent Y-shaped tripartite DNA probe to assess for the first time RNA imaging in living mice, via an *in vivo* hybridization chain reaction. In plants, applications are limited to in situ hybridization *in vitro*, as in the study by Duncan *et al*., (2016), where a single molecule fluorescence technique was applied to paraformaldehyde-fixed Arabidopsis root cells exposed to fluorescently labelled DNA oligonucleotides, capable of hybridizing with different portions of the target transcript. In previous applications, antisense oligodeoxynucleotides have been successfully administered to target specific mRNAs through hybridization of complementary sequences, through infiltration with a syringe to detached plant leaves or excised leaf segments (e.g. Dinç *et al*., 2011).

In conclusion, besides investigating the possible formation of DNA-RNA hybrids after DNA exposure as a possible mechanism for self-DNA recognition and cellular response, our methodologically innovative approach could help towards the full understanding of the interactions between eDNA and the cell environment, providing useful insights on advantages and limitations of immunoprecipitation techniques.

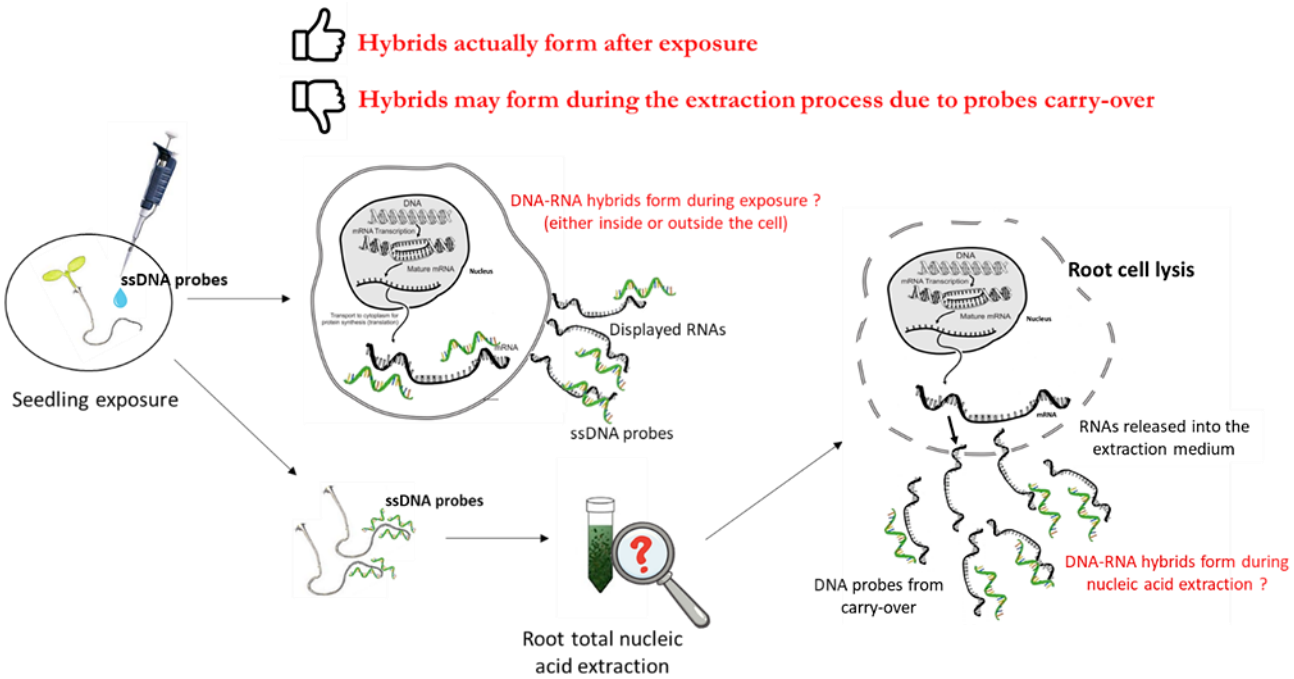

Figure 4.4. Illustration of our hypothesis according to which *in vivo* isolated DNA-RNA hybrids could form either during self-DNA exposure or during the extraction phase due to ssDNA probe carry-over on roots.

4.3. Materials and Methods

4.3.1. Gene selection, probe and primer design

Target genes were selected, after a careful bibliography research, because always highly expressed in *Arabidopsis thaliana* roots (see FPKM values in Table 4.1 by Liu *et al*., 2012). DNA probes (listed in Table 4.2) were designed through the OligoMiner application (Passaro *et al*., 2020) to bind a short fragment of the target gene RNA, less likely to form secondary structures. In particular, inputs for the OligoMiner application were exons selected from the target gene sequence: for each gene we selected one exon (neither at the beginning, nor at the end of the gene) long enough to be able to design both the probe and primers within it. The parameters for OligoMiner were set as follows: probe length (Min. 70; Max. 90 bases), probe melting temperature (Min. 52 °C; Max. 58 °C), probe GC (%) content (Min. 20%; Max. 80%). Selected probe strand (plus or minus) was set as the opposite of the target gene strand (while the input coding exon always corresponded to the gene sequence on the plus strand). The primers (listed in Table 5.2) for the target genes were designed through the Primer3web v.4.1.0 software (ELIXIR Estonia) setting the following parameters: primer length (Min. 18; Opt. 20; Max. 25 bases), primer melting temperature (Min. 58 °C; Opt. 60 °C; Max. 65 °C), and amplicon length (90–200 bases). To specifically avoid the accidental amplification of the

DNA probes, possibly still present in the final cDNA, one primer was designed to match the cDNA fragment corresponding to the probe hybridisation site, while the other was placed outside, few nucleotides away. They were strategically positioned close to the hybridization site to avoid potential amplification issues caused by the action of RNase III, which can degrade large RNA fragments forming double-stranded RNA structures (Figure 4.5). Primer specific amplification and amplicons size was verified using cDNA as template for qualitative PCR.

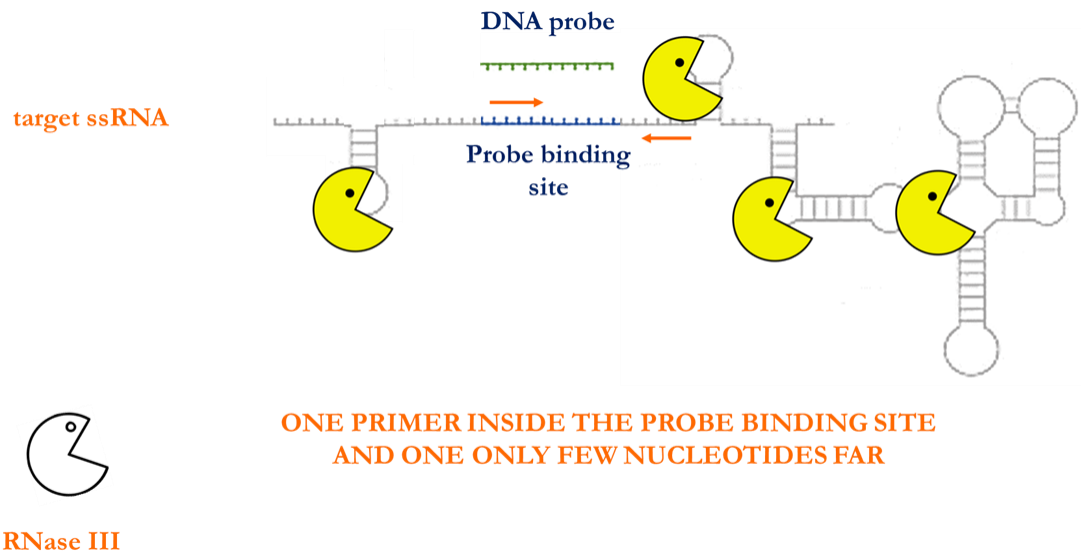

Figure 4.5. Primer designed through Primer3 software for the DNA-RNA immunoprecipitation experiment: one primer was designed to match the cDNA fragment corresponding to the probe hybridisation site, while the other was placed outside, few nucleotides away, in order to avoid amplification issues caused by the action of RNase III.

Table 4.2. In the following table we present the target genes of our DRIP experiment specifying Gene ID, Gene Name, Forward (Fwd) and Reverse (Rev) Primers and ssDNA probe. Primers were designed through the Primer3 software, while we used Oligominer application for ssDNA probes.

Gene ID	Gene Name	Primer (5'-3')	ssDNA probe
AT1G09780 Minus strand	*PGM1*	Fwd: AGCCTGGTGCTAATGACCAG Rev: CAGCATCACCGTCCACAATC	GTAACAACAGCATCACCGTCCACA ATCGGACCAACTGCTTTCCCTGAT TCATCAACAATCACAAACGGGG
AT3G24503 Minus strand	*ALDH2C4*	Fwd: GGGAAAATATGCTGATATTCCGG Rev: AAGATTGACGCGTCATTTTAAGA	CAAAGATTGACGCGTCATTTTAAGA GTCTCGCCGTGGATTTTATCTGCT GCACCCGCATTGTATCGAAAATGA CCGGCTG

AT4G37870 Minus strand	*PCKA*	Fwd: AGGAGATCCGGCGGAGAA Rev: CCAGTAGCCGGAGAAAAGAT	CACCAGTAGCCGGAGAAAAGATAGAATGATGTTGGCCGTGAGCGTACGCCGGAGTAGTTGAACCATCGGT
AT5G23020 Plus strand	*MAM3*	Fwd: CTGTCGCTCCATGGTTCTCC Rev: AACAGAGTCGCCTTGTCGTA	AACAGAGTCGCCTTGTCGTATGGACGGGTCAGGCGAAGAGAGGGAAAAGAAGATCCGATGGGTAACCCTG
AT5G43780 Minus strand	*APS4*	Fwd: CATGGGGAACCACGGCTC Rev: TCGGCTCCAAAACTTGTAAATCA	ACTTGATCGGCTCCAAAACTTGTAAATCACCTCCAATCAACCAGTTTCCAGCTTTGGTGATTGCTTCTTCCGCATAAGG
AT1G01580 Plus strand	*FRO2*	Fwd: CCACATATCCGAAGATAAGGAGA Rev: GATGAAGGAGAAACTTATGCCGA	AGCGATGAAGGAGAAACTTATGCCGACGTGGAGGACAAAGAAGAGCATGAAGACGATGTAGAGATAGTGAGTGTAGAAGAAGACTTCGAA
AT2G25980 Minus strand	*JAL20*	Fwd: CATCAATAGAAGTGACCTGTGACA Rev: CTCGCTCTTACGTCCATATGT	CGCTCGCTCTTACGTCCATATGTAGGAGATGTTCTGTCTTTTGATGTCTTGAAACTCAACGACCTAACTCGGTTTGTATTGCCAGAGACT
AT3G14940 Plus strand	*PPC3*	Fwd: TTGACATCAGGCAAGAGTCTG Rev: GACCAGTCTCTATAGGAGGAACC	AGACCAGTCTCTATAGGAGGAACCGATGTCCAAGTGCTTGGTGATAGCATCCAAGACATCTGTGTGGCGT
AT3G23430 Minus strand	*PHO1*	Fwd: AGGAGAACTAAGTGAGATACAAAGT Rev: GCCTCCTTTTGTTTTGCTCC	GCCTCCTTTTGTTTTGCTCCTCGTTGCAGAGTTTATGAAACTCACACCGTTCCTCTCTAAGGCCTCTATGATTTCATCTGTTCTTGATGT
AT3G44300 Plus strand	*NIT2*	Fwd: GGATCGGAGCTGGTTGTGTT Rev: TTCGTTATGAACTCCCACCCC	CCTTCTTCGTTATGAACTCCCACCCCTAAACCAAACCTAAAACCTCGAGGATAACCACCGATAAACGCCTCCG
AT4G38470 Plus strand	*STY46*	Fwd: TTGCAGAGCCAAAGCTGG Rev: ATTGGGTATTGGAACATGCGT	TGGCACCTGTTTGCCCATTTTCCTTTTCCGGAGAGAAGGATTGCTGCATAGGCCAGCTTTGGCTCTGCAA
AT5G44790 Minus strand	*RAN1*	Fwd: TTCAACTAACATGGATGTGCTCG Rev: GAGACCAAAATCCAGTGACTGC	GGAGACCAAAATCCAGTGACTGCTCCATATAAAAGAGCCCCAACAGAGTAGAAGTAAGAAGCAGACGTGCCCAGAG

4.3.2. *In vitro* testing of DNA-RNA immunoprecipitation (DRIP) protocol

The following procedure has been adapted from the Sanz & Chedin, (2019) protocol, normally used *in vitro* to map genomic R-loops. The protocol has undergone the following modifications and was initially tested *in vitro* before being applied *in vivo* to investigate hybrid formation following self-DNA exposure.

4.3.2.1. RNA-DNA hybridization and dsRNA purification

RNA was extracted from *Arabidopsis thaliana* seedling roots with Spectrum™ Plant Total RNA Kit (STRN50, Sigma-Aldrich) following manufacturer's instructions. Extracted RNA was treated with DNase I (AMPD1, Sigma-Aldrich, 1 unit/µL), at least 1 unit per µg of RNA treated (one unit completely digests 1 µg of plasmid DNA to oligonucleotides in 10 min. at 37 °C.), to eliminate residual genomic DNA. The solution containing RNA, DNase I and DNase I buffer was kept in agitation at room temperature for 15 min. Afterwards, the solution was precipitated overnight at -20 °C by adding sodium acetate (1/10 of the Volume) and cold isopropanol (2/3 of final volume). We centrifugated the solution at 4 °C for 15 min at 14000 rpm and eliminated the supernatant. The pellet was washed with 500 µL of 80% ethanol and we repeated the centrifugation and supernatant elimination step. Residual ethanol was air-dried (keeping the tube in ice) and the pellet was resuspended in sterile water. Absence of genomic DNA was tested by running a 2% agarose gel with the products of a qualitative PCR (same PCR cycle and reagents presented below) performed with the designed primers and extracted RNA, expecting complete absence of amplification. Extracted RNA was quantified by fluorimeter Qubit 3.0 (Life Technology, Carlsbad, CA, USA), the quality was assessed by spectrophotometer Nanodrop ND 1000 (Thermo Fisher Scientific, Waltham, MA, USA) and its integrity was evaluated on 1% agarose gel.

Moving forward, 5 µg of the extracted RNA were transferred in a PCR strip tube along with 500 ng of each of the selected ssDNA probes (four probes in total, ~ 5 µL of each probe 5 µM, Figure 4.6). The DNA-RNA hybrids were formed through the following thermal profile:

1. Heat to 95 °C and maintain the temperature for 2 min (denaturation step);
2. Cool gradually to 90 °C and maintain the temperature for 2.5 min;
3. Repeat step 2, cooling down of 5 °C each time, until reaching 25 °C;
4. Cool in ice for temporary storage.

At the completion of the cycle, the DNA-RNA solution was treated with RNase III (Ambion™ RNase III, AM2290, ThermoFisher). We added 6 µL of RNase III (equal to 6 units, where 1 unit is defined by the producer as the amount of enzyme catalysing the cleavage of 1 µg of 500 bp dsRNA substrate to approximately 12–30 bp fragments in 60 min at 37°C), 3 µL of buffer for RNase III (10X RNase III Reaction Buffer: 500 mM NaCl; 100 mM Tris pH 7.9; 100 mM $MgCl_2$; 10 mM DTT), 2 µL of buffer for RNase H (RNase H; New England BioLabs, cat. no. M0297S; 10X RNase H Reaction Buffer: 500 mM Tris-HCl; 750 mM KCl; 30 mM $MgCl_2$; 100 mM DTT, pH 8.3) and sterile water to a final volume of 50 µL. We then incubated the sample at 37 °C for 1.5 hour. Negative controls were contemporary treated also with 4 µL of

RNase H (equal to 20 units, where 1 unit is defined by the producer as the amount of enzyme required to produce 1 nmol of ribonucleotides from 20 picomoles of a fluorescently labelled 50 base pair RNA-DNA hybrid in a total reaction volume of 50 µl in 20 minutes at 37°C). We expected lack of amplification of the ssDNA probe corresponding genes in the negative controls, since RNase H degrades RNA in DNA-RNA hybrids. This would prove that signal found in positive controls derives indeed from hybrid formation. After treatment, the DNA-RNA solution was immediately cooled down in ice.

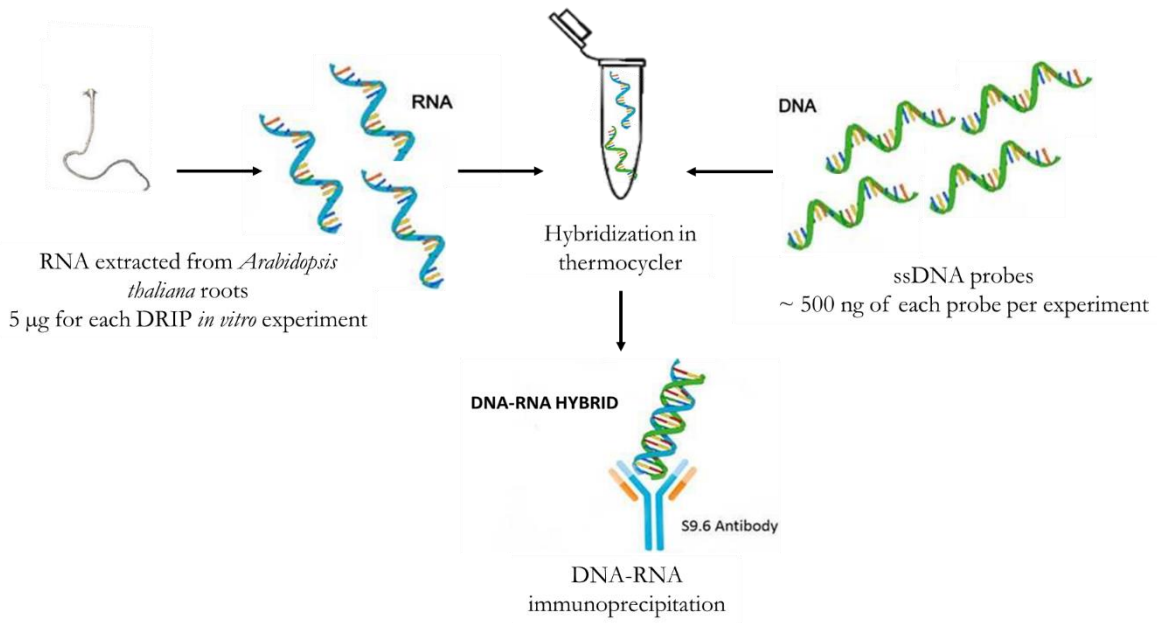

Figure 4.6. During the *in vitro* verification of our modified DRIP protocol, we triggered DNA-RNA hybrid formation by mixing extracted RNA (5 µg) with 500 ng of each of the four selected probe. The solution was incubated in a thermal cycler where it was subjected to a slow temperature decrease (starting from denaturing temperature, 95 °C) to favour the DNA-RNA annealing process.

4.3.2.2. DNA-RNA immunoprecipitation (DRIP)

Composition of the reagents used for the hybrid immunoprecipitation:

- TE buffer → 10 mM Tris, pH8, and 1 mM EDTA.
- 1 M Sodium phosphate, pH 7 → 39 mL of 2 M monobasic sodium phosphate, 61 mL of 2 M dibasic sodium phosphate and 100 mL of Nanopure water.
- 10× DRIP binding buffer → 100 mM sodium phosphate, pH 7, 1.4 M NaCl and 0.5% (vol/vol) Triton X-100. The 1x binding buffer consists of the 10x binding buffer diluted ten times in TE buffer.
- DRIP elution buffer → 50 mM Tris, pH 8, 10 mM EDTA, pH 8, and 0.5% (vol/vol) SDS.

- 80% (vol/vol) Ethanol → absolute ethanol (four parts) diluted with molecular biology-grade water (one part).

The DNA-RNA solution was transferred into a 1.5 ml Eppendorf where we also added 150 µl of TE buffer, 22 µl of 10× DRIP binding buffer and 2 µL of the S9.6 antibody (Anti-DNA-RNA Hybrid Antibody, clone S9.6, MABE1095, Sigma-Aldrich). The solution was incubated for 17 hours at 4 °C while gently inverting on a mini-tube rotator (~10 r.p.m.). After incubation, 100 µl of magnetic beads (Dynabeads™ Protein A, 10001D, ThermoFisher) were washed with 700 µL of 1× DRIP binding buffer by inverting the tube on a mini-tube rotator for 10 min. at room temperature. Beads were put on a magnetic rack to discard the supernatant. The wash was repeated one more time. The DNA-RNA solution was added to the washed magnetic beads and incubated for 2 hours at 4 °C while gently inverting on a mini-tube rotator (~10 r.p.m.). During this incubation time, the magnetic beads bind the antibody, already bound to the DNA-RNA hybrids (100 µL of Dynabeads Protein A will isolate approximately 25–30 µg human IgG from a sample containing 20–200 µg IgG/mL). The solution with the beads was then put on the magnetic rack and the supernatant was discarded. The beads were washed with 750 µl of 1× DRIP binding buffer by inverting the tube on a mini-tube rotator for 15 min. at room temperature. The solution was put on a magnetic rack to discard the supernatant. The wash was repeated one more time. 300 µl of DRIP elution buffer and 7 µL of proteinase K (20 mg/mL) were added to the beads (in order to detach the antibody-hybrids from the beads). The tube was incubated with rotation at 55 °C for 45 min. in a temperature-controlled rotating oven. After incubation, the solution with the beads was put on a magnetic rack. Meanwhile, a 2-mL phase-lock gel tube was spinned for 1 min. at 16,000g to pellet the gel. The supernatant of the tube with beads (this time containing the DNA-RNA hybrids) was transferred to the 2-mL phase-lock tube and 300 µl of phenol/chloroform/isoamyl alcohol (25:24:1) were added to separate the phase, nucleic acids from the rest. The tube was inverted gently four to five times and spinned down at 16,000g for 10 min. at room temperature. The DNA-RNA hybrids (top aqueous phase, around 290 µL) were transferred from the phase-lock gel tube into a clean 1.5-mL tube and mixed with 1.5 µl of glycogen, 29 µl of 3 M NaOAc, pH 5.2 (1/10 of the Volume), and 725 µl of 100% (vol/vol) ethanol (2.5 times the initial Volume). The tube was inverted four to six times and incubated overnight at –20 °C to increase precipitation yield. Then, the tube was spinned at 16,000g for 35 min at 4 °C. The supernatant was discarded and the pellet was washed with 200 µL of room-temperature 80% (vol/vol) ethanol. The tube was spinned for 10 min at 16,000g at 4 °C and the supernatant

discarded. The pellet was air-dried for 10–15 min and resuspended in 10 µL of RNase-free TE buffer.

4.3.2.3. DNase treatment, RNA reverse transcription and PCR amplification

In the resuspended solution were added 3 µl of Dnase I (AMPD1, Sigma-Aldrich, to eliminate the DNA strand in the DNA-RNA hybrid), 1.44 µl of 10x buffer for DNase I and the mixture was incubated at 37 °C for 45 min in gentle agitation. Then, 0.5 µL of the stop solution (0.5 M EDTA, pH 8) were added and the tube was incubated at 70 °C for 10 min to heat-inactivate the DNase I enzyme. At this point of the protocol we are left only with the RNA strands of the DNA-RNA hybrids captured by the antibody and we can proceed with the reverse transcription. Since RNA is very sensitive to environmental RNase and prone to degradation (Kagzi *et al*., 2022) the following passages are to be handled with extreme care and in complete sterile conditions in order to avoid loss of material. For the Reverse Transcription step we used the SuperScript II Reverse Transcriptase (18064022, ThermoFisher Scientific, 200 U/µL, one unit incorporates 1 nmole of dTTP into acid-precipitable material in 10 min. at 37°C using poly(A)•oligo$(dT)_{25}$ as template-primer), which is able to synthesize first-strand cDNA at higher temperatures than conventional reverse transcriptase, providing increased specificity, higher yields of cDNA, and more full-length product. I. The following reaction was set up in a PCR strip tube:

- ~16 µl of the hybrid RNA;
- 1 µl Deoxynucleotide mix (10 mM dATP, 10 mM dCTP, 10 mM dTTP, 10 mM dGTP);
- 1 µl Random nonamers (50 µM in water);
- 6 µl buffer 5x (250 mM Tris-HCl, pH 8.3; 375 mM KCl; 15 mM $MgCl_2$);
- 1 µl SuperScript II Reverse Transcriptase (200 U/µL) ;
- 1 µl RNase inhibitor (20 units/µl);
- 3 µl DTT (100 mM);

to a final volume of ~30 µL.

The reaction was mixed by pipetting gently and incubated at 25 °C for 15 min. and at 42 °C for 50 min., following the instructions of the RT enzyme manufacturer. After incubation, the PCR reactions were prepared in a PCR strip as illustrated in Table 4.3. PCR reactions were exposed to the thermal cycle presented in Table 4.4.

Table 4.3. Qualitative PCR reaction mix.

Component	25 µl reaction
10 µM Forward Primer	0.5 µl
10 µM Reverse Primer	0.5 µl
Template DNA	1.5 µl
One*Taq* 2X Master Mix with Standard Buffer (M0482, NEB)	12.5 µl
Nuclease-free water	to 25 µl

Table 4.4. Qualitative PCR reaction thermal cycle.

STEP	TEMP	TIME
Initial Denaturation	94 °C	30 seconds
26 Cycles		
Denaturation	94 °C	30 seconds
Annealing	60 °C	30 seconds
Extension	68 °C	30 seconds
Final Extension	68 °C	5 minutes
Hold	4-10 °C	∞

4.3.2.4. Non-denaturing Polyacrylamide Gel Electrophoresis

Results from the PCR amplification were visualized on non-denaturing polyacrylamide gel electrophoresis. Each gel was hand-casted with the following reagent volume (Table 4.5) and run at 100 V for 50 min. The gel was visualized under UV lights. Expected results included amplification of target amplicons (gene sequences corresponding to the given probes at the beginning of the protocol) and non-amplification of the control genes for which probes were not provided. For the samples treated with RNase H, we expected complete absence of amplification for both target amplicons (probes provided) and controls genes (probes not provided). This would confirm that the observed amplifications in the samples not treated with RNase H indeed derive from hybrid formation.

Table 4.5. Polyacrylamide gel formula.

Gel %	30% Acrylamide (29:1)	H2O (ml)	5x TBE (ml)	APS (µl)	TEMED (µl)
10 %	4.0 ml	5.6	2.4	200	10

To summarize, in Figure 4.7 the workflow of the *in vitro* experiment is showed.

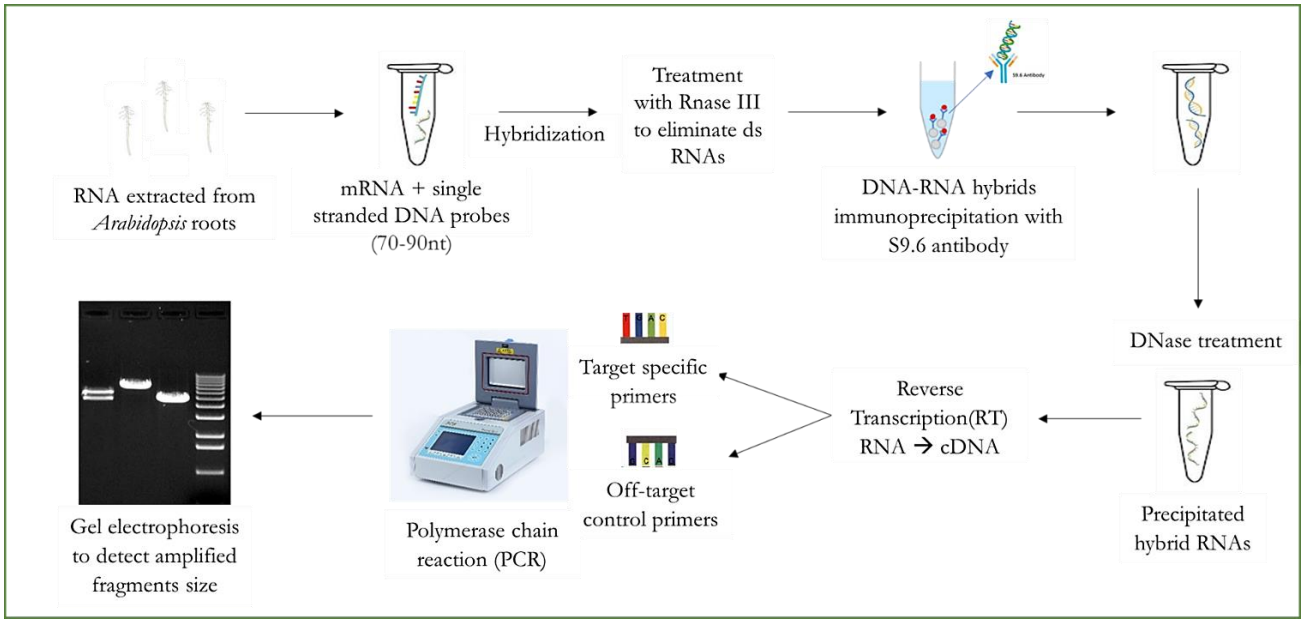

Figure 4.7. *In vitro* experiment workflow. Experiment steps include: RNA extraction from Arabidopsis roots; RNA and ssDNA probe hybridization; RNase III treatment to eliminate dsRNAs; DNA-RNA hybrid immunoprecipitation; DNase I treatment to remove the DNA moiety of the hybrid; Reverse Transcription to convert precipitated RNAs to first strand cDNA; qualitative PCR amplification of target (probe provided at the beginning of the experiment) and control genes (probe not provided) with the designed primers.

4.3.3. *In vivo* investigation of DNA-RNA hybrid formation after self-DNA exposure

4.3.3.1. Seed sterilization, vernalization and germination

Arabidopsis thaliana Col 0 seeds were sterilized with 1% NaClO solution for 5 min., then rinsed 5 times with sterile water during 1 min. for each wash. Seeds were placed on a filter paper in a Petri dish and incubated at 4 °C for 48 hours (vernalization). For each *in vivo* DRIP experiment, we sterilized 90 seeds, which were distributed on 3 Petri dishes (30 seeds per dish), filled with Murashige and Skoog growth medium (1 L made with: 4.4 g Murashige-Skoog basal medium with Gamborg's vitamins – Sigma Aldrich –; 30 g sucrose; 16 g agar; sterile water to final volume), above mesh (Figure 5.7). The Petri dishes were hermetically closed and placed in a growth chamber under standard controlled conditions (22 ± 2 °C, 50% RH, 16 h day and 8 h night photoperiod) for about 10 days, over an inclined plane to favour straight root growth through geotropism and prevent root from growing inside the growth medium.

4.3.3.2. Self-DNA exposure

When their roots reached around 1.5 - 2 cm, Arabidopsis seedlings were moved onto a Petri dish lid (Figure 4.8) and exposed to 5 µl of selected self-DNA probe solution (six probes in

total) for 1 hour at room temperature and at the concentration of 80 ng/µl per probe (Figure 4.9). Roots were exposed by micro pipetting along the root and in particular the root apex. The lid was partially closed with another Petri lid to limit solution evapotranspiration. After exposure, roots were separated from the rest of the plant, collected and washed with sterile water. Collected roots were stored at - 80 °C.

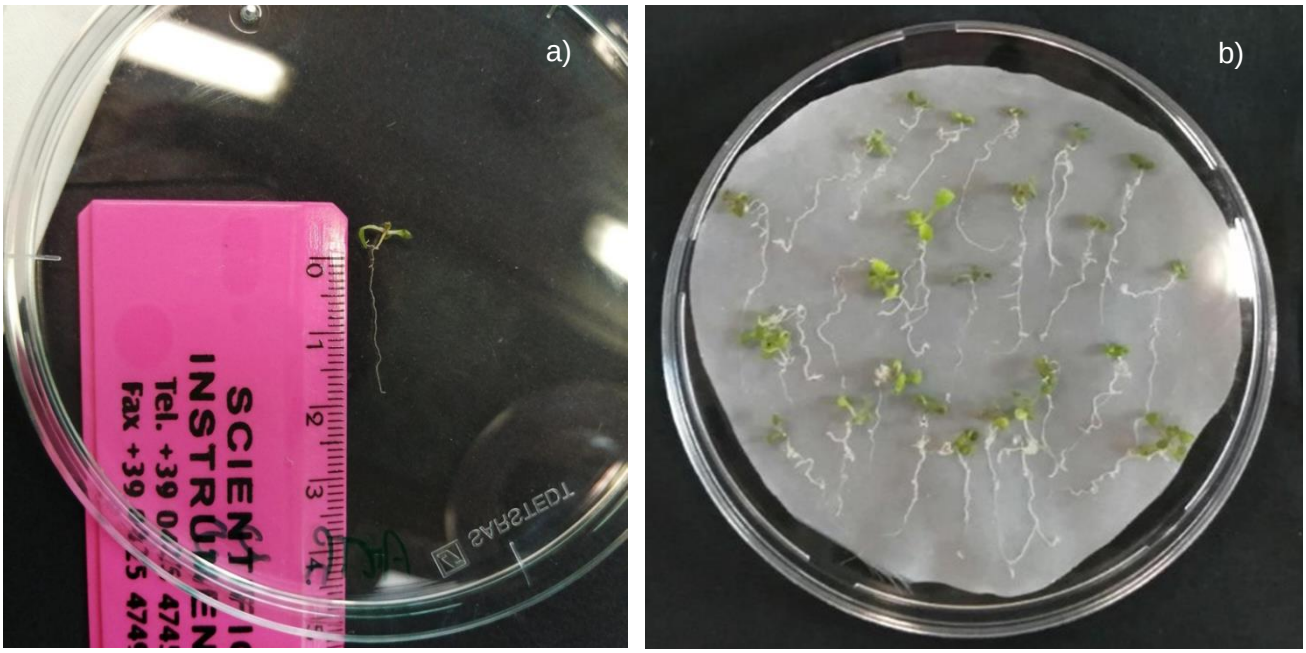

Figure 4.8. a) *Arabidopsis* seedling selected for self-DNA exposure with root of 1.5 - 2 cm; b) Arabidopsis seedlings placed on mesh on a Petri lid for self-DNA exposure.

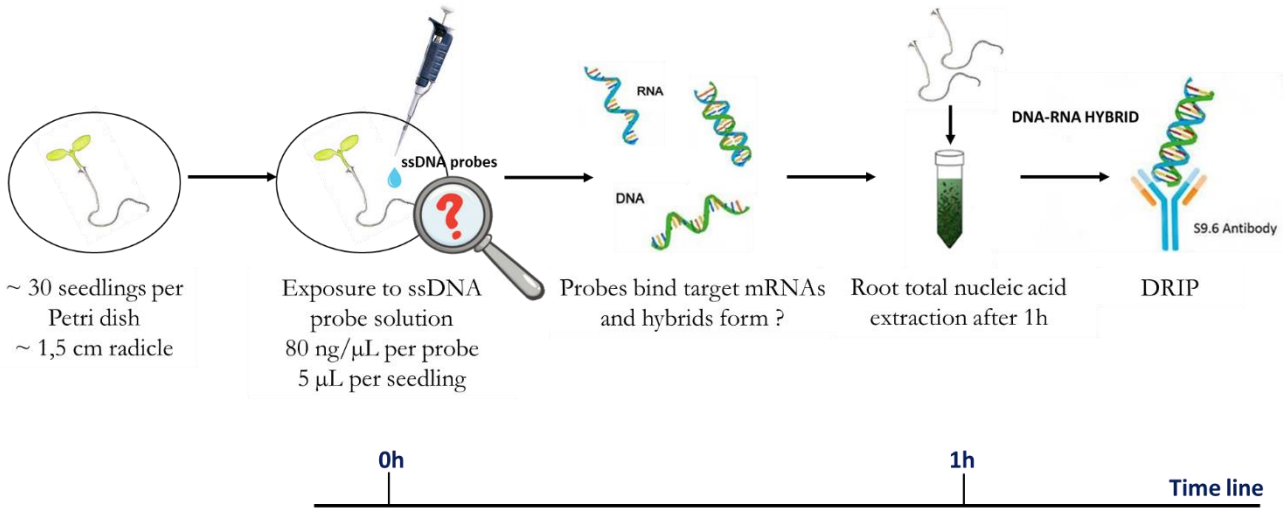

Figure 4.9. Arabidopsis seedling exposure to ssDNA probe solution by micro pipetting the root apex; roots collection after 1 h exposure; and total nucleic acid extraction followed by immunoprecipitation of potentially formed DNA-RNA hybrids.

4.3.3.3. Total nucleic acid extraction

The following passages are adapted from Doyle & Doyle, (1987) nucleic acid extraction protocol. Collected roots (around 20 mg per experiment) were powdered with liquid nitrogen and a small pestle. 900 µL of warm lysis buffer (2 mL 2.5% CTAB buffer; 20 µL β-mercaptoethanol; 0.5 µL proteinase K, 20 mg/mL), previously prepared was added. The material was incubated at 65 °C for 30 minutes, shaking occasionally, then transferred on ice for 10 min. 900 µL of chloroform:isoamyl alcohol 24:1 (v/v) were added and the tube was inverted gently for 10 min. After spinning at 16000g for 30 min. at 4 °C, the aqueous phase (~ 800 µL) was transferred into a clean tube, where were also added 80 µL of sodium acetate (1/10 of the volume) and 590 µL of cold isopropanol (2/3 of the final volume). The tube was inverted gently and placed at - 20 °C for at least 30 min. After spinning for 30 min. at 4 °C, the supernatant was discarded, and the pellet washed twice with 500 µL of 80% ethanol. Finally, ethanol was removed and air dried and the pellet resuspended in sterile water.

The extracted material was then treated with RNase III, immunoprecipitated, treated with DNase I, reverse transcribed and amplified in qualitative PCR as for the *in vitro* experiment (Figure 4.10). The absence of genomic DNA contamination in the final cDNA was confirmed by employing specific primers designed to be placed on two contiguous exons. This approach enabled the detection of any potential genomic DNA traces through qualitative PCR, where the amplicon size would encompass the intron length. Like before, we expect the amplification of target amplicons (gene sequences corresponding to the exposure probes at the beginning of the protocol) and non-amplification of the control genes for which probes were not provided.

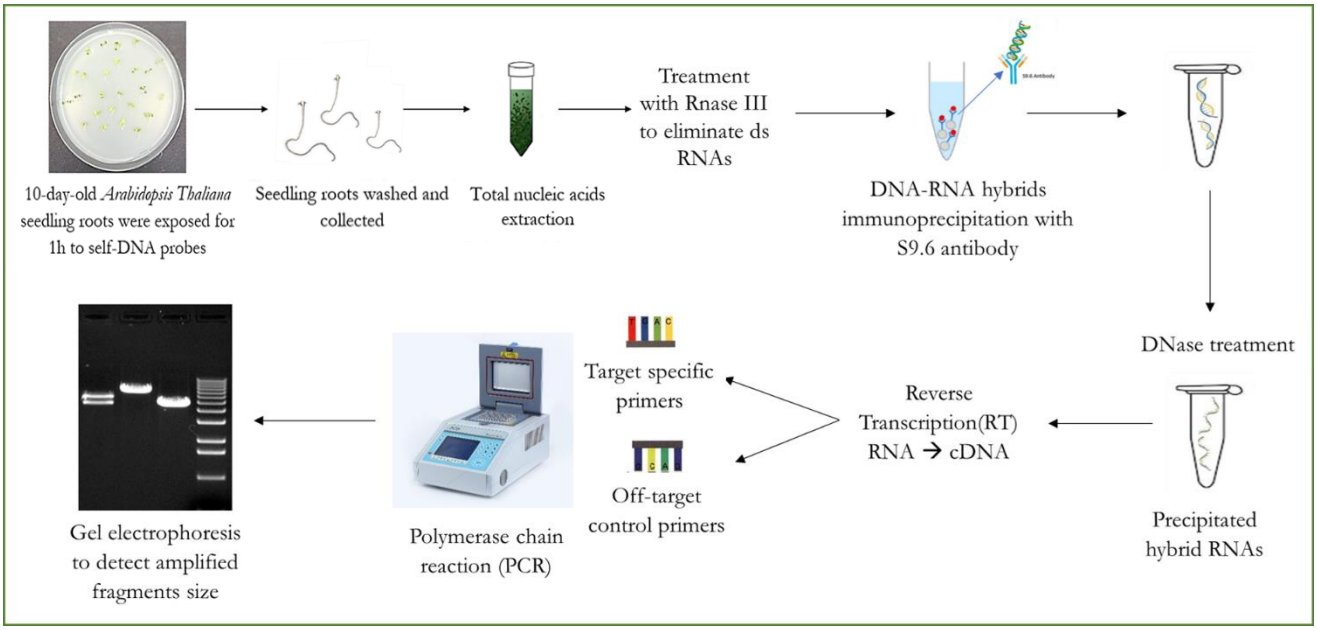

Figure 4.10. *In vivo* experiment workflow. Experiment steps include: Arabidopsis seedling exposure to selected self-DNA probe solution for 1 h; seedling roots were then washed and collected; a total nucleic acid extraction from the collected roots was performed and the extracted DNA-RNA mixture was treated with RNase III like in the *in vitro* experiment; the solution was immunoprecipitated and treated with DNase I to remove the DNA moiety of the hybrid; precipitated RNAs were converted to first strand cDNA through Reverse Transcription; finally, qualitative PCR amplification of target and control genes was carried out with the designed primers.

4.3.4. Verification of the actual molecular process causing hybrid formation *in vivo*

4.3.4.1. Testing hybrid formation during the extraction phase due to probe carry-over

After *in vivo* isolation of DNA-RNA hybrids, we verified whether their formation actually occurs during self-DNA exposure or during the extraction, due to ssDNA probe carry-over on roots (see introduction of this section for details). In order to do so, we did not expose Arabidopsis seedlings to the self-DNA probes, but we added 1 µL for each of the selected probes at 100 µM (~ 2 µg of each probe, six probes in total) directly into the extraction medium (lysis buffer), to simulate the potential carry over (Figure 4.11). Considering that for each *in vivo* experiment we collected roots from 90 seedlings, each exposed to 5 µL at the concentration of 80 ng/µL per probe (six probes in total), adding 12 µg of self-DNA probes to the root mixture means that we are taking into account a root carry-over of 5% (80 ng x 5 x 6 x 90 = ~216 µg of self-DNA; $\frac{12\ \mu g \times 100}{216\ \mu g}$ = ~5%). The lysis buffer was then added to the collected roots, already pestled in liquid nitrogen. The following passages are the same as those performed during the *in vivo* protocol (see section 4.2.3).

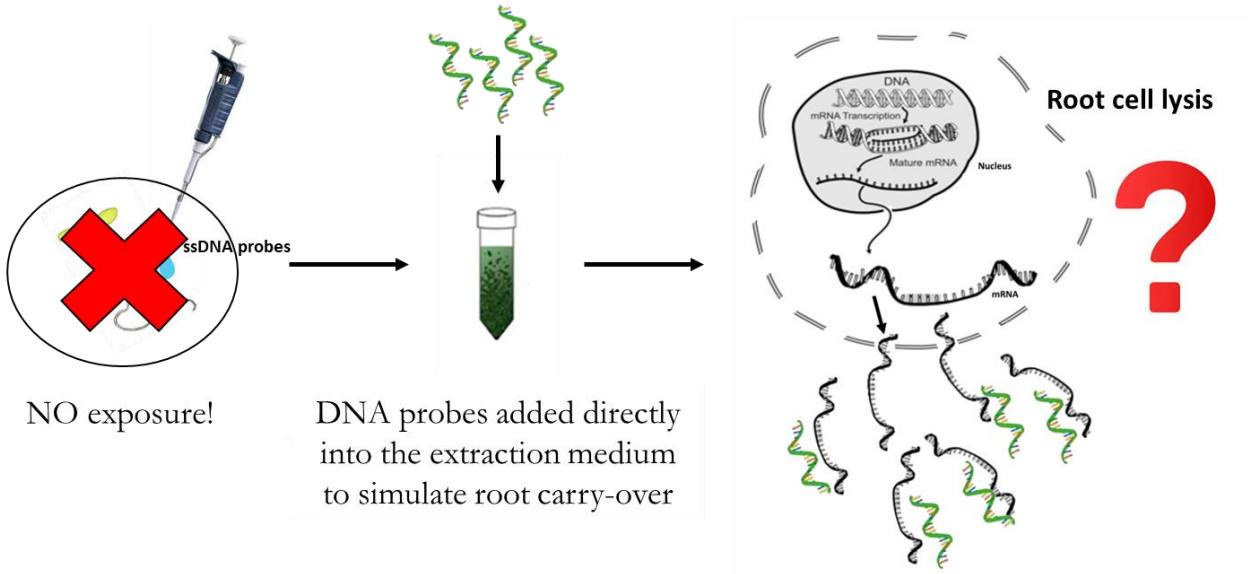

Figure 4.11. Testing the potential formation of DNA-RNA hybrids during the extraction phase, due to cell lysis, cell nucleic acid release and annealing with DNA probes, possibly carried over on roots.

4.3.4.2. Preventing hybrid formation during the extraction phase

Since the results were positive, confirming that the hybrids can form during the extraction phase in case of DNA probe carry-over on roots, we tested a DNase treatment to eliminate this potential carry-over. After collecting not exposed roots, we added the probes directly in the collection tube (1 µL per selected probe at 2000 ng/µL concentration, 6 µL in total), with enough sterile water to cover the roots. Then, we added ~15 µL of DNase I and buffer 10x and incubated the solution at 37 °C for 30 min. Considering we are adding to the roots 12 µg of DNA probes (5% carry-over), the ratio probes:DNAse is 1:1.25. After treatment, we added 15 µL of stop solution, the roots were pestled directly in the liquid, keeping the tube on ice, and the lysis buffer was added to proceed with total nucleic acid extraction and immunoprecipitation (Figure 4.12). A controlled sample was included in the experiment and not treated with DNase. This sample underwent the same incubation process but with the use of water instead of DNase reagents. At the end of this experiment, we expected non amplification in the treated sample and amplification of probe target genes in the non-treated one.

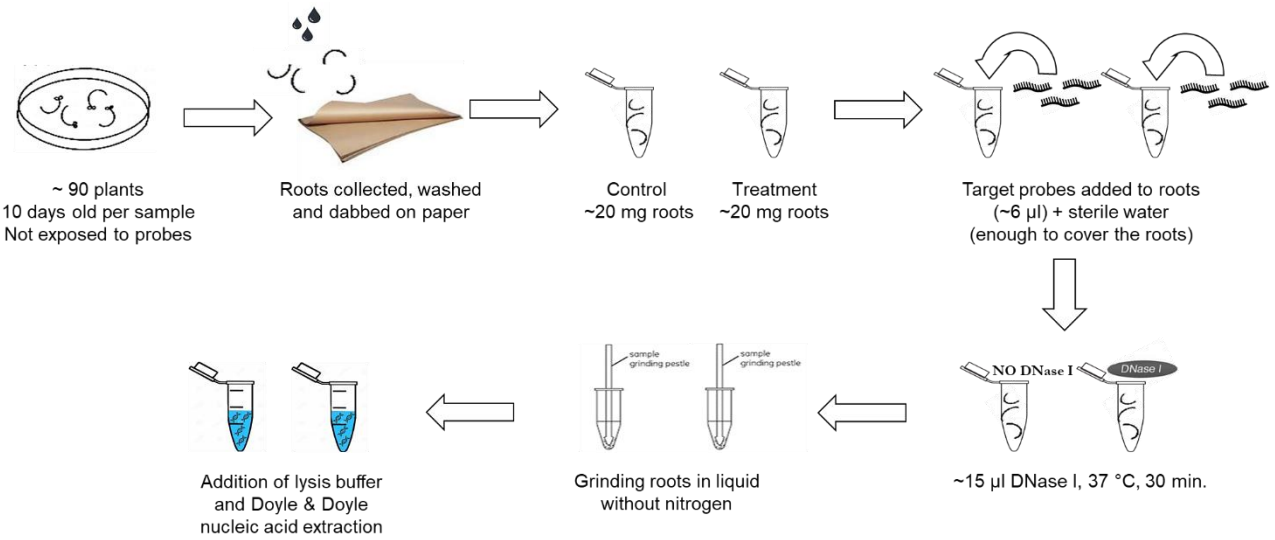

Figure 4.12. DNase I treatment to avoid hybrid formation during the extraction phase due to DNA probe carry over on roots. Self-DNA probes were added directly to the collected roots to simulate carry-over; the roots were then treated with DNase I (not the control sample), grinded directly in the liquid and finally nucleic acids were extracted to perform the immunoprecipitation.

Afterwards, we performed again the *in vivo* protocol, this time exposing the seedlings to one set of three probes for 1 h (5 µL per seedling at 80 ng/µL concentration per probe) and adding another set of three probes directly in the tube with the collected roots (1 µL per selected probe at 2000 ng/µL concentration, 3 µL in total), with enough sterile water to cover them. By adding 6 µg of DNA probe to roots, we are hypothesizing again a carry-over of ~5% (80 ng x 5 x 3 x 90 = 108 µg of self-DNA to expose 90 seedlings; $\frac{6\ \mu g \times 100}{108\ \mu g}$ = ~5%). Then, we added ~15 µL of DNase I and buffer 10x and incubated the solution at 37 °C for 30 min. Indeed, we need to also consider the potential carry-over from the probes in exposure, which means in total 12 µg of DNA to be degraded by DNase (1:1.25 ratio, like in the previous experiment). After treatment, we added 15 µL of stop solution, roots were pestled directly in the liquid, keeping the tube on ice, and the lysis buffer was added to proceed with total nucleic acid extraction and immunoprecipitation (Figure 4.13). The desirable result would be the amplification of the exposure probe genes, but not of those corresponding to the probes added to the roots to resemble probe carry-over: this would confirm that the DNase I treatment is efficient in removing potential probe carry-over on roots and that DNA-RNA hybrids can form during exposure to self-DNA probes. Finally, in the latter two experiments, we grinded the roots and added the lysis buffer only after the DNase I treatment, to avoid the degradation of the DNA moiety of any hybrids that might have already formed inside the cells during the exposure phase.

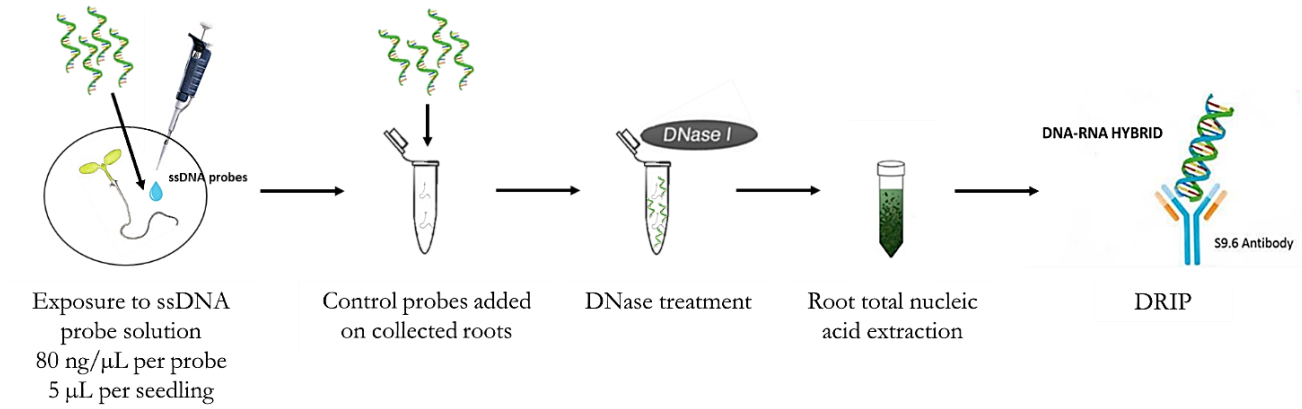

Figure 4.13. DNase I treatment to avoid hybrid formation during the extraction phase due to DNA probe carry over on roots. Arabidopsis seedlings were exposed to one set of probes while another set was added to the collected roots; the roots were then treated with DNase I, grinded directly in the liquid and finally nucleic acids were extracted to perform the immunoprecipitation.

4.4. Results

4.4.1. *In vitro* results

In the first *in vitro* experiment (Experiment 1), we used one set of four probes (matching the genes *PGM1*, *ALDH2C4*, *PCKA* and *MAM3*) to hybridize with extracted RNA, while in the second experiment (Experiment 2) we used another set of probes (*APS4*, *PHO1*, *NIT2* and *RAN1*). The genes for which we did not hybridize the corresponding probes (therefore hybrids should not have formed), respectively *APS4*, *PHO1*, *NIT2* and *RAN1* in the first experiment and *PGM1*, *ALDH2C4*, *PCKA* and *MAM3* in the second experiment, were used as controls (Table 4.6). Results highlighted the expected pattern, confirming the efficiency of our adapted DRIP protocol in isolating hybrids *in vitro*: in the first experiment, the primer target sequences of the genes *PGM1*, *ALDH2C4*, *PCKA* and *MAM3* have been amplified and are visible on the polyacrylamide gel, while there is no visible signal for the non-target genes *APS4*, *PHO1*, *NIT2* and *RAN1*; vice versa, in the second experiment, the target sequences of the genes *APS4*, *PHO1*, *NIT2* and *RAN1* have been amplified and are visible on the polyacrylamide gel, while there is no visible signal for the non-target genes *PGM1*, *ALDH2C4*, *PCKA* and *MAM3* (Figure 4.14). Moreover, respective negative control samples treated with RNase H, which degrades the RNA moiety in the hybrid impeding its precipitation by the antibody, did not show any amplification signal of the target genes, showing that the amplicons observed in the positive samples derive indeed from hybrid formation. The *in vitro* study included two additional control samples. In particular, a control sample where no probes were hybridized and only extracted RNA was precipitated, which confirmed absence of amplification, and

another where only probes where precipitated without RNA, which again confirmed no amplification signal, proving that our primers cannot amplify our DNA probes. At least two replicas were carried out for each experiment combination.

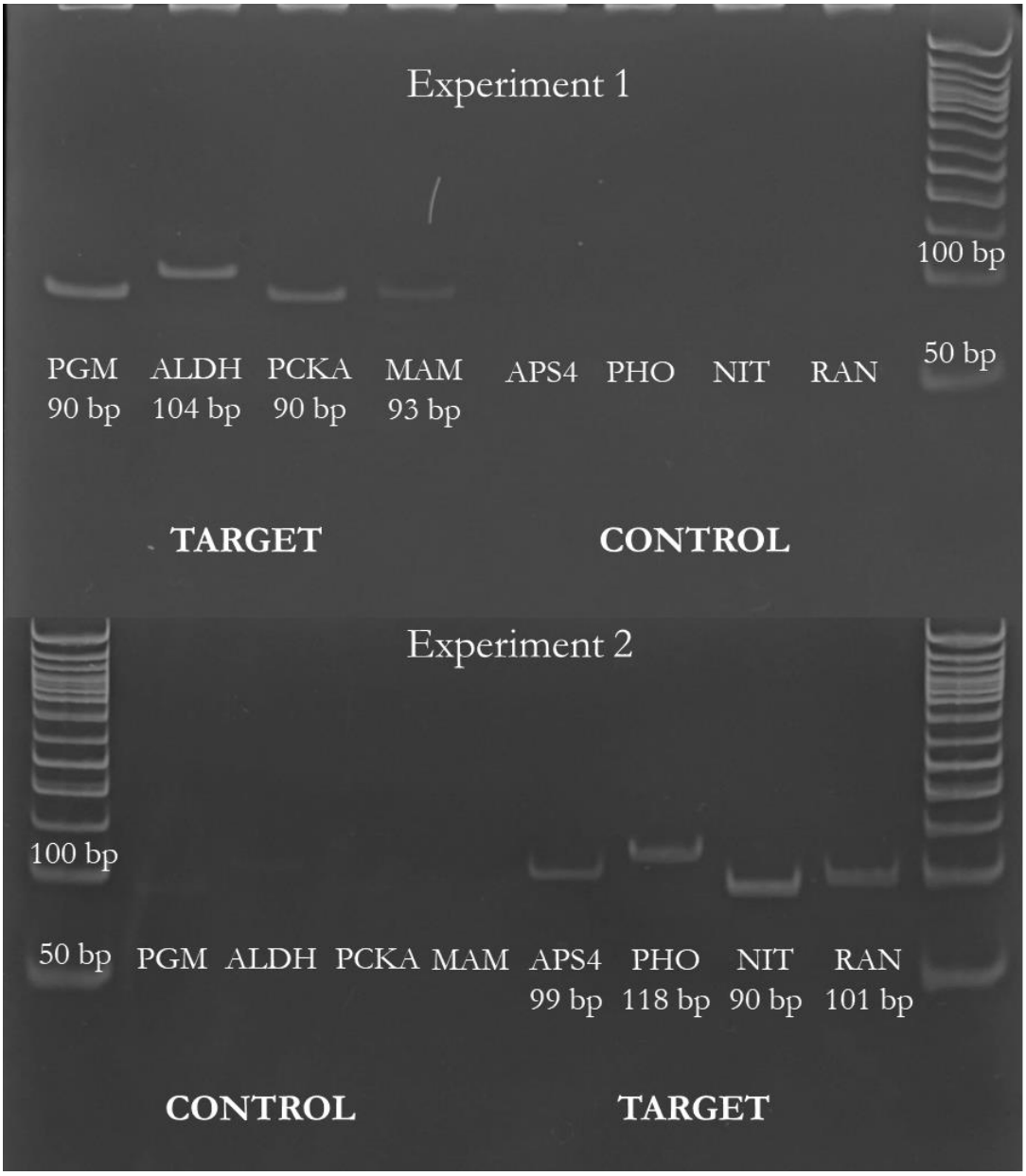

Figure 4.14. Results on polyacrylamide gel of the *in vitro* Experiment 1 and 2 showing the expected amplification and amplicon size of target genes and non-amplification of control genes (see Table 4.6).

Table 4.6. List of target (expected amplification) and control (non-amplification) genes for the *in vitro* Experiment 1 and 2. Target genes are those for which the corresponding probes have been hybridize with RNA at the beginning of the protocol; vice versa, for the control genes probes were not hybridize (therefore DNA-RNA hybrids should not have formed and cannot be precipitated).

Gene_ID	Gene_Name	Expected fragment size	Experiment 1 *in vitro*	Experiment 2 *in vitro*
AT1G09780	PGM1	90 nt	Target	Control
AT3G24503	ALDH2C4	104 nt	Target	Control
AT4G37870	PCKA	90 nt	Target	Control
AT5G23020	MAM3	93 nt	Target	Control
AT5G43780	APS4	99 nt	Control	Target
AT3G23430	PHO1	118 nt	Control	Target
AT3G44300	NIT2	90 nt	Control	Target
AT5G44790	RAN1	101 nt	Control	Target

4.4.2. *In vivo* results

Results of the *in vivo* Experiment 1, 2, 3 and 4 are presented, respectively, in Figure 4.15, 4.16, 4.17 and 4.18. For each of the following experiments, at least two replicas were conducted. In the *in vivo* Experiment 1, we exposed *Arabidopsis* seedlings for 1 h to six self-DNA probes, corresponding to the following genes: *PGM1*, *ALDH2C4*, *PCKA*, *APS4*, *PHO1* and *NIT2*. The genes *MAM3*, *FRO2*, *JAL20*, *PPC3*, *STY46* and *RAN1* were used as controls, therefore no PCR amplification was expected (Table 4.7). The results of this first *in vivo* experiment, showed in Figure 4.15, revealed the expected amplification of target genes and the non-amplification of control genes, confirming *in vivo* DNA-RNA hybrid formation. Additional control samples were carried out, in particular, a sample where seedlings were not exposed to probes (to confirm that our target sequences on the selected genes do not correspond to naturally occurring genomic R-loops) and a negative control sample treated with RNase H, both showing no amplification signal.

Table 4.7. List of target (expected amplification) and control (non-amplification) genes for the *in vivo* Experiment 1. Target genes are those for which the corresponding probes have been used to expose Arabidopsis seedlings at the beginning of the protocol; vice versa, probes of the control genes were not used (therefore DNA-RNA hybrids should not have formed and cannot be precipitated).

Gene_ID	Gene_Name	Expected fragment size	Experiment 1 *in vivo*
AT1G09780	PGM1	90 nt	Target
AT3G24503	ALDH2C4	104 nt	Target
AT4G37870	PCKA	90 nt	Target
AT5G43780	APS4	99 nt	Target
AT3G23430	PHO1	118 nt	Target
AT3G44300	NIT2	90 nt	Target
AT5G23020	MAM3	93 nt	Control
AT1G01580	FRO2	116 nt	Control
AT2G25980	JAL20	113 nt	Control
AT3G14940	PPC3	91 nt	Control
AT4G38470	STY46	93 nt	Control
AT5G44790	RAN1	101 nt	Control

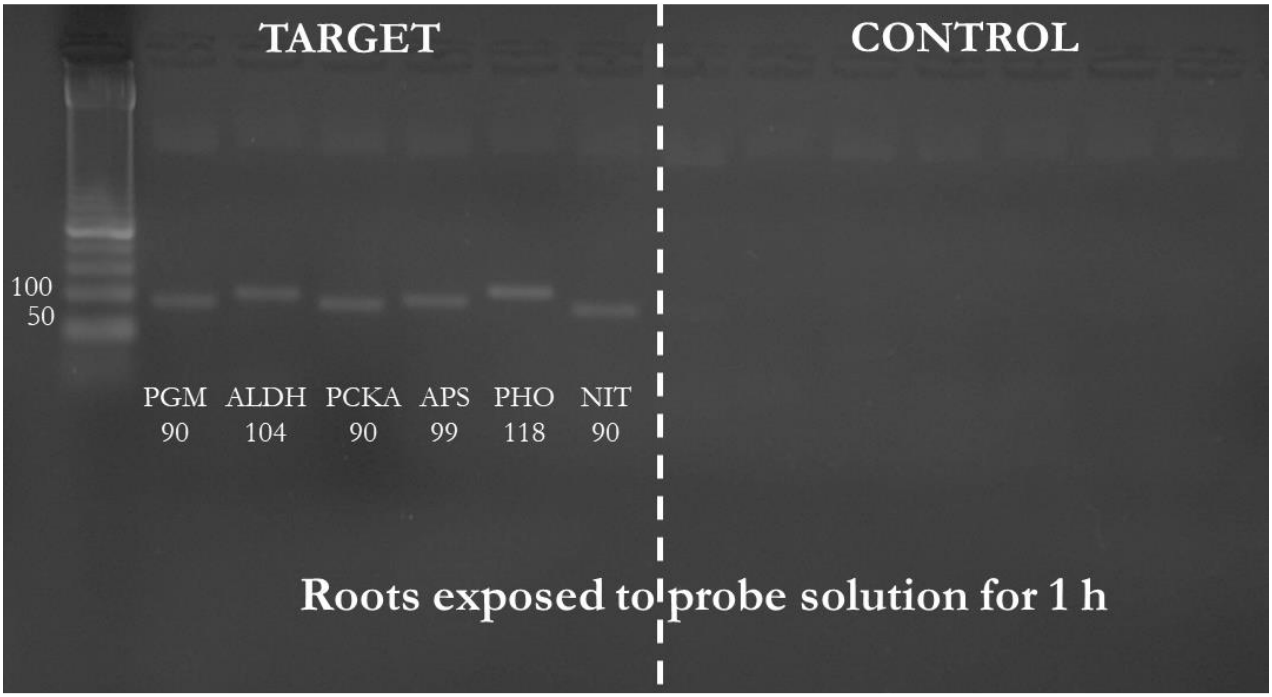

Figure 4.15. Results on polyacrylamide gel of the *in vivo* Experiment 1 showing the expected amplification and amplicon size of target genes and non-amplification of control genes (see Table 5.7).

The second *in vivo* experiment (Experiment 2 *in vivo*) was aimed to verify whether DNA-RNA hybrids can form *in vivo* during the extraction phase due to probe carry-over on roots. Therefore, we added the six selected probes (genes *PGM1*, *ALDH2C4*, *PCKA*, *APS4*, *PHO1* and *NIT2*) directly in the extraction medium (lysis buffer) together with the pestled roots (not previously exposed) to simulate the carry-over. Genes for which probes were not added (*MAM3*, *FRO2*, *JAL20*, *PPC3*, *STY46* and *RAN1*) were used as controls (Table 4.8). Results showed the amplification of amplicons belonging to the genes for which probes were added and the non-amplification of the control ones, confirming that hybrids can form during the extraction phase of the DRIP protocol in the case of self-DNA probe carry-over on roots (Figure 4.16).

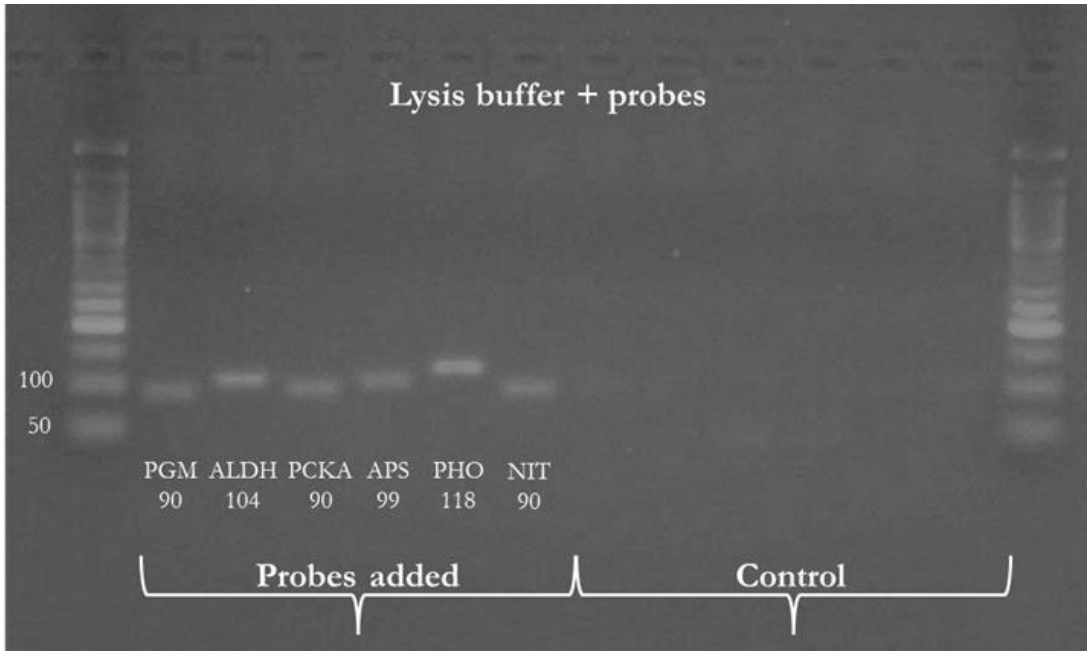

Figure 4.16. Results on polyacrylamide gel of the *in vivo* Experiment 2 showing the amplification of genes for which probes have been added in the extraction medium. This confirms that DNA-RNA hybrids can form during the extraction phase in case of probe carry-over on roots.

After having verified the *in vivo* hybrid formation during the extraction phase, in the following *in vivo* experiments (Experiment 3 and 4) we tested DNase I treatment to prevent probe carry-over on roots. In the *in vivo* Experiment 3 we did not expose Arabidopsis seedlings, but we added the probes (same as Table 4.8) to the collected roots with sterile water. After, we proceeded with DNase I treatment, root grinding in the solution, adding of lysis buffer, total nucleic acid extraction and immunoprecipitation. Also, we tested a control sample not treated with DNase. Results (Figure 4.17) showed that the DNase treatment was able to eliminate the amplification signal observed in the non-treated sample.

Table 4.8. List of genes for which probes have been added in the lysis buffer during the extraction phase in the *in vivo* Experiment 2 and 3 and control genes for which probes have not been added.

Gene_ID	Gene_Name	Expected fragment size	Experiment 2 and 3 *in vivo*
AT1G09780	PGM1	90 nt	Added to lysis or roots
AT3G24503	ALDH2C4	104 nt	Added to lysis or roots
AT4G37870	PCKA	90 nt	Added to lysis or roots
AT5G43780	APS4	99 nt	Added to lysis or roots
AT3G23430	PHO1	118 nt	Added to lysis or roots
AT3G44300	NIT2	90 nt	Added to lysis or roots
AT5G23020	MAM3	93 nt	Control
AT1G01580	FRO2	116 nt	Control
AT2G25980	JAL20	113 nt	Control
AT3G14940	PPC3	91 nt	Control
AT4G38470	STY46	93 nt	Control
AT5G44790	RAN1	101 nt	Control

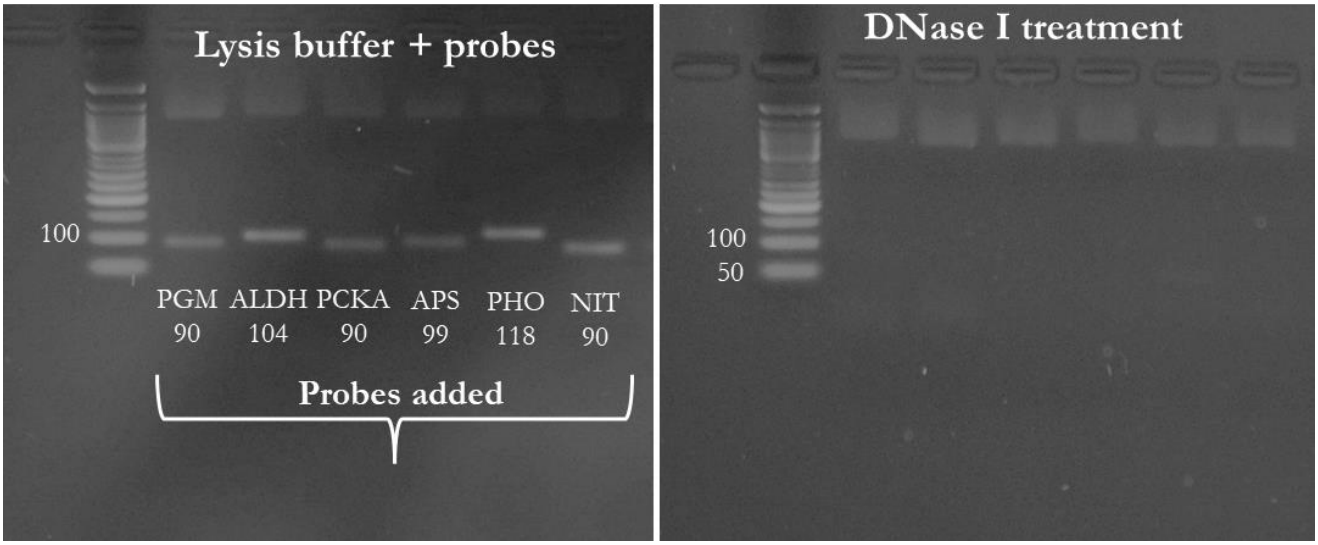

Figure 4.17. Results on polyacrylamide gel of the *in vivo* Experiment 3 showing that DNase treatment is efficient in removing DNA probe carry-over on roots, therefore preventing hybrid formation.

Finally, in our last experiment, we exposed Arabidopsis seedlings to only three probes (for the genes *PGM1*, *ALDH2C4* and *PCKA*) and added to the collected roots other three probes (genes APS4, PHO1 and NIT2), in order to minimize the amount of DNase needed to remove the probes added during the extraction phase and the same amount of potential carry-over coming from the exposure probes, hypothesized at 5% (Table 4.9). Unfortunately, results for

this experiment were inconclusive, as we observed the amplification of both the genes of the exposure probes and the genes of the probes added to roots before DNase treatment and extraction (Figure 4.18).

Table 4.9. List of genes for which probes have been either used to expose Arabidopsis seedlings or added to the collected roots before DNase treatment and extraction in the *in vivo* Experiment 4.

Gene_ID	Gene_Name	Expected fragment size	Experiment 4 *in vivo*
AT1G09780	PGM1	90 nt	Exposure
AT3G24503	ALDH2C4	104 nt	Exposure
AT4G37870	PCKA	90 nt	Exposure
AT5G43780	APS4	99 nt	Added to roots
AT3G23430	PHO1	118 nt	Added to roots
AT3G44300	NIT2	90 nt	Added to roots

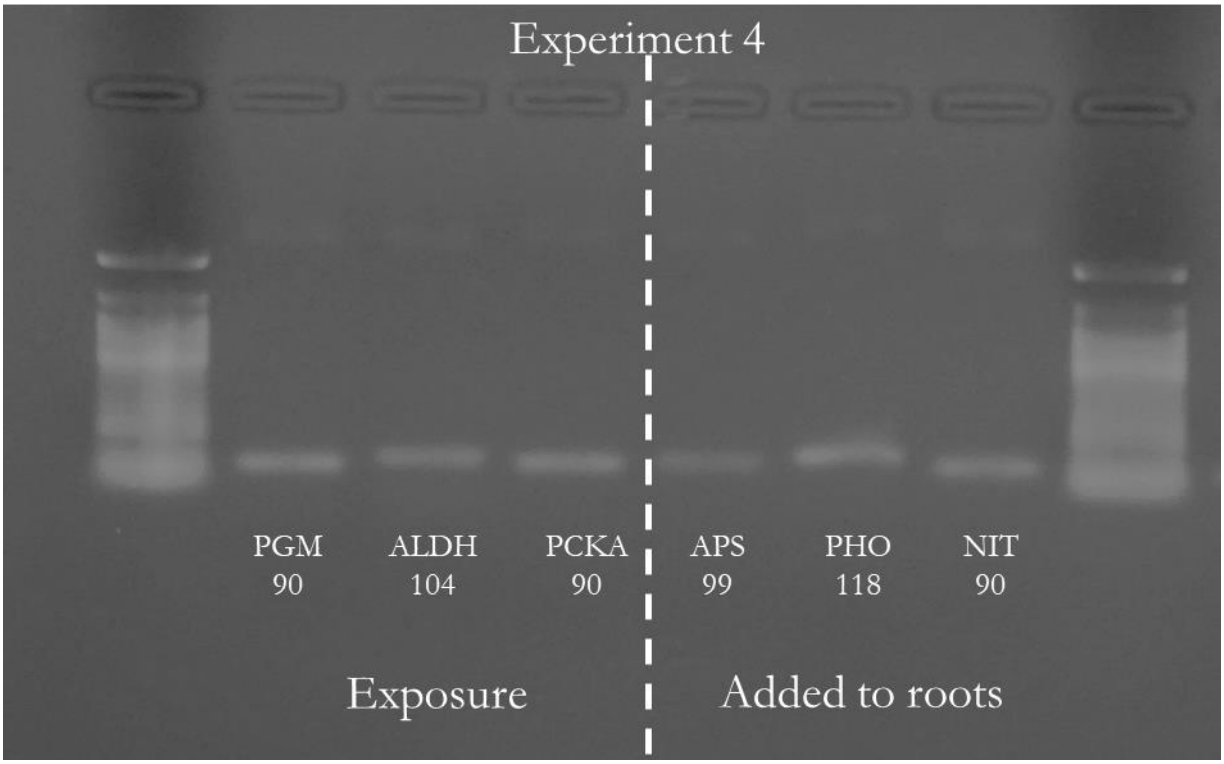

Figure 4.18. Results on polyacrylamide gel of the *in vivo* Experiment 4 showing the amplification of both the genes of the exposure probes and the genes of the probes added to roots before DNase treatment and extraction.

4.5. Conclusive remarks and perspectives

The setting up and fine-tuning of the experiment presented in this chapter have brought many challenges. In particular, some of them are summarized in the table below (Table 4.10) with the respective resolution we implemented in the protocol.

Table 4.10. List of challenges and respective resolutions we implemented during the application of the DRIP protocol to investigate DNA-RNA hybrid formation after self-DNA probe exposure.

Challenge	Resolution
Since PCR amplification and agarose gel visualization are powerful and very sensitive tools, able to detect even small DNA traces, our protocol carries a high risk of contamination from environmental nucleic acids.	We performed all the passages until the immunoprecipitation step under sterile hood. The rest of the DRIP protocol was conducted in a controlled laboratory environment, adopting rigorous sterile techniques, utilizing appropriate protective equipment, and implementing strict isolation procedures for sample handling and processing.
In the event of any residual genomic DNA in the final cDNA derived from the DRIP protocol, there is the possibility of amplifying genomic DNA fragments instead of cDNA originating from the retro transcribed hybrid RNAs.	This issue was resolved through two approaches: – extracted RNA was used as template in a qualitative PCR with all our designed primers, expecting no amplification (for the *in vitro* experiment); – we employed specific primers placed on two contiguous exons to span an intronic region, enabling us to detect genomic traces through qualitative PCR with amplicon sizes encompassing the intron length.
S9.6 monoclonal antibody exhibits high affinity not only for DNA-RNA hybrids but also for double-stranded RNA (dsRNA), characteristic that poses a potential challenge to the specificity of the immunoprecipitation process (Phillips *et al*., 2013; Sanz & Chédin, 2019).	Total extracted nucleic acids (or in case of the *in vitro* experiment, the DNA-RNA mixture after hybridization) were treated with RNase III, which specifically cleaves dsRNA, before the immunoprecipitation step with the antibody (Hartono *et al*., 2018).
RNase III can degrade large RNA regions forming secondary structures posing challenges for the detection and amplification of our hybrid region if the primers are placed too far from the DNA probe binding site.	For each primer pair of the selected genes, one primer was designed to match the cDNA fragment corresponding to the probe hybridization site, while the other was placed outside, but only few nucleotides away. In this way, we also hoped to prevent aspecific amplification of the corresponding gene probe.
To ensure that what we immunoprecipitated and amplified truly derived from hybrid formation and not from other origins (for examples residual DNA probes in the final cDNA that our primers may be able to amplify, or genomic R-loops in the *in vivo* experiment) we needed to implement several control samples.	The control samples included: – immunoprecipitation protocol performed only with extracted RNA, without hybridization with DNA probes; – immunoprecipitation protocol performed only with DNA probes, without hybridization with extracted RNA; – immunoprecipitation protocol with total extracted nucleic acid from seedling roots not exposed to self-DNA probes;

	– negative control samples treated with RNase H, an enzyme that specifically cleaves the RNA moiety of DNA/RNA hybrids impeding hybrid isolation (Cerritelli & Crouch, 2008; Lee *et al*., 2022). In all these cases we expected lack of amplification signal.

During our experimental study, we have successfully adapted and verified an *in vitro* immunoprecipitation protocol to capture DNA-RNA hybrids. Unfortunately, the *in vivo* investigation of DNA-RNA hybrid formation after self-DNA exposure resulted more challenging, with numerous still unresolved issues and questions. In particular, in our experiments, we did verify the *in vivo* hybrid amplification post exposure to self-DNA probes (Experiment 1 *in vivo*) but we also highlighted that this formation can occur during the exposure phase in case of probe carry-over on roots (Experiment 2 and 3 *in vivo*). Root treatment with DNase I seemed to be effective in removing probe carry-over (Experiment 3), but results are still preliminary and inconclusive (Experiment 4 *in vivo*). Especially, it is not easy to predict a plausible percentage of probe carry-over that may be transported on roots into the extraction phase and the consequent dose of DNase I to utilize, together with the most suitable experiment setup to carry out. In this context, it is challenging to ascertain whether the hybrids we isolated *in vivo* originated from hybrid formation during the exposure phase to self-DNA probes or occurred during the extraction process due to cell lysis and the binding of carried-over DNA probes with the released RNAs in the extraction medium. The same issue and experimental question should be posed for the DRIP protocol implementing similar procedures to map genomic R-loops: consistently, many DNA-RNA hybrid structures may form during the extraction phase before immunoprecipitation creating a strong bias for presence and frequency of genomic R-loops. Moreover, these protocols include a fragmentation process post extraction that may favour the annealing of shorter fragments. Nonetheless, Sanz & Chédin, (2019) consider the formation of *de novo* R-loops during the process of DNA extraction highly unlikely due to the high energy barrier to R-loop formation from DNA and RNA outside of the immediate vicinity of the transcription bubble and that promoting such RNA strand invasion, in a highly complex mixture of genomic DNA and RNA, would in addition require a homology search process and energy to melt the duplex DNA over hundreds of base pairs. Also, they highlight the highly robustness and reproducibility of the signals seen in DRIP based approaches, suggesting that the likelihood of this event is extremely low, even though not impossible. In addition, R-loops, or DNA-RNA hybrids,

particularly if short, represent unstable structures that can easily fall apart during extraction and fragmentation processes, therefore leading to an underestimation of their formation. Another big limitation of this protocol is the substantial residual affinity for dsRNA of the S9.6 monoclonal antibody (Phillips *et al*., 2013). Also, it has been reported that single-stranded RNA (ssRNA) species may interfere with DRIP efficiency and that RNase A or RNase T1 treatment is advisable (Zhang *et al*., 2015).

Currently, we are actively exploring various approaches to address the challenges associated with our protocol. These include developing washing methods, optimizing DNase treatments with different enzyme doses based on hypothesized carry-over percentages on roots, and refining our experimental setups, with the aim of isolating hybrids that are potentially formed exclusively during the exposure phase to self-DNA probes, while minimizing their formation during the extraction process. It is important to acknowledge that self-DNA sensing may not necessarily rely on DNA-RNA hybrid formation. Consequently, the signals observed *in vivo* could be attributed solely to probe carry-over on roots and hybrids formed during extraction. Alternatively, it is also plausible that our current protocol may not be ideally suited for investigating this specific issue. To further explore this, we are considering conducting a quantitative assessment of the immuno-precipitates using techniques such as RT-qPCR, library construction, and sequencing. This would enable us to evaluate the relative abundance of target genes compared to control genes, as well as the abundance of exposure genes relative to those for which probes were added during extraction to simulate carry-over. In addition, we are contemplating the preparation of a methodological article that outlines the challenges and critical points encountered in the application of similar protocols for isolating DNA-RNA hybrids. Such an article could provide valuable insights and guidance to other researchers working in this field. Finally, DRIP represents a highly reproducible and high-resolution procedure, that warrants further investigation and implementation. Its potential and effectiveness in studying DNA-RNA hybrids make it an exciting avenue for future research. By continuing to refine and optimize the protocol, we can enhance its reliability and applicability in a variety of biological contexts. The valuable insights gained from DRIP experiments, like the successful application of DRIP *in vivo* attempted in this study for the first time, can contribute to our understanding of hybrid formation, epigenetic modifications, and related molecular mechanisms. Therefore, investing in further exploration and utilization of DRIP holds great promise for advancing our knowledge in this field.

Chapter 5: Investigation of epigenetic changes in *Arabidopsis thaliana* seedlings exposed to self-DNA

5.1. Introduction

In the last activity of my PhD research, we investigated the possibility of epigenetic changes as a consequence of the exposition to self-DNA and the correlation to changes in gene expression in *Arabidopsis thaliana* roots. Epigenetics refers to the study of heritable phenotypic modifications that do not involve alterations in DNA sequence. The organization and modifications of chromatin are critical for regulating gene expression and various cellular processes in living organisms. Chemical modifications, such as DNA methylation and histone modifications (such as histone acetylation, phosphorylation, and methylation), can alter the structure of chromatin and influence the accessibility of genes to the transcriptional machinery. These modifications, known as epigenetic marks, can activate or repress gene expression. In particular, in our work we focused on the exploration of genomic DNA methylation changes after exposure to self-DNA, since there is substantial evidence demonstrating DNA methylation changes in response to abiotic and biotic stress in plants, showing rapid changes in methylation levels within a limited time frame. Moreover, self-DNA exposure was found to cause changes in CpG DNA methylation and defense-related responses in *Lactuca sativa*.

Based on these findings, this study aimed to investigate changes in cytosine methylation across the genome and gene expression levels in *Arabidopsis thaliana* seedlings exposed to self-DNA solution for 6 and 24 hours. Whole Genome Bisulfite Sequencing (WGBS) and RNA sequencing (RNA-seq) analyses were performed on DNA and RNA extracted from root samples of *Arabidopsis thaliana* seedlings to investigate methylation changes in root genome and in gene expression after exposition to self-DNA. WGBS is a high-resolution technique used to obtain DNA methylation information in the genome, while RNA-seq allows for gene expression analysis. Seed sterilization and germination were carried out using *Arabidopsis thaliana* Col 0 seeds, which were then grown on Murashige and Skoog growth medium. After the roots reached a length of approximately 3 cm, the growth medium with the seedlings was divided into slices. Slices were exposed to *Arabidopsis* DNA solution for 6 and 24 hours. Control samples exposed to sterile water were also collected. Roots from each group of slices were washed, collected, and stored in separate tubes for DNA and RNA extraction. In total, 15 samples, including control and treated replicas, were collected and stored for subsequent analysis. RNA extraction was performed using the Spectrum™ Plant Total RNA Kit, and RNA quality and quantity were assessed using spectrophotometry and gel electrophoresis. RNA-seq libraries were prepared using the Universal Plus mRNA-Seq kit, and sequencing was

performed on a NovaSeq 6000 platform. DNA extraction was performed using the MagMAX Plant DNA Isolation Kit, and DNA quality and quantity were assessed using spectrophotometry. Bisulfite treatment, library preparation, and sequencing for WGBS were performed using the Ultralow Methyl-Seq System.

Principal Component Analysis (PCA) was conducted to visualize gene expression patterns using the methylKit and R packages. Initial results indicated noticeable differences in gene expression levels between samples treated with self-DNA and controls, particularly after 24 hours of exposure. Differences in DNA methylation levels, particularly in CHG and CHH contexts, were also observed and require further verification. The sequencing data from this study are currently undergoing more detailed analysis for a manuscript preparation. Differentially Expressed Genes (DEGs) analysis, Gene Ontology (GO) enrichment analysis, and Differentially Methylated Regions (DMRs) analysis, presented in this chapter, provide a deeper understanding of the gene expression and DNA methylation changes associated with self-DNA exposure in *Arabidopsis thaliana*.

In conclusion, this study provides preliminary findings on the molecular responses of *Arabidopsis thaliana* seedlings to self-DNA exposure. The results suggest differential gene expression and DNA methylation patterns associated with self-DNA treatment. Further analysis and validation of these findings will contribute to a better understanding of the plant's molecular response to self-DNA and its potential implications in stress responses and phenotypic plasticity.

5.2. Introduction

The genetic information in a cell is encoded by DNA. Many proteins — namely, histones — package the massive amount of DNA in a genome into a highly compact form that can fit in the cell nucleus, called chromatin. Chromatin refers to a mixture of DNA and proteins that form the chromosomes found in the cells of humans and other higher organisms (Figure 5.1) (Wolffe, 1998; Van Holde, 2012). These proteins play a crucial role in regulating gene expression and controlling access to the DNA. Chromatin, in fact, can exist in two main forms: euchromatin and heterochromatin (Figure 5.2). Euchromatin refers to the less condensed and more accessible form of chromatin that is associated with active gene expression. It contains genes that are actively transcribed into RNA and is generally less tightly packed. In contrast, heterochromatin is highly condensed and transcriptionally silent. It contains genes that are usually not actively transcribed and is characterized by a more tightly packed

structure. The organization and modifications of chromatin play a vital role in regulating gene expression and various cellular processes (Babu & Verma, 1987). Chemical modifications, such as DNA methylation and histone modifications (e.g. histone acetylation, phosphorylation, methylation), can alter the structure of chromatin and influence the accessibility of genes to the transcriptional machinery (Bannister & Kouzarides, 2011; Li *et al*., 2022). These modifications, often referred to as epigenetic marks, can result in the activation or repression of gene expression (Vining *et al*., 2012; Morgan & Shilatifard, 2020). Understanding the organization and dynamics of chromatin is crucial for unravelling the mechanisms of gene regulation, development, and diseases.

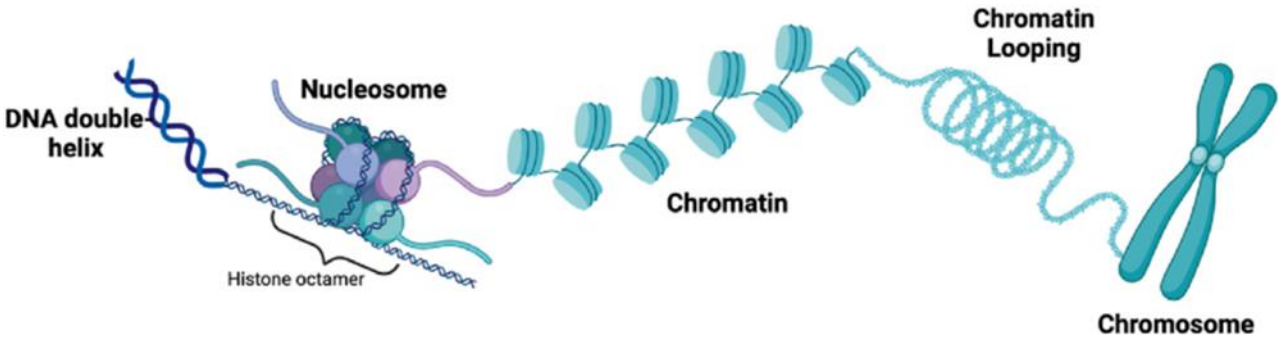

Figure 5.1. DNA molecules first wrap around the histone proteins forming beads on string structure called nucleosomes. Nucleosomes further coil and condense to form fibrous material which is called chromatin. Chromatin fibers can unwind for DNA replication and transcription. When cells replicate, duplicated chromatins condense further into chromosomes, visible under microscope, which are separated into daughter cells during cell division (source: Clarke & Mostoslavsky, 2022).

An important mechanism that determines epigenetic changes in plants is represented by noncoding RNAs. Extensive transcriptome analyses have revealed that up to 90% of eukaryotic genomes are transcribed (Wilhelm *et al*., 2008), whereas only 1–2% of the genome encodes proteins (The ENCODE Project Consortium, 2007). This suggests that a large proportion of the eukaryotic genome produces an unexpected plethora of RNA molecules that have no protein coding potential. These are collectively called noncoding RNAs (ncRNAs) although they can be grouped into two classes according to the size of transcripts and the mode of action. NcRNAs with less than 200 nucleotides, often in the 20 to 30 nt range, are considered small RNAs and include microRNA (miRNAs), small interfering RNAs (siRNAs), and Piwi-interacting RNAs (piRNAs) (Ghildiyal & Zamore 2009). Certain small RNAs induce transcriptional gene silencing by directing the formation of

heterochromatin at corresponding genomic sites, while others trigger posttranscriptional gene silencing by promoting mRNA degradation or inhibiting translation (Heo *et al*., 2013). The plant genome encodes an array of small RNAs that are involved in the development, reproduction, defence and genome reprogramming, besides contributing to phenotypic plasticity. DICER-like proteins (DCLs) help create small RNA molecules by synthesizing 21–24 nucleotide RNA molecules (Dar *et al*., 2022). Small RNAs (sRNAs) play a significant role in both defence and epigenetic responses. They are now known to be a core component of a signaling network that mediates epigenetic modifications in plants. Epigenetic regulation can be mediated through a dynamic interplay between sRNAs, DNA methylation, and histone modifications, which together modulate transcriptional silencing of DNA (Simon & Meyers, 2011). Regulatory sRNAs are short (approximately 20–24 nt in length), noncoding RNAs produced through the RNA interference (RNAi) pathway that involves the plant-specific DNA-dependent RNA polymerases Pol IV and Pol V (Wierzbicki *et al*., 2008; Zhang *et al*., 2007), the RNA-dependent RNA polymerase RDR2 (Lu *et al*., 2006; Xie *et al*., 2004), the double-stranded RNA endonuclease DICER-LIKE3 (DCL3) (Kasschau *et al*., 2007), and at least two Argonautes, AGO4 and AGO6 (Qi *et al*., 2006; Zheng *et al*., 2007). In plants, small RNAs are divided into microRNA (miRNA) and small interfering RNA (siRNA) by their origin, structure, and pathways they regulate. sRNAs 21 nt in length are typically microRNAs (miRNAs) that participate in posttranscriptional gene silencing in plants by cleaving transcripts or repressing translation. Many small interfering RNAs (siRNAs) typically 24 nt in length are involved in PTGS but a majority of them are involved with heterochromatin formation and transcriptional gene silencing by guiding sequence-specific DNA and histone methylation through a pathway termed RNA-directed DNA methylation (RdDM) and transcriptional gene silencing (TGS) (Gao *et al*., 2010). RdDM is the *de novo* methylation caused by double-stranded RNA (ds-RNA) molecules. The interrelation between RdDM and RNA interference (RNAi) suggests that small RNAs guide cytosine methylation. RdDM pathways help in adaptation responses to various stresses, maintaining genome stability and regulation of development (Sudan *et al*., 2018). Small RNAs and long noncoding RNAs (lncRNAs) have come out as key regulators of chromatin structure in eukaryotic cells. In addition to RNA degradation, translational suppression, chromatin modification, and RNA interference (RNAi) pathways, small RNAs are also involved in targeted gene expression. Nuclear RNAi pathways repress transcription through histone or DNA methylation. Using A. thaliana as a model system, scientists first demonstrated that DNA methylation of target genes, as well as posttranscriptional gene

silencing, was associated with small interfering RNA (siRNA) production, linking RNA-directed DNA methylation to the RNAi pathway (Holoch & Moazed, 2015).

Long non-coding RNAs (lncRNAs), surpassing 200 nucleotides in length, play crucial roles in regulating gene expression. They achieve this by interacting with various DNA/RNA molecules or protein complexes, contributing to processes such as chromatin remodelling and small RNA biogenesis. Additionally, lncRNAs can counteract specific small RNA regulatory circuits, adding another layer of complexity to the intricate network of gene regulation (Ariel *et al*., 2020). In plants, a few lncRNAs have been identified and functionally characterized (Ben Amor *et al*., 2009; Heo & Sung 2011; Swiezewski *et al*., 2009). They function in gene silencing, flowering time control, organogenesis in roots, photomorphogenesis in seedlings, abiotic stress responses, and reproduction (Zhang *et al*., 2014; Yuan *et al*., 2016; Matzke & Mosher, 2014; Wang *et al*., 2014). lncRNAs can act in cis or trans, function by sequence complementarity to RNA or DNA, and be recognized via specific sequence motifs or secondary/tertiary structures (Wang & Chekanova, 2017). At the simplest level, lncRNAs can serve as precursors to smRNAs, as in the case of RNA Pol IV transcripts (Wierzbicki *et al*., 2008). Some lncRNAs keep regulatory proteins or microRNAs from interacting with their DNA or RNA targets by acting as decoys that mimic the targets. Some of the plant examples include the *Arabidopsis* microRNA target mimics IPS1 lncRNA and the decoy ASCO-lncRNA (Franco-Zorrilla *et al*., 2007). Different types of lncRNAs associate with chromatin and act as scaffolds that allow the assembly of complexes of chromatin-modifying enzymes involved in chromatin remodeling and transcriptional regulation. By interacting with these proteins, lncRNAs contribute to the formation of higher-order chromatin structures and influence the accessibility of DNA to transcriptional machinery. The lncRNA COOLAIR in Arabidopsis interacts with the chromatin-remodeling protein LIKE HETEROCHROMATIN PROTEIN 1 (LHP1), leading to the formation of chromatin loops and the regulation of gene expression during vernalization (Ariel *et al*., 2020). Recruitment of these proteins can require small RNAs or not. For example, the siRNA-directed DNA methylation (RdDM) pathway, which occurs specifically in plants, requires small RNAs (Matzke & Mosher, 2014). Other lncRNAs can recruit complexes of enzymes that remodel chromatin but do not require smRNAs. The mechanism that provides targeting specificity for these lncRNAs remains to be discovered (Wang & Chekanova, 2017). Other lncRNAs interact with proteins, chromatin-modifying complexes that modify histones with repressive marks, such as Polycomb Repressive Complex 2 (PRC2), to repress transcription via methylation of histone H3K27. Plant lncRNAs can guide chromatin modifiers, such as

Polycomb Repressive Complexes (PRCs) or DNA methyltransferases, to specific genomic loci, leading to the establishment of repressive epigenetic marks, such as histone methylation or DNA methylation, respectively (Tsai *et al*., 2010). The best-studied RNAi-independent pathway that relies on lncRNAs interacting with Polycomb is epigenetic regulation via histone modifications and expression of Arabidopsis FLOWERING LOCUS C (FLC). The lncRNA COLDAIR recruits PRC2 to the FLC locus, resulting in the repression of flowering time genes through H3K27me3 deposition (Heo & Sung, 2011). Furthermore, lncRNAs can function in a trans-acting manner to modulate the expression of distant target genes. These lncRNAs often exhibit complementary sequence motifs to their target genes and form RNA-DNA hybrids, known as R-loops, at the target sites. The formation of R-loops can impact chromatin structure and gene expression. APOLO (AUXIN REGULATED PROMOTER LOOP) is an example of a trans-acting lncRNA in Arabidopsis that recognizes multiple distal genomic loci through R-loop formation and influences chromatin loop dynamics and transcriptional regulation (Ariel *et al*., 2020). The coordinated regulation induced by APOLO involved the decoying of the plant Polycomb Repressive Complex 1 component LHP1 from target loci. The expression of APOLO was found to be modulated by auxin, a hormone involved in plant development, and it was demonstrated that APOLO directly co-regulates auxin-responsive genes during lateral root formation in *Arabidopsis* (Ariel *et al*., 2014). By recognizing multiple distant independent loci through R-loop formation, APOLO influences chromatin conformation and the transcriptional activity of its targets, including auxin-responsive genes involved in lateral root formation (Ariel *et al*., 2020).

Epigenetic modifications encompass chemical alterations to DNA and histones that are linked to changes in gene expression. These modifications are heritable but do not modify the underlying DNA sequence itself (Egger *et al*., 2004). One prominent example of an epigenetic modification is DNA methylation, which involves the addition of a methyl group to a cytosine base. DNA methylation is evolutionarily conserved and is associated with gene silencing in eukaryotic organisms (Bird, 1986). In mammals, DNA methylation predominantly occurs in the symmetric CG context, with an estimated 70-80% of CG dinucleotides throughout the genome being methylated (Ehrlich et al., 1982). The remaining unmethylated CG dinucleotides are often concentrated near gene promoters in clusters known as CpG islands (Suzuki & Bird, 2008; Cedar & Bergman, 2009). However, studies have uncovered the presence of non-CG methylation in certain cell types such as embryonic stem cells and brain cells (Ramsahoye et al., 2000; Xie et al., 2012; Varley et al., 2013). In contrast, plants exhibit DNA methylation in multiple sequence contexts, including symmetric CG and CHG contexts

(where H represents A, T, or C) and the asymmetric CHH context (Henderson & Jacobsen, 2007). For instance, in Arabidopsis thaliana, approximately 24% of CG, 6.7% of CHG, and 1.7% of CHH sites in the genome are methylated (Cokus et al., 2008). Notably, DNA methylation in plants is predominantly found on transposons and other repetitive DNA elements, unlike the mammalian system where it has a broader distribution across the genome (Zhang et al., 2006).

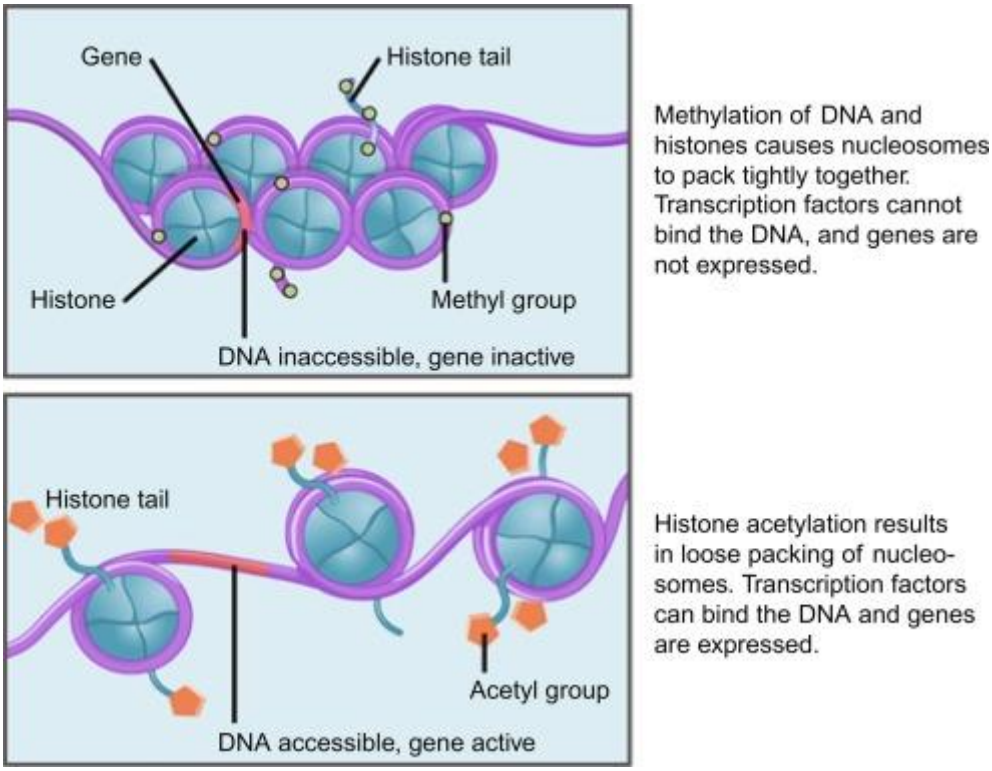

Figure 5.2. Epigenetic modifications contribute to the regulation of DNA transcription. Methylation promotes the formation of heterochromatin (top). Genes present in heterochromatin are not accessible for transcription. Acetylation promotes the formation of euchromatin (bottom) that allows the transcription of genes in these regions (source: Mobley, 2019).

In mammals, the establishment of DNA methylation patterns is mediated by the DNA methyltransferase 3 (DNMT3) family of de novo methyltransferases, while maintenance of methylation is carried out by the maintenance methyltransferase DNMT1 (Kim *et al*., 2009; Goll & Bestor, 2005; Cheng & Blumenthal, 2008). In plants, de novo methylation is catalysed by DOMAINS REARRANGED METHYLTRANSFERASE 2 (DRM2), which shares homology with the DNMT3 methyltransferases. The maintenance of DNA methylation in plants involves different pathways: CG methylation is maintained by DNA METHYLTRANSFERASE 1 (MET1, also known as DMT1), which is the plant homolog of DNMT1; CHG methylation is maintained by CHROMOMETHYLASE 3 (CMT3), a plant-specific DNA methyltransferase;

and asymmetric CHH methylation is persistently maintained through de novo methylation by DRM2 (Chan *et al*., 2005). While DNA methylation is generally considered a stable epigenetic mark, both plants and mammals can undergo a reduction in methylation levels during development. This net loss of methylation can occur either passively, through replication in the absence of functional maintenance methylation pathways (Jullien *et al*., 2008; McCabe *et al*., 2005; Kimura *et al*., 2003; McCabe *et al*, 2006), or actively, by the removal of methylated cytosines (Ikeda & Kinoshita, 2009; Zhu, 2009; Reik, 2007; Sasaki & Matsui, 2008). However, the specific pathways that regulate the establishment, maintenance, and removal of DNA methylation are still not fully characterized (Law & Jacobsen, 2010).

Plant studies have discovered important epigenetic mechanisms, including paramutation (Chandler & Stam, 2004), small interfering RNAs (siRNAs) (Hamilton & Baulcombe, 1999) and RNA-directed DNA methylation (Wassenegger *et al*., 1994). Most of these epigenetic mechanisms are related to silencing of repetitive sequences, such as transposable elements (TEs) (Comfort, 2001), parasitic DNAs that can amplify copies in the genome, and disrupt gene functions by insertion (Miryeganeh & Saze, 2019). Indeed, epigenetic control of gene expression mostly originate from regulation of TEs inserted near genes (Slotkin & Martienssen, 2007). Transposable elements, also known as "jumping genes" or transposons, are sequences of DNA that move (or jump) from one location in the genome to another and can be mutagenic (Bourque *et al*., 2018). They have been identified in all organisms, prokaryotic and eukaryotic, and can occupy a high proportion of a species' genome, for example, transposable elements comprise approximately 10% of several fish species (Muñoz-López & García-Pérez, 2010), 12% of the *Caenorhabditis elegans* genome (*C. elegans* Sequencing Consortium, 1998; Stein *et al*., 2003), 37% of the mouse genome (Mouse Genome Sequencing Consortium, 2002), 45% of the human genome (International Human Genome Sequencing Consortium, 2001), and up to >80% of the genome of some plants like maize (SanMiguel *et al*., 1996). The mobilization of TEs (transposition or retrotransposition, depending on the nature of the intermediate used for mobilization) can positively and negatively impact a genome; for example, TE mobilization can promote gene inactivation, modulate gene expression or induce illegitimate recombination, introducing a new piece of DNA into a gene (Muñoz-López & García-Pérez, 2010). In the model plant *Arabidopsis thaliana*, the overarching effect of TE methylation is to silence transposition (Zhang, 2008). In addition to preventing proliferation of new TE sequences, silencing of TEs near genes may also prevent the production of aberrant transcripts via read-through transcription beyond TE termini (Barkan & Martienssen, 1991). However, methylated

sequences may also affect the expression of nearby genes, typically reducing expression, implying a negative correlation between gene expression and the density of silenced TEs (Jahner & Jaenisch, 1985; Lippman *et al*., 2004; Zhang *et al*., 2008). Indeed, a major role of DNA demethylation in plants is to activate genes in response to biotic or abiotic stimuli, in many cases by targeting TE sequences located at their 5´ regions (Parrilla-Doblas *et al*., 2019); temporary loss of DNA methylation and subsequent reactivation of TEs, as during stress-induced bursts of TEs, can be a source of novel genetic variation in plant evolution (Belyayev, 2014; Daccord *et al*., 2017). On occasion, the reduction of gene expression could prove adaptive. For example, Lippman *et al*. (2004) demonstrated that expression of the flowering time gene FWA is correlated with the methylation status of a nearby SINE-like TE. More generally, however, one might expect that alteration of gene expression due to methylation of nearby TEs may have deleterious effects on gene and genome function. In plant genomes, CG and non-CG methylation are important for transcriptional silencing of TEs (Miryeganeh & Saze, 2019). In particular, non-CG methylation is often critical to protecting genes from adverse effects of neighbouring TEs (Kenchanmane Raju *et al*., 2019). For example, CHH islands are regions of high CHH methylation at euchromatin/heterochromatin borders, originally identified in *Z. mays*. They have been proposed to reinforce TE silencing by creating boundaries between highly methylated (CG and CHG), silenced chromatin of the TE and active chromatin of the adjacent gene (Gent *et al*., 2012; Li *et al*., 2015).

Cytosine methylation can also occur at some differentially regulated promoters and within the protein-coding regions of highly expressed genes (Zilberman *et al*. 2007). High levels of 5mC (5-Methylcytosine) in CpG-rich promoter regions are strongly associated with transcriptional repression (Figure 5.3), whereas CpG poor genomic regions exhibit a more complex and context-dependent relationship between DNA methylation and transcriptional activity (Jones, 2012). Gene body methylation (gbM) is an epigenetic mark where gene exons are methylated in the CG context only and it is transmitted trans generationally in plants, opening the possibility that gbM may be shaped by adaptation (Muyle *et al*., 2022). In contrast, CHH methylation is mostly erased by demethylation in the *A. thaliana* male germline and later reset during embryonic development (Calarco *et al*., 2012). Therefore, CHH methylation is only transmitted partially over, at most, one or a few generations. The transgenerational inheritance of the third context—CHG methylation—remains unclear. Although CHG methylation is retained during gametogenesis (Calarco *et al*. 2012), epimutation accumulation lines in *A. thaliana* do not diverge for CHG methylation over generations (van der Graaf *et al*., 2015), suggesting that CHG methylation is not inherited at a genome-wide

scale. To summarize, of the three methylation contexts in plants, methylation in CG dinucleotides is most prone to transgenerational inheritance and is therefore the best candidate for epigenetic adaptation. Overall, a growing body of literature finds that gbM correlates with levels and patterns of gene expression. It is not clear, however, if this is a causal relationship.

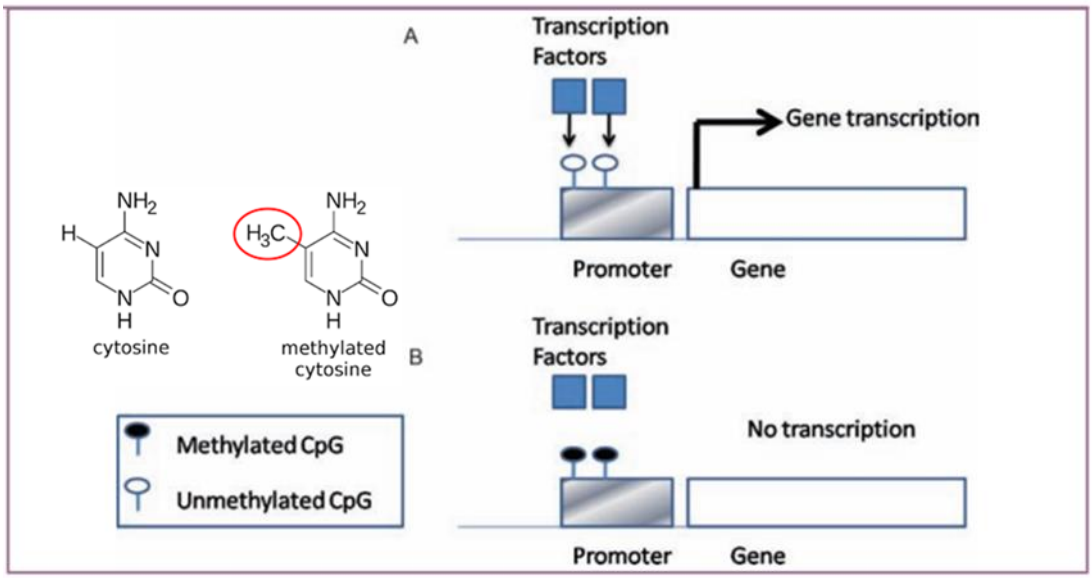

Figure 5.3. DNA methylation regulating gene expression. (A) The CpG island promoter is unmethylated and allows binding of transcription factors, which is required for transcription initiation. (B) The CpG island promoter methylation prevents binding of transcription factors and results in gene silencing (source: Lim & Maher, 2010).

Beside gene expression stabilization and upregulation, other important potential functions of gbM comprehend inhibition of aberrant transcription (reverse and internal), prevention of aberrant intron retention, and protection against TE insertions (Muyle *et al*., 2022). Also, gene body CG methylation enrichment within exons suggests a potential role in pre-mRNA splicing (Pikaard & Scheid, 2014). In *A. thaliana* genic methylation levels across genes are associated with expression levels: methylated genes tend to be intermediately to highly expressed, with lower expression variance among tissues (Zhang *et al*., 2006; Zilberman *et al*., 2007; Takuno & Gaut, 2012). These patterns have been interpreted in two ways: either gbM might affect expression patterns or, conversely, active transcription might drive gbM (Teixeira & Colot, 2009). Many highly expressed genes do not have gbM in *A. thaliana* (Zhang *et al*., 2006; Zilberman *et al*., 2007), an observation that discounts the second hypothesis or at least suggests that the relationship is not completely straightforward. Moreover, it is now known that CMT3 does not depend on gene expression to methylate genes but instead on

inaccessible chromatin marks and heterochromatin histone variants (Wendte *et al*., 2019; Papareddy *et al*., 2021), although it remains possible that the initial recruitment of CMT3 requires or depends on gene expression.

In this context, DNA methylation is especially relevant to evolution, due to its immediate impact on gene expression, as well as its more indirect effects due to suppression and reactivation of TEs (Kashkush *et al*., 2003; Madlung *et al*., 2005). In addition, DNA methylation itself is mutagenic, because spontaneous deamination of methyl-cytosine results in thymine formation (Rideout *et al*., 1990). Methylation of DNA can be the major epigenetic mark that is stably inherited for multiple generations through mitoses and meiosis (Schmitz *et al*., 2013; Eichten *et al*., 2014) and it also represents the most widely studied epigenetic mechanism in plants (Fulnecek, *et al*., 2002; Robertson & Wolffe, 2000). It is important to discriminate between inheritance of established epigenetic marks upon formation of specialized cell files in multicellular organisms (intra-organismal inheritance), and the inheritance of such epigenetic marks across generations. Transgenerational epigenetic inheritance requires the passage of epigenetic marks, such as DNA methylation, through the germline without being erased by surveillance mechanisms at the onset of ontogenesis (Reik *et al*., 2001; Lange & Schneider; 2010). Erasure of epigenetic marks, in early developmental stages, is well documented in mammals, but its relevance for developmental decisions made during plant embryogenesis is less well understood but it is seemingly a leaky process (Jullien & Berger, 2010). Now we know that heritable variation in plant phenotypes can be caused by both DNA sequence change and epigenetic variation and that plants modulate various aspects of developmental processes, including flowering and senescence time, and gametogenesis, by regulating epigenetic modifications on their genomic DNA (Miryeganeh & Saze, 2019). However, there are not many studies about plant responses to environmental factors in non-model species, due to a lack of genomic data and the complexity of real environmental conditions. Being sessile organisms, the control of gene expression is critical for plant responses to environmental stressors (Yaish *et al*., 2017), and epigenetic changes manipulate expression levels of specific genes (Baulcombe & Dean, 2014). Accumulated epigenetic alteration of stressed plants can then be transferred to their progeny as epigenetic transgenerational memory (Figure 5.4). Such transgenerational epigenetic memory may result from reassembly of parental nucleosomes during DNA replication (Alabert *et al*., 2015; Iglesias & Cerdan, 2016) and stable maintenance of DNA methylation and histone modification patterns after DNA replication (Johannes *et al*., 2009; Cortijo *et al*., 2014). Although the functional role of environment-induced DNA methylation is not always evident

(Secco *et al*., 2015; Bewick & Schmitz, 2017), it is often proposed that DNA methylation can translate environmental signals to modified gene expression profiles, thus acting as a regulating mechanism for the expression of phenotypic plasticity (Herrel *et al*., 2020; Skinner & Nilsson, 2021). Several studies have reported that cytosine contexts and genomic features are differentially impacted by stress and could thus play different roles in mediating stress responses (Gallego-Bartolomé, 2020; Kumar & Mohapatra, 2021). Furthermore, while plant methylome responses to both biotic and abiotic stresses may be common, further studies suggest differences in how DNA methylation responds to stress both within and across plant species (Dubin *et al*., 2015; Galanti *et al*., 2022; Peña-Ponton *et al*., 2022). Thus, better insights in the generalities and specificities in DNA methylation stress responses across plant species are needed. A better understanding of these aspects of the methylation response to stress may help to establish how important environmentally induced DNA methylation variations are in regulating stress responses.

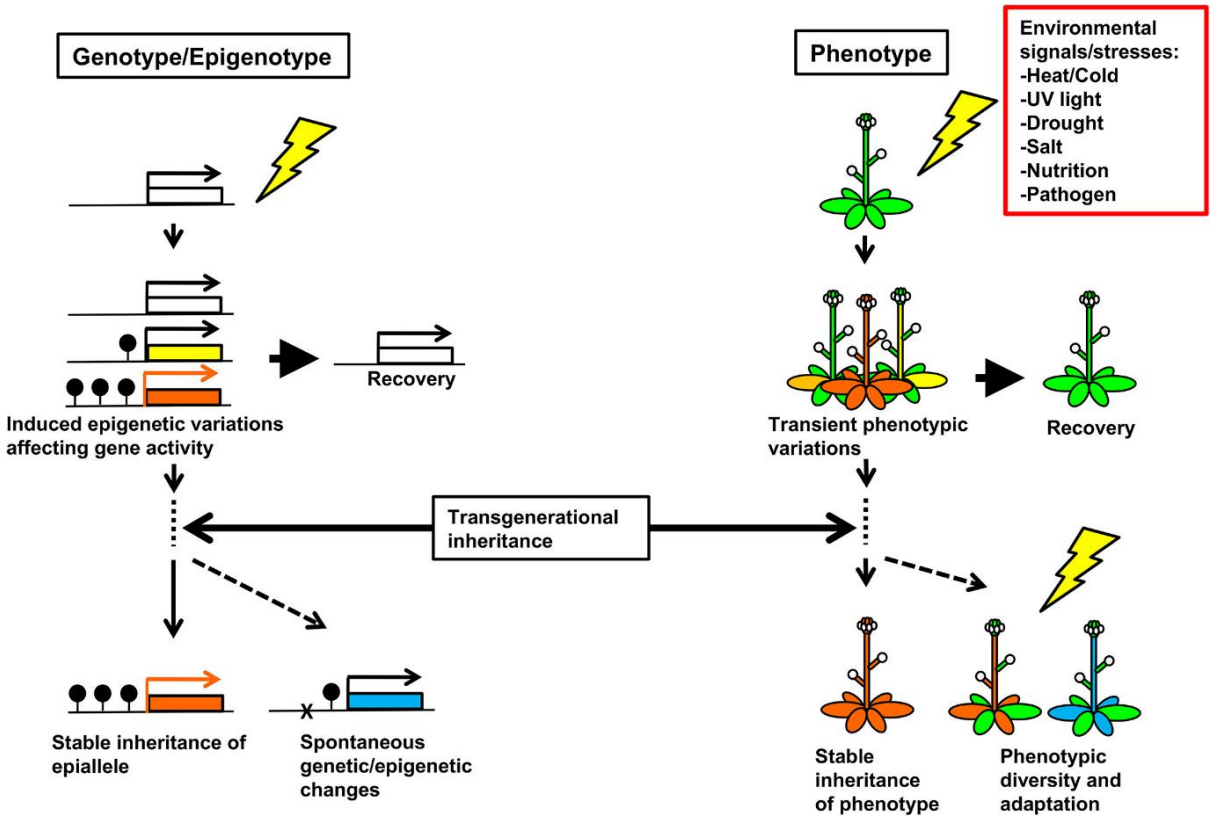

Figure 5.4. A model for epigenetic inheritance in plants. Genetic/epigenetic changes (left) and phenotypic changes (right) are shown separately. Environmental signals/stimuli (red box) perceived by individual plants may induce epigenetic variations in the genome of a plant population. In this figure, induction of epigenetic modification is shown (as lollypops), while a loss of existing modifications can also be occurred. In most cases, these epigenetic changes would be transient, reverting to the initial epigenetic state. In some cases, induced epigenetic changes may be transmitted

trans generationally. Inherited epigenetic changes may become adaptive if offspring experiences environmental signals/stimuli similarly to the previous generations. If epigenetic changes are associated with genetic changes (e.g., transposon insertions) they can be stably, or variably maintained as epialleles. Otherwise, epigenetic changes spontaneously revert to their initial states, or deamination of methyl-cytosines induces genetic changes. Different colours represent gene loci with altered activities due to epigenetic changes. Lollypops represent chromatin modifications such as DNA methylation. X indicates a genetic mutation (source: Miryeganeh & Saze, 2019).

There are numerous evidence that testify DNA methylation changes in response to abiotic and biotic stress in plants (Arora *et al*., 2022), that often highlight its dynamic and changeable character observing very fast changes in methylation level and status in a limited time (e.g. herbicide stress-induced increase in DNA methylation level after 6 h resulted in a lower ability to cope with stress, Tyczewska *et al*., 2021; after 24 h of cold stress treatment, DNA methylation levels in the repeats of the gene promoters were significantly reduced, Yang *et al*., 2022; decrease of the global DNA methylation level 1 h after wounding-induced oxidative burst, Lewandowska-Gnatowska *et al*., 2014; differentially methylated and differentially expressed genes after 3 h of desiccation and salinity stress exposure, Rajkumar *et al*., 2020). In particular, in the article by Vega-Muñoz *et al*., (2018) they observed that self-DNA exposure causes changes in CpG DNA methylation and defence-related responses in *Lactuca sativa.* For the first time, they demonstrated that self DNA acts as a DAMP in plants, changing CpG DNA methylation levels as well as increasing the production of secondary metabolites associated with defence responses to stress. Specifically, the DAMP effect of sDNA in the present work displayed significant changes in CpG DNA hypomethylation levels, gene expression associated with the oxidative burst generated in plant defence responses (superoxide dismutase: sod; catalase: cat), and phenylpropanoid production (phenylalanine ammonia lyase: pal), as well as the production of secondary metabolites (phenylpropanoids measured as total phenolics and flavonoids) in the first development stages in *L. sativa*. Interestingly, the results regarding changes in CpG DNA methylation and defence related responses in *L. sativa* were more similar for both sDNA (*L. sativa*) and nsDNA from chili pepper (*Capsicum chinense* Murray) (both species belong to the *Asterids* clade) than for nsDNA from *Acaciella angustissima* (Mill.) Britton & Rose (belonging to the *Rosids* I clade), thus suggesting a clear phylogenetic closeness effect for extracellular DNA as a DAMP. In light of this evidence, in this activity we present a Whole Genome Bisulfite Sequencing (WGBS) and RNA sequencing (RNA-seq) analysis of, respectively, DNA and RNA extracted from sample roots of *Arabidopsis thaliana* seedlings exposed to self-DNA solution for 6 h and 24 h with the aim of investigating changes in cytosine methylation across genome and gene

expression level. Whole Genome Bisulfite Sequencing or Reduced Representation Bisulfite Sequencing (RRBS) are the golden standard techniques used to obtain high-resolution DNA methylation information in the genome (Laine *et al*., 2022), but these techniques require the availability of a reference genome which are rarely available in plant species (Kress *et al*., 2022). Bisulphite ions (HSO_3^-) selectively deaminate unmethylated but not methylated Cs, giving rise to Us, which are replaced by Ts during subsequent PCR amplification (Figure 5.5).

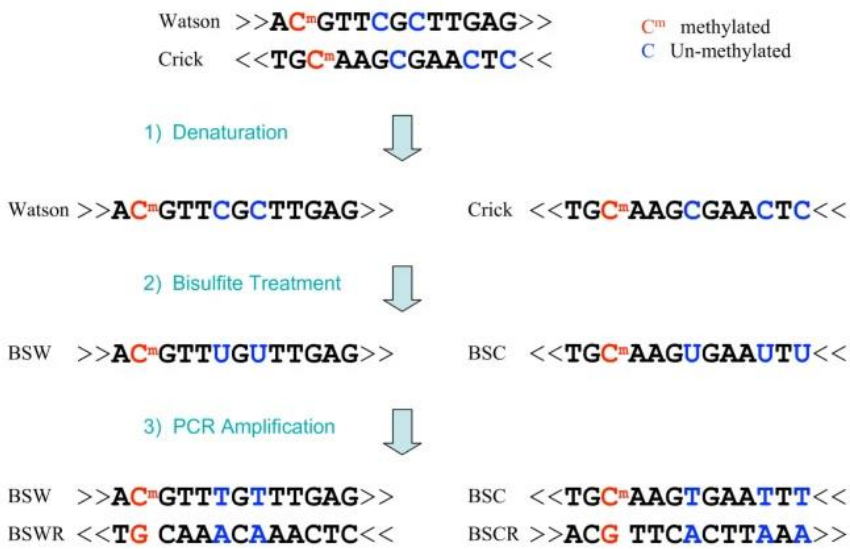

Figure 5.5. Pipeline of bisulfite sequencing. 1) Denaturation: separating Watson and Crick strands; 2) Bisulfite treatment: converting un-methylated cytosines (blue) to uracils; methylated cytosines (red) remain unchanged; 3) PCR amplification of bisulfite-treated sequences resulting in four distinct strands: Bisulfite Watson (BSW), bisulfite Crick (BSC), reverse complement of BSW (BSWR), and reverse complement of BSC (BSCR) (source: Xi & Li, 2009).

As a result of DNA treatment with the bisulphite chemical, the vast majority of unmethylated Cs (cytosines) appears as Ts (thymine) among the sequencing reads, whereas methylated Cs are largely protected from bisulphite-induced conversion. After bisulphite conversion and amplification, the DNA is adapter ligated and used to prepare a sequencing library. Following sequencing, DNA is bioinformatically analysed to reveal methylated cytosines across the entire genome. To calculate absolute DNA methylation levels (percentage of methylated alleles for a given C; this value is always binary – 0% or 100% – for single alleles but can take any value between 0% and 100% when averaging over many cells) from bisulphite sequencing data, sequencing reads are aligned to the positions in the reference genome from which they were most likely to be derived, and the percentage of Cs and Ts are determined among all reads aligned to each C in the genomic DNA sequence. The alignment of

bisulphite-sequencing reads needs to account for the selective depletion of unmethylated Cs (Bock, 2012). One of the most used alignment approaches, the “three-letter aligners” (used by software like Bismark, Krueger & Andrews, 2011), simplify bisulphite alignment by converting all Cs into Ts in the reads and for both strands of the genomic DNA sequence. This way, they can carry out the alignment exclusively on a three-letter alphabet (namely, A, G and T) using a standard aligner, such as Bowtie (Figure 5.6) (Langmead *et al*., 2009). Three-letter aligners purge the remaining Cs from the bisulphite sequencing reads and thereby decrease the sequence complexity, such that a larger percentage of reads is discarded owing to ambiguous alignment positions; this strategy allows this method to avoid introducing some bias but also leads to an inferior coverage compared to other methods (e.g. wild-card aligners, Bock, 2012).

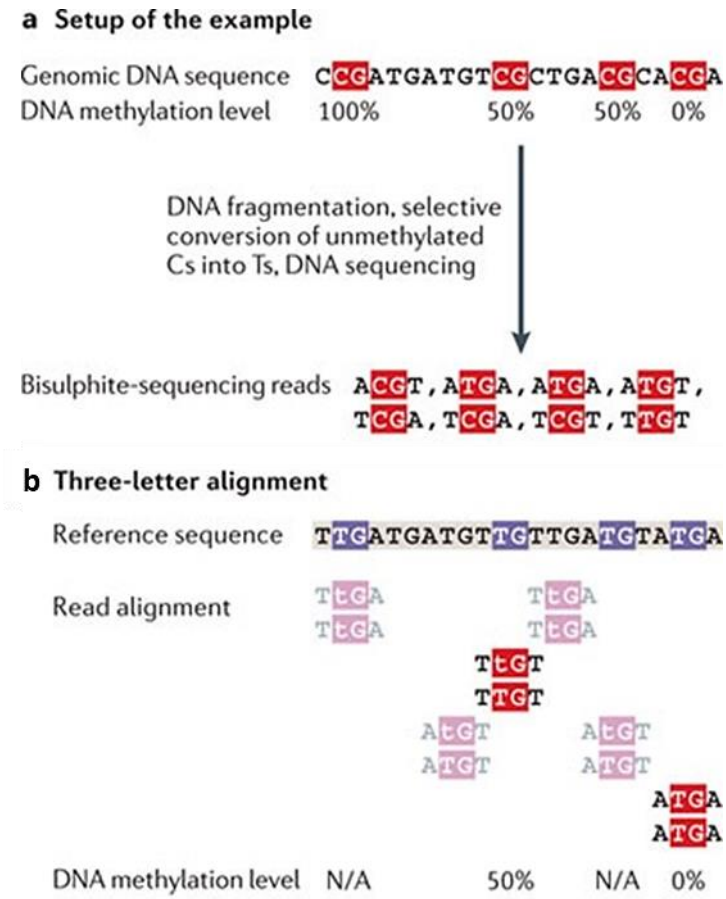

Figure 5.6. A strategy example for bisulphite alignment. a) An illustrative example of bisulphite sequencing for a DNA fragment with known DNA methylation levels at four CpGs and a total of eight bisulphite-sequencing reads (two for each highlighted CG regions). For easier visualization, the sequencing reads are four bases long (realistic numbers would be 50 to 200 bases), and the size of the genomic DNA sequence is just 23 bases (3 gigabases would be a realistic number for the human

genome). b) The alignment carried out by a three-letter aligner tolerates zero mismatches and zero gaps. The aligner replaces each C in the reference sequence by an upper-case T and each C in the sequencing reads by a lower-case t, with no distinction being made between upper-case T and lower-case t during the alignment. As a result of the reduced sequencing complexity with only three letters remaining, a larger number of reads align to more than one position in the reference sequence and are discarded (ambiguous reads). The three-letter alignment avoids incorrect results in this example, but it fails to provide any values for the first and third CpG (adapted from Bock, 2012).

After the bisulphite alignment has been completed, absolute DNA methylation levels are inferred from the frequency of Cs and Ts that align to each C in the genomic DNA sequence and data are further bioinformatically analysed, visualized and biologically interpreted. In Figure 5.7 is presented a simplified workflow for bisulphite analysis and data processing (Block, 2012).

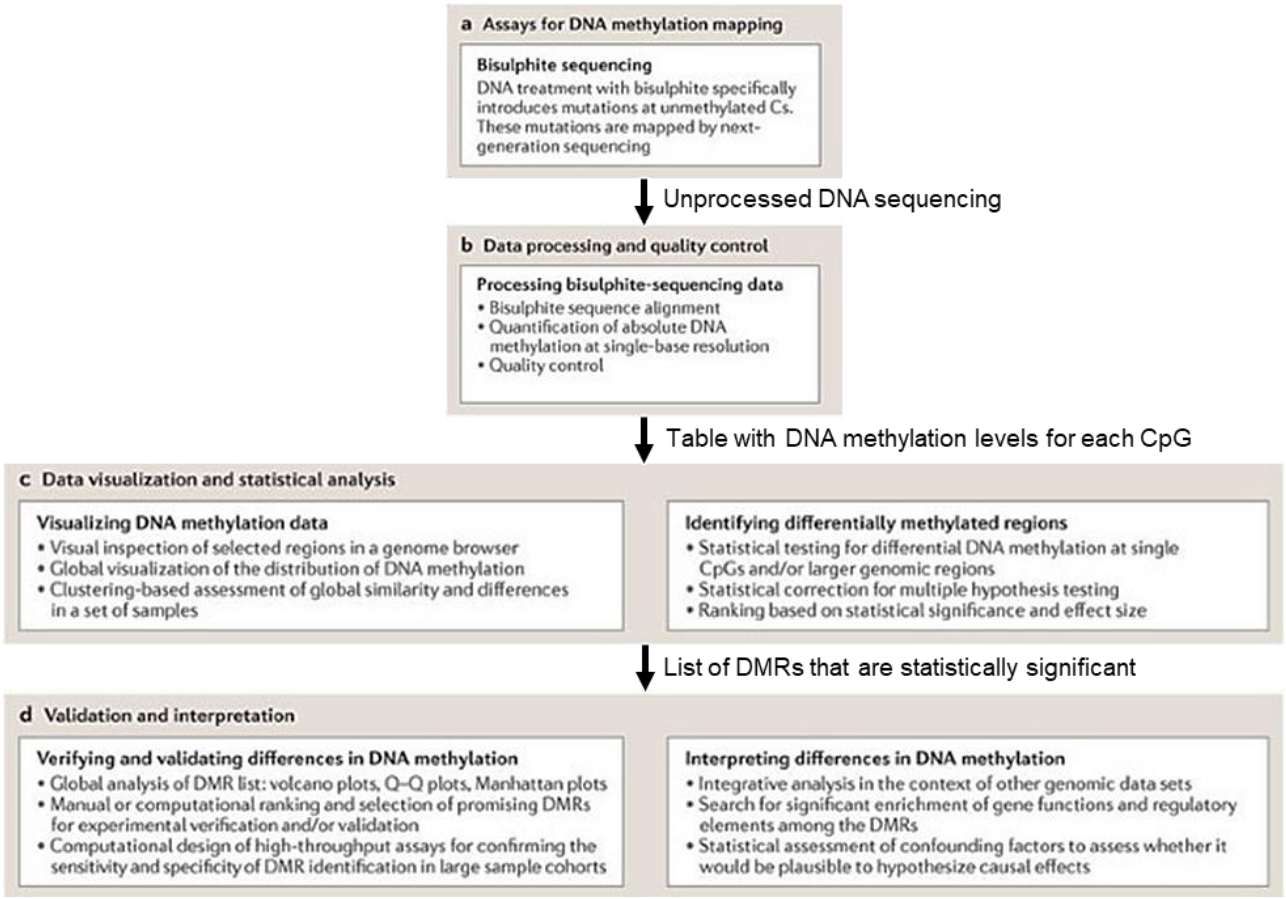

Figure 5.7. Workflow for analysing and interpreting DNA methylation data. a) Genome-wide DNA methylation is mapped through bisulphite analysis, resulting in methylation-specific DNA sequencing. b) These raw data are processed and quality-controlled using assay-specific algorithms and software. The main result of data normalization is an assay-independent CpG methylation table that contains absolute DNA methylation levels for all covered CpGs. c) Data visualization and statistical analysis

identifies relevant associations and derives a list of differentially methylated regions (DMRs) between cases and controls. d) The resulting DMR list is validated both computationally and experimentally, and biological interpretation is assisted by computational tools (adapted from Bock, 2012).

The sequencing data from our study is currently undergoing detailed analysis. While the complete results are still pending, this thesis presents preliminary findings through the utilization of Principal Component Analysis (PCA) graphs. PCA is a statistical procedure that enables the summarization of information contained in large data tables by generating a smaller set of "summary indices." These indices can be more readily visualized and analysed, thereby facilitating the reduction of multidimensional data to lower dimensions while retaining a significant portion of the information. The fundamental idea behind PCA is to decrease the dimensionality of a dataset while preserving as much variability or statistical information as possible. This process involves creating new uncorrelated variables, known as principal components (PCs), which maximize the variance. These principal components describe the variation in the data and account for the diverse influences of the original characteristics. Essentially, the objective is to identify new variables that are linear combinations of the original dataset's variables, progressively maximizing variance and ensuring their lack of correlation with one another. This entails solving an eigenvalue/eigenvector problem to determine these principal components. Consequently, a PCA plot visually represents clusters of samples based on their similarity. It is worth emphasizing that the primary utility of PCA lies in its descriptive nature rather than its inferential capacity (Jolliffe & Cadima, 2016).
Moving on to the expected outcomes of our study, we anticipate identifying differential DNA methylation patterns between the treatment samples and control group. Additionally, we aim to uncover differential methylation associated with genes involved in stress response pathways, as well as discern differences in root gene expression between the treatment samples and controls. Furthermore, we will explore the potential correlation between differential DNA methylation and gene expression changes. Through our analysis, we hope to provide new insights into the molecular aspects involved in self-DNA response. By elucidating the connections between DNA methylation, gene expression, and treatment outcomes, we anticipate contributing valuable knowledge to the field. However, it is important to note that our study is still in progress, and these expectations are subject to further investigation and validation.

5.3. Materials and Methods

5.3.1. Seed sterilization and germination

Arabidopsis thaliana Col 0 seeds were sterilized with 1% NaClO solution for 5 min., then rinsed 5 times with sterile water during 1 min. for each wash. Sterilized seeds were distributed in lines with a pipette on fifteen 150 mm Petri dishes (each representing a separate biological replica) filled with a thin layer of Murashige and Skoog growth medium (1 L made with: 4.4 g Murashige-Skoog basal medium with Gamborg's vitamins – Sigma Aldrich –; 30 g sucrose; 16 g agar; sterile water to final volume). The Petri dishes were hermetically closed and placed in a growth chamber under standard controlled conditions (22 ± 2 °C, 50% RH, 16 h day and 8 h night photoperiod) for about 15 days, over an inclined plane to favour straight root growth through geotropism and prevent root from growing inside the growth medium.

5.3.2. Growth medium slices preparation

When seedling roots reached around 3 cm, the growth medium with the seedlings grown over it in each Petri dish was divided into slices of 35 mm (length) x 40 mm (height) with a sterile scalpel under sterile hood. We selected a total of 60 slices, the most densely occupied by Arabidopsis seedlings. Each slice was delicately placed inside a pocket of a 20-pocket plastic coin holder sheet (each pocket measuring 45 mm x 30 mm) (Figure 5.8). The 3-cm-roots were completely enclosed within the plastic pocket, while the green top portion, approximately 0.5-1 cm, remained outside of it. The three plastic coin holder sheets filled with the slices were hung under a sterile hood to keep them as straight and firm as possible (Figure 5.9).

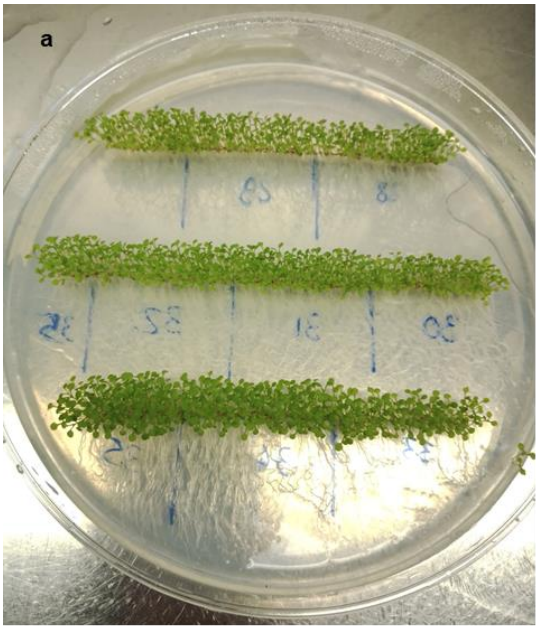

Figure 5.8.

a) Slices preparation involved working with growth medium containing Arabidopsis seedlings. The medium was initially divided into slices by marking and measuring designated areas on the back of a Petri dish using a marker and ruler. Subsequently, the demarcated slices (~35 mm x 40 mm) were carefully cut using a sterile scalpel within a sterile hood environment.

b) Each slice was carefully placed inside a pocket of a 20-pocket plastic coin holder sheet (each pocket measuring 45 mm x 30 mm). The 3-cm-roots were completely enclosed within the plastic pocket, while the green top portion, approximately 0.5-1 cm, remained outside of it.

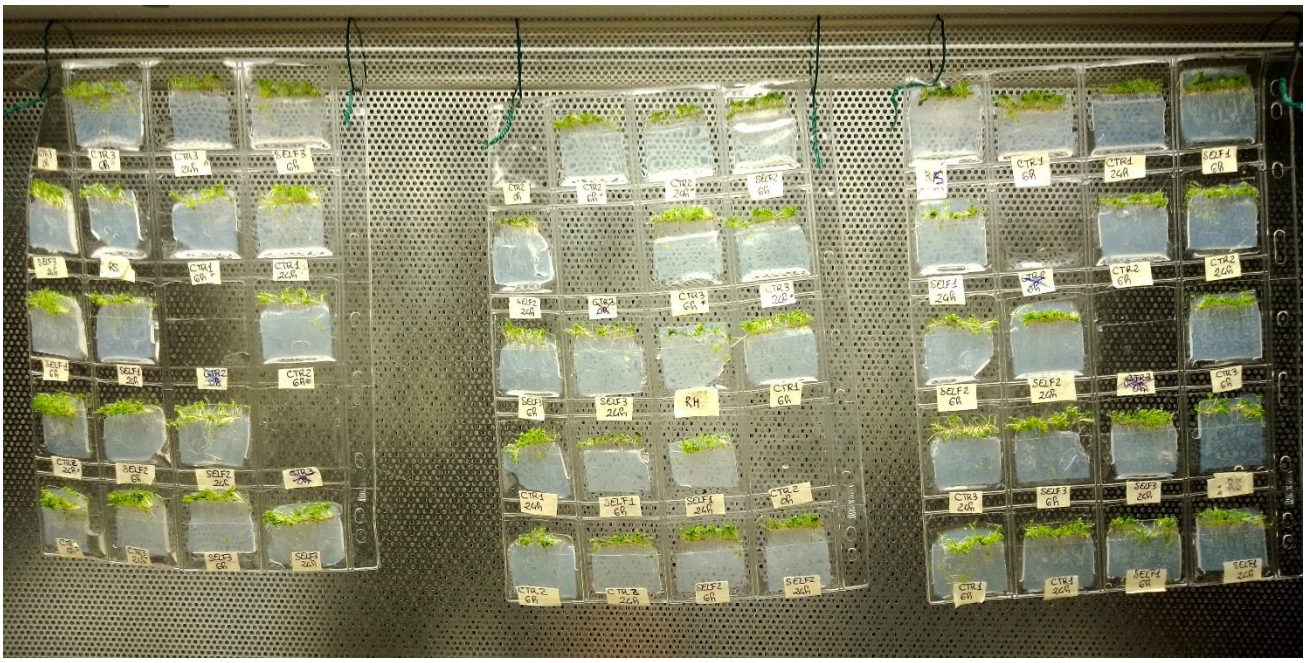

Figure 5.9. Once all 60 pockets were filled with the cut growing medium slices, the three plastic coin holder sheets were hung under a sterile hood and kept as straight and firm as possible. Each biological sample included 4 growth medium slices.

5.3.3. Self-DNA exposure and root collection

Each biological sample consisted of 4 random slices. Twelve slices were immediately collected to serve as three control replicas at the beginning of the experiment (time 0 h). Collected slices were gently put on a Petri dish lid and the green top was cut off with the sterile scalpel, always remaining under the sterile hood. From each group (replica) of 4 slices, roots were delicately gathered with a sterile spatula (Figure 5.10), washed in sterile water, dried on paper, and weighted. Each replica's roots were collected into two Eppendorf: the first tube, destined to DNA extraction, contained ~50-70 mg of roots (fresh weight); the second tube, destined to RNA extraction, contained ~15-25 mg of roots. Both tubes of each replica were stored at -80°C. Afterwards, 24 slice-containing-pockets were filled with 1 mL of Arabidopsis DNA solution at the concentration of ~60 ng/µL, while all the other slice-containing-pockets were exposed to sterile water. DNA was extracted from Arabidopsis leaves and provided from the University of Naples. The DNA was subjected to the same treatments described in section 2.2.2 and 2.2.3, namely RNase treatment, precipitation and sonication, to reach the desired fragment size range (below or around ~1500 bp). Purity and quantity were assessed with, respectively, spectrophotometer Nanodrop ND 1000 (Thermo Fisher Scientific, Waltham, MA, USA) and fluorimeter Qubit 3.0 (Life Technology, Carlsbad, CA, USA). During exposure time, the air flux of the hood was kept on, while lights were turned off to limit heating the solution and prevent excessive evapotranspiration. After 6 h of self-DNA exposure, other 24 slices were collected, specifically 12 slices exposed to self-DNA (3 treated replicas each including 4 slices) and 12 exposed to sterile water (3 control replicas each including 4 slices). For each replica, roots were washed, collected, divided in two tubes and stored as described above. The same procedure was repeated after 24 h from the beginning of exposure. In total, 15 samples (Figure 5.11), between control and treated replicas at three time points, were collected and stored for subsequent analysis. Considering that each sample included two Eppendorf tubes (one for DNA and one for RNA extraction) 30 tubes in total were stored, each labelled with the respective sample indication.

Figure 5.10.

a) Collected slices were gently put on a Petri dish lid and the green top was cut off with a sterile scalpel.

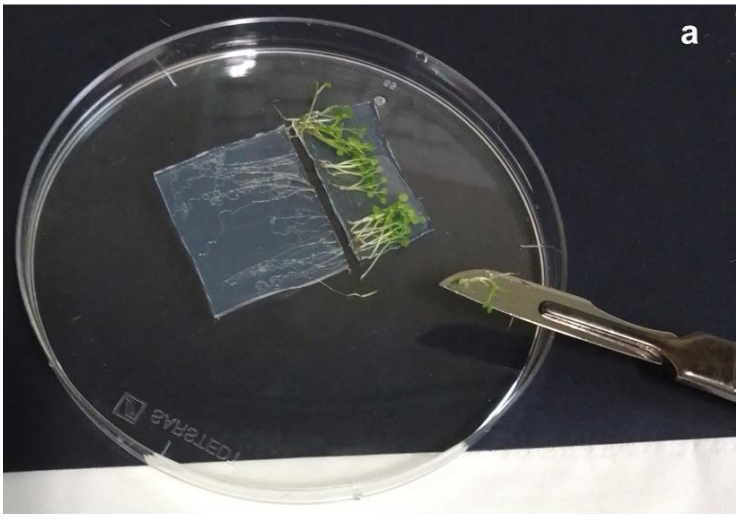

b) From each group (replica) of 4 growth medium slices, roots were delicately gathered with a sterile spatula, washed in sterile water, dried on paper, weighted and stored in two separate Eppendorf tubes, one for DNA extraction and the other for RNA extraction.

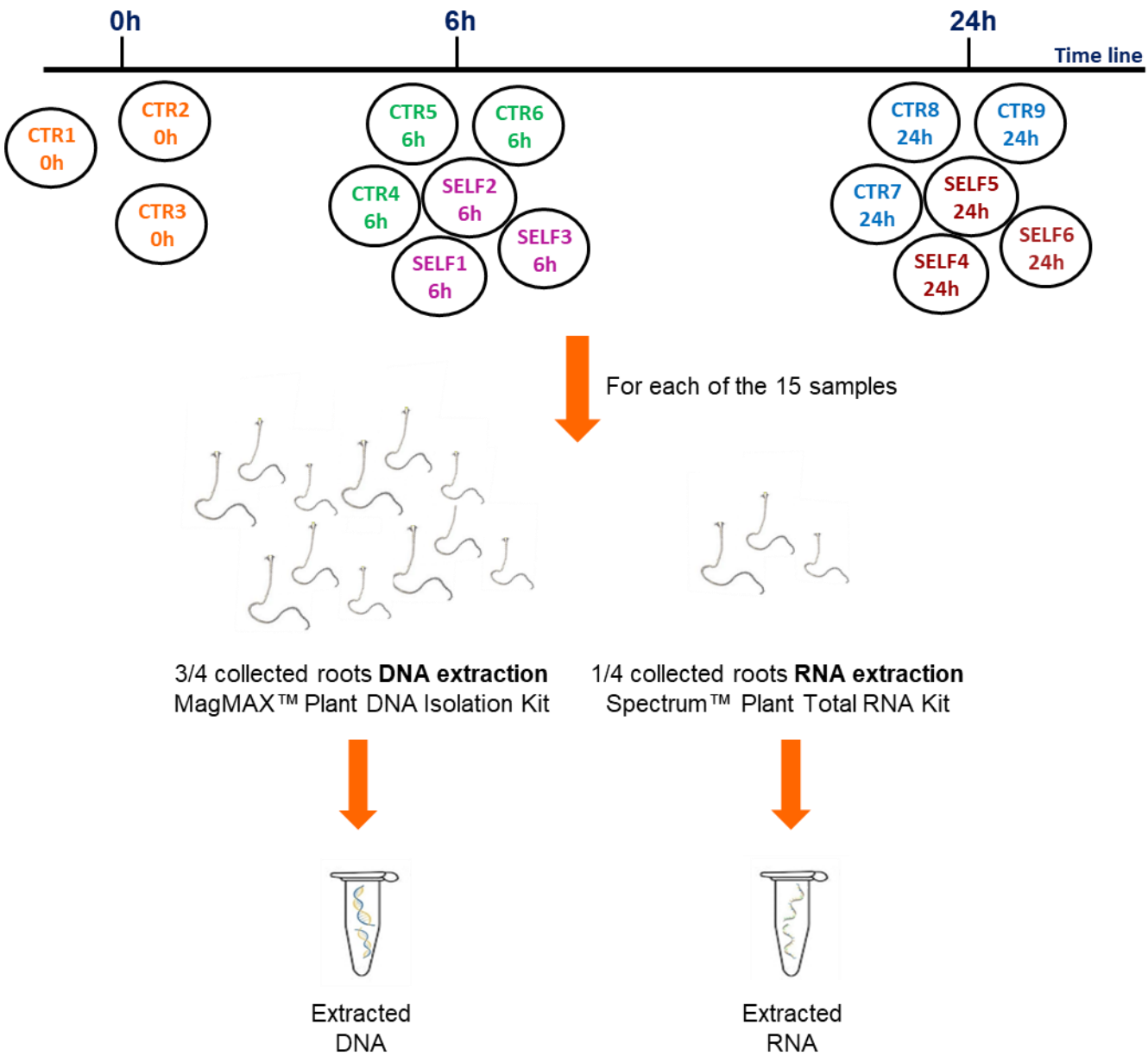

Figure 5.11. Root exposure to self-DNA (~ 60 ng/µL) or sterile water and root collection. CTR refers to samples exposed to water while SELF refers to samples exposed to self-DNA. Three biological replicas were carried out per each treatment and exposure time (15 samples in total). Roots were collected at 0 h, 6 h and 24 h (CTR 0h, CTR 6h, SELF 6h, CTR 24 h, SELF 24 h). Per each sample (4 slices of growth medium with seedlings) 3/4 of the roots (~50-70 mg) were collected and stored for DNA extraction, while the remaining 1/4 (~15-25 mg) was collected and stored for RNA extraction.

5.3.4. RNA extraction and mRNA sequencing

For each of the 15 samples, RNA extraction was performed using the Eppendorf tube containing less root material (~15-25 mg). RNA was extracted with the Spectrum™ Plant Total RNA Kit (Sigma-Aldrich, St. Louis, MO, USA), scaling the reagent volumes recommended by the manufacturer to the low amount of root material per sample, as follows:

300 µL of the Lysis Solution/2-ME Mixture, 500 µL of the Binding Solution, 300 µL for every washing step, and one elution with 35 µL of the Elution Solution (see also section 3.2.3 of this thesis). RNA quality was checked using Nanodrop ND 1000 Spectrophotometer (Thermo Fisher Scientific, Waltham, MA, USA) and assessed by 1% electrophoresis agarose gel. RNA quantity was determined with Qubi RNA Broad-Range Assay kit (Thermo Fisher Scientific) using Qubit 3.0 Fluorometer (Thermo Fisher Scientific). RNA integrity was measured by on-chip capillary electrophoresis using Agilent 2100 Bioanalyzer RNA assay (Agilent technologies, Santa Clara, CA) by IGA Technology Services Srl (https://igatechnology.com/), before performing mRNA-seq.

Universal Plus mRNA-Seq kit (Tecan Genomics, Redwood City, CA) has been used for library preparation of the 15 RNA samples following the manufacturer's instructions (library type: fr-secondstrand). Final libraries were checked with both Qubit 2.0 Fluorometer (Invitrogen, Carlsbad, CA) and Agilent Bioanalyzer DNA assay. Libraries were then prepared for sequencing and sequenced on paired-end 150 bp mode (~23 Millions spots paired-end with reads of 150 bp, total of 7 Gbp) on NovaSeq 6000 (Illumina, San Diego, CA). RNA-Seq library construction and sequencing were performed by IGA Technology Services Srl (https://igatechnology.com/).

5.3.5. DNA extraction and Whole Genome Bisulfite Sequencing analysis

For each of the 15 samples, DNA extraction was performed using the Eppendorf tube containing more root material (~50-70 mg). DNA was extracted with the MagMAX Plant DNA Isolation Kit (A32549, ThermoFisher Scientific) following manufacturer's instructions. DNA quality was checked using NanoDrop ND 1000 Spectrophotometer (ThermoFisher Scientific), whereas DNA quantity was determined using Qubit dsDNA Broad-Range Assay kit (Thermo Fisher Scientific) with Qubit 3.0 Fluorometer (ThermoFisher Scientific). Bisulfite treatment, BS-Seq library construction and sequencing were performed by IGA Technology Services Srl (https://igatechnology.com/). Ultralow Methyl-Seq System (Tecan/NuGEN, Redwood City, CA) has been used for library preparation following the manufacturer's instructions. The system produces directional bisulfite-converted libraries. The forward sequencing reads correspond to a bisulfite-converted version of either the original top or the original bottom strand (the C-to-T reads) and the reverse sequencing reads correspond to the complement of the original top or the complement of the original bottom strand (the G-to-A reads). Delivered DNA samples were quantified with Qubit 2.0 Fluorometer (Invitrogen, Carlsbad, CA). Final libraries were checked with both Qubit 2.0 Fluorometer (Invitrogen, Carlsbad, CA)

and Agilent Bioanalyzer DNA assay (Agilent technologies, Santa Clara, CA). Libraries were then prepared for sequencing and sequenced on paired-end 150 bp mode (~23 Millions spots paired-end with reads of 150 bp, total of 7 Gbp) on NovaSeq 6000 (Illumina, San Diego, CA).

5.3.6. Bioinformatic analysis

All bioinformatic analyses were performed *in silico* using MobaXterm, a command-line interface SSH client with a Unix-like environment. These analyses were conducted remotely on a Linux server with version 3.16.0-4-amd64, gcc version 4.8.4 (Debian 4.8.4-1), which was equipped with 64 computing nodes (Intel(R) Xeon(R) CPU E5-4610 v2 @ 2.30GHz) and 128 GB of available RAM. This server is located in the Department of Agricultural, Environmental, and Animal Sciences (DI4A) at the University of Udine.

Firstly, sequencing adapters and low-quality bases of raw reads (from both RNA-seq and WGBS) were trimmed using TrimGalore (Krueger, 2021) and quality controlled using FastQC (Andrews, 2010). Reads from WGBS were also deduplicated in order to discard putative PCR duplicates by retaining only one read per start and end position in the reference genome and prevent bias (Bock, 2012). Bisulphite read mapping against the TAIR10 version of *Arabidopsis thaliana* genome and conversion to cytosine-specific DNA methylation levels were performed using the bisulphite sequencing alignment tool Bismark V0.22.3 (Krueger & Andrews, 2011). DNA methylation-based PCA was performed using the methylKit R package (Akalin *et al*., 2012) with default parameters and a Q-value cutoff of 0.01. RNA-seq reads were mapped to the TAIR10 version of *Arabidopsis thaliana* genome using STAR software package v2.7.9a (Dobin *et al*., 2013) with default parameters. Read counting per gene was carried out with STAR using the "--quantMode GeneCounts" option, to produce counts coinciding with those produced by htseq-count with default parameters. Principal Component Analysis was performed using the standard R prcomp function with STAR gene counts normalized by the regularized-logarithm transformation method of the DESeq2 R package (Love *et al*., 2014). The resulting principal component matrix was plotted using the ggplot2 R package (Wickham, 2016).

5.4. Results

5.4.1. RNA-seq and gene expression in treated vs control samples

Average RNA extraction yield over the 15 samples was 400 ng/mg of roots (fresh weight), Nanodrop ratios 260/280 and 260/230 were always > 2 and average RIN (RNA integrity number) was 6.40, spanning between 5 and 8.50. At least 500 ng for each sample were

delivered to IGA for RNA-seq analysis. In Figure 5.12 are presented the results of the gene expression PCA. Principal components comprehend groups of genes whose expression level differences among samples explain most of the variability. In Table 5.1 the number of reads (in millions) produced for each sample are listed.

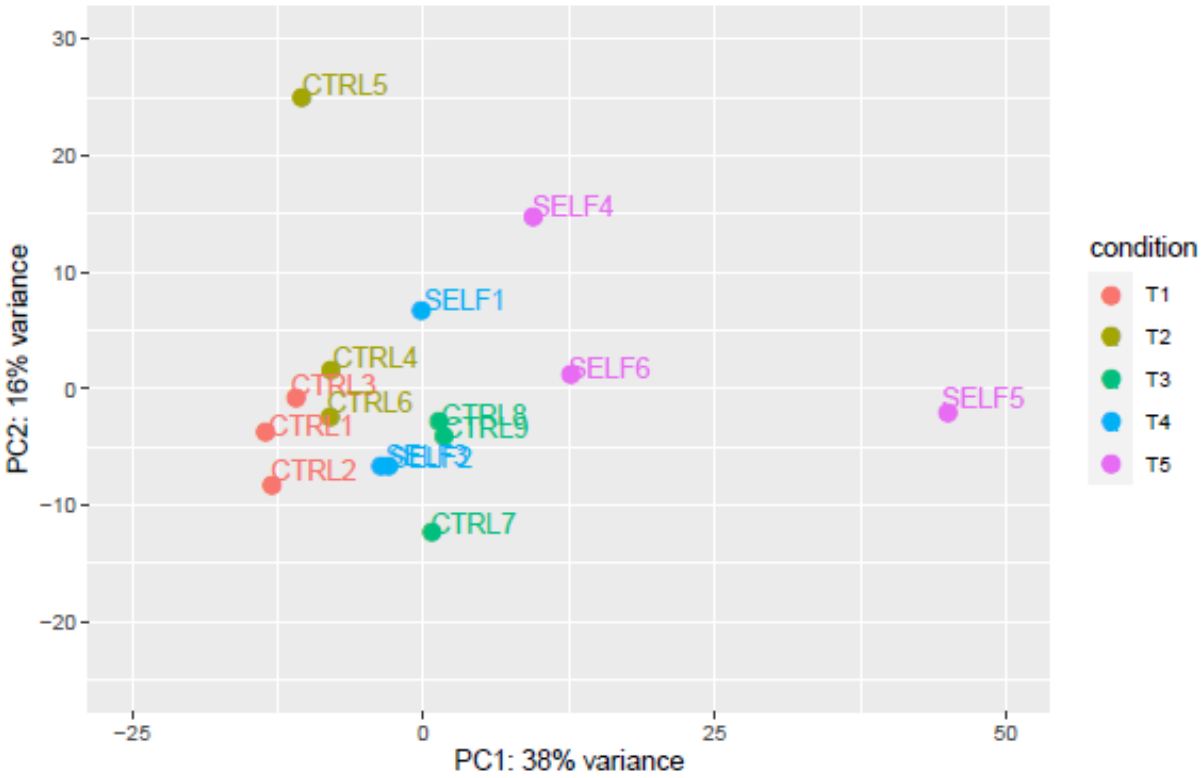

Figure 5.12. Gene expression PCA results showing experiment samples divided in clusters based on the variance explained by PC1 (38%) and PC2 (16%).

Table 5.1. List of sample ID, sample description and number of reads (in millions) produced for each RNA sample.

Sample_ID	Sample description	Number of reads (Millions)
CTRL1	RNA CTR1 0h	44.17
CTRL2	RNA CTR2 0h	47.32
CTRL3	RNA CTR3 0h	39.88
CTRL4	RNA CTR4 6h	55.56
CTRL5	RNA CTR5 6h	32.57
CTRL6	RNA CTR6 6h	40.20
CTRL7	RNA CTR7 24h	49.48
CTRL8	RNA CTR8 24h	108.83
CTRL9	RNA CTR9 24h	44.44
SELF1	RNA SELF1 6h	57.05
SELF2	RNA SELF2 6h	93.34
SELF3	RNA SELF3 6h	85.02
SELF4	RNA SELF4 24h	56.08
SELF5	RNA SELF5 24h	46.95
SELF6	RNA SELF6 24h	60.60

From a first qualitative analysis and representation of our gene expression data (Figure 5.12), we can infer that there is a difference in gene expression levels between samples treated with self-DNA and control samples. In particular, along PC1, a clear spreading of the samples is evident according to the interaction of two main conditions: i) harvest timing (i.e. 0, 6 and 24 h), with early-harvested samples showing lower factorial scores compared to late-harvested samples within either treatment group (i.e. self-DNA exposed and controls); ii) treatment group, with control samples consistently showing lower factorial scores on the PC1 as compared to the corresponding treated samples. In detail, samples treated with self-DNA for 6 h (SELF1, 2 and 3) and relative controls (CTRL4 and 6), were clearly separated. However, CTRL5 showed much higher factorial score than CTRL4 and 6 on PC2, appearing as a possible outlier. Interestingly, CTRL5 is also the sample with the least number of reads (Table 5.1). Seemingly, the three samples treated for 6 h, are closely clustered on PC1, while SELF1 shows a higher factorial score on PC2, indicating a different gene expression pattern in this sample as compared to SELF2 and SELF3. A more relevant difference in gene expression levels (Figure 5.12) was found between samples treated with self-DNA for 24 h (SELF4 and 6) and the respective controls (CTRL7, 8 and 9), evident on both principal components. In particular, control samples at 24 h are clustered very closely, with only a small variability on the PC1, and more divergent on the PC2, confirming data reliability for these control replicates. On the other hand, SELF samples at 24 h showed a higher between-replicates variability of gene expression, with SELF5 in particular appearing as a possible outlier. This sample is among those with the least reads count.

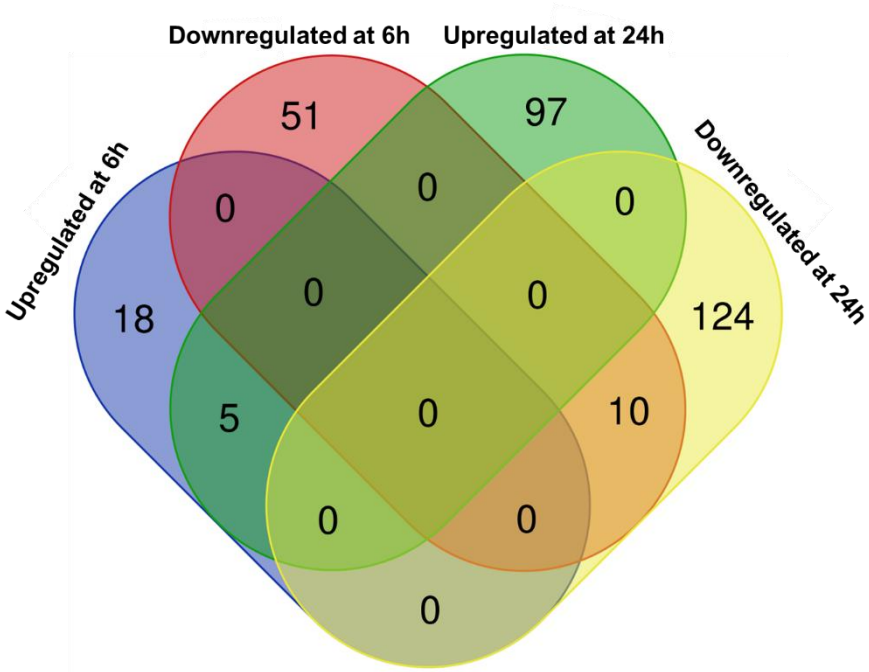

Figure 5.13. Venn diagram showing numbers of differentially expressed genes (DEG) in each of the four groups (Upregulated at 6h; Downregulated at 6h; Upregulated at 24h; Downregulated at 24h).

The Venn diagram in Figure 5.13 numerically represents the genes up- and downregulated compared to the control at 6 and 24h. These differentially expressed genes (DEGs) are more numerous at 24h compared to 6h. At both time points, the downregulated genes are more abundant than the upregulated ones (~73% at 6h and ~57% at 24h). A small portion of the DEGs (15 genes) is shared between 6 and 24h, and it reflects the proportion in favour of the downregulated genes.

In the following tables (Table 5.2, 5.3, 5.4, 5.5, 5.6, 5.7) we present the Gene Ontology (GO) biological processes and molecular functions that are over or under-represented, respectively, in DEGs at 6h, at 24h, and DEGs in common between 6 and 24h. In the comparisons between treated and control, outlier samples highlighted during PCS analysis (Figure 5.12) were not considered. DEG lists are elaborated through the PANTHER Classification System which contains up to date GO annotation data for *Arabidopsis* and other plant species. DEG lists are reported in this thesis in the Appendices. In the presented tables, the first column contains the name of the annotation data category. The second column contains the number of genes in the reference list (*Arabidopsis thaliana* REF) that map to this particular annotation data category. The third column contains the number of genes in my uploaded list that map to this annotation data category. The fourth column contains the expected value, which is the number of genes you would expect in my list for

this category, based on the reference list. The fifth column shows the Fold Enrichment of the genes observed in the uploaded list over the expected (number in my list divided by the expected number): if it is greater than 1, it indicates that the category is overrepresented, conversely, the category is underrepresented if it is less than 1. The sixth column has either a + or -, where a plus sign indicates over-representation of this category in my experiment, that is more genes than expected based on the reference list (for this category, the number of genes in your list is greater than the expected value); conversely, a negative sign indicates under-representation. The seventh column is the raw p-value as determined by Fisher's exact test. This is the probability that the number of genes observed in this category occurred by chance (randomly), as determined by the reference list. Bonferroni's correction for multiple comparisons is applied. Only the categories with Bonferroni-corrected p-value better than 0.05 are displayed in tables. The results are sorted by the Fold Enrichment of the most specific categories.

Table 5.2. GO biological process for DEGs at 6h.

GO biological process complete (6h)	*Arabidopsis thaliana* (REF)	Listed num of genes	Expected num of genes	Fold Enrichment	+/-	P value
protein complex oligomerization	55	9	.17	54.08	+	9.48E-10
response to hydrogen peroxide	76	9	.23	39.14	+	1.35E-08
protein folding	188	13	.57	22.85	+	1.15E-10
cellular response to hypoxia	239	14	.72	19.36	+	9.65E-11
response to heat	395	15	1.20	12.55	+	4.43E-09
cellular response to organic cyclic compound	298	9	.90	9.98	+	1.13E-03
defense response to fungus	930	17	2.81	6.04	+	8.31E-06
response to fatty acid	709	12	2.15	5.59	+	5.04E-03
response to salt stress	711	12	2.15	5.58	+	5.18E-03
cellular response to lipid	837	13	2.53	5.13	+	4.56E-03
regulation of response to stress	1018	13	3.08	4.22	+	3.69E-02
defense response to bacterium	1105	14	3.34	4.19	+	1.79E-02
cellular response to endogenous stimulus	1160	14	3.51	3.99	+	3.08E-02

Table 5.3. GO molecular function for DEGs at 6h.

GO molecular function complete (6h)	*Arabidopsis thaliana* (REF)	Listed num of genes	Expected num of genes	Fold Enrichment	+/-	P value
unfolded protein binding	100	10	.30	33.05	+	2.33E-09
protein self-association	122	10	.37	27.09	+	1.47E-08

Table 5.4. GO biological process for DEGs at 24h.

GO biological process complete (24h)	*Arabidopsis thaliana* (REF)	Listed num of genes	Expected num of genes	Fold Enrichment	+/-	P value
zinc ion transmembrane transport	23	6	.19	31.25	+	3.64E-04
photosynthesis, light reaction	165	13	1.38	9.44	+	1.01E-05
cellular response to extracellular stimulus	259	13	2.16	6.01	+	1.47E-03
root morphogenesis	689	21	5.75	3.65	+	1.63E-03
secondary metabolic process	789	20	6.59	3.04	+	4.41E-02
response to chemical	5314	77	44.36	1.74	+	1.12E-03
protein modification process	3177	7	26.52	.26	-	1.70E-02

Table 5.5. GO molecular function for DEGs at 24h.

GO molecular function complete (24h)	*Arabidopsis thaliana* (REF)	Listed num of genes	Expected num of genes	Fold Enrichment	+/-	P value
zinc ion transmembrane transporter activity	26	6	.22	27.64	+	4.06E-04
catalytic activity	8339	100	69.62	1.44	+	4.64E-02

Table 5.6. GO biological process for DEGs in common at 6 and 24h..

GO biological process complete (Overlap)	*Arabidopsis thaliana* (REF)	Listed num of genes	Expected num of genes	Fold Enrichment	+/-	P value
protein complex oligomerization	55	5	.03	> 100	+	3.70E-07
response to hydrogen peroxide	76	5	.04	> 100	+	1.72E-06
protein folding	188	5	.10	48.63	+	1.38E-04
cellular response to hypoxia	239	4	.13	30.61	+	2.26E-02
response to heat	395	5	.22	23.15	+	5.08E-03

Table 5.7. GO molecular function for DEGs in common at 6 and 24h..

GO molecular function complete (Overlap)	*Arabidopsis thaliana* (REF)	Listed num of genes	Expected num of genes	Fold Enrichment	+/-	P value
unfolded protein binding	100	5	.05	91.43	+	3.85E-06
protein self-association	122	5	.07	74.95	+	1.01E-05

5.4.2. WGBS and methylation level in treated vs control samples

Average DNA extraction yield over the 15 samples was 5 ng/mg of roots (fresh weight). Average Nanodrop ratio 260/280 was 1.80 and ratio 260/230 was 1.52. At least 100 ng for each sample were delivered to IGA for WGBS analysis. In Figure 4.13, the results of the DNA methylation based PCA for the methylation contexts CG, CHG and CHH, are presented. Principal components comprehend groups of cytosines whose methylation level differences among samples explain most of the variability. In Table 5.8 the number of reads (in millions) produced for each sample is listed.

Table 5.8. List of sample ID, sample description and number of reads (in millions) produced for each sample.

Sample_ID	Sample description	Number of reads (Millions)
CTRL1	DNA CTR1 0h	63.16
CTRL2	DNA CTR2 0h	58.77
CTRL3	DNA CTR3 0h	53.47
CTRL4	DNA CTR4 6h	76.14
CTRL5	DNA CTR5 6h	63.41
CTRL6	DNA CTR6 6h	42.91
CTRL7	DNA CTR7 24h	82.90
CTRL8	DNA CTR8 24h	63.91
CTRL9	DNA CTR9 24h	63.59
SELF1	DNA SELF1 6h	57.67
SELF2	DNA SELF2 6h	73.52
SELF3	DNA SELF3 6h	69.70
SELF4	DNA SELF4 24h	63.57
SELF5	DNA SELF5 24h	47.69
SELF6	DNA SELF6 24h	76.49

Based on the exploratory PCA analysis of the cytosine methylation distribution in samples treated with self-DNA compared to control samples (Figure 5.13), it is not possible to draw conclusive evidence about the relationship between self-DNA exposure, its timing and the distribution of cytosine methylation across the genome. Apparently, there is no overall differences among the samples in any of the methylation contexts (CG, CHG, CHH), with a

possible exception for the samples treated with self-DNA for 24 h. In particular, in the CG context, all samples appear clustered together except for CTRL4 and SELF5. CTRL4 is among the samples with the highest number of reads and diverge from the main cluster only on the y axis, the principal component explaining the least variability. SELF5, on the other hand, is among the samples with the lowest number of reads and diverge from the main cluster on both the PC2 and, especially, the PC1. Since both SELF4 and 6 are clustered with the rest of the samples with only a minor difference, it is possible that the divergency evidenced by SELF5 may be due to its low number of reads. Differently, in the CHG methylation context, all the samples are even more closely clustered together, except for SELF4 and, again, CTRL4 and SELF5. CTRL4 diverge only slightly from the main cluster this time, while the samples treated with self-DNA for 24 h SELF4 and 5 are more distant: SELF4 only on the y axis, while SELF5 mostly on the PC1. Very interestingly, the very same pattern is observed for the methylation context CHH, where samples SELF4 and SELF5 differentiate from the main cluster. SELF5 is the most divergent sample in all the methylation contexts and in particular on the PC1; therefore, this sample will be most likely reprocessed, also to confirm the high variability in methylation level among the replicas SELF4, SELF5 and SELF6.

In Figure 5.14, 5.15 and 5.16 are presented the metanalysis for methylation levels in genic and intragenic regions, derived from DMRs (Differential Methylated Regions) analysis. Respectively, Figure 5.14 displays the results for the comparison between control samples at 6 and 24h in the three methylation context (CG, CHG, CHH); Figure 5.15 for the comparison between treated and control samples at 6h; and Figure 5.16 for the comparison between treated and control samples at 24h.

In all three cases, the 24-hour control shows an increase in methylation, especially in intergenic regions (flanking the gene region). This demonstrates that the treatment under these experimental conditions elicits a stress-induced response. Comparing the treated and control at 6-hour, in all three contexts, the presence of self-DNA leads to increased methylation in the intragenic regions, a phenomenon observed in the 24-hour controls. It is as if the presence of self-DNA triggers an early stress response in the plant. In this context, the effect of self-DNA drastically reduces the levels of methylation, both in the intragenic regions where it returns to normal, and in the genes in the comparison between treated and control samples at 24h. It would be interesting, for example, to have a 36-hour control to see if it reflects the decrease in methylation observed at 24 hours. This would confirm that the

presence of self-DNA leads to anticipatory changes in methylation levels that also occur in controls, but at a later stage, in response to stress conditions.

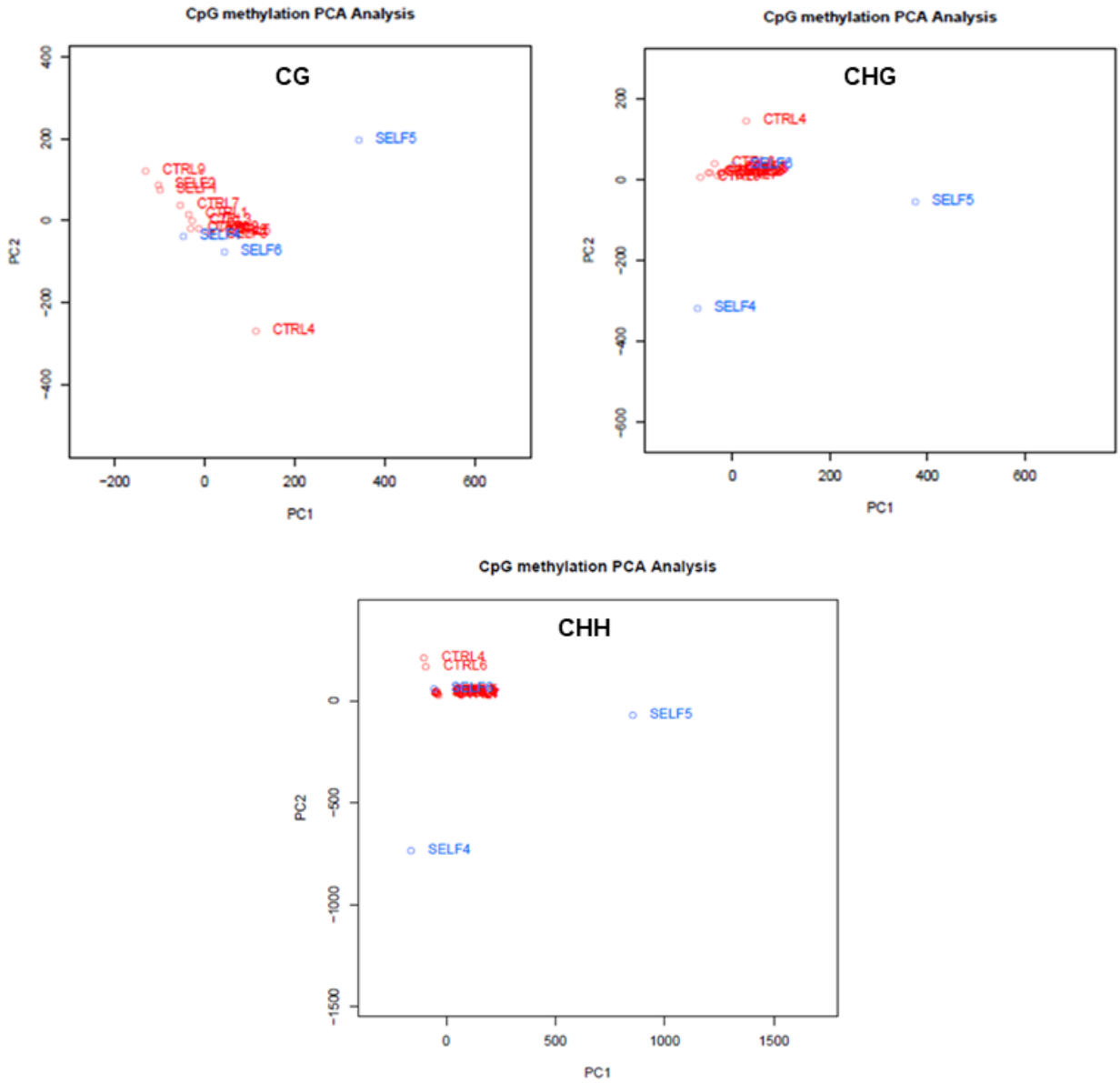

Figure 5.13. Methylation-based PCA results for context CG, CHG and CHH, each showing experiment samples divided in clusters based on the variance explained by PC1 and PC2.

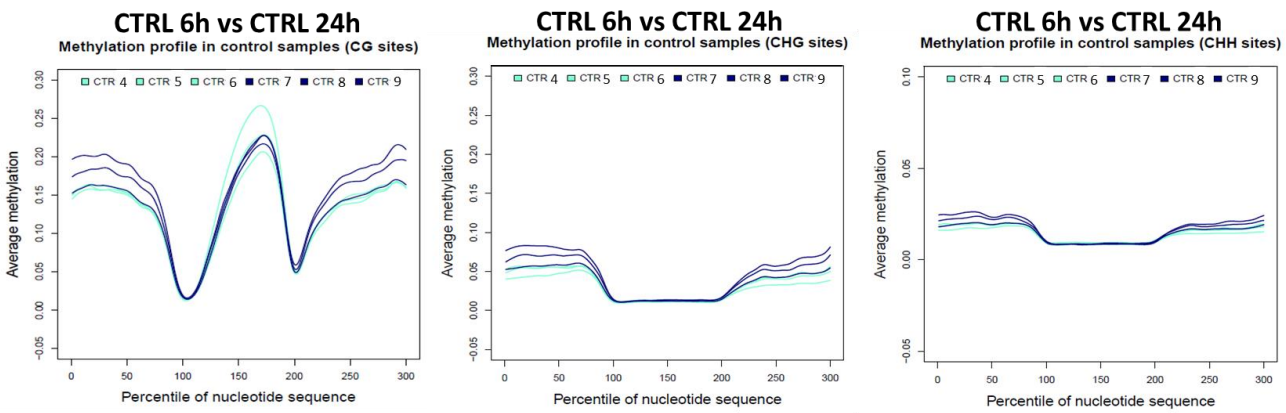

Figure 5.14. Metanalysis for methylation levels in genic and intragenic regions, derived from DMRs (Differential Methylated Regions) analysis for the comparison between control samples at 6 and 24h in the three methylation contexts (CG, CHG, CHH)

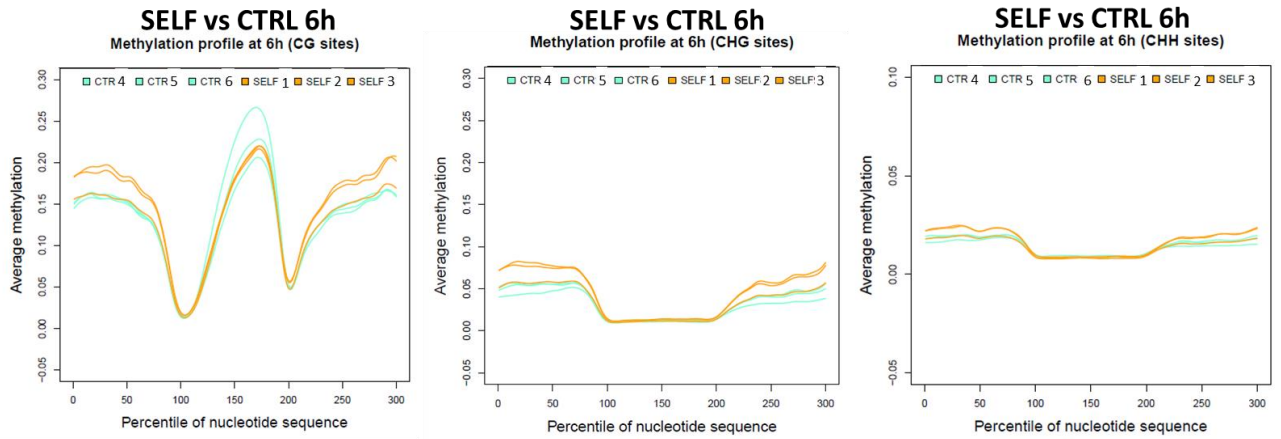

Figure 5.15. metanalysis for methylation levels in genic and intragenic regions, derived from DMRs (Differential Methylated Regions) analysis for the comparison between treated and control samples at 6h in the three methylation contexts (CG, CHG, CHH).

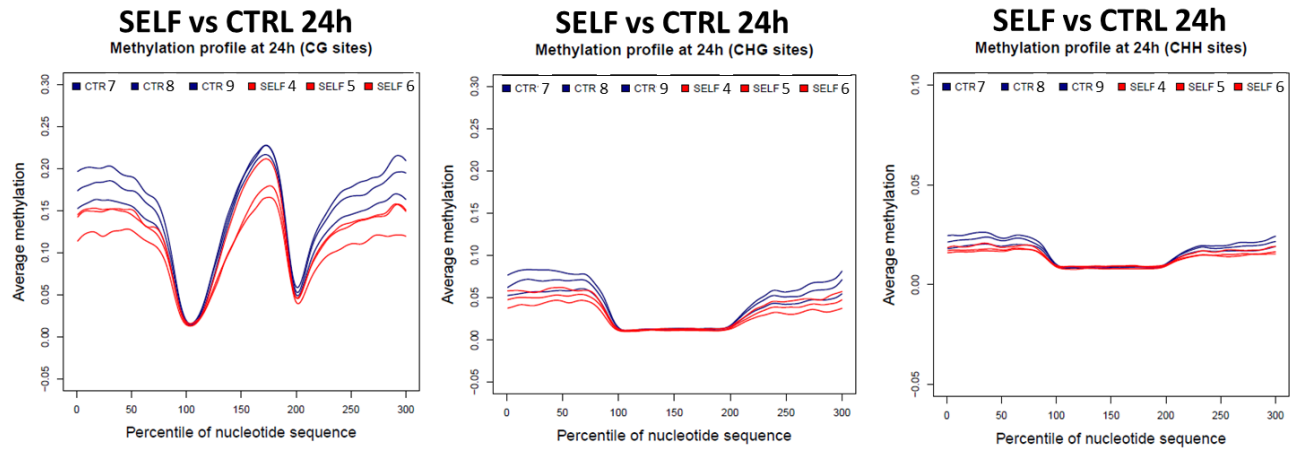

Figure 5.16. metanalysis for methylation levels in genic and intragenic regions, derived from DMRs (Differential Methylated Regions) analysis for the comparison between treated and control samples at 24h in the three methylation contexts (CG, CHG, CHH).

5.5. Conclusive remarks and perspectives

In this activity, we presented the first, exploratory results of a preliminary bioinformatic analysis of the RNA-seq and WHBS data provided by IGA Technology Services Srl. Initial results highlight an appreciable difference in gene expression levels between samples treated with self-DNA and control, especially regarding the 24 h exposure time. Differences in DNA methylation levels are less clear, but there are hints of a possible involvement of CHG and CHH methylation contexts in the plant response to 24 h exposure to self-DNA, that require further verification.

These data will undergo further processing and analysis, with the specific objective of preparing a manuscript. In particular, some samples will be reprocessed to verify the observed pattern and high variability between replicas. Moreover, we will perform a Differentially Expressed Genes (DEGs) analysis to explore more in detail which genes are significantly differentially expressed in the samples (Kumar *et al*., 2020) and their relative function, metabolic pathway and belonging genic family to produce a final Gene Ontology (GO) enrichment analysis. The Gene Ontology (GO) is the most widely used ontology for specifying cellular location, molecular function, and biological process participation of human and model organism genes (Ashburner *et al*., 2000). The GO enrichment analysis is predominantly used to gain insight into the biological significance of the alterations in gene expression levels. With this method, it is possible to determine whether GO terms about specific biological processes, molecular functions, or cellular components are over- or under-represented (Khatri *et al*., 2012). Differentially Expressed Genes statistical analysis will also help to understand and collocate, in terms of gene expression, the variability between replicas of the same treatment. Concerning methylation analysis, we will further investigate our data through a Differentially methylated regions (DMRs) analysis. DMRs are genomic regions that exhibit statistically significant differences in DNA methylation patterns among multiple samples (Rakyan *et al*., 2011). Therefore, identification of DMRs is critical and fundamental in analysing these functional regions that may be involved in transcriptional regulation (Chen *et al*., 2016). For example, it will be important to assess if differential methylation is associated with genes involved in stress response pathways and their expression. This analysis will also help us to better understand the variability observed in some replicas, especially in those treated with self-DNA for 24 h. Finally, since the exposure time of 24 h is the one reporting the major interesting changes and differences (but also the highest variability between

replicas) in gene expression and methylation levels, the experiment with this time frame will be repeated to provide more soundness and reliability to our data and statistical analysis. Overall, this explorative and initial analysis pointed out some interesting aspects, providing valuable insights on the plant molecular response to self-DNA treatment that require further investigation with larger and more in-depth analysis. Also, we tested an innovative experiment set up that will help future investigations on the topic to save precious genomic material during the exposure phase.

Chapter 6: General conclusions

In the previous chapters, the thesis explored several aspects of self-DNA inhibition research, covering species-specificity, gene expression analysis, potential mechanisms for distinguishing self-DNA from non-self-DNA and epigenetic changes in response to self-DNA exposure. These topics share the common goal of exploring plant early molecular response mechanisms to self-DNA, deepening our knowledge of extracellular DNA interactions in plants, toward the understading of its roles in natural ecosystems. Undoubtedly, the inhibitory effect of self-DNA has garnered substantial evidence; however, the precise underlying mechanisms remain largely unresolved. Given the growing significance of this natural phenomenon and its potential implications in plant-soil negative feedback and the shaping of ecosystem biodiversity patterns, it is fundamental to expand research efforts into this area, specifically targeting the molecular pathways that govern growth inhibition. Furthermore, recognizing its potential as a valuable resource for agricultural applications, such as the development of natural pesticides and weedicides, the widespread implementation of self-DNA inhibition in open field settings cannot be carried out before a deeper comprehension of its functioning. Therefore, it is crucial to advance our understanding of self-DNA inhibition to fully harness its benefits for both scientific exploration and practical utilization in agriculture.

Considering the potential practical applications of this principle, our primary concern and area of investigation revolved around the species-specificity of the self-DNA inhibition effect. While previous studies had provided evidence of species-specificity at the suprageneric and infrageneric level, we aimed to deepen into this aspect and contextualize it within the realm of agricultural application. Building upon prior evidence, our hypothesis posited that species-specificity of self-DNA inhibition would persist even in closely related species, including weed plants that are typically more resistant to allelopathic effects. In line with previous studies, our results on a cross-factorial experiment with cultivated vs weedy congeneric *Setaria italica* and *Setaria* provided confirmatory evidence of concentration dependency and species-specificity in self-DNA inhibition. Notably, we confirmed that the inhibitory effect of self-DNA holds true at the infrageneric level for congeneric species with distinct ecological traits. However, our research also raised critical concerns that warrant verification through appropriate field tests on a larger scale. For instance, the extent of potential inhibition of crop species treated with DNA targeting closely related weeds requires further investigation. Therefore, our initial work not only offers positive insights into the specificity of the self-DNA approach in the field but also emphasizes the importance of carefully considering doses and concentrations to avoid harm to congeneric crop species. Indeed, we observed an increased risk at higher concentrations for congeneric species, whereas lower concentrations seemed

to be sufficient for conspecific inhibition. The concentration efficiency for the self-inhibition effect is species-specific, depending on the sensitivity of the species, and necessitates evaluation on a case-by-case basis through biological assays based on highly purified solutions in realistic settlements resembling open field conditions. From an application perspective, the evidence of species-specific self-DNA inhibition on the invasive weed *S. pumila*, but not on the cultivated species *S. italica*, presents promising data for innovative and sustainable weedicide treatments in agriculture. Furthermore, attention must be posed not only towards the level of concentration, but also on the degree of purity of the treatment solutions to avoid unexpected and aspecific effects. The findings of our research have been published in the Plants journal, providing further accessibility to our work (Ronchi, A., Foscari, A., Zaina, G., De Paoli, E., & Incerti, G. (2023). Self-DNA Early Exposure in Cultivated and Weedy Setaria Triggers ROS Degradation Signaling Pathways and Root Growth Inhibition. Plants (Basel, Switzerland), 12(6), 1288. https://doi.org/10.3390/plants12061288).

In our following investigation, we aimed to explore the early expression of genes responsive to abiotic stress in the two *Setaria* species over the time window spanning between 1 and 3 h since exposure to self-DNA, under the hypothesis that early exposure to self-DNA triggers molecular pathways associated with abiotic stress responses. Our study represents the first exploration of the early molecular response to self-DNA inhibition in C4 model plants. We observed differential expression in four genes in *S. italica* (*FSD2*, *ALDH22A1*, *WD40-155*, *MPK17*) and five genes in *S. pumila* (*FSD2*, *ALDH22A1*, *CSD3*, *WD40-155*, *MPK17*) consistently after 1 and 3 hours of exposure. These findings confirmed the involvement of abiotic stress pathways in the early response to self-DNA. Significantly, our experiment revealed a clear functional association between self-DNA exposure and the production of reactive oxygen species (ROS) during the early stages, as evidenced by the upregulation of genes associated with antioxidant activity. Furthermore, our analysis confirmed that invasive species demonstrate greater resilience compared to cultivated species, likely due to a more rapid and efficient initiation of the immune response, with a crucial role played by superoxide dismutase (SOD) proteins. Collectively, our exploratory molecular experiment yields valuable insights, paving the way for future investigations targeting more specific cellular processes with fully representative gene sets. The results of our work have been published in the same paper of the previous activity.

In my third research activity, I focused on studying the cellular sensing and discrimination mechanisms between self and non-self DNA, specifically through sequence-specific recognition involving RNA/DNA interactions. This hypothesis suggests the formation of DNA-

RNA hybrids for self-DNA recognition and was experimentally tested by assessing DNA-RNA hybrid formation *in vivo* for specific target genes, which, to the best of our knowledge, has never been performed in plants. However, this line of investigation presented significant challenges in setting up and fine-tuning the experiment. Nonetheless, during our experimental study, we successfully adapted and verified an *in vitro* immunoprecipitation protocol to capture DNA-RNA hybrids. Unfortunately, the *in vivo* investigation of DNA-RNA hybrid formation after exposure to self-DNA proved to be even more challenging, with numerous still unresolved issues and questions. In particular, our experiments revealed the amplification of *in vivo* hybrids following exposure to self-DNA probes, but we also observed that this formation could occur during the exposure phase due to probe carry-over on roots. Root treatment with DNase I appeared to effectively remove probe carry-over, but the results are still preliminary and inconclusive. Thus, it remains difficult to ascertain whether the *in vivo* hybrids we isolated originated from hybrid formation during the exposure phase to self-DNA probes or if they occurred during the extraction process as a result of cell lysis and the binding of carried-over DNA probes with the released RNAs in the extraction medium. Even though the results are difficult to interpret, we still successfully applied a DRIP protocol in vivo for the first time, obtaining encouraging results for the further development and applicability of this technique. Currently, we are actively exploring various approaches to address the challenges associated with our *in vivo* protocol. These include developing washing methods, optimizing DNase treatments with different enzyme doses based on hypothesized carry-over percentages on roots, and refining our experimental setups. Our aim is to isolate hybrids that are potentially formed exclusively during the exposure phase to self-DNA probes while minimizing their formation during the extraction process. Additionally, we are considering conducting a quantitative assessment of the immuno-precipitates using techniques such as RT-qPCR, library construction, and sequencing to further explore this aspect. It is important to note that self-DNA sensing may not necessarily rely on DNA-RNA hybrid formation, or our current protocol may not be ideally suited for investigating this specific issue. In light of this, we are contemplating the preparation of a methodological article that outlines the challenges and critical points encountered in the application of similar protocols for isolating DNA-RNA hybrids. Such an article could provide valuable insights and guidance to other researchers working in this field, particularly considering that DRIP (DNA-RNA Immunoprecipitation) represents a highly reproducible and high-resolution procedure that merits further investigation and implementation. The potential and effectiveness of DRIP in studying DNA-RNA hybrids make it an exciting avenue for future research and by continuing to refine and

optimize the protocol, we can enhance its reliability and applicability in various biological contexts.

In our investigation of the early molecular mechanisms involved in self-DNA recognition and response in plants, our latest activity focused on exploring epigenetic changes, specifically methylation changes, that may occur in response to self-DNA exposure in the genome of the recipient plant (*Arabidopsis thaliana* seedlings), together with changes in gene expression level. Previous studies have suggested and reported methylation changes as a response mechanism to self-DNA in plants (Vega-Muñoz *et al*., 2018). In this activity we presented only exploratory results from bioinformatic analysis of the RNA-seq and WHBS data provided by IGA Technology Services Srl. Due to time constraints, logistic challenges, and scheduling of externalized activities, the results presented here are still limited. However, such preliminary evidence indicate notable differences in gene expression levels between samples treated with self-DNA and the control groups, progressively increasing with exposure time. On the other hand, differences in DNA methylation levels are less clear, although there are indications of potential involvement of CHG and CHH methylation contexts in the plant response to 24-hour exposure to self-DNA, which require further verification. These data will undergo further processing and analysis, with the specific objective of providing a more detailed result, increasing knowledge of the relationships between self-DNA exposure and epigenetic patterns, prospectively receipt into a research manuscript. In particular, after analytically reprocessing some critical samples, a Differentially Expressed Genes (DEGs) and a Gene Ontology (GO) enrichment analysis should be carried out, in order to understand the genes, their functions, metabolic pathways, and families responsible for self-recognition and root growth inhibition. Regarding the methylation analysis, a further investigation of our data shall be based on a Differentially Methylated Regions (DMRs) analysis, to identify regions that exhibit statistically significant differences in DNA methylation patterns among multiple samples. Furthermore, the involvement of these regions in transcriptional regulation will be addressed. Since the 24-hour exposure time showed the most interesting changes and differences in gene expression and methylation levels, despite the higher variability between replicates, it is planned to repeat the experiment within this timeframe to provide more robustness and reliability to our data and statistical analysis. Overall, this exploratory and initial analysis has revealed intriguing aspects and provided valuable insights into the plant molecular response to self-DNA treatment. However, further investigation with larger and more comprehensive analyses is necessary. Additionally, we have tested an innovative

experimental setup using a plastic coin holder sheet, which will help future investigations on this topic preserve precious genomic material during the exposure phase.

In conclusion, still many unanswered questions about self-DNA sensing and response mechanisms remain, creating opportunities for further studies. While some aspects of my PhD work have provided valuable findings and confirmatory evidence, additional analysis and manuscript preparation are still underway. Unfortunately, due to various reasons such as time constraints, as related to the pandemic global emergency, logistical challenges, experiment complexity, and delays in external laboratories, two manuscripts related to this thesis are still in preparation, and one of them requires further in-depth analysis. Nonetheless, the initial results are promising and suggest interesting outcomes that can contribute to a deeper understanding of the mechanisms underlying self-DNA exposure. Finally, the chapters of this thesis represent a comprehensive exploration of some of the main aspects and open questions pertaining to the early response of plants exposed to self-DNA. All these aspects are closely intertwined with each other, as the investigation of plant sensing of extracellular DNA and the discrimination mechanism between self and nonself-DNA can help us understand the following signaling cascade that determines the activation or silencing of specific genes, possibly through changes in DNA methylation, involved in the species-specific growth inhibition response observed phenomenologically. In summary, through these exploratory experiments, we have analyzed plant response mechanism to self-DNA in different of its interconnected aspects, highlighting and synthesizing important insights that enrich our understanding of the topic and its implications and applications in plant biology. As a result, exciting opportunities for future research and advancements in this intriguing field are revealed, opening up new avenues for scientific progress.

159

References

Abobatta, W.F. Drought adaptive mechanisms of plants—A review. Adv. Agric. Environ. Sci. 2019, 2, 42–45.

Akira, S., Uematsu, S., & Takeuchi, O. (2006). Pathogen Recognition and Innate Immunity. *Cell*, *124*(4), 783–801. https://doi.org/10.1016/j.cell.2006.02.015

Alabert, C., Barth, T. K., Reverón-Gómez, N., Sidoli, S., Schmidt, A., Jensen, O. N., Imhof, A., & Groth, A. (2015). Two distinct modes for propagation of histone PTMs across the cell cycle. *Genes & Development*, *29*(6), 585–590. https://doi.org/10.1101/gad.256354.114

Alizadeh Behbahani, B., Tabatabaei Yazdi, F., Shahidi, F., Hesarinejad, M. A., Mortazavi, S. A., & Mohebbi, M. (2017). Plantago major seed mucilage: Optimization of extraction and some physicochemical and rheological aspects. *Carbohydrate Polymers*, *155*, 68–77. https://doi.org/10.1016/j.carbpol.2016.08.051

Altfeld, M., & Gale Jr, M. (2015). Innate immunity against HIV-1 infection. *Nature Immunology*, *16*(6), 554–562. https://doi.org/10.1038/ni.3157

An, M., Pratley, J. E., & Haig, T. (2001). Phytotoxicity of vulpia residues: IV. Dynamics of allelochemicals during decomposition of vulpia residues and their corresponding phytotoxicity. *Journal of Chemical Ecology*, *27*(2), 395–409. https://doi.org/10.1023/a:1005692724885

Anjum, S.A.; Xie, X.Y.; Wang, L.C.; Saleem, M.F.; Man, C.; Lei, W. Morphological, physiological and biochemical responses of plants to drought stress. Afr. J. Agric. Res. 2011, 6, 2026–2032.

Arora, H., Singh, R. K., Sharma, S., Sharma, N., Panchal, A., Das, T., Prasad, A., & Prasad, M. (2022). DNA methylation dynamics in response to abiotic and pathogen stress in plants. *Plant Cell Reports*, *41*(10), 1931–1944. https://doi.org/10.1007/s00299-022-02901-x

Ashburner, M., Ball, C. A., Blake, J. A., Botstein, D., Butler, H., Cherry, J. M., Davis, A. P., Dolinski, K., Dwight, S. S., Eppig, J. T., Harris, M. A., Hill, D. P., Issel-Tarver, L., Kasarskis, A., Lewis, S., Matese, J. C., Richardson, J. E., Ringwald, M., Rubin, G. M., & Sherlock, G. (2000). Gene Ontology: Tool for the unification of biology. *Nature Genetics*, *25*(1), 25–29. https://doi.org/10.1038/75556

Aslam, M., Fakher, B., Ashraf, M. A., Cheng, Y., Wang, B., & Qin, Y. (2022). Plant Low-Temperature Stress: Signaling and Response. *Agronomy*, *12*(3), 702. https://doi.org/10.3390/agronomy12030702

Aubin, E., El Baidouri, M., & Panaud, O. (2021). Horizontal Gene Transfers in Plants. *Life (Basel, Switzerland)*, *11*(8), 857. https://doi.org/10.3390/life11080857

Babu, A., & Verma, R. S. (1987). Chromosome Structure: Euchromatin and Heterochromatin. In *International Review of Cytology* (Vol. 108, pp. 1–60). Elsevier. https://doi.org/10.1016/S0074-7696(08)61435-7

Bacete, L., Mélida, H., Miedes, E., & Molina, A. (2018). Plant cell wall-mediated immunity: Cell wall changes trigger disease resistance responses. *The Plant Journal*, *93*(4), 614–636. https://doi.org/10.1111/tpj.13807

Bannister, A. J., & Kouzarides, T. (2011). Regulation of chromatin by histone modifications. *Cell Research*, *21*(3), 381–395. https://doi.org/10.1038/cr.2011.22

Barbero, F., Guglielmotto, M., Capuzzo, A., & Maffei, M. (2016). Extracellular Self-DNA (esDNA), but Not Heterologous Plant or Insect DNA (etDNA), Induces Plasma Membrane Depolarization and Calcium Signaling in Lima Bean (Phaseolus lunatus) and Maize (Zea mays). *International Journal of Molecular Sciences*, *17*(10), 1659. https://doi.org/10.3390/ijms17101659

Barbero, F., Guglielmotto, M., Islam, M., & Maffei, M. E. (2021). Extracellular Fragmented Self-DNA Is Involved in Plant Responses to Biotic Stress. *Frontiers in Plant Science*, *12*, 686121. https://doi.org/10.3389/fpls.2021.686121

Barkan, A., & Martienssen, R. A. (1991). Inactivation of maize transposon Mu suppresses a mutant phenotype by activating an outward-reading promoter near the end of Mu1. *Proceedings of the National Academy of Sciences*, *88*(8), 3502–3506. https://doi.org/10.1073/pnas.88.8.3502

Barrat, F. J., Meeker, T., Gregorio, J., Chan, J. H., Uematsu, S., Akira, S., Chang, B., Duramad, O., & Coffman, R. L. (2005). Nucleic acids of mammalian origin can act as endogenous ligands for Toll-like receptors and may promote systemic lupus erythematosus. *Journal of Experimental Medicine*, *202*(8), 1131–1139. https://doi.org/10.1084/jem.20050914

Barton, G. M., Kagan, J. C., & Medzhitov, R. (2006). Intracellular localization of Toll-like receptor 9 prevents recognition of self DNA but facilitates access to viral DNA. *Nature Immunology*, *7*(1), 49–56. https://doi.org/10.1038/ni1280

Baulcombe, D. C., & Dean, C. (2014). Epigenetic Regulation in Plant Responses to the Environment. *Cold Spring Harbor Perspectives in Biology*, *6*(9), a019471–a019471. https://doi.org/10.1101/cshperspect.a019471

Beckman Coulter (2016). Agencourt AMPure XP Information for Use Guide PCR Purification; Beckman Coulter, Inc.: Brea, CA, USA, p. 36.

Belyayev, A. (2014). Bursts of transposable elements as an evolutionary driving force. *Journal of Evolutionary Biology*, *27*(12), 2573–2584. https://doi.org/10.1111/jeb.12513

Bennett, J. A., & Klironomos, J. (2019). Mechanisms of plant–soil feedback: Interactions among biotic and abiotic drivers. *New Phytologist*, *222*(1), 91–96. https://doi.org/10.1111/nph.15603

Bennetzen, J. L., Schmutz, J., Wang, H., Percifield, R., Hawkins, J., Pontaroli, A. C., Estep, M., Feng, L., Vaughn, J. N., Grimwood, J., Jenkins, J., Barry, K., Lindquist, E., Hellsten, U., Deshpande, S., Wang, X., Wu, X., Mitros, T., Triplett, J., … Devos, K. M. (2012). Reference genome sequence of the model plant Setaria. *Nature Biotechnology*, *30*(6), 555–561. https://doi.org/10.1038/nbt.2196

Bever, J. D. (2003). Soil community feedback and the coexistence of competitors: Conceptual frameworks and empirical tests. *New Phytologist*, *157*(3), 465–473. https://doi.org/10.1046/j.1469-8137.2003.00714.x

Bever, J. D., Westover, K. M., & Antonovics, J. (1997). Incorporating the Soil Community into Plant Population Dynamics: The Utility of the Feedback Approach. *The Journal of Ecology*, *85*(5), 561. https://doi.org/10.2307/2960528

Bewick, A. J., & Schmitz, R. J. (2017). Gene body DNA methylation in plants. *Current Opinion in Plant Biology*, *36*, 103–110. https://doi.org/10.1016/j.pbi.2016.12.007

Bhat, A., & Ryu, C.-M. (2016). Plant Perceptions of Extracellular DNA and RNA. *Molecular Plant*, *9*(7), 956–958. https://doi.org/10.1016/j.molp.2016.05.014

Bird, A. P. (1986). CpG-rich islands and the function of DNA methylation. *Nature*, *321*(6067), 209–213. https://doi.org/10.1038/321209a0

Bock, C. (2012). Analysing and interpreting DNA methylation data. *Nature Reviews Genetics*, *13*(10), 705–719. https://doi.org/10.1038/nrg3273

Bonanomi, G., Antignani, V., Barile, E., Lanzotti, V., & Scala, F. (2011). Decomposition of Medicago Sativa Residues Affects Phytotoxicity, Fungal Growth and Soil-Borne Pathogen Diseases. *Journal of Plant Pathology = Rivista Di Patologia Vegetale : An International Journal of the Italian Society of Plant Pathology : 93, 1, 2011*, *93, 1*. https://doi.org/10.1400/169642

Bonanomi, G., Zotti, M., Idbella, M., Termolino, P., De Micco, V., & Mazzoleni, S. (2022). Field evidence for litter and SELF-DNA inhibitory effects on *Alnus glutinosa* roots. *New Phytologist*, *236*(2), 399–412. https://doi.org/10.1111/nph.18391

Bourque, G., Burns, K. H., Gehring, M., Gorbunova, V., Seluanov, A., Hammell, M., Imbeault, M., Izsvák, Z., Levin, H. L., Macfarlan, T. S., Mager, D. L., & Feschotte, C. (2018). Ten things you should know about transposable elements. *Genome Biology*, *19*(1), 199. https://doi.org/10.1186/s13059-018-1577-z

Brázda, V., Coufal, J., Liao, J. C. C., & Arrowsmith, C. H. (2012). Preferential binding of IFI16 protein to cruciform structure and superhelical DNA. *Biochemical and Biophysical Research Communications*, *422*(4), 716–720. https://doi.org/10.1016/j.bbrc.2012.05.065

Brigham, L. A., Woo, H.-H., Wen, F., & Hawes, M. C. (1998). Meristem-Specific Suppression of Mitosis and a Global Switch in Gene Expression in the Root Cap of Pea by Endogenous Signals. *Plant Physiology*, *118*(4), 1223–1231. https://doi.org/10.1104/pp.118.4.1223

Calarco, J. P., Borges, F., Donoghue, M. T. A., Van Ex, F., Jullien, P. E., Lopes, T., Gardner, R., Berger, F., Feijó, J. A., Becker, J. D., & Martienssen, R. A. (2012). Reprogramming of DNA Methylation in Pollen Guides Epigenetic Inheritance via Small RNA. *Cell*, *151*(1), 194–205. https://doi.org/10.1016/j.cell.2012.09.001

Carminati, A., & Vetterlein, D. (2013). Plasticity of rhizosphere hydraulic properties as a key for efficient utilization of scarce resources. *Annals of Botany*, *112*(2), 277–290. https://doi.org/10.1093/aob/mcs262

Cartenì, F., Bonanomi, G., Giannino, F., Incerti, G., Vincenot, C. E., Chiusano, M. L., & Mazzoleni, S. (2016). Self-DNA inhibitory effects: Underlying mechanisms and ecological implications. *Plant Signaling & Behavior*, *11*(4), e1158381. https://doi.org/10.1080/15592324.2016.1158381

Ceccherini, M., Poté, J., Kay, E., Van, V. T., Maréchal, J., Pietramellara, G., Nannipieri, P., Vogel, T. M., & Simonet, P. (2003). Degradation and Transformability of DNA from Transgenic Leaves. *Applied and Environmental Microbiology*, *69*(1), 673–678. https://doi.org/10.1128/AEM.69.1.673-678.2003

Ceccherini, M. T., Ascher, J., Agnelli, A., Borgogni, F., Pantani, O. L., & Pietramellara, G. (2009). Experimental discrimination and molecular characterization of the extracellular soil DNA fraction. *Antonie van Leeuwenhoek*, *96*(4), 653–657. https://doi.org/10.1007/s10482-009-9354-3

Cedar, H., & Bergman, Y. (2009). Linking DNA methylation and histone modification: Patterns and paradigms. *Nature Reviews Genetics*, *10*(5), 295–304. https://doi.org/10.1038/nrg2540

Cerritelli, S. M., & Crouch, R. J. (2009). Ribonuclease H: The enzymes in eukaryotes. *The FEBS Journal*, *276*(6), 1494–1505. https://doi.org/10.1111/j.1742-4658.2009.06908.x

Chan, S. W.-L., Henderson, I. R., & Jacobsen, S. E. (2005). Gardening the genome: DNA methylation in Arabidopsis thaliana. *Nature Reviews Genetics*, *6*(5), 351–360. https://doi.org/10.1038/nrg1601

Chandler, V. L., & Stam, M. (2004). Chromatin conversations: Mechanisms and implications of paramutation. *Nature Reviews Genetics*, *5*(7), 532–544. https://doi.org/10.1038/nrg1378

Chen, D.-P., Lin, Y.-C., & Fann, C. S. J. (2016). Methods for identifying differentially methylated regions for sequence- and array-based data: Table 1. *Briefings in Functional Genomics*, elw018. https://doi.org/10.1093/bfgp/elw018

Cheng, X., & Blumenthal, R. M. (2008). Mammalian DNA Methyltransferases: A Structural Perspective. *Structure*, *16*(3), 341–350. https://doi.org/10.1016/j.str.2008.01.004

Chiusano, M. L., Incerti, G., Colantuono, C., Termolino, P., Palomba, E., Monticolo, F., Benvenuto, G., Foscari, A., Esposito, A., Marti, L., De Lorenzo, G., Vega-Muñoz, I., Heil, M., Carteni, F., Bonanomi, G., & Mazzoleni, S. (2021). Arabidopsis thaliana Response to Extracellular DNA: Self Versus Nonself Exposure. *Plants*, *10*(8), 1744. https://doi.org/10.3390/plants10081744

Clarke, T. L., & Mostoslavsky, R. (2022). DNA repair as a shared hallmark in cancer and ageing. *Molecular Oncology*, *16*(18), 3352–3379. https://doi.org/10.1002/1878-0261.13285

Clements, D. R., & Jones, V. L. (2021). Rapid Evolution of Invasive Weeds Under Climate Change: Present Evidence and Future Research Needs. *Frontiers in Agronomy*, *3*, 664034. https://doi.org/10.3389/fagro.2021.664034

Cokus, S. J., Feng, S., Zhang, X., Chen, Z., Merriman, B., Haudenschild, C. D., Pradhan, S., Nelson, S. F., Pellegrini, M., & Jacobsen, S. E. (2008). Shotgun bisulphite sequencing of the Arabidopsis genome reveals DNA methylation patterning. *Nature*, *452*(7184), 215–219. https://doi.org/10.1038/nature06745

Comfort, N. (2001). From controlling elements to transposons: Barbara McClintock and the Nobel Prize1. *Trends in Genetics*, *17*(8), 475–478. https://doi.org/10.1016/S0168-9525(01)02383-6

Cortijo, S., Wardenaar, R., Colomé-Tatché, M., Gilly, A., Etcheverry, M., Labadie, K., Caillieux, E., Hospital, F., Aury, J.-M., Wincker, P., Roudier, F., Jansen, R. C., Colot, V., & Johannes, F. (2014). Mapping the Epigenetic Basis of Complex Traits. *Science*, *343*(6175), 1145–1148. https://doi.org/10.1126/science.1248127

Couto, D., & Zipfel, C. (2016). Regulation of pattern recognition receptor signalling in plants. *Nature Reviews Immunology*, *16*(9), 537–552. https://doi.org/10.1038/nri.2016.77

Crecchio, C., Ruggiero, P., Curci, M., Colombo, C., Palumbo, G., & Stotzky, G. (2005). Binding of DNA from *Bacillus subtilis* on Montmorillonite-Humic Acids-Aluminum or Iron Hydroxypolymers: Effects on Transformation and Protection against DNase. *Soil Science Society of America Journal*, *69*(3), 834–841. https://doi.org/10.2136/sssaj2004.0166

Daccord, N., Celton, J.-M., Linsmith, G., Becker, C., Choisne, N., Schijlen, E., Van De Geest, H., Bianco, L., Micheletti, D., Velasco, R., Di Pierro, E. A., Gouzy, J., Rees, D. J. G., Guérif, P., Muranty, H., Durel, C.-E., Laurens, F., Lespinasse, Y., Gaillard, S., … Bucher, E. (2017). High-quality de novo

assembly of the apple genome and methylome dynamics of early fruit development. *Nature Genetics*, *49*(7), 1099–1106. https://doi.org/10.1038/ng.3886

Dar, N. A., Amin, I., Wani, W., Wani, S. A., Shikari, A. B., Wani, S. H., & Masoodi, K. Z. (2017). Abscisic acid: A key regulator of abiotic stress tolerance in plants. *Plant Gene*, *11*, 106–111. https://doi.org/10.1016/j.plgene.2017.07.003

De Lorenzo, G., Ferrari, S., Cervone, F., & Okun, E. (2018). Extracellular DAMPs in Plants and Mammals: Immunity, Tissue Damage and Repair. *Trends in Immunology*, *39*(11), 937–950. https://doi.org/10.1016/j.it.2018.09.006

DeFalco, T. A., & Zipfel, C. (2021). Molecular mechanisms of early plant pattern-triggered immune signaling. *Molecular Cell*, *81*(17), 3449–3467. https://doi.org/10.1016/j.molcel.2021.07.029

Demanèche, S., Jocteur-Monrozier, L., Quiquampoix, H., & Simonet, P. (2001). Evaluation of Biological and Physical Protection against Nuclease Degradation of Clay-Bound Plasmid DNA. *Applied and Environmental Microbiology*, *67*(1), 293–299. https://doi.org/10.1128/AEM.67.1.293-299.2001

Dempsey, A., & Bowie, A. G. (2015). Innate immune recognition of DNA: A recent history. *Virology*, *479–480*, 146–152. https://doi.org/10.1016/j.virol.2015.03.013

Desmet, C. J., & Ishii, K. J. (2012). Nucleic acid sensing at the interface between innate and adaptive immunity in vaccination. *Nature Reviews Immunology*, *12*(7), 479–491. https://doi.org/10.1038/nri3247

Dinç, E., Tóth, S. Z., Schansker, G., Ayaydin, F., Kovács, L., Dudits, D., Garab, G., & Bottka, S. (2011). Synthetic Antisense Oligodeoxynucleotides to Transiently Suppress Different Nucleus- and Chloroplast-Encoded Proteins of Higher Plant Chloroplasts. *Plant Physiology*, *157*(4), 1628–1641. https://doi.org/10.1104/pp.111.185462

Doerfler, W. (1991). Patterns of DNA methylation—Evolutionary vestiges of foreign DNA inactivation as a host defense mechanism. A proposal. *Biological Chemistry Hoppe-Seyler*, *372*(8), 557–564.

Doyle, J.J.; Doyle, J.L. (1987). A rapid DNA isolation procedure for small quantities of fresh leaf tissue. Phytochem. Bull., 19, 11–15.

Doust, A. (2016). *Genetics and genomics of setaria*. Springer Science+Business Media.

Driouich, A., Follet-Gueye, M.-L., Vicré-Gibouin, M., & Hawes, M. (2013). Root border cells and secretions as critical elements in plant host defense. *Current Opinion in Plant Biology*, *16*(4), 489–495. https://doi.org/10.1016/j.pbi.2013.06.010

Driouich, A., Smith, C., Ropitaux, M., Chambard, M., Boulogne, I., Bernard, S., Follet-Gueye, M., Vicré, M., & Moore, J. (2019). Root extracellular traps *versus* neutrophil extracellular traps in host defence, a case of functional convergence? *Biological Reviews*, *94*(5), 1685–1700. https://doi.org/10.1111/brv.12522

Dubin, M. J., Zhang, P., Meng, D., Remigereau, M.-S., Osborne, E. J., Paolo Casale, F., Drewe, P., Kahles, A., Jean, G., Vilhjálmsson, B., Jagoda, J., Irez, S., Voronin, V., Song, Q., Long, Q., Rätsch, G., Stegle, O., Clark, R. M., & Nordborg, M. (2015). DNA methylation in Arabidopsis has a genetic basis and shows evidence of local adaptation. *ELife*, *4*, e05255. https://doi.org/10.7554/eLife.05255

Duncan, S., Olsson, T. S. G., Hartley, M., Dean, C., & Rosa, S. (2016). A method for detecting single mRNA molecules in Arabidopsis thaliana. *Plant Methods*, *12*(1), 13. https://doi.org/10.1186/s13007-016-0114-x

Duran-Flores, D., & Heil, M. (2014). Damaged-self recognition in common bean (Phaseolus vulgaris) shows taxonomic specificity and triggers signaling via reactive oxygen species (ROS). *Frontiers in Plant Science*, *5*. https://doi.org/10.3389/fpls.2014.00585

Duran-Flores, D., & Heil, M. (2015). Growth inhibition by self-DNA: A phenomenon and its multiple explanations. *New Phytologist*, *207*(3), 482–485. https://doi.org/10.1111/nph.13542

Duran-Flores, D., & Heil, M. (2016). Sources of specificity in plant damaged-self recognition. *Current Opinion in Plant Biology*, *32*, 77–87. https://doi.org/10.1016/j.pbi.2016.06.019

Duran-Flores, D., & Heil, M. (2018). Extracellular self-DNA as a damage-associated molecular pattern (DAMP) that triggers self-specific immunity induction in plants. *Brain, Behavior, and Immunity*, *72*, 78–88. https://doi.org/10.1016/j.bbi.2017.10.010

Egger, G., Liang, G., Aparicio, A., & Jones, P. A. (2004). Epigenetics in human disease and prospects for epigenetic therapy. *Nature*, *429*(6990), 457–463. https://doi.org/10.1038/nature02625

Ehrenfeld, J. G., Ravit, B., & Elgersma, K. (2005). FEEDBACK IN THE PLANT-SOIL SYSTEM. *Annual Review of Environment and Resources*, *30*(1), 75–115. https://doi.org/10.1146/annurev.energy.30.050504.144212

Ehrlich, M., Gama-Sosa, M. A., Huang, L.-H., Midgett, R. M., Kuo, K. C., McCune, R. A., & Gehrke, C. (1982). Amount and distribution of 5-methylcytosine in human DNA from different types of tissues or cells. *Nucleic Acids Research*, *10*(8), 2709–2721. https://doi.org/10.1093/nar/10.8.2709

Eichten, S. R., Schmitz, R. J., & Springer, N. M. (2014). Epigenetics: Beyond Chromatin Modifications and Complex Genetic Regulation. *Plant Physiology*, *165*(3), 933–947. https://doi.org/10.1104/pp.113.234211

Fahad, S., Bajwa, A. A., Nazir, U., Anjum, S. A., Farooq, A., Zohaib, A., Sadia, S., Nasim, W., Adkins, S., Saud, S., Ihsan, M. Z., Alharby, H., Wu, C., Wang, D., & Huang, J. (2017). Crop Production under Drought and Heat Stress: Plant Responses and Management Options. *Frontiers in Plant Science*, *8*, 1147. https://doi.org/10.3389/fpls.2017.01147

Fernandes-Alnemri, T., Yu, J.-W., Datta, P., Wu, J., & Alnemri, E. S. (2009). AIM2 activates the inflammasome and cell death in response to cytoplasmic DNA. *Nature*, *458*(7237), 509–513. https://doi.org/10.1038/nature07710

Ferrusquía-Jiménez, N. I., Chandrakasan, G., Torres-Pacheco, I., Rico-Garcia, E., Feregrino-Perez, A. A., & Guevara-González, R. G. (2021). Extracellular DNA: A Relevant Plant Damage-Associated Molecular Pattern (DAMP) for Crop Protection Against Pests—A Review. *Journal of Plant Growth Regulation*, *40*(2), 451–463. https://doi.org/10.1007/s00344-020-10129-w

Ferrusquía-Jiménez, N. I., Serrano-Jamaica, L. M., Martínez-Camacho, J. E., Sáenz De La O, D., Villagomez-Aranda, A. L., González-Chavira, M. M., Guerrero-Aguilar, B. Z., Torres-Pacheco, I., Feregrino-Pérez, A. A., Medina-Ramos, G., & Guevara-González, R. G. (2022). Extracellular self-DNA plays a role as a damage-associated molecular pattern (DAMP) delaying zoospore germination rate and inducing stress-related responses in *Phytophthora capsici*. *Plant Pathology*, *71*(5), 1066–1075. https://doi.org/10.1111/ppa.13545

Filippou, P., Bouchagier, P., Skotti, E., & Fotopoulos, V. (2014). Proline and reactive oxygen/nitrogen species metabolism is involved in the tolerant response of the invasive plant species Ailanthus altissima to drought and salinity. *Environmental and Experimental Botany*, *97*, 1–10. https://doi.org/10.1016/j.envexpbot.2013.09.010

Fraire-Velazquez, S., & Emmanuel, V. (2013). Abiotic Stress in Plants and Metabolic Responses. In K. Vahdati (Ed.), *Abiotic Stress—Plant Responses and Applications in Agriculture*. InTech. https://doi.org/10.5772/54859

Frick, E. M., & Strader, L. C. (2018). Kinase MPK17 and the Peroxisome Division Factor PMD1 Influence Salt-induced Peroxisome Proliferation. *Plant Physiology*, *176*(1), 340–351. https://doi.org/10.1104/pp.17.01019

Fulneček, J., Matyášek, R., & Kovařík, A. (2002). Distribution of 5-methylcytosine residues in 5S rRNA genes in Arabidopsis thaliana and Secale cereale. *Molecular Genetics and Genomics*, *268*(4), 510–517. https://doi.org/10.1007/s00438-002-0761-7

Galanti, D., Ramos-Cruz, D., Nunn, A., Rodríguez-Arévalo, I., Scheepens, J. F., Becker, C., & Bossdorf, O. (2022). Genetic and environmental drivers of large-scale epigenetic variation in Thlaspi arvense. *PLOS Genetics*, *18*(10), e1010452. https://doi.org/10.1371/journal.pgen.1010452

Gallego-Bartolomé, J. (2020). DNA methylation in plants: Mechanisms and tools for targeted manipulation. *New Phytologist*, *227*(1), 38–44. https://doi.org/10.1111/nph.16529

Gallucci, S., & Maffei, M. E. (2017). DNA Sensing across the Tree of Life. *Trends in Immunology*, *38*(10), 719–732. https://doi.org/10.1016/j.it.2017.07.012

Garg, A. D., Galluzzi, L., Apetoh, L., Baert, T., Birge, R. B., Bravo-San Pedro, J. M., Breckpot, K., Brough, D., Chaurio, R., Cirone, M., Coosemans, A., Coulie, P. G., De Ruysscher, D., Dini, L., De Witte, P., Dudek-Peric, A. M., Faggioni, A., Fucikova, J., Gaipl, U. S., … Agostinis, P. (2015). Molecular and Translational Classifications of DAMPs in Immunogenic Cell Death. *Frontiers in Immunology*, *6*. https://doi.org/10.3389/fimmu.2015.00588

Gent, J. I., Dong, Y., Jiang, J., & Dawe, R. K. (2012). Strong epigenetic similarity between maize centromeric and pericentromeric regions at the level of small RNAs, DNA methylation and H3 chromatin modifications. *Nucleic Acids Research*, *40*(4), 1550–1560. https://doi.org/10.1093/nar/gkr862

Germoglio, M., Adamo, A., Incerti, G., Cartenì, F., Gigliotti, S., Storlazzi, A., & Mazzoleni, S. (2022). Self-DNA Exposure Induces Developmental Defects and Germline DNA Damage Response in Caenorhabditis elegans. *Biology*, *11*(2), 262. https://doi.org/10.3390/biology11020262

Ginno, P. A., Lott, P. L., Christensen, H. C., Korf, I., & Chédin, F. (2012). R-Loop Formation Is a Distinctive Characteristic of Unmethylated Human CpG Island Promoters. *Molecular Cell*, *45*(6), 814–825. https://doi.org/10.1016/j.molcel.2012.01.017

Givnish, T. J. (1999). On the causes of gradients in tropical tree diversity. *Journal of Ecology*, *87*(2), 193–210. https://doi.org/10.1046/j.1365-2745.1999.00333.x

Godoy, O., De Lemos-Filho, J. P., & Valladares, F. (2011). Invasive species can handle higher leaf temperature under water stress than Mediterranean natives. *Environmental and Experimental Botany*, *71*(2), 207–214. https://doi.org/10.1016/j.envexpbot.2010.12.001

Goll, M. G., & Bestor, T. H. (2005). EUKARYOTIC CYTOSINE METHYLTRANSFERASES. *Annual Review of Biochemistry*, *74*(1), 481–514. https://doi.org/10.1146/annurev.biochem.74.010904.153721

Greenland, D. J. (1979). THE PHYSICS AND CHEMISTRY OF THE SOIL-ROOT INTERFACE: SOME COMMENTS. In *The Soil–Root Interface* (pp. 83–98). Elsevier. https://doi.org/10.1016/B978-0-12-325550-1.50013-6

Groneberg, J., Brown, D. T., & Doerfler, W. (1975). Uptake and fate of the DNA of adenovirus type 2 in KB cells. *Virology*, *64*(1), 115–131. https://doi.org/10.1016/0042-6822(75)90084-7

Gruenert, D. C. (1999). Opportunities and challenges in targeting genes for therapy. *Gene Therapy*, *6*(8), 1347–1348. https://doi.org/10.1038/sj.gt.3301011

Gruenert, D. C., Bruscia, E., Novelli, G., Colosimo, A., Dallapiccola, B., Sangiuolo, F., & Goncz, K. K. (2003). Sequence-specific modification of genomic DNA by small DNA fragments. *Journal of Clinical Investigation*, *112*(5), 637–641. https://doi.org/10.1172/JCI19773

Gunawardena, A. H. L. A. N., Sault, K., Donnelly, P., Greenwood, J. S., & Dengler, N. G. (2005). Programmed cell death and leaf morphogenesis in Monstera obliqua (Araceae). *Planta*, *221*(5), 607–618. https://doi.org/10.1007/s00425-005-1545-1

Gunawardena, U., & Hawes, M. C. (2002). Tissue Specific Localization of Root Infection by Fungal Pathogens: Role of Root Border Cells. *Molecular Plant-Microbe Interactions®*, *15*(11), 1128–1136. https://doi.org/10.1094/MPMI.2002.15.11.1128

Guo, Q., Major, I. T., & Howe, G. A. (2018). Resolution of growth–defense conflict: Mechanistic insights from jasmonate signaling. *Current Opinion in Plant Biology*, *44*, 72–81. https://doi.org/10.1016/j.pbi.2018.02.009

Gust, A. A., Pruitt, R., & Nürnberger, T. (2017). Sensing Danger: Key to Activating Plant Immunity. *Trends in Plant Science*, *22*(9), 779–791. https://doi.org/10.1016/j.tplants.2017.07.005

Halverson, T. W. R., Wilton, M., Poon, K. K. H., Petri, B., & Lewenza, S. (2015). DNA Is an Antimicrobial Component of Neutrophil Extracellular Traps. *PLOS Pathogens*, *11*(1), e1004593. https://doi.org/10.1371/journal.ppat.1004593

Hamilton, A. J., & Baulcombe, D. C. (1999). A Species of Small Antisense RNA in Posttranscriptional Gene Silencing in Plants. *Science*, *286*(5441), 950–952. https://doi.org/10.1126/science.286.5441.950

Hartono, S. R., Malapert, A., Legros, P., Bernard, P., Chédin, F., & Vanoosthuyse, V. (2018). The Affinity of the S9.6 Antibody for Double-Stranded RNAs Impacts the Accurate Mapping of R-Loops in Fission Yeast. *Journal of Molecular Biology*, *430*(3), 272–284. https://doi.org/10.1016/j.jmb.2017.12.016

Hawes, M. C., Curlango-Rivera, G., Wen, F., White, G. J., VanEtten, H. D., & Xiong, Z. (2011). Extracellular DNA: The tip of root defenses? *Plant Science*, *180*(6), 741–745. https://doi.org/10.1016/j.plantsci.2011.02.007

Hawes, M. C., Curlango-Rivera, G., Xiong, Z., & Kessler, J. O. (2012). Roles of root border cells in plant defense and regulation of rhizosphere microbial populations by extracellular DNA 'trapping'. *Plant and Soil*, *355*(1–2), 1–16. https://doi.org/10.1007/s11104-012-1218-3

Hawes, M. C., Wen, F., & Elquza, E. (2015). Extracellular DNA: A Bridge to Cancer. *Cancer Research*, *75*(20), 4260–4264. https://doi.org/10.1158/0008-5472.CAN-15-1546

Hawes, M., McLain, J., Ramirez-Andreotta, M., Curlango-Rivera, G., Flores-Lara, Y., & Brigham, L. (2016). Extracellular Trapping of Soil Contaminants by Root Border Cells: New Insights into Plant Defense. *Agronomy*, *6*(1), 5. https://doi.org/10.3390/agronomy6010005

Heil, M. (2002). Fitness costs of induced resistance: Emerging experimental support for a slippery concept. *Trends in Plant Science*, *7*(2), 61–67. https://doi.org/10.1016/S1360-1385(01)02186-0

Heil, M. (2009). Damaged-self recognition in plant herbivore defence. *Trends in Plant Science*, *14*(7), 356–363. https://doi.org/10.1016/j.tplants.2009.04.002

Heil, M., & Land, W. G. (2014). Danger signals â€“ damaged-self recognition across the tree of life. *Frontiers in Plant Science*, *5*. https://doi.org/10.3389/fpls.2014.00578

Heil, M., & Vega-Muñoz, I. (2019). Nucleic Acid Sensing in Mammals and Plants: Facts and Caveats. In *International Review of Cell and Molecular Biology* (Vol. 345, pp. 225–285). Elsevier. https://doi.org/10.1016/bs.ircmb.2018.10.003

Hemmi, H., Takeuchi, O., Kawai, T., Kaisho, T., Sato, S., Sanjo, H., Matsumoto, M., Hoshino, K., Wagner, H., Takeda, K., & Akira, S. (2000). A Toll-like receptor recognizes bacterial DNA. *Nature*, *408*(6813), 740–745. https://doi.org/10.1038/35047123

Henderson, I. R., & Jacobsen, S. E. (2007). Epigenetic inheritance in plants. *Nature*, *447*(7143), 418–424. https://doi.org/10.1038/nature05917

Herrel, A., Joly, D., & Danchin, E. (2020). Epigenetics in ecology and evolution. *Functional Ecology*, *34*(2), 381–384. https://doi.org/10.1111/1365-2435.13494

Herzner, A.-M., Hagmann, C. A., Goldeck, M., Wolter, S., Kübler, K., Wittmann, S., Gramberg, T., Andreeva, L., Hopfner, K.-P., Mertens, C., Zillinger, T., Jin, T., Xiao, T. S., Bartok, E., Coch, C., Ackermann, D., Hornung, V., Ludwig, J., Barchet, W., … Schlee, M. (2015). Sequence-specific activation of the DNA sensor cGAS by Y-form DNA structures as found in primary HIV-1 cDNA. *Nature Immunology*, *16*(10), 1025–1033. https://doi.org/10.1038/ni.3267

Hodge, A. (2004). The plastic plant: Root responses to heterogeneous supplies of nutrients. *New Phytologist*, *162*(1), 9–24. https://doi.org/10.1111/j.1469-8137.2004.01015.x

Hornung, V., Ablasser, A., Charrel-Dennis, M., Bauernfeind, F., Horvath, G., Caffrey, Daniel. R., Latz, E., & Fitzgerald, K. A. (2009). AIM2 recognizes cytosolic dsDNA and forms a caspase-1-activating inflammasome with ASC. *Nature*, *458*(7237), 514–518. https://doi.org/10.1038/nature07725

Huang, N., Fan, X., Zaleta-Rivera, K., Nguyen, T. C., Zhou, J., Luo, Y., Gao, J., Fang, R. H., Yan, Z., Chen, Z. B., Zhang, L., & Zhong, S. (2020). Natural display of nuclear-encoded RNA on the cell surface and its impact on cell interaction. *Genome Biology*, *21*(1), 225. https://doi.org/10.1186/s13059-020-02145-6

Iglesias, F. M., & Cerdán, P. D. (2016). Maintaining Epigenetic Inheritance During DNA Replication in Plants. *Frontiers in Plant Science*, *7*. https://doi.org/10.3389/fpls.2016.00038

Ikeda, Y., & Kinoshita, T. (2009). DNA demethylation: A lesson from the garden. *Chromosoma*, *118*(1), 37–41. https://doi.org/10.1007/s00412-008-0183-3

International Human Genome Sequencing Consortium. (2001). Correction: Initial sequencing and analysis of the human genome. *Nature*, *412*(6846), 565–566. https://doi.org/10.1038/35087627

Jähner, D., & Jaenisch, R. (1985). Retrovirus-induced de novo methylation of flanking host sequences correlates with gene inactivity. *Nature*, *315*(6020), 594–597. https://doi.org/10.1038/315594a0

Jaroszuk-Ściseł, J., Kurek, E., Rodzik, B., & Winiarczyk, K. (2009). Interactions between rye (Secale cereale) root border cells (RBCs) and pathogenic and nonpathogenic rhizosphere strains of Fusarium culmorum. *Mycological Research*, *113*(10), 1053–1061. https://doi.org/10.1016/j.mycres.2009.07.001

Johannes, F., Porcher, E., Teixeira, F. K., Saliba-Colombani, V., Simon, M., Agier, N., Bulski, A., Albuisson, J., Heredia, F., Audigier, P., Bouchez, D., Dillmann, C., Guerche, P., Hospital, F., & Colot, V. (2009). Assessing the Impact of Transgenerational Epigenetic Variation on Complex Traits. *PLoS Genetics*, *5*(6), e1000530. https://doi.org/10.1371/journal.pgen.1000530

Jolliffe, I. T., & Cadima, J. (2016). Principal component analysis: A review and recent developments. *Philosophical Transactions of the Royal Society A: Mathematical, Physical and Engineering Sciences*, *374*(2065), 20150202. https://doi.org/10.1098/rsta.2015.0202

Jones, P. A. (2012). Functions of DNA methylation: Islands, start sites, gene bodies and beyond. *Nature Reviews Genetics*, *13*(7), 484–492. https://doi.org/10.1038/nrg3230

Jounai, N., Kobiyama, K., Takeshita, F., & Ishii, K. J. (2013). Recognition of damage-associated molecular patterns related to nucleic acids during inflammation and vaccination. *Frontiers in Cellular and Infection Microbiology*, *2*. https://doi.org/10.3389/fcimb.2012.00168

Jullien, P. E., & Berger, F. (2010). DNA methylation reprogramming during plant sexual reproduction? *Trends in Genetics*, *26*(9), 394–399. https://doi.org/10.1016/j.tig.2010.06.001

Jullien, P. E., Mosquna, A., Ingouff, M., Sakata, T., Ohad, N., & Berger, F. (2008). Retinoblastoma and Its Binding Partner MSI1 Control Imprinting in Arabidopsis. *PLoS Biology*, *6*(8), e194. https://doi.org/10.1371/journal.pbio.0060194

Kaczmarek, A., Vandenabeele, P., & Krysko, D. V. (2013). Necroptosis: The Release of Damage-Associated Molecular Patterns and Its Physiological Relevance. *Immunity*, *38*(2), 209–223. https://doi.org/10.1016/j.immuni.2013.02.003

Kagzi, K., Hechler, R. M., Fussmann, G. F., & Cristescu, M. E. (2022). Environmental RNA degrades more rapidly than environmental DNA across a broad range of pH conditions. *Molecular Ecology Resources*, *22*(7), 2640–2650. https://doi.org/10.1111/1755-0998.13655

Kardol, P., Cornips, N. J., Van Kempen, M. M. L., Bakx-Schotman, J. M. T., & Van Der Putten, W. H. (2007). MICROBE-MEDIATED PLANT–SOIL FEEDBACK CAUSES HISTORICAL CONTINGENCY EFFECTS IN PLANT COMMUNITY ASSEMBLY. *Ecological Monographs*, *77*(2), 147–162. https://doi.org/10.1890/06-0502

Kashkush, K., Feldman, M., & Levy, A. A. (2003). Transcriptional activation of retrotransposons alters the expression of adjacent genes in wheat. *Nature Genetics*, *33*(1), 102–106. https://doi.org/10.1038/ng1063

Kenchanmane Raju, S. K., Ritter, E. J., & Niederhuth, C. E. (2019). Establishment, maintenance, and biological roles of non-CG methylation in plants. *Essays in Biochemistry*, *63*(6), 743–755. https://doi.org/10.1042/EBC20190032

Khatri, P., Sirota, M., & Butte, A. J. (2012). Ten Years of Pathway Analysis: Current Approaches and Outstanding Challenges. *PLoS Computational Biology*, *8*(2), e1002375. https://doi.org/10.1371/journal.pcbi.1002375

Kim, J. K., Samaranayake, M., & Pradhan, S. (2009). Epigenetic mechanisms in mammals. *Cellular and Molecular Life Sciences: CMLS*, *66*(4), 596–612. https://doi.org/10.1007/s00018-008-8432-4

Kim, J.-H. (2021). Multifaceted Chromatin Structure and Transcription Changes in Plant Stress Response. *International Journal of Molecular Sciences*, *22*(4), 2013. https://doi.org/10.3390/ijms22042013

Kimura, H. (2003). Transcription of mouse DNA methyltransferase 1 (Dnmt1) is regulated by both E2F-Rb-HDAC-dependent and -independent pathways. *Nucleic Acids Research*, *31*(12), 3101–3113. https://doi.org/10.1093/nar/gkg406

Knee, E. M., Gong, F.-C., Gao, M., Teplitski, M., Jones, A. R., Foxworthy, A., Mort, A. J., & Bauer, W. D. (2001). Root Mucilage from Pea and Its Utilization by Rhizosphere Bacteria as a Sole Carbon Source. *Molecular Plant-Microbe Interactions®*, *14*(6), 775–784. https://doi.org/10.1094/MPMI.2001.14.6.775

Koocheki, A., Taherian, A. R., & Bostan, A. (2013). Studies on the steady shear flow behavior and functional properties of Lepidium perfoliatum seed gum. *Food Research International*, *50*(1), 446–456. https://doi.org/10.1016/j.foodres.2011.05.002

Kozera, B., & Rapacz, M. (2013). Reference genes in real-time PCR. *Journal of Applied Genetics*, *54*(4), 391–406. https://doi.org/10.1007/s13353-013-0173-x

Kress, W. J., Soltis, D. E., Kersey, P. J., Wegrzyn, J. L., Leebens-Mack, J. H., Gostel, M. R., Liu, X., & Soltis, P. S. (2022). Green plant genomes: What we know in an era of rapidly expanding opportunities. *Proceedings of the National Academy of Sciences of the United States of America*, *119*(4), e2115640118. https://doi.org/10.1073/pnas.2115640118

Krueger, F., & Andrews, S. R. (2011). Bismark: A flexible aligner and methylation caller for Bisulfite-Seq applications. *Bioinformatics*, *27*(11), 1571–1572. https://doi.org/10.1093/bioinformatics/btr167

Ku, Y.-S., Sintaha, M., Cheung, M.-Y., & Lam, H.-M. (2018). Plant Hormone Signaling Crosstalks between Biotic and Abiotic Stress Responses. *International Journal of Molecular Sciences*, *19*(10), 3206. https://doi.org/10.3390/ijms19103206

Kulmatiski, A., Beard, K. H., Stevens, J. R., & Cobbold, S. M. (2008). Plant-soil feedbacks: A meta-analytical review. *Ecology Letters*, *11*(9), 980–992. https://doi.org/10.1111/j.1461-0248.2008.01209.x

Kumar, K., Muthamilarasan, M., & Prasad, M. (2013). Reference genes for quantitative real-time PCR analysis in the model plant foxtail millet (Setaria italica L.) subjected to abiotic stress conditions. *Plant Cell, Tissue and Organ Culture (PCTOC)*, *115*(1), 13–22. https://doi.org/10.1007/s11240-013-0335-x

Kumar, S., & Mohapatra, T. (2021). Dynamics of DNA Methylation and Its Functions in Plant Growth and Development. *Frontiers in Plant Science*, *12*, 596236. https://doi.org/10.3389/fpls.2021.596236

Kuriyama, H., & Fukuda, H. (2002). Developmental programmed cell death in plants. *Current Opinion in Plant Biology*, *5*(6), 568–573. https://doi.org/10.1016/S1369-5266(02)00305-9

Laine, V. N., Sepers, B., Lindner, M., Gawehns, F., Ruuskanen, S., & Oers, K. (2022). An ecologist's guide for studying DNA methylation variation in wild vertebrates. *Molecular Ecology Resources*, 1755-0998.13624. https://doi.org/10.1111/1755-0998.13624

Lambers, H., Mougel, C., Jaillard, B., & Hinsinger, P. (2009). Plant-microbe-soil interactions in the rhizosphere: An evolutionary perspective. *Plant and Soil*, *321*(1–2), 83–115. https://doi.org/10.1007/s11104-009-0042-x

Land, W. G. (2015). The Role of Damage-Associated Molecular Patterns in Human Diseases: Part I - Promoting inflammation and immunity. *Sultan Qaboos University Medical Journal*, *15*(1), e9–e21.

Lange, U. C., & Schneider, R. (2010). What an epigenome remembers. *BioEssays*, *32*(8), 659–668. https://doi.org/10.1002/bies.201000030

Langmead, B., Trapnell, C., Pop, M., & Salzberg, S. L. (2009). Ultrafast and memory-efficient alignment of short DNA sequences to the human genome. *Genome Biology*, *10*(3), R25. https://doi.org/10.1186/gb-2009-10-3-r25

Lanzotti, V., Grauso, L., Mangoni, A., Termolino, P., Palomba, E., Anzano, A., Incerti, G., & Mazzoleni, S. (2022). Metabolomics and molecular networking analyses in Arabidopsis thaliana show that extracellular self-DNA affects nucleoside/nucleotide cycles with accumulation of cAMP, cGMP and N6-methyl-AMP. *Phytochemistry*, *204*, 113453. https://doi.org/10.1016/j.phytochem.2022.113453

Lata, C., Sahu, P. P., & Prasad, M. (2010). Comparative transcriptome analysis of differentially expressed genes in foxtail millet (Setaria italica L.) during dehydration stress. *Biochemical and Biophysical Research Communications*, *393*(4), 720–727. https://doi.org/10.1016/j.bbrc.2010.02.068

Law, J. A., & Jacobsen, S. E. (2010). Establishing, maintaining and modifying DNA methylation patterns in plants and animals. *Nature Reviews Genetics*, *11*(3), 204–220. https://doi.org/10.1038/nrg2719

Leal, R. P., Silveira, M. J., Petsch, D. K., Mormul, R. P., & Thomaz, S. M. (2022). The success of an invasive Poaceae explained by drought resilience but not by higher competitive ability. *Environmental and Experimental Botany*, *194*, 104717. https://doi.org/10.1016/j.envexpbot.2021.104717

Leclerc, X., Danos, O., Scherman, D., & Kichler, A. (2009). A comparison of synthetic oligodeoxynucleotides, DNA fragments and AAV-1 for targeted episomal and chromosomal gene repair. *BMC Biotechnology*, *9*(1), 35. https://doi.org/10.1186/1472-6750-9-35

Lee, H., Cho, H., Kim, J., Lee, S., Yoo, J., Park, D., & Lee, G. (2022). RNase H is an exo- and endoribonuclease with asymmetric directionality, depending on the binding mode to the structural variants of RNA:DNA hybrids. *Nucleic Acids Research*, *50*(4), 1801–1814. https://doi.org/10.1093/nar/gkab1064

Lee, J.-H., Yoon, H.-J., Terzaghi, W., Martinez, C., Dai, M., Li, J., Byun, M.-O., & Deng, X. W. (2010). DWA1 and DWA2, Two *Arabidopsis* DWD Protein Components of CUL4-Based E3 Ligases, Act Together as Negative Regulators in ABA Signal Transduction. *The Plant Cell*, *22*(6), 1716–1732. https://doi.org/10.1105/tpc.109.073783

Levy-Booth, D. J., Campbell, R. G., Gulden, R. H., Hart, M. M., Powell, J. R., Klironomos, J. N., Pauls, K. P., Swanton, C. J., Trevors, J. T., & Dunfield, K. E. (2007). Cycling of extracellular DNA in the soil environment. *Soil Biology and Biochemistry*, *39*(12), 2977–2991. https://doi.org/10.1016/j.soilbio.2007.06.020

Lewandowska-Gnatowska, E., Polkowska-Kowalczyk, L., Szczegielniak, J., Barciszewska, M., Barciszewski, J., & Muszyńska, G. (2014). Is DNA methylation modulated by wounding-induced oxidative burst in maize? *Plant Physiology and Biochemistry*, *82*, 202–208. https://doi.org/10.1016/j.plaphy.2014.06.003

Li, Q., Gent, J. I., Zynda, G., Song, J., Makarevitch, I., Hirsch, C. D., Hirsch, C. N., Dawe, R. K., Madzima, T. F., McGinnis, K. M., Lisch, D., Schmitz, R. J., Vaughn, M. W., & Springer, N. M. (2015). RNA-directed DNA methylation enforces boundaries between heterochromatin and euchromatin in the maize genome. *Proceedings of the National Academy of Sciences*, *112*(47), 14728–14733. https://doi.org/10.1073/pnas.1514680112

Li, Q., Wang, C., & Mou, Z. (2020). Perception of Damaged Self in Plants. *Plant Physiology*, *182*(4), 1545–1565. https://doi.org/10.1104/pp.19.01242

Li, S., Peng, Y., & Panchenko, A. R. (2022). DNA methylation: Precise modulation of chromatin structure and dynamics. *Current Opinion in Structural Biology*, *75*, 102430. https://doi.org/10.1016/j.sbi.2022.102430

Lim, D. H. K., & Maher, E. R. (2010). DNA methylation: A form of epigenetic control of gene expression. *The Obstetrician & Gynaecologist*, *12*(1), 37–42. https://doi.org/10.1576/toag.12.1.037.27556

Lippman, Z., Gendrel, A.-V., Black, M., Vaughn, M. W., Dedhia, N., Richard McCombie, W., Lavine, K., Mittal, V., May, B., Kasschau, K. D., Carrington, J. C., Doerge, R. W., Colot, V., & Martienssen, R. (2004). Role of transposable elements in heterochromatin and epigenetic control. *Nature*, *430*(6998), 471–476. https://doi.org/10.1038/nature02651

Liu, J., Jung, C., Xu, J., Wang, H., Deng, S., Bernad, L., Arenas-Huertero, C., & Chua, N.-H. (2012). Genome-Wide Analysis Uncovers Regulation of Long Intergenic Noncoding RNAs in *Arabidopsis*. *The Plant Cell*, *24*(11), 4333–4345. https://doi.org/10.1105/tpc.112.102855

Lowes, H., Pyle, A., Santibanez-Koref, M., & Hudson, G. (2020). Circulating cell-free mitochondrial DNA levels in Parkinson's disease are influenced by treatment. *Molecular Neurodegeneration*, *15*(1), 10. https://doi.org/10.1186/s13024-020-00362-y

Madlung, A., Tyagi, A. P., Watson, B., Jiang, H., Kagochi, T., Doerge, R. W., Martienssen, R., & Comai, L. (2004). Genomic changes in synthetic Arabidopsis polyploids: Genomic changes in Arabidopsis polyploids. *The Plant Journal*, *41*(2), 221–230. https://doi.org/10.1111/j.1365-313X.2004.02297.x

Mareri, L., Parrotta, L., & Cai, G. (2022). Environmental Stress and Plants. *International Journal of Molecular Sciences*, *23*(10), 5416. https://doi.org/10.3390/ijms23105416

Martignago, D., Rico-Medina, A., Blasco-Escámez, D., Fontanet-Manzaneque, J. B., & Caño-Delgado, A. I. (2020). Drought Resistance by Engineering Plant Tissue-Specific Responses. *Frontiers in Plant Science*, *10*, 1676. https://doi.org/10.3389/fpls.2019.01676

Matsuyama, T., Yasumura, N., Funakoshi, M., Yamada, Y., & Hashimoto, T. (1999). Maize Genes Specifically Expressed in the Outermost Cells of Root Cap. *Plant and Cell Physiology*, *40*(5), 469–476. https://doi.org/10.1093/oxfordjournals.pcp.a029566

Mazzoleni, S., Bonanomi, G., Giannino, F., Rietkerk, M., Dekker, S., & Zucconi, F. (2007). Is plant biodiversity driven by decomposition processes? An emerging new theory on plant diversity. *Community Ecology*, *8*(1), 103–109. https://doi.org/10.1556/ComEc.8.2007.1.12

Mazzoleni, S., Bonanomi, G., Incerti, G., Chiusano, M. L., Termolino, P., Mingo, A., Senatore, M., Giannino, F., Cartenì, F., Rietkerk, M., & Lanzotti, V. (2015a). Inhibitory and toxic effects of extracellular self- DNA in litter: A mechanism for negative plant–soil feedbacks? *New Phytologist*, *205*(3), 1195–1210. https://doi.org/10.1111/nph.13121

Mazzoleni, S., Cartenì, F., Bonanomi, G., Incerti, G., Chiusano, M. L., Termolino, P., Migliozzi, A., Senatore, M., Giannino, F., Rietkerk, M., Risitano, A., & Lanzotti, V. (2014). New perspectives on the use of nucleic acids in pharmacological applications: Inhibitory action of extracellular self-DNA in biological systems. *Phytochemistry Reviews*, *13*(4), 937–946. https://doi.org/10.1007/s11101-014-9386-9

Mazzoleni, S. (2014) Composition Comprising Nucleic Acids of Parasitic, Pathogenic or Weed Biological Systems for Inhibiting and/or Controlling the Growth of Said Systems. International Patent WO 2014020624 A9.

Mazzoleni, S., Cartenì, F., Bonanomi, G., Incerti, G., Chiusano, M. L., Termolino, P., Migliozzi, A., Senatore, M., Giannino, F., Rietkerk, M., Risitano, A., & Lanzotti, V. (2014b). New perspectives on the use of nucleic acids in pharmacological applications: Inhibitory action of extracellular self-DNA in biological systems. *Phytochemistry Reviews*, *13*(4), 937–946. https://doi.org/10.1007/s11101-014-9386-9

Mazzoleni, S., Cartenì, F., Bonanomi, G., Senatore, M., Termolino, P., Giannino, F., Incerti, G., Rietkerk, M., Lanzotti, V., & Chiusano, M. L. (2015b). Inhibitory effects of extracellular self- DNA: A general biological process? *New Phytologist*, *206*(1), 127–132. https://doi.org/10.1111/nph.13306

McCabe, M. T., Davis, J. N., & Day, M. L. (2005). Regulation of DNA Methyltransferase 1 by the pRb/E2F1 Pathway. *Cancer Research*, *65*(9), 3624–3632. https://doi.org/10.1158/0008-5472.CAN-04-2158

McCabe, M. T., Low, J. A., Imperiale, M. J., & Day, M. L. (2006). Human polyomavirus BKV transcriptionally activates DNA methyltransferase 1 through the pRb/E2F pathway. *Oncogene*, *25*(19), 2727–2735. https://doi.org/10.1038/sj.onc.1209266

McCarthy, B., Casey, D., Devane, D., Murphy, K., Murphy, E., & Lacasse, Y. (2015). Pulmonary rehabilitation for chronic obstructive pulmonary disease. *Cochrane Database of Systematic Reviews*, *2015*(4). https://doi.org/10.1002/14651858.CD003793.pub3

Mcnear, D. (2013). The rhizosphere-roots, soil and everything in between. *Nature Education Knowledge*. 4.

Mench, M., Morel, J. L., & Guckert, A. (1987). Metal binding properties of high molecular weight soluble exudates from maize (Zea mays L.) roots. *Biology and Fertility of Soils*, *3*(3), 165–169. https://doi.org/10.1007/BF00255778

Miryeganeh, M., & Saze, H. (2020). Epigenetic inheritance and plant evolution. *Population Ecology*, *62*(1), 17–27. https://doi.org/10.1002/1438-390X.12018

Mishra, A. K., Muthamilarasan, M., Khan, Y., Parida, S. K., & Prasad, M. (2014). Genome-Wide Investigation and Expression Analyses of WD40 Protein Family in the Model Plant Foxtail Millet (Setaria italica L.). *PLoS ONE*, *9*(1), e86852. https://doi.org/10.1371/journal.pone.0086852

Moazed, D. (2009). Small RNAs in transcriptional gene silencing and genome defence. *Nature*, *457*(7228), 413–420. https://doi.org/10.1038/nature07756

Mobley, A. S. (2019). Induced Pluripotent Stem Cells. In *Neural Stem Cells and Adult Neurogenesis* (pp. 67–94). Elsevier. https://doi.org/10.1016/B978-0-12-811014-0.00004-4

Monticolo, F., Palomba, E., Termolino, P., Chiaiese, P., De Alteriis, E., Mazzoleni, S., & Chiusano, M. L. (2020). The Role of DNA in the Extracellular Environment: A Focus on NETs, RETs and Biofilms. *Frontiers in Plant Science*, *11*, 589837. https://doi.org/10.3389/fpls.2020.589837

Moore, R., Evans, M. L., & Fondren, W. M. (1990). Inducing Gravitropic Curvature of Primary Roots of *Zea mays* cv Ageotropic. *Plant Physiology*, *92*(2), 310–315. https://doi.org/10.1104/pp.92.2.310

Morgan, M. A. J., & Shilatifard, A. (2020). Reevaluating the roles of histone-modifying enzymes and their associated chromatin modifications in transcriptional regulation. *Nature Genetics*, *52*(12), 1271–1281. https://doi.org/10.1038/s41588-020-00736-4

Morrone, O. (Ed.). (2014). *Revision of the Old World Species of Setaria (Poaceae: Panicoideae: Paniceae)*. American Soc. of Plant Taxonomists.

Mouse Genome Sequencing Consortium. (2002). Initial sequencing and comparative analysis of the mouse genome. *Nature*, *420*(6915), 520–562. https://doi.org/10.1038/nature01262

Moustafa, K., Lefebvre-De Vos, D., Leprince, A.-S., Savouré, A., & Laurière, C. (2008). Analysis of the Arabidopsis Mitogen-Activated Protein Kinase Families: Organ Specificity and Transcriptional Regulation upon Water Stresses. *Scholarly Research Exchange*, *2008*, 1–12. https://doi.org/10.3814/2008/143656

Munoz-Lopez, M., & Garcia-Perez, J. (2010). DNA Transposons: Nature and Applications in Genomics. *Current Genomics*, *11*(2), 115–128. https://doi.org/10.2174/138920210790886871

Muyle, A. M., Seymour, D. K., Lv, Y., Huettel, B., & Gaut, B. S. (2022). Gene Body Methylation in Plants: Mechanisms, Functions, and Important Implications for Understanding Evolutionary Processes. *Genome Biology and Evolution*, *14*(4), evac038. https://doi.org/10.1093/gbe/evac038

Nagler, M., Insam, H., Pietramellara, G., & Ascher-Jenull, J. (2018). Extracellular DNA in natural environments: Features, relevance and applications. *Applied Microbiology and Biotechnology*, *102*(15), 6343–6356. https://doi.org/10.1007/s00253-018-9120-4

Nisa, M.-U., Huang, Y., Benhamed, M., & Raynaud, C. (2019). The Plant DNA Damage Response: Signaling Pathways Leading to Growth Inhibition and Putative Role in Response to Stress Conditions. *Frontiers in Plant Science*, *10*, 653. https://doi.org/10.3389/fpls.2019.00653

Orlandi, S., Nucera, E., Mosimann, E., D'Adda, G., Garzoli, D., Bertossa, M., Lonati, M., & Lombardi, G. (2017). Drivers of *Setaria pumila* (Poir.) Roem. Et Schult growth and impact on forage quality in lowland Switzerland meadows. *Grass and Forage Science*, *72*(1), 154–162. https://doi.org/10.1111/gfs.12200

Packer, A., & Clay, K. (2000). Soil pathogens and spatial patterns of seedling mortality in a temperate tree. *Nature*, *404*(6775), 278–281. https://doi.org/10.1038/35005072

Palomba, E., Chiaiese, P., Termolino, P., Paparo, R., Filippone, E., Mazzoleni, S., & Chiusano, M. L. (2022). Effects of Extracellular Self- and Nonself-DNA on the Freshwater Microalga Chlamydomonas reinhardtii and on the Marine Microalga Nannochloropsis gaditana. *Plants*, *11*(11), 1436. https://doi.org/10.3390/plants11111436

Pan, J., Zhang, M., Kong, X., Xing, X., Liu, Y., Zhou, Y., Liu, Y., Sun, L., & Li, D. (2012). ZmMPK17, a novel maize group D MAP kinase gene, is involved in multiple stress responses. *Planta*, *235*(4), 661–676. https://doi.org/10.1007/s00425-011-1510-0

Papareddy, R. K., & Nodine, M. D. (2021). Plant Epigenetics: Propelling DNA Methylation Variation across the Cell Cycle. *Current Biology*, *31*(3), R129–R131. https://doi.org/10.1016/j.cub.2020.11.049

Parrilla-Doblas, J. T., Roldán-Arjona, T., Ariza, R. R., & Córdoba-Cañero, D. (2019). Active DNA Demethylation in Plants. *International Journal of Molecular Sciences*, *20*(19), 4683. https://doi.org/10.3390/ijms20194683

Passaro, M., Martinovic, M., Bevilacqua, V., Hershberg, E. A., Rossetti, G., Beliveau, B. J., Bonnal, R. J. P., & Pagani, M. (2020). OligoMinerApp: A web-server application for the design of genome-scale oligonucleotide in situ hybridization probes through the flexible OligoMiner environment. *Nucleic Acids Research*, *48*(W1), W332–W339. https://doi.org/10.1093/nar/gkaa251

Paungfoo-Lonhienne, C., Lonhienne, T. G. A., Mudge, S. R., Schenk, P. M., Christie, M., Carroll, B. J., & Schmidt, S. (2010). DNA Is Taken Up by Root Hairs and Pollen, and Stimulates Root and Pollen Tube Growth. *Plant Physiology*, *153*(2), 799–805. https://doi.org/10.1104/pp.110.154963

Paungfoo-Lonhienne, C., Lonhienne, T. G. A., & Schmidt, S. (2010). DNA uptake by Arabidopsis induces changes in the expression of CLE peptides which control root morphology. *Plant Signaling & Behavior*, *5*(9), 1112–1114. https://doi.org/10.4161/psb.5.9.12477

Pearce, G., Yamaguchi, Y., Barona, G., & Ryan, C. A. (2010). A subtilisin-like protein from soybean contains an embedded, cryptic signal that activates defense-related genes. *Proceedings of the National Academy of Sciences*, *107*(33), 14921–14925. https://doi.org/10.1073/pnas.1007568107

Peña-Ponton, C., Diez-Rodriguez, B., Perez-Bello, P., Becker, C., McIntyre, L. M., Van Der Putten, W., De Paoli, E., Heer, K., Opgenoorth, L., & Verhoeven, Kjf. (2022). *High-resolution methylome analysis in the clonal* Populus nigra *cv. 'Italica' reveals environmentally sensitive hotspots and drought-responsive TE superfamilies* [Preprint]. Genomics. https://doi.org/10.1101/2022.10.18.512698

Phillips, D. D., Garboczi, D. N., Singh, K., Hu, Z., Leppla, S. H., & Leysath, C. E. (2013). The sub-nanomolar binding of DNA-RNA hybrids by the single-chain Fv fragment of antibody S9.6: ANTIBODY RECOGNITION OF DNA-RNA HYBRIDS. *Journal of Molecular Recognition*, *26*(8), 376–381. https://doi.org/10.1002/jmr.2284

Pietramellara, G., Ascher, J., Borgogni, F., Ceccherini, M. T., Guerri, G., & Nannipieri, P. (2009). Extracellular DNA in soil and sediment: Fate and ecological relevance. *Biology and Fertility of Soils*, *45*(3), 219–235. https://doi.org/10.1007/s00374-008-0345-8

Pikaard, C. S., & Mittelsten Scheid, O. (2014). Epigenetic Regulation in Plants. *Cold Spring Harbor Perspectives in Biology*, *6*(12), a019315–a019315. https://doi.org/10.1101/cshperspect.a019315

Plancot, B., Santaella, C., Jaber, R., Kiefer-Meyer, M. C., Follet-Gueye, M.-L., Leprince, J., Gattin, I., Souc, C., Driouich, A., & Vicré-Gibouin, M. (2013). Deciphering the Responses of Root Border-Like

Cells of Arabidopsis and Flax to Pathogen-Derived Elicitors. *Plant Physiology*, *163*(4), 1584–1597. https://doi.org/10.1104/pp.113.222356

Podda, L., Santo, A., Leone, C., Mayoral, O., & Bacchetta, G. (2017). Seed germination, salt stress tolerance and seedling growth of Opuntia ficus—Indica (Cactaceae), invasive species in the Mediterranean Basin. *Flora*, *229*, 50–57. https://doi.org/10.1016/j.flora.2017.02.002

Qamer, Z., Chaudhary, M. T., Du, X., Hinze, L., & Azhar, M. T. (2021). Review of oxidative stress and antioxidative defense mechanisms in Gossypium hirsutum L. in response to extreme abiotic conditions. *Journal of Cotton Research*, *4*(1), 9. https://doi.org/10.1186/s42397-021-00086-4

Quintana-Rodriguez, E., Duran-Flores, D., Heil, M., & Camacho-Coronel, X. (2018). Damage-associated molecular patterns (DAMPs) as future plant vaccines that protect crops from pests. *Scientia Horticulturae*, *237*, 207–220. https://doi.org/10.1016/j.scienta.2018.03.026

Raaijmakers, J. M., Paulitz, T. C., Steinberg, C., Alabouvette, C., & Moënne-Loccoz, Y. (2009). The rhizosphere: A playground and battlefield for soilborne pathogens and beneficial microorganisms. *Plant and Soil*, *321*(1–2), 341–361. https://doi.org/10.1007/s11104-008-9568-6

Rajkumar, M. S., Shankar, R., Garg, R., & Jain, M. (2020). Bisulphite sequencing reveals dynamic DNA methylation under desiccation and salinity stresses in rice cultivars. *Genomics*, *112*(5), 3537–3548. https://doi.org/10.1016/j.ygeno.2020.04.005

Rakyan, V. K., Down, T. A., Balding, D. J., & Beck, S. (2011). Epigenome-wide association studies for common human diseases. *Nature Reviews Genetics*, *12*(8), 529–541. https://doi.org/10.1038/nrg3000

Ramsahoye, B. H., Biniszkiewicz, D., Lyko, F., Clark, V., Bird, A. P., & Jaenisch, R. (2000). Non-CpG methylation is prevalent in embryonic stem cells and may be mediated by DNA methyltransferase 3a. *Proceedings of the National Academy of Sciences*, *97*(10), 5237–5242. https://doi.org/10.1073/pnas.97.10.5237

Rassizadeh, L., Cervero, R., Flors, V., & Gamir, J. (2021). Extracellular DNA as an elicitor of broad-spectrum resistance in Arabidopsis thaliana. *Plant Science*, *312*, 111036. https://doi.org/10.1016/j.plantsci.2021.111036

Reigosa, M. J., Pedrol, N., & González, L. (Eds.). (2006). *Allelopathy*. Kluwer Academic Publishers. https://doi.org/10.1007/1-4020-4280-9

Reik, W. (2007). Stability and flexibility of epigenetic gene regulation in mammalian development. *Nature*, *447*(7143), 425–432. https://doi.org/10.1038/nature05918

Reik, W., Dean, W., & Walter, J. (2001). Epigenetic Reprogramming in Mammalian Development. *Science*, *293*(5532), 1089–1093. https://doi.org/10.1126/science.1063443

Rideout, W. M., Coetzee, G. A., Olumi, A. F., & Jones, P. A. (1990). 5-Methylcytosine as an Endogenous Mutagen in the Human LDL Receptor and p53 Genes. *Science*, *249*(4974), 1288–1290. https://doi.org/10.1126/science.1697983

Rietkerk, M. (2022). Spatial pattern formation, community assembly and resilience. *Physics of Life Reviews*, *40*, 51–53. https://doi.org/10.1016/j.plrev.2021.11.002

Robertson, K. D., & Wolffe, A. P. (2000). DNA methylation in health and disease. *Nature Reviews Genetics*, *1*(1), 11–19. https://doi.org/10.1038/35049533

Roh, J. S., & Sohn, D. H. (2018). Damage-Associated Molecular Patterns in Inflammatory Diseases. *Immune Network*, *18*(4), e27. https://doi.org/10.4110/in.2018.18.e27

Ronald, P. C., & Beutler, B. (2010). Plant and Animal Sensors of Conserved Microbial Signatures. *Science*, *330*(6007), 1061–1064. https://doi.org/10.1126/science.1189468

Ronchi, A., Foscari, A., Zaina, G., De Paoli, E., & Incerti, G. (2023). Self-DNA Early Exposure in Cultivated and Weedy Setaria Triggers ROS Degradation Signaling Pathways and Root Growth Inhibition. *Plants (Basel, Switzerland)*, *12*(6), 1288. https://doi.org/10.3390/plants12061288

Rudi, K., Kroken, M., Dahlberg, O. J., Deggerdal, A., Jakobsen, K. S., & Larsen, F. (1997). Rapid, Universal Method to Isolate PCR-Ready DNA Using Magnetic Beads. *BioTechniques*, *22*(3), 506–511. https://doi.org/10.2144/97223rr01

Rykova, E., Sizikov, A., Roggenbuck, D., Antonenko, O., Bryzgalov, L., Morozkin, E., Skvortsova, K., Vlassov, V., Laktionov, P., & Kozlov, V. (2017). Circulating DNA in rheumatoid arthritis: Pathological changes and association with clinically used serological markers. *Arthritis Research & Therapy*, *19*(1), 85. https://doi.org/10.1186/s13075-017-1295-z

SanMiguel, P., Tikhonov, A., Jin, Y.-K., Motchoulskaia, N., Zakharov, D., Melake-Berhan, A., Springer, P. S., Edwards, K. J., Lee, M., Avramova, Z., & Bennetzen, J. L. (1996). Nested Retrotransposons in the Intergenic Regions of the Maize Genome. *Science*, *274*(5288), 765–768. https://doi.org/10.1126/science.274.5288.765

Santos-Pereira, J. M., & Aguilera, A. (2015). R loops: New modulators of genome dynamics and function. *Nature Reviews Genetics*, *16*(10), 583–597. https://doi.org/10.1038/nrg3961

Sanz, L. A., & Chédin, F. (2019). High-resolution, strand-specific R-loop mapping via S9.6-based DNA–RNA immunoprecipitation and high-throughput sequencing. *Nature Protocols*, *14*(6), 1734–1755. https://doi.org/10.1038/s41596-019-0159-1

Sasaki, H., & Matsui, Y. (2008). Epigenetic events in mammalian germ-cell development: Reprogramming and beyond. *Nature Reviews Genetics*, *9*(2), 129–140. https://doi.org/10.1038/nrg2295

Satchivi, N. M., deBoer, G. J., & Bell, J. L. (2017). Understanding the Differential Response of *Setaria viridis* L. (green foxtail) and *Setaria pumila* Poir. (Yellow foxtail) to Pyroxsulam. *Journal of Agricultural and Food Chemistry*, *65*(34), 7328–7336. https://doi.org/10.1021/acs.jafc.7b01453

Scandalios, J. G. (1993). Oxygen Stress and Superoxide Dismutases. *Plant Physiology*, *101*(1), 7–12. https://doi.org/10.1104/pp.101.1.7

Schmitz, R. J., He, Y., Valdés-López, O., Khan, S. M., Joshi, T., Urich, M. A., Nery, J. R., Diers, B., Xu, D., Stacey, G., & Ecker, J. R. (2013). Epigenome-wide inheritance of cytosine methylation variants in a recombinant inbred population. *Genome Research*, *23*(10), 1663–1674. https://doi.org/10.1101/gr.152538.112

Secco, D., Wang, C., Shou, H., Schultz, M. D., Chiarenza, S., Nussaume, L., Ecker, J. R., Whelan, J., & Lister, R. (2015). Stress induced gene expression drives transient DNA methylation changes at adjacent repetitive elements. *ELife*, *4*, e09343. https://doi.org/10.7554/eLife.09343

Seong, S.-Y., & Matzinger, P. (2004). Hydrophobicity: An ancient damage-associated molecular pattern that initiates innate immune responses. *Nature Reviews Immunology*, *4*(6), 469–478. https://doi.org/10.1038/nri1372

Serrano-Jamaica, L. M., Villordo-Pineda, E., González-Chavira, M. M., Guevara-González, R. G., & Medina-Ramos, G. (2021). Effect of Fragmented DNA From Plant Pathogens on the Protection Against Wilt and Root Rot of Capsicum annuum L. Plants. *Frontiers in Plant Science*, *11*, 581891. https://doi.org/10.3389/fpls.2020.581891

Seybold, H., Trempel, F., Ranf, S., Scheel, D., Romeis, T., & Lee, J. (2014). Ca^{2+} signalling in plant immune response: From pattern recognition receptors to Ca^{2+} decoding mechanisms. *New Phytologist*, *204*(4), 782–790. https://doi.org/10.1111/nph.13031

Shao, H.-B., Chu, L.-Y., Jaleel, C. A., & Zhao, C.-X. (2008). Water-deficit stress-induced anatomical changes in higher plants. *Comptes Rendus Biologies*, *331*(3), 215–225. https://doi.org/10.1016/j.crvi.2008.01.002

Singh, H. P. ; Batish, R. Daizy ; Kohli, R. K. (1999) Autotoxicity: Concept, organisms, and ecological significance Critical Reviews in Plant Sciences, 18 (6). Pp. 757-772. ISSN 0735-2689. (n.d.).

Singh, S., Brocker, C., Koppaka, V., Chen, Y., Jackson, B. C., Matsumoto, A., Thompson, D. C., & Vasiliou, V. (2013). Aldehyde dehydrogenases in cellular responses to oxidative/electrophilicstress. *Free Radical Biology and Medicine*, *56*, 89–101. https://doi.org/10.1016/j.freeradbiomed.2012.11.010

Sirois, C. M., Jin, T., Miller, A. L., Bertheloot, D., Nakamura, H., Horvath, G. L., Mian, A., Jiang, J., Schrum, J., Bossaller, L., Pelka, K., Garbi, N., Brewah, Y., Tian, J., Chang, C., Chowdhury, P. S., Sims, G. P., Kolbeck, R., Coyle, A. J., … Latz, E. (2013). RAGE is a nucleic acid receptor that promotes inflammatory responses to DNA. *Journal of Experimental Medicine*, *210*(11), 2447–2463. https://doi.org/10.1084/jem.20120201

Skinner, M. K., & Nilsson, E. E. (2021). Role of environmentally induced epigenetic transgenerational inheritance in evolutionary biology: Unified Evolution Theory. *Environmental Epigenetics*, *7*(1), dvab012. https://doi.org/10.1093/eep/dvab012

Slotkin, R. K., & Martienssen, R. (2007). Transposable elements and the epigenetic regulation of the genome. *Nature Reviews Genetics*, *8*(4), 272–285. https://doi.org/10.1038/nrg2072

Son, Y., Cheong, Y.-K., Kim, N.-H., Chung, H.-T., Kang, D. G., & Pae, H.-O. (2011). Mitogen-Activated Protein Kinases and Reactive Oxygen Species: How Can ROS Activate MAPK Pathways? *Journal of Signal Transduction*, *2011*, 1–6. https://doi.org/10.1155/2011/792639

Stein, L. D., Bao, Z., Blasiar, D., Blumenthal, T., Brent, M. R., Chen, N., Chinwalla, A., Clarke, L., Clee, C., Coghlan, A., Coulson, A., D'Eustachio, P., Fitch, D. H. A., Fulton, L. A., Fulton, R. E., Griffiths-Jones, S., Harris, T. W., Hillier, L. W., Kamath, R., … Waterston, R. H. (2003). The Genome Sequence of Caenorhabditis briggsae: A Platform for Comparative Genomics. *PLoS Biology*, *1*(2), e45. https://doi.org/10.1371/journal.pbio.0000045

Suzuki, M. M., & Bird, A. (2008). DNA methylation landscapes: Provocative insights from epigenomics. *Nature Reviews Genetics*, *9*(6), 465–476. https://doi.org/10.1038/nrg2341

Szczesny, B., Marcatti, M., Ahmad, A., Montalbano, M., Brunyánszki, A., Bibli, S.-I., Papapetropoulos, A., & Szabo, C. (2018). Mitochondrial DNA damage and subsequent activation of Z-DNA binding

protein 1 links oxidative stress to inflammation in epithelial cells. *Scientific Reports*, *8*(1), 914. https://doi.org/10.1038/s41598-018-19216-1

Takaoka, A., Wang, Z., Choi, M. K., Yanai, H., Negishi, H., Ban, T., Lu, Y., Miyagishi, M., Kodama, T., Honda, K., Ohba, Y., & Taniguchi, T. (2007). DAI (DLM-1/ZBP1) is a cytosolic DNA sensor and an activator of innate immune response. *Nature*, *448*(7152), 501–505. https://doi.org/10.1038/nature06013

Takuno, S., & Gaut, B. S. (2012). Body-Methylated Genes in Arabidopsis thaliana Are Functionally Important and Evolve Slowly. *Molecular Biology and Evolution*, *29*(1), 219–227. https://doi.org/10.1093/molbev/msr188

Tang, D., Kang, R., Coyne, C. B., Zeh, H. J., & Lotze, M. T. (2012). PAMPs and DAMPs: Signal 0s that spur autophagy and immunity. *Immunological Reviews*, *249*(1), 158–175. https://doi.org/10.1111/j.1600-065X.2012.01146.x

Teixeira, F. K., & Colot, V. (2009). Gene body DNA methylation in plants: A means to an end or an end to a means? *The EMBO Journal*, *28*(8), 997–998. https://doi.org/10.1038/emboj.2009.87

The C. elegans Sequencing Consortium*. (1998). Genome Sequence of the Nematode *C. elegans*: A Platform for Investigating Biology. *Science*, *282*(5396), 2012–2018. https://doi.org/10.1126/science.282.5396.2012

Thierry, A. R., El Messaoudi, S., Gahan, P. B., Anker, P., & Stroun, M. (2016). Origins, structures, and functions of circulating DNA in oncology. *Cancer and Metastasis Reviews*, *35*(3), 347–376. https://doi.org/10.1007/s10555-016-9629-x

Tjia, T. O. S., Meitha, K., Septiani, P., Awaludin, R., & Sumardi, D. (2023). Extracellular self-DNA induces local inhibition of growth, regulates production of reactive oxygen species, and gene expression in rice roots. *Biologia Plantarum*, *67*, 9–18. https://doi.org/10.32615/bp.2022.037

Toussaint, M., Jackson, D. J., Swieboda, D., Guedán, A., Tsourouktsoglou, T.-D., Ching, Y. M., Radermecker, C., Makrinioti, H., Aniscenko, J., Bartlett, N. W., Edwards, M. R., Solari, R., Farnir, F., Papayannopoulos, V., Bureau, F., Marichal, T., & Johnston, S. L. (2017). Host DNA released by NETosis promotes rhinovirus-induced type-2 allergic asthma exacerbation. *Nature Medicine*, *23*(6), 681–691. https://doi.org/10.1038/nm.4332

Tozer, K. N., Cameron, C. A., & Matthews, L. (2015). Grazing defoliation and nutritive value of Setaria pumila and Digitaria sanguinalis in Lolium perenne-based swards. *Crop and Pasture Science*, *66*(2), 184. https://doi.org/10.1071/CP14079

Tran, T. M., MacIntyre, A., Hawes, M., & Allen, C. (2016). Escaping Underground Nets: Extracellular DNases Degrade Plant Extracellular Traps and Contribute to Virulence of the Plant Pathogenic Bacterium Ralstonia solanacearum. *PLOS Pathogens*, *12*(6), e1005686. https://doi.org/10.1371/journal.ppat.1005686

Trifonova, R., Postma, J., Verstappen, F. W. A., Bouwmeester, H. J., Ketelaars, J. J. M. H., & Van Elsas, J.-D. (2008). Removal of phytotoxic compounds from torrefied grass fibres by plant-beneficial microorganisms: Removal of phytotoxic compounds from torrefied grass fibres. *FEMS Microbiology Ecology*, *66*(1), 158–166. https://doi.org/10.1111/j.1574-6941.2008.00508.x

Tyczewska, A., Gracz-Bernaciak, J., Szymkowiak, J., & Twardowski, T. (2021). Herbicide stress-induced DNA methylation changes in two Zea mays inbred lines differing in Roundup® resistance. *Journal of Applied Genetics*, *62*(2), 235–248. https://doi.org/10.1007/s13353-021-00609-4

Udhaya Kumar, S., Thirumal Kumar, D., Bithia, R., Sankar, S., Magesh, R., Sidenna, M., George Priya Doss, C., & Zayed, H. (2020). Analysis of Differentially Expressed Genes and Molecular Pathways in Familial Hypercholesterolemia Involved in Atherosclerosis: A Systematic and Bioinformatics Approach. *Frontiers in Genetics*, *11*, 734. https://doi.org/10.3389/fgene.2020.00734

R Core Team. (2019) R: A Language and Environment for Statistical Computing; R Foundation for Statistical Computing: Vienna, Austria.

Rogers, H. T., Pearson, R. W., and Pierre, W. H. (1942). THE SOURCE AND PHOSPHATASE ACTIVITY OF EXOENZYME SYSTEMS OF CORN AND TOMATO ROOTS. *Soil Sci*. *54*, 353.

Rice, E.L. (1984) Allelopathy. 2nd Edition, Academic Press, New York, 422.

Rizvi, S.J.H. and Rizvi, V. (1992) Allelopathy; Basic and Applied Aspects. Chapman and Hall, New York, 480.

Van Der Graaf, A., Wardenaar, R., Neumann, D. A., Taudt, A., Shaw, R. G., Jansen, R. C., Schmitz, R. J., Colomé-Tatché, M., & Johannes, F. (2015). Rate, spectrum, and evolutionary dynamics of spontaneous epimutations. *Proceedings of the National Academy of Sciences*, *112*(21), 6676–6681. https://doi.org/10.1073/pnas.1424254112

Van Der Putten, W. H., Bardgett, R. D., Bever, J. D., Bezemer, T. M., Casper, B. B., Fukami, T., Kardol, P., Klironomos, J. N., Kulmatiski, A., Schweitzer, J. A., Suding, K. N., Van De Voorde, T. F. J., & Wardle, D. A. (2013). Plant-soil feedbacks: The past, the present and future challenges. *Journal of Ecology*, *101*(2), 265–276. https://doi.org/10.1111/1365-2745.12054

Van Holde, K. E. (1989). Chromatin Structure and Transcription. In A. Rich (Ed.), *Chromatin* (pp. 355–408). Springer New York. https://doi.org/10.1007/978-1-4612-3490-6_8

Varley, K. E., Gertz, J., Bowling, K. M., Parker, S. L., Reddy, T. E., Pauli-Behn, F., Cross, M. K., Williams, B. A., Stamatoyannopoulos, J. A., Crawford, G. E., Absher, D. M., Wold, B. J., & Myers, R. M. (2013). Dynamic DNA methylation across diverse human cell lines and tissues. *Genome Research*, *23*(3), 555–567. https://doi.org/10.1101/gr.147942.112

Vega-Muñoz, I., Feregrino-Pérez, A. A., Torres-Pacheco, I., & Guevara-González, R. G. (2018). Exogenous fragmented DNA acts as a damage-associated molecular pattern (DAMP) inducing changes in CpG DNA methylation and defence-related responses in Lactuca sativa. *Functional Plant Biology*, *45*(10), 1065. https://doi.org/10.1071/FP18011

Vega-Muñoz, I., Herrera-Estrella, A., Martínez-de La Vega, O., & Heil, M. (2023). ATM and ATR, two central players of the DNA damage response, are involved in the induction of systemic acquired resistance by extracellular DNA, but not the plant wound response. *Frontiers in Immunology*, *14*, 1175786. https://doi.org/10.3389/fimmu.2023.1175786

Vénéreau, E., Ceriotti, C., & Bianchi, M. E. (2015). DAMPs from Cell Death to New Life. *Frontiers in Immunology*, *6*. https://doi.org/10.3389/fimmu.2015.00422

Vining, K. J., Pomraning, K. R., Wilhelm, L. J., Priest, H. D., Pellegrini, M., Mockler, T. C., Freitag, M., & Strauss, S. H. (2012). Dynamic DNA cytosine methylation in the Populus trichocarpa genome:

Tissue-level variation and relationship to gene expression. *BMC Genomics*, *13*(1), 27. https://doi.org/10.1186/1471-2164-13-27

Vos, I. A., Verhage, A., Schuurink, R. C., Watt, L. G., Pieterse, C. M. J., & Van Wees, S. C. M. (2013). Onset of herbivore-induced resistance in systemic tissue primed for jasmonate-dependent defenses is activated by abscisic acid. *Frontiers in Plant Science*, *4*. https://doi.org/10.3389/fpls.2013.00539

Wang, F., Alain, T., Szretter, K. J., Stephenson, K., Pol, J. G., Atherton, M. J., Hoang, H.-D., Fonseca, B. D., Zakaria, C., Chen, L., Rangwala, Z., Hesch, A., Chan, E. S. Y., Tuinman, C., Suthar, M. S., Jiang, Z., Ashkar, A. A., Thomas, G., Kozma, S. C., … Lichty, B. D. (2016). S6K-STING interaction regulates cytosolic DNA–mediated activation of the transcription factor IRF3. *Nature Immunology*, *17*(5), 514–522. https://doi.org/10.1038/ni.3433

Wang, K., Guo, Q., Froehlich, J. E., Hersh, H. L., Zienkiewicz, A., Howe, G. A., & Benning, C. (2018). Two Abscisic Acid-Responsive Plastid Lipase Genes Involved in Jasmonic Acid Biosynthesis in *Arabidopsis thaliana*. *The Plant Cell*, *30*(5), 1006–1022. https://doi.org/10.1105/tpc.18.00250

Wang, L., Wen, M., & Cao, X. (2019). Nuclear hnRNPA2B1 initiates and amplifies the innate immune response to DNA viruses. *Science*, *365*(6454), eaav0758. https://doi.org/10.1126/science.aav0758

Wang, T., Song, H., Zhang, B., Lu, Q., Liu, Z., Zhang, S., Guo, R., Wang, C., Zhao, Z., Liu, J., & Peng, R. (2018). Genome-wide identification, characterization, and expression analysis of superoxide dismutase (SOD) genes in foxtail millet (Setaria italica L.). *3 Biotech*, *8*(12), 486. https://doi.org/10.1007/s13205-018-1502-x

Wassenegger, M., Heimes, S., Riedel, L., & Sänger, H. L. (1994). RNA-directed de novo methylation of genomic sequences in plants. *Cell*, *76*(3), 567–576. https://doi.org/10.1016/0092-8674(94)90119-8

Weiller, F., Moore, J. P., Young, P., Driouich, A., & Vivier, M. A. (2016). The Brassicaceae species *Heliophila coronopifolia* produces root border-like cells that protect the root tip and secrete defensin peptides. *Annals of Botany*, mcw141. https://doi.org/10.1093/aob/mcw141

Wen, F., Curlango-Rivera, G., & Hawes, M. C. (2007). Proteins Among the Polysaccharides: A New Perspective on Root Cap 'Slime'. *Plant Signaling & Behavior*, *2*(5), 410–412. https://doi.org/10.4161/psb.2.5.4344

Wen, F., Curlango-Rivera, G., Huskey, D. A., Xiong, Z., & Hawes, M. C. (2017). Visualization of extracellular DNA released during border cell separation from the root cap. *American Journal of Botany*, *104*(7), 970–978. https://doi.org/10.3732/ajb.1700142

Wen, F., VanEtten, H. D., Tsaprailis, G., & Hawes, M. C. (2007). Extracellular Proteins in Pea Root Tip and Border Cell Exudates. *Plant Physiology*, *143*(2), 773–783. https://doi.org/10.1104/pp.106.091637

Wen, F., White, G. J., VanEtten, H. D., Xiong, Z., & Hawes, M. C. (2009). Extracellular DNA Is Required for Root Tip Resistance to Fungal Infection. *Plant Physiology*, *151*(2), 820–829. https://doi.org/10.1104/pp.109.142067

Wendte, J. M., Zhang, Y., Ji, L., Shi, X., Hazarika, R. R., Shahryary, Y., Johannes, F., & Schmitz, R. J. (2019). Epimutations are associated with CHROMOMETHYLASE 3-induced de novo DNA methylation. *ELife*, *8*, e47891. https://doi.org/10.7554/eLife.47891

Whipps, J. M. (2001). Microbial interactions and biocontrol in the rhizosphere. *Journal of Experimental Botany*, *52*(suppl 1), 487–511. https://doi.org/10.1093/jexbot/52.suppl_1.487

Wolffe, A. (2000). Chromatin Structure. In *Chromatin* (pp. 7–172). Elsevier. https://doi.org/10.1016/B978-012761914-9/50004-0

Wu, H., Chen, T.-T., Wang, X.-N., Ke, Y., & Jiang, J.-H. (2020). RNA imaging in living mice enabled by an *in vivo* hybridization chain reaction circuit with a tripartite DNA probe. *Chemical Science*, *11*(1), 62–69. https://doi.org/10.1039/C9SC03469B

Wu, J., & Chen, Z. J. (2014). Innate Immune Sensing and Signaling of Cytosolic Nucleic Acids. *Annual Review of Immunology*, *32*(1), 461–488. https://doi.org/10.1146/annurev-immunol-032713-120156

Wu, J., Sun, L., Chen, X., Du, F., Shi, H., Chen, C., & Chen, Z. J. (2013). Cyclic GMP-AMP Is an Endogenous Second Messenger in Innate Immune Signaling by Cytosolic DNA. *Science*, *339*(6121), 826–830. https://doi.org/10.1126/science.1229963

Xi, Y., & Li, W. (2009). BSMAP: Whole genome bisulfite sequence MAPping program. *BMC Bioinformatics*, *10*(1), 232. https://doi.org/10.1186/1471-2105-10-232

Xie, W., Barr, C. L., Kim, A., Yue, F., Lee, A. Y., Eubanks, J., Dempster, E. L., & Ren, B. (2012). Base-Resolution Analyses of Sequence and Parent-of-Origin Dependent DNA Methylation in the Mouse Genome. *Cell*, *148*(4), 816–831. https://doi.org/10.1016/j.cell.2011.12.035

Yaish, M. W. (2017). Editorial: Epigenetic Modifications Associated with Abiotic and Biotic Stresses in Plants: An Implication for Understanding Plant Evolution. *Frontiers in Plant Science*, *8*, 1983. https://doi.org/10.3389/fpls.2017.01983

Yakushiji, S., Ishiga, Y., Inagaki, Y., Toyoda, K., Shiraishi, T., & Ichinose, Y. (2009). Bacterial DNA activates immunity in Arabidopsis thaliana. *Journal of General Plant Pathology*, *75*(3), 227–234. https://doi.org/10.1007/s10327-009-0162-4

Yang, L., Lang, C., Wu, Y., Meng, D., Yang, T., Li, D., Jin, T., & Zhou, X. (2022). ROS1-mediated decrease in DNA methylation and increase in expression of defense genes and stress response genes in Arabidopsis thaliana due to abiotic stresses. *BMC Plant Biology*, *22*(1), 104. https://doi.org/10.1186/s12870-022-03473-4

Yeats, T. H., & Rose, J. K. C. (2013). The Formation and Function of Plant Cuticles. *Plant Physiology*, *163*(1), 5–20. https://doi.org/10.1104/pp.113.222737

Yong-Quan, L., Zi-Hong, Y., & Wei-Ren, W. (2006). Analysis of the Phylogenetic Relationships Among Several Species of Gramineae Using ACGM Markers. *Acta Genetica Sinica*, *33*(12), 1127–1131. https://doi.org/10.1016/S0379-4172(06)60151-0

Zerebecki, R. A., & Sorte, C. J. B. (2011). Temperature Tolerance and Stress Proteins as Mechanisms of Invasive Species Success. *PLoS ONE*, *6*(4), e14806. https://doi.org/10.1371/journal.pone.0014806

Zhang, Q., & Bartels, D. (2018). Molecular responses to dehydration and desiccation in desiccation-tolerant angiosperm plants. *Journal of Experimental Botany*, *69*(13), 3211–3222. https://doi.org/10.1093/jxb/erx489

Zhang, X., Shiu, S., Cal, A., & Borevitz, J. O. (2008). Global Analysis of Genetic, Epigenetic and Transcriptional Polymorphisms in Arabidopsis thaliana Using Whole Genome Tiling Arrays. *PLoS Genetics*, *4*(3), e1000032. https://doi.org/10.1371/journal.pgen.1000032

Zhang, X., Yazaki, J., Sundaresan, A., Cokus, S., Chan, S. W.-L., Chen, H., Henderson, I. R., Shinn, P., Pellegrini, M., Jacobsen, S. E., & Ecker, J. R. (2006). Genome-wide High-Resolution Mapping and Functional Analysis of DNA Methylation in Arabidopsis. *Cell*, *126*(6), 1189–1201. https://doi.org/10.1016/j.cell.2006.08.003

Zhang, Z. Z., Pannunzio, N. R., Hsieh, C.-L., Yu, K., & Lieber, M. R. (2015). Complexities due to single-stranded RNA during antibody detection of genomic rna:dna hybrids. *BMC Research Notes*, *8*(1), 127. https://doi.org/10.1186/s13104-015-1092-1

Zhou, J.-M., & Zhang, Y. (2020). Plant Immunity: Danger Perception and Signaling. *Cell*, *181*(5), 978–989. https://doi.org/10.1016/j.cell.2020.04.028

Zhou, X., Gao, H., Zhang, X., Khashi U Rahman, M., Mazzoleni, S., Du, M., & Wu, F. (2023). Plant extracellular self-DNA inhibits growth and induces immunity via the jasmonate signaling pathway. *Plant Physiology*, kiad195. https://doi.org/10.1093/plphys/kiad195

Zhu, C., Ming, C., Zhao-shi, X., Lian-cheng, L., Xue-ping, C., & You-zhi, M. (2014). Characteristics and Expression Patterns of the Aldehyde Dehydrogenase (ALDH) Gene Superfamily of Foxtail Millet (Setaria italica L.). *PLoS ONE*, *9*(7), e101136. https://doi.org/10.1371/journal.pone.0101136

Zhu, Z., Wang, T., Lan, J., Ma, J., Xu, H., Yang, Z., Guo, Y., Chen, Y., Zhang, J., Dou, S., Yang, M., Li, L., & Liu, G. (2022). Rice MPK17 Plays a Negative Role in the Xa21-Mediated Resistance Against Xanthomonas oryzae pv. Oryzae. *Rice*, *15*(1), 41. https://doi.org/10.1186/s12284-022-00590-4

Zilberman, D., Gehring, M., Tran, R. K., Ballinger, T., & Henikoff, S. (2007). Genome-wide analysis of Arabidopsis thaliana DNA methylation uncovers an interdependence between methylation and transcription. *Nature Genetics*, *39*(1), 61–69. https://doi.org/10.1038/ng1929

Appendices

Appendix A. List of sample DEGs with pvalue adjusted <= 0.05 after 6h treatment. Gene expression level comparison have been carried out between treated (SELF1, SLEF2) and control (CTRL4, CTRL6) samples at 6h. The table displays the gene name, the mean expression value among all samples, the log2FoldChange, the standard error (lfcSE), the p value and the pvalue adjusted for multiple comparisons. Also, expression level of genes for each individual sample (CTRL1, CTRL2, CTRL3, CTRL4, CTRL6, CTRL7, CTRL8, CTRL9, SELF1, SELF2, SELF4, SELF6) are presented.

Gene	baseMean	log2FoldChange	lfcSE	stat	pvalue	padj	CTRL1	CTRL2	CTRL3	CTRL4	CTRL6	CTRL7	CTRL8	CTRL9	SELF1	SELF2	SELF4	SELF6
AT1G07000	357.04	-1.11	0.31	-3.56	0	0.05	253.00	284.34	296.78	482.96	443.04	334.03	356.91	419.62	242.45	186.75	347.09	637.57
AT1G07400	548.13	-2.00	0.53	-3.79	0	0.03	1213.59	749.62	400.98	489.28	898.69	384.93	1134.77	598.32	168.89	178.48	145.01	214.92
AT1G08920	1441.15	-1.15	0.32	-3.58	0	0.05	3116.33	2545.55	1824.22	1331.53	2251.64	775.17	1149.24	1107.96	819.57	799.32	798.96	774.26
AT1G10970	454.70	1.40	0.34	4.12	0	0.01	151.53	194.43	208.41	271.72	231.33	150.58	115.70	211.80	502.51	829.06	1400.51	1188.81
AT1G11670	2599.35	-1.19	0.28	-4.21	0	0.01	1586.50	1886.97	1675.17	3694.89	4776.68	3488.79	2861.99	3208.71	2422.43	1296.20	2108.72	2185.18
AT1G12010	257.91	1.07	0.24	4.48	0	0.01	162.08	151.72	166.20	163.40	187.87	243.90	302.68	285.92	375.07	361.92	368.61	325.53
AT1G13210	1342.34	-1.34	0.33	-4.02	0	0.02	1067.33	936.18	1271.54	1782.00	2018.91	1900.27	1502.53	1745.99	982.24	521.68	879.41	1499.95
AT1G14780	397.58	-1.52	0.40	-3.81	0	0.03	1174.06	664.20	444.51	523.59	472.48	306.46	387.90	240.92	173.03	174.63	106.65	102.51
AT1G15405	161.54	1.95	0.55	3.53	0	0.05	274.08	87.66	133.22	58.68	47.67	138.92	199.89	291.22	273.53	140.47	116.94	176.25
AT1G16030	695.43	-2.69	0.60	-4.47	0	0.01	1297.92	886.73	455.07	775.45	2133.87	398.72	1157.50	418.30	212.40	237.98	110.39	260.78
AT1G17180	1810.84	1.20	0.30	4.03	0	0.02	1482.40	2447.78	2620.91	1243.97	1351.55	1136.77	1419.37	938.52	2803.72	3173.58	1740.12	1371.36
AT1G17340	907.92	-1.63	0.31	-5.23	0	0.00	1056.79	1010.35	770.31	1181.68	1847.86	829.25	978.79	1098.69	584.37	393.32	667.05	476.60
AT1G18390	501.06	-1.10	0.26	-4.27	0	0.01	528.39	554.07	543.44	769.13	524.35	560.96	489.14	618.18	285.97	319.51	358.31	461.32
AT1G19530	3058.57	1.98	0.41	4.78	0	0.00	1116.08	913.70	1750.35	1056.20	1072.54	4096.41	5030.30	5718.50	2681.46	5727.43	2448.33	5091.56
AT1G20380	519.61	2.04	0.51	4.02	0	0.02	65.88	57.32	91.01	63.19	79.92	97.56	29.96	115.16	192.72	391.67	2567.14	2483.73
AT1G22030	142.10	1.44	0.36	4.05	0	0.02	131.77	134.86	142.46	67.71	63.09	107.10	143.59	104.57	150.24	204.92	275.99	178.95
AT1G25390	382.93	-1.12	0.27	-4.12	0	0.01	484.91	425.94	440.56	575.94	465.47	339.33	377.57	402.41	295.29	186.20	275.99	325.53
AT1G53540	2364.12	-1.45	0.41	-3.55	0	0.05	5422.29	3242.35	2512.75	3691.28	4437.39	963.92	2228.75	1301.22	1544.84	1438.88	634.30	951.41
AT1G54050	189.25	-2.37	0.61	-3.86	0	0.02	413.75	256.24	193.90	166.10	280.40	78.47	428.70	236.95	50.77	35.81	58.00	71.94
AT1G55810	508.53	1.55	0.42	3.73	0	0.03	210.83	321.43	291.51	302.42	267.79	1141.01	438.52	630.09	634.10	1035.64	367.67	461.32
AT1G59860	183.51	-3.41	0.66	-5.19	0	0.00	388.72	192.18	118.71	185.06	552.40	95.44	241.73	270.04	41.44	28.09	28.07	60.25
AT1G61360	464.69	-1.04	0.26	-4.05	0	0.02	495.45	639.48	510.46	618.37	548.19	500.52	511.86	434.18	297.36	269.38	304.99	446.03

AT1G68570	200.82	1.58	0.40	3.90	0	0.02	267.49	110.14	162.24	142.63	112.16	131.49	133.78	119.14	467.29	295.82	232.02	235.60
AT1G70740	536.91	-1.31	0.30	-4.35	0	0.01	534.98	413.58	534.21	929.82	677.17	502.64	505.66	656.57	370.93	279.84	412.58	624.98
AT1G72540	159.59	-2.23	0.50	-4.44	0	0.01	278.03	104.52	129.26	225.68	206.10	239.66	322.30	154.88	54.91	38.01	67.36	94.42
AT1G72790	846.63	-1.31	0.38	-3.49	0	0.05	520.49	409.09	713.59	1438.96	1801.59	787.89	821.25	1010.00	893.13	415.36	539.81	808.43
AT1G77500	678.23	-1.08	0.25	-4.39	0	0.01	768.21	818.17	786.14	852.18	771.11	560.96	765.99	713.49	374.04	394.43	544.49	789.54
AT1G80920	1073.77	1.38	0.37	3.70	0	0.04	728.68	956.41	623.90	633.72	814.57	1524.89	1001.52	942.49	1190.49	2568.17	863.51	1036.84
AT2G20960	750.98	-1.03	0.26	-3.92	0	0.02	782.71	809.18	927.28	1146.47	759.89	775.17	607.93	681.72	460.03	473.20	675.47	912.74
AT2G25460	2683.12	-1.29	0.35	-3.68	0	0.04	2516.79	1758.85	2713.24	2973.61	3957.90	2214.16	2630.59	3768.65	1538.63	1293.45	2364.13	4467.48
AT2G29500	3326.50	-1.24	0.34	-3.62	0	0.05	5598.86	4190.89	3690.64	6061.87	6435.26	1041.33	2121.31	1847.92	2342.65	2960.94	1426.71	2199.57
AT2G31865	214.95	-1.33	0.35	-3.80	0	0.03	318.88	197.80	247.98	290.68	377.14	150.58	189.04	211.80	150.24	115.68	129.11	200.53
AT2G41830	246.71	-1.18	0.31	-3.76	0	0.03	283.30	259.61	275.68	389.08	436.03	229.05	255.67	226.36	241.41	126.15	111.33	126.79
AT2G44500	1491.56	-1.38	0.33	-4.21	0	0.01	1656.34	1281.21	1448.29	2210.80	2541.86	1214.18	982.40	1580.53	1157.34	674.82	1228.37	1922.60
AT2G46240	917.41	-1.79	0.44	-4.07	0	0.02	980.36	1032.83	778.23	883.78	3326.99	597.02	581.08	610.24	594.73	623.59	421.00	579.12
AT3G02550	1059.02	2.10	0.51	4.10	0	0.01	380.81	528.22	638.41	466.71	416.40	2370.04	731.38	976.91	1620.48	2155.57	667.98	1755.34
AT3G09640	642.49	-1.55	0.39	-3.93	0	0.02	1183.28	668.70	565.86	1547.29	1479.13	116.65	220.03	232.98	495.26	536.00	260.08	404.66
AT3G10040	501.69	2.44	0.57	4.27	0	0.01	129.13	253.99	300.74	211.24	169.64	1056.18	410.63	402.41	636.17	1428.41	283.47	738.29
AT3G12750	876.69	1.45	0.42	3.50	0	0.05	454.60	434.94	551.35	475.74	464.07	206.78	457.63	598.32	947.01	1626.73	2554.05	1749.04
AT3G14870	174.67	-1.19	0.32	-3.75	0	0.03	160.76	168.58	197.85	326.79	286.01	177.09	154.95	153.55	169.92	101.91	88.88	109.71
AT3G25610	1020.88	-1.23	0.27	-4.60	0	0.01	1188.56	1166.57	1296.61	1336.95	1481.93	1280.99	770.63	1107.96	567.79	633.50	602.49	816.52
AT3G27220	945.50	1.52	0.40	3.83	0	0.03	419.03	423.70	523.65	665.32	395.37	1676.53	737.58	1106.64	1572.82	1479.64	824.22	1521.53
AT3G27850	230.90	1.40	0.39	3.57	0	0.05	156.80	112.39	258.53	158.88	127.58	206.78	145.14	177.38	305.65	452.82	319.96	348.91
AT3G28580	150.92	1.59	0.44	3.60	0	0.05	60.61	88.79	85.74	97.50	64.49	199.36	136.88	285.92	314.98	178.48	132.85	165.46
AT3G46230	2968.62	-1.92	0.54	-3.59	0	0.05	6019.20	2963.63	2209.37	6319.15	7760.17	831.37	2668.81	1285.34	1788.33	1931.36	523.91	1322.80
AT3G56200	461.28	-1.41	0.33	-4.29	0	0.01	606.14	666.45	495.95	695.11	630.91	541.88	418.89	430.21	231.05	267.72	180.56	370.49
AT3G56410	554.69	-1.26	0.31	-4.06	0	0.02	549.48	515.85	557.95	807.95	593.05	767.74	404.94	561.26	282.86	304.08	579.10	731.99
AT3G59930	3100.97	3.51	1.00	3.51	0	0.05	22.40	11.24	3.96	32.50	102.35	41.36	249.47	80.75	545.00	981.66	22992.96	12147.99
AT3G62010	4009.80	-1.88	0.43	-4.34	0	0.01	3003.01	2266.84	2382.17	6101.59	13209.81	3496.21	3929.62	4611.86	3937.23	1324.85	1882.32	1972.06
AT4G04990	319.75	-2.01	0.51	-3.91	0	0.02	827.51	685.56	498.59	540.74	164.04	170.73	227.26	165.47	52.84	120.64	154.37	229.31
AT4G08770	386.20	1.69	0.47	3.61	0	0.05	131.77	366.38	455.07	213.95	186.47	482.49	348.13	676.42	697.30	597.70	264.76	214.02
AT4G10250	1945.36	-2.19	0.51	-4.34	0	0.01	5629.17	2366.86	1669.89	4904.56	4297.19	258.74	572.81	454.04	1270.27	745.88	428.48	746.38

AT4G19520	203.96	-2.52	0.57	-4.46	0	0.01	205.56	113.51	142.46	544.35	235.54	338.27	233.46	180.03	106.72	30.85	123.49	193.34
AT4G22970	152.57	-2.04	0.55	-3.73	0	0.03	281.99	118.01	179.39	164.30	347.70	79.53	198.34	136.34	56.99	67.21	130.04	71.04
AT4G25200	310.77	-2.14	0.59	-3.63	0	0.04	756.35	412.46	251.93	430.60	433.22	165.43	570.23	300.49	122.26	74.37	61.75	150.18
AT4G26690	1981.15	-1.83	0.38	-4.79	0	0.00	2504.93	1595.89	2142.10	3262.48	4204.65	1682.89	1175.58	1945.88	1300.32	803.72	1017.88	2137.52
AT4G29440	747.82	-1.01	0.25	-3.97	0	0.02	909.21	742.87	870.56	794.41	849.62	840.91	791.81	720.11	433.10	386.16	631.49	1003.57
AT4G30270	3173.86	-1.50	0.38	-3.93	0	0.02	3379.87	2064.54	2913.74	6866.20	4909.87	5330.74	2106.85	3075.02	1951.00	2211.76	1433.26	1843.47
AT4G35380	473.64	-1.53	0.36	-4.29	0	0.01	768.21	506.86	495.95	841.35	541.18	671.25	520.64	432.86	297.36	185.09	191.79	231.11
AT4G37530	478.21	-1.80	0.33	-5.43	0	0.00	864.40	841.77	651.60	1002.04	619.69	378.57	380.67	226.36	227.94	237.43	174.01	133.99
AT4G37890	170.06	1.53	0.41	3.72	0	0.03	188.43	262.98	246.66	65.00	79.92	103.92	88.32	111.19	147.13	266.62	310.60	169.96
AT4G39400	1462.67	-1.00	0.26	-3.78	0	0.03	1819.73	1704.90	1857.19	2565.57	1556.24	1546.09	1162.15	1518.31	1130.40	931.53	837.32	922.63
AT5G01040	4433.67	-1.84	0.51	-3.58	0	0.05	3644.73	1928.55	3531.04	8562.44	11750.31	4657.37	3551.53	5591.42	4710.17	970.09	2153.63	2152.81
AT5G06330	188.90	-1.79	0.50	-3.56	0	0.05	224.01	287.71	233.47	239.22	133.19	290.56	161.15	234.30	32.12	74.37	109.46	247.29
AT5G10210	411.75	1.43	0.33	4.26	0	0.01	143.63	147.23	245.34	209.43	325.27	374.33	470.03	529.49	779.16	653.34	579.10	484.70
AT5G12020	514.94	-2.61	0.55	-4.72	0	0.00	1174.06	619.25	480.13	688.79	1598.30	219.51	580.56	276.66	244.52	130.56	60.81	106.11
AT5G15640	224.78	-1.06	0.26	-4.06	0	0.02	337.33	339.41	266.44	284.36	339.29	183.45	149.79	154.88	158.53	139.92	174.95	169.06
AT5G16910	3209.51	-1.44	0.35	-4.13	0	0.01	4005.77	2135.34	3269.87	5269.26	4933.70	3592.71	2358.91	3883.81	2288.77	1466.97	2150.82	3158.17
AT5G24030	896.14	-1.48	0.32	-4.64	0	0.00	1326.91	841.77	1061.82	1668.25	1456.70	408.26	692.12	778.35	500.44	620.28	683.89	714.91
AT5G25340	223.71	1.25	0.31	4.09	0	0.01	185.79	282.09	224.23	129.09	113.56	265.11	193.69	238.27	312.91	266.62	259.15	214.02
AT5G27350	1248.86	-1.38	0.39	-3.57	0	0.05	2590.58	1917.31	1751.67	2136.77	1301.07	866.36	994.28	807.47	375.07	945.30	605.30	695.12
AT5G38710	223.41	-1.53	0.40	-3.83	0	0.03	262.22	385.49	312.61	300.61	461.26	163.30	106.92	191.94	158.53	105.77	145.01	87.23
AT5G39890	349.28	2.35	0.54	4.36	0	0.01	27.67	35.96	84.42	103.81	85.52	840.91	350.71	659.22	350.21	618.63	328.38	705.91
AT5G41080	773.78	-1.82	0.50	-3.66	0	0.04	329.42	334.91	857.37	1030.02	1930.58	726.39	646.16	1111.93	439.31	401.59	468.71	1008.96
AT5G41100	507.42	-1.25	0.33	-3.77	0	0.03	507.31	449.55	573.78	684.27	688.39	466.59	445.23	726.73	346.06	232.47	376.09	592.61
AT5G41810	772.09	-1.30	0.29	-4.48	0	0.01	1222.82	863.13	768.99	1017.38	1141.24	632.01	763.92	871.01	521.16	357.52	529.52	576.42
AT5G45070	860.70	-1.45	0.41	-3.55	0	0.05	1539.06	1477.88	1357.28	1471.46	492.11	759.26	488.62	642.01	305.65	411.50	615.59	767.96
AT5G46470	420.76	-1.18	0.30	-3.96	0	0.02	445.38	333.79	456.38	555.18	480.89	351.00	438.00	575.82	256.96	202.72	434.09	518.87
AT5G48570	867.75	-1.36	0.27	-5.01	0	0.00	1561.46	1205.91	1077.65	1273.76	1543.62	505.82	639.44	526.84	574.01	523.33	394.80	586.31
AT5G52640	2351.63	-1.32	0.34	-3.87	0	0.02	3335.07	2084.77	1627.68	3276.03	5535.17	1310.68	1656.45	1502.43	1681.61	1857.54	1940.33	2411.79
AT5G53050	357.53	-1.26	0.36	-3.51	0	0.05	304.39	251.75	338.99	446.85	926.73	293.74	323.85	349.46	354.35	219.80	238.56	241.90
AT5G55050	234.68	-1.19	0.33	-3.60	0	0.05	351.82	291.08	257.21	247.35	403.78	229.05	303.19	226.36	145.06	139.92	94.49	126.79

AT5G59720	7023.72	-1.27	0.29	-4.35	0	0.01	20356.98	17398.55	16717.37	9997.79	7333.96	932.11	1643.02	1433.60	4000.43	3176.88	552.91	740.98
AT5G64120	791.47	2.02	0.57	3.55	0	0.05	185.79	529.34	837.58	257.28	356.11	628.83	865.67	1358.14	656.90	1834.41	1001.97	985.58

Appendix B. List of sample DEGs with pvalue adjusted <= 0.05 after 24h treatment. Gene expression level comparison have been carried out between treated (SELF4, SLEF6) and control (CTRL7, CTRL8, CTRL9) samples at 24h. The table displays the gene name, the mean expression value among all samples, the log2FoldChange, the standard error (lfcSE), the p value and the pvalue adjusted for multiple comparisons. Also, expression level of genes for each individual sample (CTRL1, CTRL2, CTRL3, CTRL4, CTRL6, CTRL7, CTRL8, CTRL9, SELF1, SELF2, SELF4, SELF6) are presented.

gene	baseMean	log2FoldChange	lfcSE	stat	pvalue	padj	CTRL1	CTRL2	CTRL3	CTRL4	CTRL6	CTRL7	CTRL8	CTRL9	SELF1	SELF2	SELF4	SELF6
AT1G01610	598.31	1.49	0.30	5.00	0	0.00	673.34	923.82	936.51	538.93	431.82	320.25	253.09	326.96	620.63	476.51	1085.24	592.61
AT1G04020	31.42	-2.03	0.56	-3.60	0	0.03	14.49	31.47	23.74	37.01	35.05	42.42	42.87	62.22	36.26	27.54	14.97	8.99
AT1G05300	94.64	3.03	0.37	8.26	0	0.00	35.58	38.21	40.89	29.79	28.04	37.11	32.54	55.60	66.31	100.26	382.64	288.66
AT1G05562	877.95	1.42	0.33	4.36	0	0.00	1196.46	1039.57	1200.32	547.96	337.89	459.16	479.84	602.30	584.37	1332.56	1313.51	1441.50
AT1G05680	897.60	1.57	0.45	3.53	0	0.04	656.21	712.53	613.35	1228.62	398.17	759.26	537.17	285.92	858.94	1578.25	1481.91	1660.92
AT1G06980	13.90	-4.63	1.35	-3.43	0	0.05	3.95	0.00	3.96	16.25	14.02	13.79	74.38	11.91	17.61	8.26	0.00	2.70
AT1G07400	548.13	-1.97	0.48	-4.10	0	0.01	1213.59	749.62	400.98	489.28	898.69	384.93	1134.77	598.32	168.89	178.48	145.01	214.92
AT1G07720	469.78	1.96	0.48	4.05	0	0.01	1278.16	618.13	743.93	494.70	405.18	119.83	48.04	150.90	336.74	623.04	565.07	253.59
AT1G08650	553.15	-1.12	0.29	-3.90	0	0.02	550.79	606.89	477.49	573.24	679.98	490.97	749.97	514.93	537.74	917.75	261.02	276.97
AT1G08840	750.62	-1.08	0.30	-3.56	0	0.04	909.21	1065.42	652.92	719.48	686.99	656.40	1111.02	722.75	1035.08	663.80	375.15	409.16
AT1G09155	111.11	4.15	0.77	5.39	0	0.00	89.60	61.81	68.59	27.98	58.88	28.63	5.17	30.45	18.65	201.62	396.67	345.31
AT1G10960	543.88	1.40	0.35	4.05	0	0.01	469.10	515.85	664.79	710.45	622.50	189.82	193.18	416.97	673.47	670.41	830.77	569.23
AT1G10970	454.70	3.03	0.31	9.76	0	0.00	151.53	194.43	208.41	271.72	231.33	150.58	115.70	211.80	502.51	829.06	1400.51	1188.81
AT1G11190	152.28	-1.68	0.48	-3.48	0	0.05	313.61	257.37	205.77	143.53	103.75	110.28	287.70	91.34	86.00	125.05	58.94	44.06
AT1G11450	585.14	-1.06	0.30	-3.57	0	0.04	451.97	749.62	527.61	612.05	902.90	689.27	581.08	634.06	780.19	484.22	300.31	308.44
AT1G12030	41.53	6.18	0.83	7.40	0	0.00	0.00	2.25	6.60	4.51	2.80	3.18	2.58	3.97	3.11	15.42	318.09	135.79
AT1G12040	46.01	-8.38	1.70	-4.94	0	0.00	27.67	16.86	178.07	68.61	40.66	27.57	46.49	95.31	14.51	36.36	0.00	0.00
AT1G13300	704.38	-2.19	0.55	-3.99	0	0.01	646.99	731.64	691.17	781.77	457.06	2399.73	522.19	434.18	535.67	760.76	218.92	272.47
AT1G14700	8.84	5.63	1.49	3.78	0	0.02	14.49	7.87	23.74	2.71	8.41	1.06	0.00	0.00	8.29	7.16	22.45	9.89
AT1G14780	397.58	-1.58	0.37	-4.25	0	0.01	1174.06	664.20	444.51	523.59	472.48	306.46	387.90	240.92	173.03	174.63	106.65	102.51
AT1G15670	891.00	-1.43	0.37	-3.86	0	0.02	1023.84	551.82	664.79	1293.62	1037.49	1201.46	918.87	902.78	1220.54	1128.19	542.62	205.93
AT1G15980	13.09	5.83	1.55	3.75	0	0.02	13.18	4.50	34.29	10.83	9.81	1.06	0.00	0.00	35.23	11.02	30.87	6.29

AT1G16410	14.73	7.25	2.00	3.63	0	0.03	36.90	1.12	72.55	0.00	0.00	0.00	0.00	0.00	12.43	3.31	49.58	0.90
AT1G17190	308.13	-2.67	0.53	-5.06	0	0.00	127.82	468.65	212.36	230.20	222.92	1043.45	389.45	333.58	265.24	219.25	100.10	84.53
AT1G17220	472.30	1.18	0.32	3.66	0	0.03	496.77	320.30	568.50	484.77	457.06	303.28	232.43	413.00	366.78	592.74	728.79	703.21
AT1G17744	987.98	1.34	0.34	3.91	0	0.02	1440.23	875.49	1231.97	824.20	901.50	871.67	434.90	375.94	902.45	1168.40	1366.84	1462.18
AT1G20380	519.61	4.99	0.45	10.97	0	0.00	65.88	57.32	91.01	63.19	79.92	97.56	29.96	115.16	192.72	391.67	2567.14	2483.73
AT1G20390	154.72	3.16	0.57	5.58	0	0.00	17.13	48.33	14.51	58.68	57.48	43.48	107.95	60.89	122.26	53.43	906.55	366.00
AT1G22650	37.97	-1.90	0.55	-3.43	0	0.05	43.48	46.08	43.53	34.30	42.06	40.30	76.96	29.12	36.26	36.91	14.03	12.59
AT1G23740	129.87	2.27	0.50	4.57	0	0.00	101.46	94.40	87.06	195.89	180.86	23.33	21.69	74.13	239.34	167.47	245.11	127.69
AT1G27140	74.19	-2.34	0.65	-3.60	0	0.04	38.21	25.85	85.74	121.87	100.95	159.06	53.72	52.95	80.82	136.07	23.39	11.69
AT1G27740	12.19	-6.19	1.68	-3.68	0	0.03	17.13	12.36	17.15	24.37	21.03	6.36	23.76	5.29	7.25	11.57	0.00	0.00
AT1G30730	619.51	-1.58	0.38	-4.15	0	0.01	701.01	757.48	720.19	1476.87	633.71	759.26	435.94	329.61	661.04	618.08	164.66	176.25
AT1G33790	312.50	-1.83	0.40	-4.58	0	0.00	220.05	161.84	395.71	415.26	534.17	378.57	420.44	242.24	351.24	435.19	72.97	122.30
AT1G42550	119.39	2.21	0.53	4.18	0	0.01	88.29	56.19	134.54	111.94	78.51	28.63	81.61	63.54	179.25	71.61	322.76	215.82
AT1G48710	282.76	-2.01	0.48	-4.21	0	0.01	426.93	534.96	505.19	374.64	253.77	349.94	234.50	319.02	76.67	168.02	29.94	119.60
AT1G49380	51.82	1.61	0.41	3.93	0	0.01	61.93	50.57	55.40	34.30	56.08	28.63	27.38	21.18	62.17	66.10	87.94	70.14
AT1G49660	482.25	1.14	0.33	3.50	0	0.04	546.84	564.18	571.14	371.93	358.92	243.90	272.20	448.74	454.85	536.55	942.10	475.70
AT1G50250	524.52	1.42	0.25	5.64	0	0.00	602.18	564.18	705.68	515.46	558.00	188.75	292.35	320.34	507.70	609.27	755.92	674.44
AT1G51850	216.38	-1.79	0.51	-3.50	0	0.05	189.75	198.92	249.30	452.27	143.01	480.37	150.82	236.95	191.68	136.07	73.91	93.52
AT1G54000	1724.15	-1.01	0.28	-3.66	0	0.03	1156.93	2288.19	1551.18	1487.71	1252.00	2758.16	2126.99	2136.49	1611.16	2002.97	1197.50	1120.47
AT1G54050	189.25	-1.94	0.56	-3.47	0	0.05	413.75	256.24	193.90	166.10	280.40	78.47	428.70	236.95	50.77	35.81	58.00	71.94
AT1G54970	39.89	-6.06	1.44	-4.20	0	0.01	3.95	28.10	138.50	38.82	19.63	22.27	40.29	120.46	27.98	36.91	0.00	1.80
AT1G55320	213.34	1.46	0.27	5.37	0	0.00	309.66	259.61	313.93	225.68	173.85	91.20	139.97	117.81	156.45	126.70	334.93	310.24
AT1G55430	24.83	-4.89	1.40	-3.49	0	0.05	39.53	12.36	27.70	40.62	19.63	45.60	30.99	3.97	64.24	11.57	0.00	1.80
AT1G55990	446.42	2.06	0.54	3.80	0	0.02	719.46	1235.13	707.00	405.33	248.16	54.08	80.06	280.63	211.37	272.68	723.18	419.95
AT1G56020	78.57	-1.57	0.43	-3.62	0	0.03	81.70	129.24	125.31	107.43	46.27	79.53	90.39	83.39	70.46	72.16	29.94	26.98
AT1G56430	499.16	3.50	0.39	8.92	0	0.00	89.60	113.51	225.55	173.33	147.21	112.40	236.05	182.67	365.75	314.00	2441.78	1588.08
AT1G57560	10.67	-6.94	1.76	-3.94	0	0.01	6.59	17.98	15.83	9.93	2.80	10.60	27.38	23.83	11.40	1.65	0.00	0.00
AT1G59860	183.51	-2.20	0.60	-3.65	0	0.03	388.72	192.18	118.71	185.06	552.40	95.44	241.73	270.04	41.44	28.09	28.07	60.25
AT1G60950	536.44	1.24	0.34	3.61	0	0.03	438.79	306.82	664.79	521.78	754.29	224.81	251.02	338.87	904.53	749.19	766.21	516.17
AT1G60960	719.03	2.21	0.31	7.07	0	0.00	737.91	781.09	608.07	628.30	358.92	264.04	311.46	303.13	682.80	1249.38	1532.43	1170.83

AT1G62750	555.81	1.35	0.30	4.55	0	0.00	419.03	359.64	572.46	456.78	415.00	275.71	392.55	460.66	548.10	856.06	929.93	983.78
AT1G62980	14.94	-7.16	1.65	-4.35	0	0.00	18.45	14.61	17.15	6.32	14.02	7.42	29.44	35.74	20.72	15.42	0.00	0.00
AT1G64770	13.64	4.61	1.31	3.51	0	0.04	5.27	4.50	13.19	19.86	0.00	2.12	1.03	2.65	14.51	11.02	81.39	8.09
AT1G66270	2671.98	-1.98	0.33	-5.92	0	0.00	1286.06	3036.68	2163.21	2551.13	2783.01	4273.50	4133.12	3239.16	2389.28	4243.37	914.03	1051.23
AT1G66280	5099.90	-1.44	0.36	-4.03	0	0.01	4173.12	9778.75	4658.81	4295.21	3558.32	9696.49	6159.91	6525.97	2620.33	4244.48	2600.82	2886.60
AT1G67100	22.39	-2.92	0.73	-3.98	0	0.01	3.95	4.50	6.60	13.54	19.63	71.05	64.05	41.04	6.22	22.59	5.61	9.89
AT1G72540	159.59	-1.57	0.45	-3.46	0	0.05	278.03	104.52	129.26	225.68	206.10	239.66	322.30	154.88	54.91	38.01	67.36	94.42
AT1G74010	403.40	-1.06	0.24	-4.35	0	0.00	673.34	590.03	519.70	569.63	555.20	277.83	330.05	377.26	361.60	272.13	143.14	170.86
AT1G74470	441.55	1.68	0.41	4.07	0	0.01	224.01	103.40	284.91	361.09	339.29	158.00	383.25	350.79	552.25	630.75	1088.04	822.82
AT1G77580	119.06	-1.66	0.48	-3.42	0	0.05	97.51	144.98	112.12	112.84	102.35	106.04	294.93	129.73	103.61	111.83	34.62	78.23
AT1G77990	37.59	-2.54	0.71	-3.59	0	0.04	35.58	42.71	46.17	71.32	30.84	27.57	97.10	41.04	27.98	11.57	9.36	9.89
AT1G78380	27687.99	1.25	0.27	4.62	0	0.00	23220.32	17758.19	24329.49	21414.68	33331.58	19468.27	16650.77	19111.96	25527.75	44103.45	42892.99	44446.43
AT1G78570	3713.67	1.50	0.28	5.38	0	0.00	6111.44	4548.28	5360.53	3143.32	3275.11	1695.61	1353.78	2659.37	3108.34	2521.35	6104.45	4682.40
AT1G78660	1654.10	-1.00	0.25	-3.95	0	0.01	1263.66	1671.19	1301.88	1622.21	2609.16	2061.46	1898.18	2035.89	1645.35	1741.86	1187.21	811.13
AT1G78820	7.18	6.78	1.83	3.70	0	0.03	2.64	0.00	11.87	6.32	8.41	0.00	0.00	0.00	12.43	8.26	30.87	5.40
AT1G79410	223.33	1.67	0.35	4.73	0	0.00	241.14	298.95	237.43	177.84	151.42	155.88	94.52	116.49	138.84	290.31	445.32	331.82
AT1G80380	1410.91	-1.30	0.37	-3.50	0	0.04	1209.64	693.42	707.00	903.64	1130.03	2940.55	2478.22	1708.93	1092.06	2138.49	696.05	1232.87
AT2G01880	119.36	-1.69	0.46	-3.67	0	0.03	67.20	198.92	96.29	138.12	85.52	236.47	152.89	161.49	82.89	98.61	60.81	53.06
AT2G02955	149.88	1.04	0.28	3.67	0	0.03	115.96	140.48	130.58	126.38	126.18	125.13	85.74	137.67	170.96	168.57	222.66	248.19
AT2G03460	55.04	1.82	0.49	3.73	0	0.02	36.90	43.83	64.63	34.30	30.84	40.30	24.79	48.98	31.08	40.76	177.75	86.33
AT2G04090	102.45	-1.78	0.51	-3.46	0	0.05	122.55	204.54	114.76	144.44	96.74	124.07	146.69	128.40	13.47	56.19	29.94	47.66
AT2G07698	214.38	-2.01	0.55	-3.65	0	0.03	438.79	356.27	274.36	306.03	138.80	92.26	393.06	259.45	107.76	82.08	35.55	88.13
AT2G16270	24.45	-2.85	0.71	-4.04	0	0.01	22.40	21.35	15.83	21.67	33.65	26.51	30.47	52.95	31.08	27.54	2.81	7.19
AT2G18480	942.84	1.41	0.38	3.73	0	0.03	1774.93	1046.32	1077.65	541.64	1556.24	396.60	431.29	496.40	731.50	911.69	1277.96	1071.91
AT2G19800	918.88	-1.81	0.37	-4.83	0	0.00	438.79	307.94	842.86	1762.14	1669.80	1240.69	1121.35	794.24	1372.85	876.44	270.37	329.13
AT2G20570	9.37	7.30	1.93	3.79	0	0.02	0.00	0.00	2.64	16.25	1.40	0.00	0.00	0.00	31.08	8.81	48.65	3.60
AT2G20950	1076.74	1.45	0.21	6.92	0	0.00	716.82	695.67	784.82	806.14	772.51	717.91	933.85	811.44	906.60	1284.64	2100.30	2390.21
AT2G21330	53.74	6.04	1.56	3.88	0	0.02	28.99	5.62	76.50	52.36	8.41	5.30	0.00	2.65	109.83	23.69	292.83	38.67
AT2G21970	379.54	1.26	0.34	3.76	0	0.02	378.18	357.39	336.35	415.26	342.09	143.16	159.60	317.69	453.82	665.45	507.07	478.40
AT2G22590	499.93	1.98	0.48	4.14	0	0.01	863.09	563.06	729.42	536.22	487.90	78.47	117.76	322.99	603.02	339.89	844.80	512.57

AT2G22970	335.14	-1.34	0.33	-4.07	0	0.01	299.12	624.87	402.30	421.58	302.84	349.94	316.10	416.97	285.97	317.85	161.85	122.30
AT2G24850	41.09	-4.14	1.08	-3.82	0	0.02	6.59	21.35	51.44	41.53	143.01	51.96	40.80	51.63	68.38	11.02	0.00	5.40
AT2G24980	51.74	-6.16	1.80	-3.42	0	0.05	10.54	42.71	174.11	104.72	15.42	26.51	10.85	157.52	14.51	62.25	0.00	1.80
AT2G27505	32.90	-2.83	0.83	-3.41	0	0.05	10.54	6.74	15.83	20.76	33.65	28.63	181.30	42.36	22.79	8.26	13.10	10.79
AT2G27830	665.21	-1.05	0.27	-3.94	0	0.01	765.58	712.53	684.58	682.47	569.22	1073.15	828.48	652.60	484.90	708.97	463.10	357.00
AT2G28790	231.43	-1.43	0.31	-4.57	0	0.00	193.70	189.93	344.27	297.00	287.41	267.23	323.34	236.95	208.26	223.65	103.85	101.62
AT2G29130	153.54	-1.68	0.45	-3.77	0	0.02	296.48	189.93	195.22	272.63	176.65	118.77	137.91	63.54	211.37	112.93	37.42	29.68
AT2G29750	222.55	-1.83	0.53	-3.49	0	0.05	271.44	330.42	271.72	482.06	173.85	335.09	154.44	150.90	283.89	96.95	53.33	66.54
AT2G29995	321.66	-1.90	0.42	-4.52	0	0.00	275.40	574.29	365.37	427.90	308.44	424.17	451.95	276.66	333.63	216.49	60.81	144.78
AT2G30130	287.04	-1.47	0.36	-4.12	0	0.01	192.38	253.99	245.34	284.36	290.22	319.19	492.75	369.32	467.29	245.14	100.10	184.35
AT2G30395	41.81	-2.63	0.64	-4.10	0	0.01	26.35	52.82	34.29	46.94	35.05	27.57	84.71	47.65	78.74	50.13	8.42	8.99
AT2G30950	741.94	1.01	0.17	6.02	0	0.00	760.31	717.03	811.20	641.84	719.24	466.59	423.54	499.04	1009.17	1000.39	944.90	910.04
AT2G31560	184.45	-1.54	0.44	-3.53	0	0.04	329.42	229.27	274.36	220.27	158.43	121.95	296.48	127.08	159.56	170.77	43.97	81.83
AT2G32270	256.50	1.96	0.52	3.76	0	0.02	140.99	285.46	201.81	287.97	128.99	218.45	119.31	78.10	144.02	395.53	420.06	657.35
AT2G33560	37.65	-2.08	0.59	-3.54	0	0.04	35.58	44.95	60.68	20.76	37.85	29.69	70.76	43.68	43.52	41.32	13.10	9.89
AT2G34910	52.54	-2.22	0.64	-3.44	0	0.05	44.80	26.97	88.37	83.05	88.33	46.66	26.34	62.22	81.85	62.80	5.61	13.49
AT2G35260	53.60	1.68	0.49	3.45	0	0.05	39.53	20.23	39.57	44.23	23.83	27.57	54.75	30.45	55.95	61.70	136.59	108.81
AT2G36255	405.50	13.84	1.77	7.81	0	0.00	0.00	2.25	0.00	4.51	1.40	0.00	0.00	0.00	0.00	2.75	3199.57	1655.52
AT2G36990	94.83	1.93	0.51	3.79	0	0.02	43.48	22.48	97.61	73.12	77.11	63.63	55.78	48.98	88.07	139.37	262.89	165.46
AT2G37660	161.40	1.38	0.37	3.74	0	0.02	113.32	116.88	191.26	130.90	89.73	104.98	113.63	138.99	170.96	147.08	404.16	214.92
AT2G38750	659.98	-1.57	0.43	-3.68	0	0.03	711.55	1283.45	426.05	700.52	1020.67	957.56	621.88	493.75	530.49	709.52	287.21	177.15
AT2G39730	805.37	1.73	0.45	3.83	0	0.02	432.20	160.71	670.07	905.44	1094.98	282.07	574.88	375.94	1203.96	1230.10	1655.92	1078.20
AT2G41170	192.11	1.22	0.34	3.63	0	0.03	235.87	313.56	340.31	140.83	183.66	73.17	102.27	132.37	132.62	175.73	281.60	193.34
AT2G41240	29.47	5.56	1.13	4.92	0	0.00	0.00	4.50	3.96	0.00	0.00	4.24	5.68	0.00	1.04	0.00	294.70	39.57
AT2G42840	656.82	-1.57	0.42	-3.78	0	0.02	260.90	529.34	770.31	888.29	1146.85	1098.60	799.56	451.39	746.00	662.70	279.73	248.19
AT2G43590	697.89	-2.01	0.42	-4.78	0	0.00	853.86	1198.04	739.98	591.29	321.06	1426.27	982.40	473.89	793.66	517.82	203.95	272.47
AT2G44370	80.49	-1.73	0.50	-3.47	0	0.05	68.52	79.79	97.61	92.98	54.68	118.77	94.52	86.04	141.95	71.06	15.90	44.06
AT2G47540	24.25	-4.15	1.20	-3.45	0	0.05	22.40	31.47	52.76	27.08	23.83	21.21	4.13	48.98	22.79	33.60	0.00	2.70
AT2G48140	320.07	1.98	0.51	3.85	0	0.02	391.35	759.73	357.46	400.81	206.10	111.34	44.94	178.70	213.44	302.98	553.84	320.13
AT3G01900	45.51	-4.65	0.83	-5.58	0	0.00	69.84	64.06	55.40	81.25	33.65	78.47	50.62	42.36	37.30	28.65	0.00	4.50

AT3G04070	476.22	-1.30	0.38	-3.41	0	0.05	1187.24	1042.95	639.73	425.19	368.73	313.88	523.74	361.38	166.81	359.17	193.66	132.19
AT3G04760	52.09	2.12	0.61	3.44	0	0.05	36.90	41.58	64.63	60.48	11.22	19.09	30.47	15.88	94.29	57.84	100.10	92.62
AT3G08040	1054.07	1.98	0.44	4.53	0	0.00	643.03	631.61	770.31	557.89	1096.38	254.50	732.41	855.13	942.86	1327.05	3075.15	1762.53
AT3G11430	146.69	1.52	0.44	3.47	0	0.05	249.04	306.82	145.09	229.29	121.98	50.90	39.25	64.86	150.24	109.62	185.24	107.91
AT3G12320	496.56	-1.89	0.47	-4.03	0	0.01	67.20	68.56	26.38	825.10	1090.77	554.60	909.58	349.46	1033.00	706.77	232.02	95.32
AT3G12750	876.69	2.35	0.38	6.21	0	0.00	454.60	434.94	551.35	475.74	464.07	206.78	457.63	598.32	947.01	1626.73	2554.05	1749.04
AT3G13100	243.69	-1.35	0.36	-3.71	0	0.03	208.19	156.22	183.35	362.00	337.89	316.01	362.07	307.10	313.94	120.09	144.07	113.31
AT3G13790	2579.92	-1.33	0.38	-3.48	0	0.05	2769.78	3968.37	3809.36	4152.58	2306.32	4032.78	2033.50	1992.21	1409.11	2348.92	798.96	1337.19
AT3G14362	86.56	-1.63	0.45	-3.62	0	0.03	54.03	110.14	69.91	112.84	138.80	111.34	118.80	60.89	93.25	105.77	24.32	38.67
AT3G15460	366.65	-1.15	0.31	-3.66	0	0.03	188.43	195.55	209.73	231.10	256.57	492.04	961.23	504.34	331.56	437.39	304.05	287.76
AT3G15500	492.23	-1.06	0.30	-3.53	0	0.04	525.76	634.98	513.10	635.53	670.16	458.10	776.32	406.38	314.98	445.66	272.24	253.59
AT3G16150	77.18	-2.15	0.41	-5.26	0	0.00	26.35	17.98	30.34	87.57	50.47	164.37	177.68	125.75	77.71	97.50	29.94	40.47
AT3G16390	35.17	-3.81	0.77	-4.92	0	0.00	18.45	44.95	47.49	55.07	22.43	41.36	45.97	47.65	40.41	51.78	3.74	2.70
AT3G21670	36.81	4.66	1.33	3.50	0	0.04	38.21	34.84	42.21	36.11	9.81	3.18	0.00	3.97	142.98	20.93	108.52	0.90
AT3G23700	74.28	2.18	0.48	4.53	0	0.00	88.29	42.71	84.42	46.94	57.48	32.87	16.53	45.01	88.07	112.38	154.37	122.30
AT3G23810	2948.71	1.66	0.32	5.12	0	0.00	4704.15	4634.82	4434.58	2100.66	3167.16	936.35	1021.66	1677.16	2863.82	2217.81	5002.37	2624.02
AT3G24170	4305.65	1.29	0.24	5.48	0	0.00	3257.33	3716.62	4365.99	5291.83	5601.06	1577.91	2201.37	2538.91	5620.91	7206.52	4824.62	5464.75
AT3G24340	19.09	-7.39	1.67	-4.43	0	0.00	35.58	5.62	23.74	21.67	39.26	13.79	46.49	23.83	11.40	7.71	0.00	0.00
AT3G26570	124.58	1.69	0.44	3.80	0	0.02	40.85	69.68	98.93	172.42	168.24	27.57	69.21	62.22	263.17	179.03	189.92	153.77
AT3G29780	38.52	-2.25	0.58	-3.87	0	0.02	10.54	31.47	30.34	53.26	35.05	57.26	89.36	74.13	31.08	18.73	12.16	18.88
AT3G46610	115.76	1.52	0.41	3.67	0	0.03	97.51	69.68	104.20	119.16	79.92	113.47	50.10	66.19	105.68	145.98	260.08	177.15
AT3G48340	332.38	-2.06	0.41	-5.00	0	0.00	307.02	756.36	430.00	343.94	220.12	388.11	200.92	277.98	426.88	499.09	58.94	79.13
AT3G49130	72.91	-1.96	0.57	-3.42	0	0.05	123.86	139.36	61.99	86.66	70.10	64.69	132.74	82.07	21.76	43.52	36.49	11.69
AT3G49570	122.66	-1.31	0.31	-4.30	0	0.00	239.82	240.51	208.41	91.18	107.96	113.47	113.12	96.63	74.60	99.16	41.16	45.86
AT3G49620	32.94	-3.36	0.97	-3.46	0	0.05	2.64	1.12	9.23	33.40	29.44	79.53	114.67	27.80	37.30	45.72	0.00	14.39
AT3G51420	14.41	6.62	1.77	3.75	0	0.02	10.54	0.00	25.06	1.81	0.00	1.06	0.00	0.00	53.88	15.42	57.07	8.09
AT3G51710	77.89	1.50	0.43	3.52	0	0.04	77.74	68.56	96.29	52.36	70.10	55.14	48.04	48.98	44.55	85.94	188.05	98.92
AT3G54580	550.91	-3.22	0.59	-5.46	0	0.00	540.25	601.27	1803.11	638.23	291.62	443.26	318.69	906.75	240.38	707.87	65.49	53.96
AT3G56000	78.19	-2.30	0.52	-4.37	0	0.00	110.69	67.43	71.23	78.54	113.56	85.89	172.00	56.92	61.13	77.67	25.26	17.99
AT3G56970	45.28	4.07	1.14	3.58	0	0.04	5.27	13.49	5.28	5.42	7.01	0.00	37.71	1.32	7.25	4.96	388.25	67.44

AT3G56980	182.32	2.55	0.73	3.49	0	0.05	40.85	78.67	142.46	29.79	42.06	71.05	169.93	74.13	27.98	278.74	909.35	322.83
AT3G57370	8.83	-5.89	1.72	-3.43	0	0.05	13.18	7.87	10.55	16.25	19.63	7.42	17.56	3.97	6.22	3.31	0.00	0.00
AT3G58120	182.34	-1.43	0.38	-3.73	0	0.03	140.99	238.26	249.30	288.88	173.85	197.24	176.13	172.08	255.92	160.30	51.46	83.63
AT3G58190	23.37	-4.35	1.24	-3.50	0	0.05	21.08	43.83	14.51	43.33	79.92	9.54	25.83	19.86	12.43	8.26	0.00	1.80
AT3G59140	265.34	1.37	0.40	3.40	0	0.05	263.54	296.70	265.12	312.35	126.18	184.51	164.25	133.70	185.46	420.87	428.48	402.86
AT3G59720	25.87	-3.36	0.96	-3.50	0	0.05	15.81	48.33	77.82	36.11	18.23	37.11	25.83	21.18	11.40	13.22	0.00	5.40
AT3G59930	3100.97	7.14	0.91	7.89	0	0.00	22.40	11.24	3.96	32.50	102.35	41.36	249.47	80.75	545.00	981.66	22992.96	12147.99
AT3G60130	917.97	-1.08	0.29	-3.66	0	0.03	1151.66	1647.59	1346.73	1205.15	827.19	1074.21	870.84	730.70	489.05	827.41	458.42	386.68
AT3G60960	77.83	1.35	0.37	3.60	0	0.03	100.14	58.44	76.50	76.73	81.32	54.08	54.23	43.68	48.70	80.43	135.65	124.10
AT3G61220	516.25	1.34	0.29	4.65	0	0.00	560.02	617.00	530.25	467.62	517.34	223.75	228.30	424.92	536.71	615.33	808.31	665.45
AT3G61970	9.78	-6.54	1.73	-3.77	0	0.02	22.40	4.50	7.91	5.42	18.23	19.09	17.04	10.59	7.25	4.96	0.00	0.00
AT4G00050	13.42	6.77	1.95	3.47	0	0.05	0.00	0.00	23.74	23.47	7.01	0.00	0.00	0.00	55.95	14.87	24.32	11.69
AT4G00080	334.04	-1.46	0.40	-3.65	0	0.03	196.34	401.22	237.43	426.09	196.28	444.32	530.97	348.14	532.56	373.49	132.85	188.84
AT4G00370	177.46	1.39	0.40	3.49	0	0.05	291.21	211.29	279.63	169.71	114.97	55.14	90.39	132.37	124.33	178.48	300.31	181.65
AT4G00820	146.84	-1.40	0.35	-3.93	0	0.01	139.68	252.87	187.30	178.74	161.23	134.67	184.39	127.08	166.81	115.68	54.26	59.35
AT4G00900	808.06	1.14	0.28	4.07	0	0.01	1254.44	976.64	957.62	816.07	893.09	412.50	349.16	664.51	700.41	588.33	1122.66	961.30
AT4G01140	23.37	-7.51	1.62	-4.63	0	0.00	10.54	3.37	10.55	51.46	67.30	15.91	46.49	29.12	34.19	11.57	0.00	0.00
AT4G04640	122.21	2.36	0.50	4.68	0	0.00	88.29	56.19	199.17	92.08	70.10	34.99	58.88	60.89	151.27	123.40	343.35	187.94
AT4G07960	22.41	-3.63	0.94	-3.86	0	0.02	15.81	22.48	30.34	25.28	33.65	14.85	42.35	43.68	11.40	23.69	0.00	5.40
AT4G10340	195.39	1.78	0.52	3.43	0	0.05	98.83	28.10	127.95	116.45	141.60	119.83	204.54	140.31	194.79	104.12	714.76	353.41
AT4G12550	353.13	-2.04	0.57	-3.55	0	0.04	18.45	98.90	56.72	50.55	61.69	537.63	676.63	2008.09	76.67	129.46	239.50	283.26
AT4G13420	371.88	-2.37	0.49	-4.83	0	0.00	577.15	366.38	432.64	455.88	319.66	674.43	439.55	362.70	517.02	127.25	120.69	69.24
AT4G15230	294.95	-1.56	0.37	-4.24	0	0.01	479.64	561.93	338.99	351.16	203.29	447.50	342.45	247.54	128.48	203.27	104.78	130.39
AT4G16370	829.09	1.50	0.38	3.95	0	0.01	330.74	310.19	519.70	466.71	413.60	554.60	1061.43	786.29	325.34	657.19	2899.26	1624.05
AT4G16980	26.70	7.43	1.46	5.10	0	0.00	14.49	3.37	10.55	47.84	22.43	1.06	0.00	0.00	84.96	23.14	97.30	15.29
AT4G17770	399.45	1.09	0.27	3.99	0	0.01	367.64	349.52	444.51	474.84	398.17	312.82	190.08	289.90	425.84	417.56	653.95	468.51
AT4G21380	12.18	-5.61	1.65	-3.41	0	0.05	14.49	31.47	39.57	7.22	5.61	8.48	8.26	7.94	8.29	14.87	0.00	0.00
AT4G21400	536.12	-1.13	0.30	-3.71	0	0.03	342.60	383.24	329.76	641.84	483.70	987.25	630.66	622.15	852.72	477.61	333.05	348.91
AT4G21830	1111.22	-1.90	0.53	-3.59	0	0.04	549.48	765.35	737.34	2105.18	1854.87	2329.75	964.84	1039.12	1871.22	344.85	490.23	282.37
AT4G22214	60.22	-3.91	0.71	-5.49	0	0.00	19.77	21.35	55.40	74.02	54.68	144.22	72.83	74.13	140.91	52.33	9.36	3.60

AT4G22230	26.14	-3.32	0.88	-3.79	0	0.02	25.04	28.10	9.23	32.50	30.84	53.02	34.61	34.42	17.61	40.21	0.00	8.09
AT4G22530	462.41	1.13	0.32	3.56	0	0.04	453.29	594.52	890.34	295.19	276.20	250.26	254.12	285.92	406.16	688.59	641.79	512.57
AT4G23600	27.81	28.52	4.74	6.02	0	0.00	0.00	0.00	0.00	8.12	0.00	0.00	0.00	0.00	318.09	0.00	7.48	0.00
AT4G24275	90.58	-1.33	0.38	-3.52	0	0.04	73.79	89.91	84.42	124.58	105.15	101.80	91.94	76.78	155.42	111.28	46.78	25.18
AT4G25350	11.08	-6.65	1.70	-3.90	0	0.02	9.22	23.60	17.15	8.12	19.63	8.48	29.44	11.91	2.07	3.31	0.00	0.00
AT4G29060	412.35	1.12	0.29	3.86	0	0.02	326.79	285.46	510.46	306.03	279.00	314.95	311.46	283.28	440.35	569.60	782.12	538.65
AT4G30090	39.36	-2.31	0.57	-4.06	0	0.01	28.99	13.49	25.06	41.53	61.69	49.84	70.76	55.60	67.35	34.15	12.16	11.69
AT4G30170	993.23	-2.03	0.37	-5.48	0	0.00	785.34	1365.50	1214.83	1334.24	576.23	1306.44	1114.63	1637.45	1076.52	845.04	249.79	412.76
AT4G30290	1115.24	-1.32	0.32	-4.10	0	0.01	781.39	603.52	906.17	1726.03	1294.06	1369.00	1624.94	1607.00	1530.34	711.18	508.00	721.20
AT4G33020	22.25	6.60	1.19	5.54	0	0.00	0.00	0.00	0.00	0.00	0.00	2.12	0.00	2.65	0.00	2.20	166.53	93.52
AT4G35250	164.94	1.74	0.38	4.57	0	0.00	122.55	144.98	154.33	160.69	203.29	73.17	53.20	125.75	163.71	224.21	333.05	220.32
AT4G35380	473.64	-1.36	0.33	-4.15	0	0.01	768.21	506.86	495.95	841.35	541.18	671.25	520.64	432.86	297.36	185.09	191.79	231.11
AT4G35770	82.20	-2.95	0.65	-4.55	0	0.00	25.04	11.24	15.83	65.00	28.04	289.49	198.86	111.19	51.81	138.27	11.23	40.47
AT4G36610	144.95	2.14	0.46	4.69	0	0.00	152.85	293.33	209.73	133.60	70.10	43.48	68.18	70.16	77.71	84.83	379.83	155.57
AT4G36820	140.21	-1.54	0.37	-4.11	0	0.01	213.47	251.75	150.37	253.67	151.42	142.10	130.16	112.52	81.85	106.87	52.39	35.97
AT4G36850	56.90	3.36	0.78	4.30	0	0.00	7.91	0.00	7.91	31.60	19.63	16.97	29.96	6.62	31.08	154.80	195.53	180.75
AT4G37070	916.41	-1.68	0.48	-3.48	0	0.05	1960.72	2276.95	1134.37	1563.54	527.16	898.18	765.99	636.71	216.55	538.75	153.43	324.63
AT4G37390	259.58	-2.62	0.60	-4.33	0	0.00	241.14	533.84	486.72	259.99	99.54	240.72	689.03	131.05	110.86	206.58	56.13	59.35
AT4G37400	487.49	-2.51	0.49	-5.09	0	0.00	363.68	193.30	313.93	650.87	740.27	902.42	946.25	591.71	707.67	153.14	110.39	176.25
AT4G37530	478.21	-1.10	0.31	-3.55	0	0.04	864.40	841.77	651.60	1002.04	619.69	378.57	380.67	226.36	227.94	237.43	174.01	133.99
AT4G37760	297.59	1.25	0.29	4.28	0	0.00	307.02	234.89	245.34	313.25	508.93	123.01	189.04	150.90	349.17	409.30	349.89	390.28
AT4G37890	170.06	1.25	0.37	3.43	0	0.05	188.43	262.98	246.66	65.00	79.92	103.92	88.32	111.19	147.13	266.62	310.60	169.96
AT4G38470	1695.20	-1.78	0.42	-4.20	0	0.01	1413.88	1398.09	1028.84	1314.38	1535.21	5280.90	1725.15	1616.27	1371.81	1979.84	905.61	772.46
AT4G40090	40.27	-5.61	1.26	-4.47	0	0.00	28.99	19.11	110.80	30.69	28.04	11.66	39.77	149.58	22.79	39.11	0.00	2.70
AT5G01870	836.40	-1.64	0.39	-4.24	0	0.01	300.43	364.13	528.93	721.29	1010.86	1147.38	2306.74	1031.18	597.84	1068.14	427.55	532.36
AT5G05500	34.24	-2.49	0.70	-3.53	0	0.04	22.40	25.85	47.49	39.72	22.43	29.69	58.37	91.34	16.58	35.81	14.97	6.29
AT5G05600	1635.52	-1.44	0.40	-3.56	0	0.04	1114.76	1298.06	1172.62	1932.76	4761.25	2636.21	1565.03	1119.87	1767.61	952.46	622.14	683.43
AT5G06090	112.27	2.15	0.44	4.88	0	0.00	173.93	161.84	142.46	103.81	71.50	37.11	27.89	64.86	87.03	100.81	257.28	118.70
AT5G06930	70.14	-1.93	0.51	-3.78	0	0.02	59.30	67.43	47.49	121.87	124.78	58.32	135.84	47.65	69.42	66.66	17.78	25.18
AT5G10510	652.02	-1.34	0.30	-4.50	0	0.00	500.72	586.66	741.29	973.15	995.43	744.42	890.47	542.73	715.95	557.48	217.98	357.90

AT5G12020	514.94	-2.11	0.51	-4.10	0	0.01	1174.06	619.25	480.13	688.79	1598.30	219.51	580.56	276.66	244.52	130.56	60.81	106.11
AT5G13580	306.83	1.46	0.37	3.97	0	0.01	512.58	674.32	514.42	367.41	213.11	76.35	105.37	145.61	249.70	224.21	391.99	206.83
AT5G13630	352.21	1.73	0.36	4.88	0	0.00	163.39	86.54	211.04	483.87	422.01	129.37	180.78	239.59	574.01	518.92	681.08	535.95
AT5G14540	1730.28	1.80	0.25	7.22	0	0.00	1689.28	1580.15	1694.95	1377.57	1278.64	1115.56	712.27	890.87	1587.33	2528.51	3408.20	2900.09
AT5G15070	158.15	-1.11	0.32	-3.44	0	0.05	137.04	207.91	216.32	196.80	204.69	195.12	154.95	158.85	164.74	104.67	75.78	80.93
AT5G17430	85.81	-1.70	0.49	-3.44	0	0.05	123.86	124.75	83.10	102.01	138.80	95.44	75.41	45.01	92.21	104.67	11.23	33.27
AT5G17820	157.06	-2.39	0.59	-4.03	0	0.01	64.57	200.05	291.51	113.74	70.10	183.45	210.22	293.87	86.00	283.70	53.33	34.17
AT5G22020	812.09	2.08	0.47	4.43	0	0.00	848.59	892.35	1192.40	705.04	665.96	143.16	248.44	710.84	710.77	529.94	1613.82	1483.77
AT5G22140	961.22	1.54	0.31	5.01	0	0.00	1009.35	663.08	964.21	514.56	859.44	440.07	632.73	730.70	995.70	1233.96	1991.78	1499.05
AT5G23220	390.25	-1.55	0.35	-4.43	0	0.00	1091.05	735.01	461.66	459.49	304.24	283.13	232.95	256.80	349.17	333.28	91.68	84.53
AT5G23870	66.85	-1.59	0.44	-3.64	0	0.03	75.11	106.77	56.72	92.98	93.94	62.56	82.64	91.34	54.91	33.05	25.26	26.98
AT5G24120	291.95	1.13	0.27	4.10	0	0.01	230.60	249.50	234.79	347.55	314.05	118.77	139.46	211.80	423.77	553.63	338.67	340.82
AT5G33355	407.04	13.85	1.25	11.04	0	0.00	1.32	0.00	0.00	0.00	0.00	0.00	0.00	0.00	5.18	2.75	3439.07	1436.11
AT5G40780	318.91	-1.54	0.39	-3.92	0	0.01	384.77	505.74	588.29	385.47	217.31	305.40	383.25	334.90	149.20	337.13	88.88	146.58
AT5G41040	531.61	1.67	0.34	4.87	0	0.00	973.77	1167.70	1374.43	462.20	318.26	120.89	116.22	242.24	262.14	330.52	584.72	426.25
AT5G42580	625.67	-1.98	0.53	-3.72	0	0.03	998.81	2341.01	836.26	995.72	346.30	629.89	337.28	415.65	101.54	272.68	140.33	92.62
AT5G42930	313.22	-1.31	0.38	-3.42	0	0.05	329.42	609.13	300.74	352.97	536.97	432.65	332.63	227.68	161.63	207.68	116.01	151.07
AT5G44120	340.24	-10.90	3.15	-3.46	0	0.05	2.64	28.10	655.56	1.81	227.13	2453.81	146.17	9.27	0.00	557.48	0.00	0.90
AT5G46890	41.35	-3.10	0.85	-3.67	0	0.03	34.26	35.96	19.79	38.82	11.22	53.02	50.10	181.35	6.22	43.52	9.36	12.59
AT5G47110	282.74	1.52	0.36	4.21	0	0.01	155.49	122.50	208.41	174.23	238.34	117.71	266.52	230.33	295.29	405.99	605.30	572.82
AT5G48110	558.95	-1.40	0.34	-4.11	0	0.01	250.36	450.67	342.95	531.71	430.42	873.79	1111.02	558.61	660.00	856.06	386.38	255.39
AT5G48880	449.18	1.62	0.36	4.51	0	0.00	492.82	551.82	618.62	320.47	305.64	147.40	382.22	326.96	292.18	187.85	1016.00	748.18
AT5G50260	96.60	-2.54	0.61	-4.18	0	0.01	454.60	169.70	126.63	56.87	47.67	68.93	104.34	55.60	24.87	23.69	7.48	18.88
AT5G50400	1618.26	1.93	0.26	7.52	0	0.00	1014.62	1203.66	1205.59	1289.11	1519.79	740.17	920.94	959.70	1395.64	2508.68	3535.43	3125.80
AT5G50740	49.70	-2.75	0.64	-4.30	0	0.00	31.62	46.08	50.12	38.82	35.05	40.30	148.24	58.24	81.85	41.32	13.10	11.69
AT5G55050	234.68	-1.20	0.31	-3.91	0	0.02	351.82	291.08	257.21	247.35	403.78	229.05	303.19	226.36	145.06	139.92	94.49	126.79
AT5G55820	167.08	-1.48	0.39	-3.74	0	0.02	129.13	194.43	153.01	125.48	207.50	211.02	387.90	169.44	122.26	119.54	93.55	91.72
AT5G56080	174.13	3.10	0.42	7.30	0	0.00	382.13	221.40	155.65	119.16	95.34	58.32	39.77	51.63	37.30	79.88	419.13	429.84
AT5G58000	226.46	1.06	0.26	4.05	0	0.01	235.87	323.67	308.65	199.50	178.06	124.07	121.38	158.85	235.20	275.44	305.92	250.89
AT5G59540	490.60	1.23	0.33	3.72	0	0.03	611.41	528.22	747.89	439.63	475.28	199.36	373.44	297.84	290.11	558.03	740.95	624.98

AT5G59720	7023.72	-1.05	0.27	-3.88	0	0.02	20356.98	17398.55	16717.37	9997.79	7333.96	932.11	1643.02	1433.60	4000.43	3176.88	552.91	740.98
AT5G62210	37.49	3.90	1.00	3.92	0	0.01	117.27	105.64	67.27	40.62	37.85	0.00	0.00	6.62	7.25	16.53	11.23	39.57
AT5G66690	1125.17	-1.14	0.26	-4.31	0	0.00	1612.85	1480.13	1253.08	1465.14	842.61	1148.44	1582.07	1588.47	651.72	566.30	652.08	659.15
AT5G67400	27.39	-7.68	1.73	-4.45	0	0.00	26.35	15.73	97.61	34.30	9.81	10.60	34.09	59.57	10.36	30.30	0.00	0.00

Appendix C. List of sample DEGs with pvalue adjusted <= 0.05 in common between 6 and 24h treatment. The table displays the gene name, the mean expression value among all samples, the log2FoldChange between treated vs control at 6h and between treated vs control at 24h.

GENE	BaseMean (all samples)	log2FoldChange (SELF 6H vs CTRL)	log2FoldChange (SELF 24H vs CTRL)
AT1G07400	548.13	-2.00	-1.97
AT1G10970	454.70	1.40	3.03
AT1G14780	397.58	-1.52	-1.58
AT1G20380	519.61	2.04	4.99
AT1G54050	189.25	-2.37	-1.94
AT1G59860	183.51	-3.41	-2.20
AT1G72540	159.59	-2.23	-1.57
AT3G12750	876.69	1.45	2.35
AT3G59930	3100.97	3.51	7.14
AT4G35380	473.64	-1.53	-1.36
AT4G37530	478.21	-1.80	-1.10
AT4G37890	170.06	1.53	1.25
AT5G12020	514.94	-2.61	-2.11
AT5G55050	234.68	-1.19	-1.20
AT5G59720	7023.72	-1.27	-1.05

Acknowledgements

I am immensely grateful to all the people who have accompanied me throughout this long journey. Foremost, I would like to express my deepest appreciation to my family, especially my mother, whose unwavering support has been a constant source of strength during challenging times. My college experience has been enriched by the remarkable people I have encountered, each contributing to my scientific knowledge, personal growth, and passion for research. I am particularly indebted to Nicoletta Felice and Giusi Zaina, whose guidance and enthusiasm have instilled in me a profound appreciation for laboratory work. They have been fundamental in shaping my understanding of laboratory techniques and etiquette. I would also like to extend my heartfelt gratitude to my two supervisors, Professor Guido Incerti and Professor Emanuele De Paoli, for their unwavering support and guidance throughout my journey. I am also grateful to Professor Mazzoleni for his valuable mentorship. To my incredible friends at the university, I am forever grateful for the memorable moments and the lasting friendships we have forged. Leaving this city will undoubtedly be a bittersweet experience, as I know how much I will miss all of them. I want to extend a special thanks to Rory, whose constant inspiration and encouragement have pushed me to strive for excellence throughout these years. Lastly, I want to express my heartfelt appreciation to my beloved cat, my ever-faithful companion, who has given me unconditional love and companionship during this entire journey.